



Résilience et vulnérabilité des savanes brésiliennes face aux incendies, au climat et aux activités anthropiques depuis la fin la dernière glaciation

Katerine Escobar Torrez

► To cite this version:

Katerine Escobar Torrez. Résilience et vulnérabilité des savanes brésiliennes face aux incendies, au climat et aux activités anthropiques depuis la fin la dernière glaciation. Biodiversité et Ecologie. Université de Montpellier, 2023. Français. NNT: 2023UMONG026 . tel-04622713

HAL Id: tel-04622713

<https://theses.hal.science/tel-04622713>

Submitted on 24 Jun 2024

HAL is a multi-disciplinary open access archive for the deposit and dissemination of scientific research documents, whether they are published or not. The documents may come from teaching and research institutions in France or abroad, or from public or private research centers.

L'archive ouverte pluridisciplinaire **HAL**, est destinée au dépôt et à la diffusion de documents scientifiques de niveau recherche, publiés ou non, émanant des établissements d'enseignement et de recherche français ou étrangers, des laboratoires publics ou privés.

THÈSE POUR OBTENIR LE GRADE DE DOCTEUR DE L'UNIVERSITÉ DE MONTPELLIER

En EERGP – Ecologie, Evolution, Ressources Génétiques, Paléobiologie
École doctorale GAIA – Biodiversité, Agriculture, Alimentation, Environnement, Terre, Eau
Unité de recherche – Institut des Sciences de l'Evolution de Montpellier – UMR 5554

Résilience et vulnérabilité des savanes brésiliennes face aux incendies, au climat et aux activités anthropiques depuis la fin la dernière glaciation

(Resilience and vulnerability of Brazilian savannahs to fires, climates and
anthropogenic activities since the end of the last glacial)

Présentée par Katerine ESCOBAR TORREZ

Le 6 octobre 2023

Sous la direction de Marie-Pierre LEDRU
et le co-encadrement de Raquel FRANCO CASSINO

Devant le jury composé de

[Dr. Christelle HÉLY, directrice d'étude, EPHE, France]

[Président du Jury]

[Dr. Vincent LEBRETON, Professeur, CNRS-HNHP, France]

[Rapporteur/Examinateur]

[Dr. Antonio MALDONADO, director de recherche, CEAZA, Chile]

[Rapporteur/Examinateur]

[Dr. Imma OLIVERAS MENOR, directrice de recherche, AMAP-IRD, France]

[Examinateuse]

[Dr. Lionel SIAME, Maître de Conférences, CEREGE, France]

[Examinateur]

[Dr. Adam A ALI, Professeur, Université de Montpellier, France]

[Examinateur Invité]



UNIVERSITÉ
DE MONTPELLIER

REMERCIEMENTS

Cette thèse représente une période d'enrichissement de trois ans dans ma vie, au cours de laquelle j'ai appris, découvert et compris ma voie dans la recherche. Ainsi, il est donc nécessaire de reconnaître que cette thèse est le résultat de la collaboration et de l'aide de personnes que j'ai rencontrées tout au long de ma carrière scientifique et autre.

Tout d'abord, je voudrais remercier ma directrice de thèse Marie-Pierre Ledru et ma co-directrice Raquel Franco Cassino. Toutes deux sont un élément fondamental et le meilleur exemple de la passion et de l'amour qui poussent à choisir la voie de la recherche. Leur guidance et leurs conseils, leur patience et leur affection, les encouragements et évidemment l'énorme savoir qu'ils m'ont transmis m'ont accompagnée tout au long de cette aventure. Aussi, des grands remerciements à mes co-auteurs pour ces contributions dans les articles écrits: Ingrid Horak-Terra, Iliana Wainer, Manuel Chevalier et Elder Yokoyama.

Un grand merci aux membres du comité de suivi de la thèse, qui m'ont accompagné par leurs conseils et leurs discussions enrichissantes tout au long de l'avancement de la thèse: Michel Brossard, Ludivine Eloy, Nicolas Galtier et Sonia Kefi.

Merci à Antonio Maldonado et Vincent Lebreton d'avoir accepté d'être rapporteurs et jury de cette thèse, ainsi qu'aux autres membres du jury qui ont pris le temps d'évaluer et de questionner mon travail de recherche: Imma Oliveras Menor, Christelle Hély et Adam A. Ali.

Merci au programme "Cerrados & Fogos" de l'IRD, soutien financier apporté par l'IRD, le FAPDF (0193.001374/2016), l'ISEM, la DEGEO-UFOP, l'IG-UnB et l'ICA/UFVJM. Au programme doctorale ARTS de l'IRD et l'Ambassade de France en Bolivie. Ce travail a également bénéficié d'une bourse "Investissement d'Avenir" gérée par l'Agence Nationale de la Recherche (CEBA, réf. ANR-10-LABX-25-01). La datation au radiocarbone a été réalisée au LMC14 (LSCE(CNRS-CEA-UVSQ)-IRD-IRSN-MC) avec le soutien financier de l'IRD.

Merci à l'équipe qui a participé au travail de terrain pour la collecte des échantillons de sédiments, sans laquelle cette thèse n'existerait pas: Ana Carolina Sena Barradas, Marco Assis Borges, Maximo Menezes Costa de l'Instituto Chico Mendes de conservação da Biodiversidade, Ludivine Eloy, Silvia Laine Borges Lucio, Christelle Hély-Alleaume pour leur aide lors du travail de terrain à la station écologique de la Serra Geral do Tocantins.

Merci à l'ISEM, le lieu qui m'a accueilli pendant le développement de la thèse, en particulier au département PAST, où j'ai rencontré des personnes merveilleuses qui m'ont accompagné pendant les heures de laboratoire: des chercheurs, des enseignants et du personnel, en particulier à: Eleonora Cagliero, Nagham Tabaja, Olga Aquino, Reyes Luelmo Lautenschlaeger, Sandrine Canal, Sylvie Rouland, Bertrand Limier, Jérôme Ros, Laurent Bremond, Sergio Xavier, Thierry Pastor, Vincent Montade, Walter Finsinger.

Un grand merci à toutes les personnes que j'ai rencontrées à l'intérieur et à l'extérieur du laboratoire, je n'aurais pas assez de place pour les remercier toutes, mais je suis satisfait de savoir qu'elles savent de qui je parle!

Un remerciement spécial à ma famille pour m'avoir poussé et soutenu à distance pendant ces trois dernières années.

Et enfin, merci à tous ceux qui liront cette thèse, j'espère qu'elle vous plaira.

DÉDICACE



à tout ce que j'aime

AVANT-PROPOS

Cette thèse a été élaborée en fonction de trois parties. Le premier sous presse, le deuxième en préparation, et le troisième en cours de révision. La Partie 1 présente le cadre général de la thèse ainsi que le matériel et les méthodes utilisés pour ces travaux. La partie 2 présente les articles, dans le **l'article 1** nous avons examiné les relations entre morphologie, syndrome de pollinisation et dépôt du grain de pollen dans les sédiments. Les **articles 2 et 3** ont été consacrés à l'étude palynologique de deux nouveaux enregistrements sédimentaires des Cerrados brésiliens. La partie 3 présente une discussion finale sur la résilience et la vulnérabilité des Cerrados d'après nos résultats. Les articles ont été rédigés en anglais, tandis que le reste de la thèse a été rédigé en français.

Comme la thèse est développée autour d'un axe central, plusieurs des études publiées utilisées comme base pour le développement du projet sont répétées dans les différents chapitres. C'est pourquoi, afin de ne pas surcharger la thèse de références répétées (y compris celles des articles), celles-ci se trouvent dans la section **Références** à la fin du document.

Liste des articles

Article 1: Katerine Escobar-Torrez, Raquel Franco Cassino, Marie-Pierre Ledru 2023. Relationships between pollination syndromes, pollen morphology and plant ecology in Quaternary deposits of the Cerrado. **Palynology**. doi : 10.1080/01916122.2023.2252871

Article 2: Katerine Escobar-Torrez, Marie-Pierre Ledru, Raquel Franco Cassino, Paula Ribeiro Bianchini, Elder Yokoyama. 2023. Long- and short-term vegetation change and inferred climate dynamics and anthropogenic activity in central Cerrado during the Holocene. **Journal of Quaternary Science**. doi: 10.1002/jqs.3567

Article 3: Katerine Escobar-Torrez, Marie-Pierre Ledru, Raquel Franco Cassino, Ingrid Horák-Terra, Ilana Wainer, Manuel Chevalier (**en preparation**) How northern hemisphere ice melting changed the biodiversity of the Cerrado.

TABLE DES MATIÈRES

REMERCIEMENTS.....	I
DEDICACE.....	II
AVANT-PROPOS	III
TABLE DES MATIERES.....	IV
LISTE DES PLANCHES.....	VII
LISTE DES FIGURES.....	VII
LISTE DES TABLEAUX.....	XI
RÉSUMÉ.....	XIII
ABSTRACT.....	XV

Partie I. Cadre général, matériel et méthodes	1
1 Contexte général du Cerrado.....	2
1.1 Les savanes tropicales et le Cerrado: origines.....	2
1.2 Importance du Cerrado.....	3
1.3 Environnement climatique actuel.....	4
1.4 Le Cerrado: principales caractéristiques.....	6
1.4.1 Végétation.....	6
1.4.2 Facteurs environnementaux	9
1.5 Problèmes actuels dans le Cerrado.....	14
2 Etat de l'art - paléoenvironnement dans le Cerrado.....	16
2.1 Études palynologiques	16
2.2 Études sur les charbons.....	17
2.3 Études paléoclimatiques du Cerrado.....	19
3 Objectifs de l'étude.....	20
4 Région d'étude.....	22
5 Matériel et méthodes.....	23
5.1 Echantillonnage et cadre chronologique.....	23
5.2 Reconstruction de la végétation	25
5.3 Reconstruction des incendies.....	26
5.4 Les autres indicateurs.....	28

Partie II.

Article 1. Relationships between pollination syndromes, pollen morphology and plant ecology in Quaternary deposits of the Cerrado.....31

Abstract.....	31
1 Introduction	32
2 Material and methods.....	33
2.1 Study area and core sampling.....	33
2.2 Climate and vegetation.....	34
2.3 Laboratory work.....	34
2.4 Pollen taxa morphology and ecology.....	35
3 Results	35
3.1 Pollen morphology and ecological information.....	35
3.2 Ecological and morphological traits of pollen taxa.....	54
4 Discussion.....	58
5 Conclusion	60
6 Acknowledgments and Funding.....	60

Article 2. Long- and short-term vegetation change and inferred climate dynamics and anthropogenic activity in central Cerrado during the Holocene.....62

Abstract.....	62
1 Introduction.....	63
2 Material and methods.....	65
2.1 Study area.....	65
2.2 Modern vegetation.....	66
2.3 Sampling and chronology.....	67
2.4 Analytical protocols.....	68
3 Results.....	69
3.1 Palynological analyses.....	70
3.2 XRF analyses.....	73
3.3 Charcoal analyses.....	73
4 Interpretation.....	74
5 Discussion.....	75
5.1 Expansion of the arboreal cerrado in Central Brazil.....	75
5.2 Climatic drivers of vegetation changes in central Brazil.....	77
5.3 Fire events in central Brazil.....	81
6 Conclusion.....	83
7 Acknowledgments and funding.....	83
8 Annex 1. Supporting information.....	84

Article 3. Link between northern hemisphere ice melting and Cerrado biodiversity	97
Abstract.....	97
1 Introduction.....	98
2 Material and methods.....	100
2.1 Study area.....	100
2.2 Modern vegetation.....	101
2.3 Sampling and chronology.....	103
2.4 Analytical methods.....	104
3 Results.....	106
3.1 Age-depth model and sedimentation rates.....	106
3.2 Elemental and isotopic proxies.....	106
3.3 Pollen analysis.....	108
3.4 Paleoclimate reconstruction based on pollen.....	112
3.5 Macrocharcoal analyses.....	112
4 Interpretation.....	113
5 Discussion.....	116
5.1 15,000 years of ecological successions in the Cerrado.....	116
5.2 Climatic drivers affecting vegetation.....	117
5.3 Fire occurrence in the “Serra Geral do Tocantins”.....	123
6 Conclusion.....	123
7 Acknowledgments and funding.....	124
8 Annex 1. Supporting information.....	125
Partie 3. Synthèse des résultats, conclusions et perspectives	136
1 Synthèse.....	137
2 Conclusion et perspectives.....	138
Références.....	141

LISTE DES PLANCHES

Planche II.1: Photomicrographs of pollen taxa identified in LFB1 and VGE-17 cores: Amaranthaceae – 1) Gomphrena, Anacardiaceae – 2) Astronium, 3) Tapirira, Apiaceae – 4) Eryngium, Aquifoliaceae – 5) Ilex, Arecaceae – 6) Euterpe type, Asteraceae – 7) Baccharis type, Boraginaceae – 8) Cordia, 9) Brassicaceae type, Burseraceae – 10) Protium, Cannabaceae – 11) Celtis, 12) Trema, Caryocaraceae – 13) Caryocar, Chloranthaceae – 14) Hedyosmum, Cunoniaceae – 15) Lamanonia, Dillenaceae – 16) Curatella, Droseraceae – 17) Drosera, 18) Ericaceae type, Euphorbiaceae – 19) Acalypha, 20) Alchornea, Fabaceae (Mimosaceae) – 21) Anadenanthera, 22) Mimosa.....	39
Planche II.2: Photomicrographs of pollen taxa LFB1 and VGE-17 cores: Fabaceae (Mimosaceae) – 23) Piptadenia, Fabaceae (papilionaceae) – 24) Dalbergia, 25) Dialium, 26) Machaerium, Icacinaceae – 27) Emmotum, Lythraceae – 28) Cuphea, Malvaceae – 29) Apeiba, 32) Eriotheca, Malpighiaceae – 30) Banisteropsis, 31) Byrsonima, 33) Melastomataceae/Combretaceae, Meliaceae – 34) Guarea, Menispermaceae – 35) Abuta, 36) Menispermaceae type, 37) Moraceae , 38) Myrtaceae , Ochnaceae – 39) Ouratea, <i>Pentaphylaceae</i> – 40) Ternstroemia, Phyllantaceae – 41) Hyeronima, Piperaceae – 42) Peperomia, 43) Poaceae , Polygonaceae – 44) Polygala, Primulaceae – 45) Cybianthus, 46) Myrsine	44
Planche II.3: Photomicrographs of pollen taxa identified in LFB1 and VGE-17 cores: Rubiaceae – 47) Guettarda, 48) Sabicea type, 49) Simira, Salicaceae – 50) Casearia, Vitaceae – 51) Cissus, Sapindaceae – 52) Matayba, 53) Paullinia, Smilaceae – 54) Smilax, Solanaceae – 55) Solanum, Urticaceae – 56) Cecropia, Verbenaceae – 57) Lippia, Xyridaceae – 58) Xyris, Arecaceae – 59) Mauritia, 60) Cyperaceae , Alismataceae – 61) Echinodorus, 62) Sagittaria, Eriocaulaceae – 63) Eriocaulon, Haloragaceae – 64) Myriophyllum, Nymphaeaceae – 65) Nymphaea.....	50

LISTE DES FIGURES

Figure I.1: Carte du Brésil représentant les 7 divisions du Cerrado (d'après Françoso et al 2019) (ligne jaune), avec les Etats du Brésil (ligne noire) et la délimitation du Cerrado (ligne rouge). NE nord-est, NW nord-ouest, CW central-ouest, SW sud-ouest, C centre, C&SE centre-sud- est.....	4
Figure I.2 : Précipitations moyennes annuelles pour les mois de janvier (Jan) (a) et de juillet (Jun) (b) au Brésil avec les frontières entre les états (ligne noire) et le biome Cerrado (ligne rouge). En a) la ligne pointillée orange représente la zone influencée par la ZCIT, la ligne pointillée verte l'emplacement de la ZCAS, les flèches bleues montrent l'incursion des alizés de l'océan Atlantique Nord qui pénètrent sur le continent et la ligne jaune le flux des masses d'air de basse altitude (SALLJ). En b) la zone d'incursion des fronts polaires (ligne jaune pointillée) et des masses d'air atlantiques (flèche bleue). (D'après Fick and Hijmans, 2017).....	5

Figure I.3 Les phytophysionomies du biome Cerrado avec a) les sols bien drainés et b) les sols inondés en permanence ou de façon saisonnière, ainsi que les trois formations, forêt, la savane et la prairie (d'après Cassino et al., 2021).....	9
Figure I.4 : Les types de sol du Cerrado avec les phytophysionomies correspondantes (d'après Lira-Martins et al., 2022).....	11
Figure I.5 : Représentation graphique montrant les différents régimes de feu observés dans les savanes et les forêts (d'après Pivello et al., 2021).....	12
Figure I.6: Carte du Brésil montrant la répartition des zones protégées (principalement en Amazonie et dans la région nord-est du Cerrado) et des territoires indigènes au Brésil (peu nombreux dans le nord-est du Cerrado) (MAPBIOMAS, 2023).....	15
Figure I.7 : Synthèse a) des changements climatiques (sec/humide). <i>wet=humide (barre bleue claire)</i> , <i>dry=sec (barre jaune)</i> . b) des physionomies dominantes et des incendies à partir des enregistrements palynologiques et des macrocharbons (barre noire). <i>grassland=savane ouvert (barre jaune)</i> , <i>savanna=savane (barre marron)</i> , <i>sav/gallery forest= savanna/forêt de galerie (barre orange)</i> , <i>gallery/moist forest= forêt de galerie/humide (barre verte)</i> .1 Caço, 2 Confusão, 3 Aguas Emendadas, 4 Lagoa Feia, 5 Pandeiros, 6 Cromínia, 7 São Jose, 8 Laçador, 9 Fazenda Urbano, 10 Pau de fruta, 11 Pinheiro, 12 Rio Preto, 13 Salitre, 14 Lagoa Santa.....	18
Figure I.8 : Variations du $\delta^{18}\text{O}$ mesuré dans les spéléothèmes localisés dans le biome Cerrado (d'après Strikis et al., 2011, 2018; Wortham et al., 2017; Azevedo et al., 2021; Wong et al., 2021).....	20
Figure I.9 : Interaction des différents forçages (climat, homme, sol, feu) montrant des réponses favorables (positives) ou défavorables (négatives) entre les différentes composantes.....	21
Figure I.10 : Cartes (a) de la distribution des précipitations pendant l'été austral (DJF) au Brésil et (b) de la topographie de la zone d'étude montrant l'emplacement des sites d'étude 1) Lagoa Feia et 2) Varjão do Getulio. Détail des types de végétation observés autour de Lagoa Feia (c) et Varjão do Getulio (d) représentés par un point noir (Fick and Hijmans, 2017; MapBiomas, 2023).....	23
Figure II.1: a) Brazilian biomes showing the location of VGE-17 (1) and LFB1 (2) sediment cores in the Cerrado area, and the b) elevation in which the two sites are emplaced, with the division territory division (red line).....	33
Figure II.2: Synthetic diagram of pollen influx ($\text{mm}^2/\text{cm}^2/\text{yr} \times 1000$) from LFB1 (A) and VGE-17 (B) sediment cores, were we showed the pollen depositions sums in relation to their pollination syndrome (purple color), the stratum from which they come (green color), and their pollen size (dark color). Additionally it has been added the pollen taxa water level-related (green-blue color), for of LFB1 (total aquatic taxa) and for VGE-17 (Mauritia). The diagram was represented in a scale of depth (cm). abiotic=anemophilous, both=biotic/abiotic, field=<50cm, shrubby=<2m, lower=2-10m, medium=>15m, small=<15 μm , med= 15-25 μm , large=26-49 μm	57

Figure II.3: Schematic representation of the principal phytophysiognomies observed at lake Feia, showing the list of main pollen taxa identified in the LFB1 core related to the determined classification based in table 1. The band on the top of the schema shows water availability on the soil, from high (blue) to low (yellow).....57

Figure II.4: Schematic representation of the principal phytophysiognomies at “Varjão do Getulio” swamp, showing the list of main pollen taxa identified in the VGE-17 core related to the determined classification based in table 1. The band on the top of the schema shows water availability on the soil, from high (blue) to low (yellow).....58

Figure III.1: (A) A map of the mean austral summer precipitation levels, showing the position of the ITCZ, the core region of the summer monsoon today (dark blue), the limit of the Cerrado biome (black line), and the location of Lake Feia and the pollen and isotopic records discussed in the text. (B) A satellite view of Lake Feia (source Google Earth) showing its location relative to Formosa and Preto River. (C) A climate diagram for the city of Formosa (INMET, 2022).....65

Figure III.2: A calibrated age-depth model for the LFB1 core from Lake Feia, with the accumulation rate curve in a/cm at the top and the position of the radiocarbon dates (Table 1) along the core lithology (in brown) at the bottom. The standardized errors are indicated by the blue boxes. The black dashed lines show the upper and lowest calibrated ages, the gray band the probability of minor or major dates for each depth, and the red dashed line the most probable age.....69

Figure III.3: Synthetic pollen influx (black bars) and frequency (curve) diagram for 20 selected pollen taxa from core LFB1, represented by PC1 scores and macrocharcoal accumulation rate (mm²/cm²/a), respectively, along a time scale. Woody cerrado taxa are shown in yellow, gallery forest taxa in green, and water level-related taxa in blue. Gray horizontal bands indicate the dry intervals. Exaggeration ($\times 10$) curves are in gray.....71

Figure III.4: A representation of the last 6000 years in the central region of the Cerrado biome. A synthetic pollen, charcoal and geochemical diagram is shown for Lake Feia (cores LF-15 and LFB1) (Cassino et al. 2020; present study) along with $\delta^{18}\text{O}$ isotopic ratios from selected speleothem records along a calibrated time scale. The percentages of terrestrial and water level-related taxa, normalized Ti/K ratios and charcoal influxes (CHARarea) are indicated. The speleothem records came from southern (Botuverá cave; Bernal et al., 2016), northern (Paraiso cave; Wang et al., 2017) and central (Angelica cave; Wong et al., 2021; Tamboril; Wortham et al., 2017) Brazil, with an insolation curve at 15°S (Laskar et al., 2011). The blue dotted line shows the main vegetation observed in central Cerrado; the gray bands represent the dry intervals.....74

Figure III.5: The last 19,000 years in central Cerrado, as represented by the Lake Feia sediment cores (Cassino et al. 2020; present study). From left to right, a synthetic pollen diagram showing arboreal pollen/non-arboreal pollen frequencies (AP and NAP, respectively), 13 selected pollen taxa, with AP cerrado taxa shown in yellow and gallery forest taxa in green, and water level-related (aquatics) in blue, plus the charcoal influx (CHARarea; mm²/cm²/a). The yellow horizontal bands show the disappearance of Lake Feia during dry episodes (from Cassino et al., 2020).....77

Figure III.6: A schematic representation of the eight climate episodes observed during the last 6000 years in the Cerrado biome, with their corresponding latitudinal boundaries. The site numbers are the same as Fig. 1. Arboreal pollen/non-arboreal pollen frequencies available from palynological sites are represented as pie diagrams.....79

Figure III.7: Summary of the main climate changes (wet/dry events) observed in the last 6000 years between the paleo-records in Figure 6, organized according to their latitude and longitude. From left to right: the age scale in cal ka BP (ka = 1000 years), the paleo-records from north to south, and finally a summary of the SASM intensity at 15°S, at lake Feia. The blue lines represent wet climate and the yellow lines represent dry climate. The number below each record indicates the name of the record shown in Figure 1 (in red the pollen records and in blue the speleothem records).....80

Figure IV.1: a) Map of northern South America showing the Cerrado biome location (dark line) inside the Brazilian territory (filled in gray) and the limits of Tocantins state (green line), and the Cerrado division of the biome defined by Fraçoso et al. (2019) – NW=northwestern, NE=northeastern, C=center, CW=central western, C&CE=central and southeastern, SW=southwestern. b) Picture of Varjão do Getulio swamp, Tocantins (by M-P Ledru) c) Map of Brazil showing the distribution of the austral summer precipitation, the limits of the biome Cerrado (red line), the states of Brazil (black line), the location of core VGE-17 (yellow rhomb), and the pollen (brown rhomb) and isotope records (yellow circle) from cerrado and adjacent areas. 1. Rahina, 2. Paraiso, 3. Lapa Sem Fim, 4. Botuverá, 5. Feia, 6. Rio Preto, 7. Caço, 8. Saquino, 9. Saci, 10. Carajas, 11. Pau de Fruta, 12. Aguas Emendadas, 13. Pandeiros, 14. Crôminia, 15. Pinheiro, 16. Confusão, 17. São Jose, 18. Salitre, 19. Varjão do Getulio (this study).....101

Figure IV.2: a) Age-depth model for the core VGE-17 based on linear interpolation between calibrated ages (Blaauw and Christen, 2011) b) sediment-accumulation rate (cm/yr) and deposition time (yr/cm) for VGE-17 core.....106

Figure IV.3: Principal component analysis from Isotopic and XRF elements from VGE-17 core. Z-scores' curves from first fourth principal components.....108

Figure IV.4: Pollen diagram of the 31 most representative terrestrial taxa from VGE-17 core along a time scale. From left to right pollen percentage (colored curves) and concentration (black bars), total of terrestrial pollen accumulation rate (PAR) (area/cm²/yr), and the pollen zones. Herbaceous taxa (yellow), shrub taxa (brown) and tree taxa (green) are presented in front of their corresponding predominant physiognomy [cerrado and gallery forest (GF)]. *Mauritia* % and accumulation rate were added to represent the general trend of water level-related pollen taxa (green-light).....111

Figure IV.5: Results of the macrocharcoal analyses of core VGE-17 with the distribution of W:L ratios for each particle per sample (blue squares) and the average of W:L ratio per sample (dark line) (red-dotted line suggest the threshold between grass <0.5 and wood particles >0.5; red stars showing the punctual events of zero fire), CHARarea (mm²/cm²/yr), red bands highlight the four macrocharcoal peaks.....113

Figure IV.6: Synthetic diagram showing the regional changes in our study area through time. From left to right, pollen frequency according to their growth forms; changes in *Mauritia* frequency (green) and pollen influx (PAR) (black bars); z-scores obtained from PC1 and PC2; $\delta^{13}\text{C}$ signal, Si/Ti and Ti/Al ratio, charcoal influx (area/cm²/yr) (red line), and the regional climatic periods. Hs1a = Heinrich stadial 1a (16,110 -14,690 yr BP), YD = Younger Dryas, EH = early Holocene, MH = mid Holocene, LH = late Holocene.....115

Figure IV.7: a) Synthesis of principal changes observed between 10,000 and 7500 cal yr BP on the VGE-17 core with pollen representation, (b) Mean annual precipitation (MAP) and precipitation of the driest quarter reconstruction made with Crest package (Chevalier et al., 2020), (c) PC2 and PC3 from XRF analyses, (d) the Insolation curve at 10°S (red curve) (Laskar et al., 2011) (e) changes in moisture from the isotopic analyses of the speleothems (Strikis et al 2011, 2015) and (f) Ti signal from Cariaco basin (Haug et al., 2001) (g) temperature reconstruction for Vostok ice core (Petit et al., 1999) and the % HSG (purple curve) representing the ice drift (Bond et al., 2001) and (h) Greenland ice core (Badgaley et al., 2020). The yellow band highlights the drier interval and the dotted black lines show the wet intervals observed at VGE-17 (this study). Light purple bands represent the bond events (from Bond et al., 2001).....121

Figure IV.8: a) Synthesis of principal changes observed between 10,000 and 7500 cal yr BP on the VGE-17 core with pollen representation, (b) Mean annual precipitation (MAP) and precipitation of the driest quarter reconstruction made with Crest package (Chevalier et al., 2020) (c) PC2 and PC3 from XRF analyses, (d) changes in moisture from the isotopic analyses of the speleothems (Strikis et al 2011, 2015), (e), Ti signal from Cariaco basin (Haug et al., 2001) (f) temperature reconstruction for Vostok (Petit et al., 1999) and Greenland (Badgaley et al., 2020) ice cores. The yellow band highlights the drier interval and the dotted black lines show the wet intervals observed at VGE-17 (this study). Light purple bands represent the bond events (from Bond et al., 2001).....122

Figure IV.9: a) December-January-February (DJF) precipitation reconstruction (PPT) at 8000 yr BP (from ref). Changes in vegetation along across a latitudinal transect b) Summary graphic showing the indicator pollen taxa used for climate and precipitation changes interpretations, with arboreal pollen (green), *Mauritia* (red) and cold and humid taxa (blue) from three records: Caço Lake (from 15,040 cal yr BP to 1997 AD) (Ledru et al., 2006), Gétulio swamp (this study) and Feia Lake (from 15,210 cal yr BP to 1990 AD) (Cassino et al., 2020; Escobar-Torrez et al., 2023a). The site names are related to the numbers in the pollen diagrams (b) in this figure.....123

LISTE DES TABLEAUX

Tableau I.1: Les espèces les plus communément observées classées par physionomie dans les trois types de formation supérieure selon Walter & Ribeiro (2008).....8

Tableau I.2: Résultats des datations radiocarbone pour la carotte LFB1.....24

Tableau I.3: Résultats des datations radiocarbone pour la carotte VGE-17.....	24
Tableau II. 1: pollen taxa classification in response to their pollination syndrome, life form, and physiognomy and strata vegetation from the Cerrado cores LFB1 and VGE-17. PS – pollination syndrome; LF – life form; P – physiognomy; S – stratum; an – anemophilous; en – entomophilous; chi – chiropterophilous; orn – ornithophilous; psy – psychophilous; zoo – zoophilous; car – carantarophilous; hyd – hydrophilous; op – open (grassland cerrado); in – intermediate (scrubby cerrado, cerrado sensu stricto); clo – closed (cerradão, gallery forest); la – lake; fi – field (< 1 m); sh – shrubby (1 – 2 m); lo – lower storey (< 10 m); me – medium storey (~15 m); up – upper storey (> 20 m).....	55
Tableau III.1: Key Cerrado species identified near Lake Feia, Brazil (Ferraz-Vicentini, 1999)....	67
Tableau III.2: Radiocarbon dates for the LFB1 sediment core taken from Lake Feia, Brazil. The 14C dates were calibrated using Calib 7.0 (Stuiver and Reimer, 1993), and values are shown to two standard deviations (2σ).....	67
Tableau IV.1: Classification of modern vegetation in the Cerrado region in comparison with the northeast Cerrado. (based upon: Felfili et al., 2007; Ribeiro and Walter, 2008; Medeiros et al., 2012; Medeiros and Walter, 2012; Lemos et al., 2013; Silva et al., 2016; Antar and Sano, 2019).....	102
Tableau IV.2: Radiocarbon dates of VGE-17 core. Calibrated ages (2σ) were obtained from Calib 8.0 (Stuiver and Reimer, 1993).....	104

RÉSUMÉ

Le biome Cerrado est le deuxième plus grand biome du Brésil, couvrant plus de 2 millions de km², soit près de 24 % du territoire brésilien. Il présente une grande variété de physionomies végétales, allant des prairies ouvertes aux formations boisées denses, qui sont le résultat de la relation étroite entre la végétation, les conditions édaphiques (disponibilité de l'eau et des nutriments dans le sol) et la fréquence des incendies. Environ 12 000 espèces végétales ont été décrites dans le Cerrado, dont près de 4 000 sont endémiques. En outre, il s'agit d'une source d'approvisionnement et d'un réservoir de ressources en eau pour le système fluvial brésilien. Néanmoins, même si le Cerrado revêt une grande importance en termes écologiques et économiques, seuls 7,5 % du biome sont protégés et plus de 50 % font l'objet d'une activité anthropique intense avec l'augmentation de l'agriculture, du pâturage et des incendies. Les prédictions montrent que ce biome aura perdu plus de 50% de sa diversité végétale d'ici 2080. Les études sur le passé peuvent nous permettre de mieux comprendre les changements en cours en les insérant dans un schéma évolutif où tour à tour le climat et l'homme sont intervenus. Nos travaux ont pour objectif de compléter nos connaissances sur les liens entre la végétation, les feux et le climat du Cerrado à partir de l'étude de deux nouveaux enregistrements sédimentaires situés dans la zone centrale et dans la zone nord-est du Cerrado.

Ainsi, l'**article 1** est consacré aux caractéristiques morphologiques et écologiques des grains de pollen (syndrome pollinique, taille des grains de pollen, strate de végétation) que nous avions identifiés lors des deux études précédentes et à leur relation avec les conditions environnementales lors de leur dépôt. L'**article 2** présente l'évolution du paysage au cours des 6 000 dernières années dans le centre du Cerrado (15°S), en complément d'une étude antérieure qui couvrait la période de 15 000 à 6 000 ans BP. Nous avons montré que le cerrado arboré s'est étendu depuis 5 000 ans BP en phase avec l'augmentation de l'insolation de l'hémisphère sud. Cette expansion a été interrompue par trois périodes sèches marquées par la baisse du niveau du lac et la régression de la forêt-galerie. Ces changements climatiques courts et abrupts reflètent des variations de l'expansion et de l'intensité de la mousson sud-américaine au cours de l'Holocène. Enfin, dans l'**article 3**, nous avons reconstruit l'évolution du paysage sur 15 000 ans dans le centre de la région nord du Cerrado (10°S) et nous avons montré comment un phénomène climatique de l'hémisphère nord avait modifié la composition de la forêt tropicale pendant un événement bref et intense entre 9 300 et 7 500 ans BP. Les deux chapitres s'accordent sur le fait que le climat est le principal moteur des changements de la végétation à l'échelle millénaire et séculaire. La composition floristique du Cerrado montre une adaptation au feu et nos résultats montrent qu'ils n'ont pas été très intenses au cours des derniers 15 000 ans sauf sur des événements courts qui semblent être causés par les activités anthropiques. La haute résolution de nos études nous a permis de définir le temps nécessaire à la récupération de la végétation en fonction des différentes contraintes.

Notre étude montre que la végétation du Cerrado est peu vulnérable aux perturbations climatiques depuis le fin du dernière période glaciaire ainsi qu'à l'augmentation de la fréquence des incendies principalement au cours des derniers 5 000 ans. Le Cerrado est un biome composé d'une multitude de physionomies distribuées en mosaïques dans le paysage, ce qui lui confère une grande capacité d'adaptation en lui permettant de répondre assez rapidement aux perturbations, en moins de 12 ans.

Mots-clefs: forêt tropicale, changement climatique, perurbation anthropique, Holocène, pollen, charbon, sédiment

ABSTRACT

The Cerrado biome is the second largest biome in Brazil, covering more than two million km², or almost 24% of Brazilian territory. It has a wide variety of plant physiognomies, ranging from open grasslands to dense woodland formations, which are the result of the close relationship between vegetation, edaphic conditions (availability of water and nutrients in the soil) and the frequency of fires. Around 12 000 plant species have been described in the Cerrado, nearly 4 000 of which are endemic. It is also a source and reservoir of water resources for the Brazilian river system. However, even though the Cerrado is of great importance in ecological and economic terms, only 7.5% of the biome is protected and over 50% is subject to intense human activity, with an increase in agriculture, grazing and fires. Predictions show that this biome will have lost more than 50% of its plant diversity by 2080. Studies of the past can give us a better understanding of the changes underway by placing them in an evolutionary framework in which climate and man have both played a part. The aim of our work is to add to our knowledge of the links between vegetation, fire and climate in the Cerrado by studying two new sedimentary records located in the central and north-eastern zones of the Cerrado.

Thus, **article 1** is devoted to the morphological and ecological characteristics of the pollen grains (pollen syndrome, pollen grain size, vegetation stratum) that we identified in the two previous studies and their relationship with the environmental conditions at the time of deposition. The **article 2** presents the evolution of the landscape over the last 6 000 years in the central Cerrado (15°S), complementing a previous study that covered the period from 15 000 to 6 000 years BP. We have shown that the cerrado woodlands have expanded over the past 5 000 years BP in phase with the increase in insolation in the southern hemisphere. This expansion was interrupted by three dry periods marked by a drop in lake level and the regression of gallery forest. These short and abrupt climatic changes reflect variations in the expansion and intensity of the South American monsoon during the HoloceneFinally, in **article 3** we reconstructed the evolution of the landscape over 15,000 years in the centre of the northern Cerrado region (10°S) and showed how a climatic phenomenon in the northern hemisphere modified the composition of the tropical forest during a brief and intense event between 9 300 to 7 500 years BP. Both chapters agree that climate is the main driver of vegetation change on millennial and centennial scales. The floristic composition of the Cerrado shows adaptation to fire, and our results show that fire has not been very intense over the last 15 000 years, except for short events that appear to have been caused by human activities. The high resolution of our studies has enabled us to define the time required for vegetation to recover as a function of the various constraints.

Our study shows that the vegetation of the Cerrado has shown little vulnerability to climatic disturbances since the end of the last ice age and to the increase in the frequency of fires, mainly

over the last 5 000 years. The Cerrado is a biome made up of a multitude of physiognomies distributed in mosaics across the landscape, which gives it a great capacity for adaptation, enabling it to respond fairly quickly to disturbances, in less than 12 years.

Keywords: tropical forest, climate change, human disturbance, Holocene, pollen, charcoal, sediment.

Partie I

Cadre général, matériel et méthodes

1 Contexte général du Cerrado

1.1 Les savanes tropicales et le Cerrado : origines

Les savanes tropicales constituent une partie importante du paysage à la surface de la terre avec environ 20 % de la surface mondiale, principalement distribuées en Afrique, en Australie et en Amérique du Sud (Pennington et al., 2014 ; Lehmann et al., 2014). Ces écosystèmes sont caractérisés par une strate continue d'herbacées C₄, des graminées tolérantes au feu et intolérantes à l'ombre, et une strate arborée plus ou moins discontinue (Ratnam et al., 2011 ; Parr et al., 2014). Ces caractéristiques sont obtenues en réponse à leur histoire évolutive qui indique une évolution liée aux variations du climat (changement de la température, de la quantité de CO₂) et l'émergence du feu en réponse à des environnements plus ouverts (Beerling et Osborne, 2006 ; Osborne et Sack, 2012). Bien que les savanes tropicales aient été un temps considérées comme d'origine anthropique, elles ont en réalité une origine plus ancienne et ces paysages auraient pu favoriser la bipédie dans l'évolution de l'homme (Parr et al., 2014).

L'apparition des savanes tropicales, il y a 25 millions d'années (Ma) a été favorisée par une réduction de la concentration CO₂ atmosphérique et de la disponibilité de l'eau qui aurait permis l'expansion des herbacées et l'émergence de plantes C₄, dans des environnements plus secs (déficit hydrique) et plus chauds (Edwards et al., 2010; Spriggs et al., 2014). L'augmentation des incendies semble avoir joué un rôle clé dans l'expansion rapide des savanes au cours de la transition du Miocène vers le Pliocène (Pennington et al., 2014; Lehmann et al., 2014; Lehmann et Hughes, 2014). En Amérique du Sud, l'adaptation au feu des arbres et des graminées est observée depuis environ 4 Ma (Simon et al., 2009) et une relation intrinsèque entre climat-incendie-végétation dans les savanes est indiscutable (Edwards et al., 2010; Pennington et al., 2014).

Bien que les savanes tropicales soient apparues à la même époque avec des adaptations évolutives similaires, elles présentent également des caractéristiques particulières qui les différencient d'un continent à l'autre. Pour revenir aux caractéristiques communes décrites ci-dessus, sur le plan physionomique, les savanes sont des écosystèmes végétaux dominés par les herbacées (principalement des graminées) contenant une proportion variable d'arbres (0-80 %), qui interagissent constamment dans le paysage en réponse aux facteurs climatiques, aux perturbations et aux caractéristiques biologiques propres des plantes (Pennington et al., 2014). Pour comprendre ces relations, Lehman et al. (2014) ont analysé la réponse de la surface terrestre des arbres à différents facteurs tels que la disponibilité en eau et les incendies sur les trois continents. Ils ont constaté une forte relation entre la distribution des précipitations et le régime des incendies sur les trois sites avec toutefois des différences sur les caractéristiques des sols (Lehmann et al., 2014). Si la température est également un facteur clé pour l'occurrence des incendies en Afrique et en Australie, il n'en est pas de même en Amérique du Sud où la nature et la fréquence des incendies peuvent varier en fonction de la répartition et de la structure de la végétation en réponse à des facteurs édaphiques (pH, nutriments) (Lira-Martins et al., 2022). Il est donc important de mieux comprendre dans quelle mesure les changements environnementaux permettent la fonctionnalité de ces écosystèmes (Lehmann et Parr, 2016).

Murphy et Bowman (2012) ont montré qu'il existait des états d'équilibre alternatifs limitant l'expansion de la forêt et qui sont maintenus par les variations de la composition floristique, les taux de croissance des arbres et la fréquence des incendies. La composition floristique varie d'une savane à l'autre (Furley, 1999 ; Lehmann et al., 2014) avec plus d'espèces semi-décidues en Afrique et en Australie qu'en Amérique du Sud (au Brésil) où ce sont les espèces d'arbres sempervirents qui dominent (Fank-de-Carvalho et al., 2015).

1.2 Importance du Cerrado

Le Cerrado est un biome qui occupe 2 millions km² sur le territoire brésilien, au sein duquel environ plus de 1000 à 1300 espèces d'arbres seulement, ont été repertoriées, soit environ 11% de la diversité végétale totale. Ce chiffre peut varier si l'on inclut les autres formes de croissance (arbuste et herbes) (Françoso et al., 2016).

A l'intérieur du Cerrado, il existe une grande variété d'écosystèmes et de climats surtout lorsque l'on compare les compositions floristiques du Cerrado de la région centrale avec celles des régions situées au contact des autres biomes (Vieira et al., 2019 ; Françoso et al., 2019 ; Couthino et al., 2021). Par conséquent, le Cerrado est divisé en régions, en groupes et en districts biogéographiques sur la base de sa composition floristique (Figure I.1) (Ratter et al., 2003, 2011; Bridgewater et al., 2004; Françoso et al., 2019). Toutefois, la zone de plus grande diversité du Cerrado est la région centrale alors que le Cerrado situé près des extrêmes climatiques (arides ou humides) présente une moindre diversité (Neves et al., 2022). Des conclusions analogues sont obtenues à partir de la diversité génétique des plantes (Neves et al., 2022).

Des reconstructions de la distribution du biome pendant les périodes glaciaires et interglaciaires ont montré que la région centrale du Cerrado est restée stable avec des refuges de végétation (Bueno et al., 2017). En essayant de caractériser la diversité des espèces, Françoso et al. (2019) observent que dans les régions les mieux conservées c'est à dire où l'on observe plus d'aires naturelles protégées, le Cerrado central et le Cerrado du nord-ouest présentent le plus grand nombre d'espèces caractéristiques (Figure I.1). D'autre part, outre la diversité végétale, plus l'habitat est hétérogène, plus la diversité des petits mammifères est élevée. Comme pour la végétation, la distance géographique et la distance entre les biomes voisins expliqueraient le taux de renouvellement des espèces dans les zones stables et écotones, par rapport aux autres biomes, comme cela a pu être observé chez les amphibiens (Alves-Ferreira et al., 2022 ; Carmignotto et al., 2022).

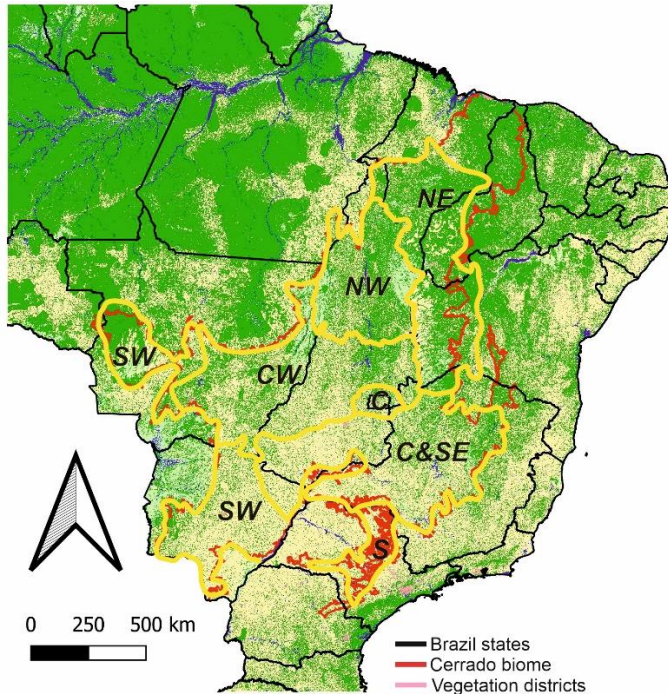


Figure I.1. Carte du Brésil représentant les 7 divisions du Cerrado (selon Françoso et al 2019) (ligne jaune), avec les Etats du Brésil (ligne noire) et la délimitation du Cerrado (ligne rouge). NE nord-est, NW nord-ouest, CW central-ouest, SW sud-ouest, C centre, C&SE centre-sud-est.

De plus, la région centrale du Cerrado est importante pour les ressources en eau du pays et contribue à 90 % du débit du fleuve São Francisco, à 50 % de celui du fleuve Paraná et à 70 % de celui du fleuve Tocantins, qui sont parmi les trois fleuves les plus importants pour l'économie brésilienne. Le Cerrado est donc aussi une région stratégique pour le secteur hydroélectrique, représentant 50 % de la production d'électricité au Brésil, en plus de son importance en tant que ressource en eau pour la consommation de la population et l'agriculture (Lima et al., 2011). Il s'agit de l'une des zones où la croissance démographique et l'utilisation des terres pour l'agriculture et l'élevage sont parmi les plus importantes.

1.3 Environnement climatique actuel

Dans le Cerrado, le climat est modulé principalement par la dynamique équatoriale (Zou et Lau, 1997) de la zone de convergence intertropicale (ZCIT), qui se déplace en fonction de la cyclicité annuelle de l'insolation (Garreaud et al., 2008). Les oscillations saisonnières de la ZCIT influencent le fonctionnement de la mousson sud-américaine (SAMS) notamment en modulant son intensité et son amplitude à l'intérieur du continent (Reboitia et al., 2016 ; Marengo et al., 2012).

Deux schémas de régime des précipitations sont observés au cours de l'année (Garreaud, 2009, Reboitia, 2010) : pendant l'été austral (DJF), la ZCIT se déplace vers sa position méridionale (5°S) (Figure I.2a) permettant ainsi l'incursion des alizés de l'est de l'océan Atlantique vers le continent. Leur trajet se trouve bloqué au niveau de la Cordillère des Andes (Insel et al., 2010) et l'augmentation de l'humidité et de l'activité convective sur le bassin amazonien génèrent un flux de vent de basse altitude connu comme « jet de basse altitude sud-américain (SALLJ) » dans une

direction NO-SE qui circule jusqu'à la latitude moyenne de 21°S vers le centre du Brésil (Garreaud, 2009). Dans le même temps, l'intensité de la mousson qui contrôle les précipitations dans le Cerrado augmente avec l'activité de la zone de convergence de l'Atlantique Sud (SACZ) (Sulca et al., 2016) (Figure I.2a). Pendant l'hiver austral (JJA), l'insolation dans l'hémisphère Sud diminue et la ZCIT est positionnée entre 10° et 5 °N. Ceci entraîne un changement dans le régime des précipitations (Garreaud, 2009). La mousson sud-américaine s'affaiblit, les précipitations diminuent dans la région centrale et dans le sud-est du Brésil et augmentent au nord du continent et dans la région nord-est du Brésil (Sulca et al., 2016). Au cours de cette période, des précipitations sporadiques sont enregistrées en réponse à l'incursion de fronts polaires (PF) et de masses d'air venant de l'Atlantique tropical (mTa) qui peuvent parfois atteindre la région centrale (Vera et al., 2006, Nascimento & Novais, 2020).

Dans le Cerrado, la variation de la température moyenne annuelle et le gradient de précipitation permettent de définir trois régions climatiques: le Nord où les températures moyennes annuelles sont plus élevées (28°C), le centre avec 24°C, et le Sud où les températures moyennes annuelles sont les plus basses (18°C) (Nascimento & Novais, 2020). En outre, bien que les précipitations moyennes annuelles soient de 1400 mm, un gradient ouest-est est observé dans le nord du Cerrado (état du Tocantins) où les précipitations se réduisent à 800 mm par an sur la région périphérique du Cerrado proche de la Caatinga (Figure I.2b) (Nascimento & Novais, 2020).

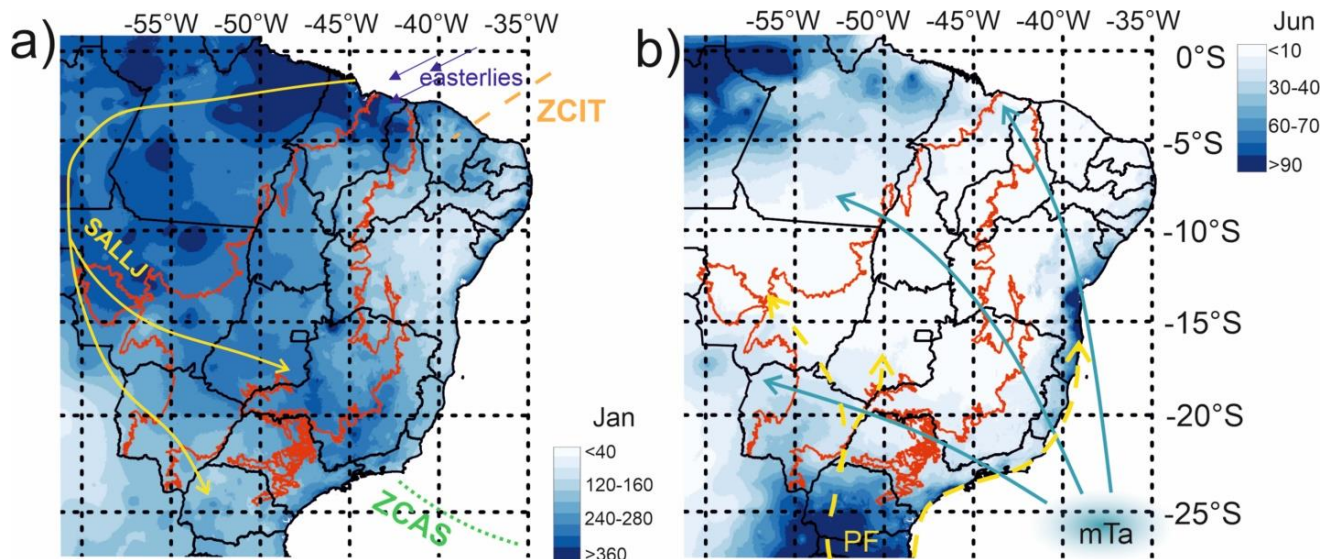


Figure I.2. Précipitations moyennes annuelles pour les mois de janvier (Jan) (a) et de juillet (Jun) (b) au Brésil avec les frontières entre les états (ligne noire) et le biome Cerrado (ligne rouge). En a) la ligne pointillée orange représente la zone influencée par la ZCIT, la ligne pointillée verte l'emplacement de la ZCAS, les flèches bleues montrent l'incursion des alizés de l'océan Atlantique Nord qui pénètrent sur le continent et la ligne jaune le flux des masses d'air de basse altitude (SALLJ). En b) la zone d'incursion des fronts polaires (ligne jaune pointillée) et des masses d'air atlantiques (flèche bleue) (d'après Fick and Hijnmans, 2017).

1.4 Le Cerrado : principales caractéristiques

1.4.1 Végétation

Le biome Cerrado est majoritairement distribué dans la région centrale du Brésil et représente le deuxième biome du pays, avec 32 % du territoire avec un gradient altitudinal variant entre 0 et 1500 mètres au-dessus du niveau de la mer et un gradient latitudinal compris entre 3°S et 24°S. A partir de sa diversité floristique, le Cerrado a été divisé en districts avec la définition de trois grands centres de diversité, au nord, au centre et au sud du biome (Vieira et al., 2020). Différentes phisionomies végétales ont également été définies à partir de la forme de croissance et des stratifications des arbres, des aspects environnementaux (comme les facteurs édaphiques) et de la composition floristique (Ribeiro et Walter, 2008). A l'intérieur du Cerrado, l'on distingue les formations forestières (avec des arbres formant une canopée plus ou moins continue), de savane (faciès avec des arbres et des arbustes dispersés et une strate herbacée, sans formation continue de la canopée) et savane ouverte (faciès avec une prédominance d'espèces herbacées et quelques arbustes) (Tableau I.1) (Figure I.3 a,b). À l'intérieur de chaque formation, une autre sub-division est définie à partir du degré de couverture des arbres et de la disponibilité en eau et en nutriments dans le sol (Ribeiro et Walter, 2008).

Les formations forestières du biome Cerrado

La **forêt ciliaire** est observée le long des cours d'eau de moins de 100 m de largeur. Elle est caractérisée par des arbres de 20 à 25 m de hauteur et est principalement composée d'espèces feuillues avec différents degrés de caducifoliés. La couverture de la canopée varie de 90 % pendant la saison humide à 50 % pendant la saison sèche (Ribeiro et Walter, 2008).

La **forêt-galerie** est sempervirente et forme des couloirs fermés le long et autour des cours d'eau. Elle est presque toujours accompagnée de formations non forestières, en transition abrupte avec la formation de savane boisée et/ou ouverte. Les arbres peuvent atteindre une hauteur de 20 à 30 m, et la canopée couvre 70 à 95 % du couvert forestier ce qui contribue au maintien d'une forte humidité où la saison sèche impactera peu la forêt. En fonction de la topographie et des variations de la nappe phréatique, elle est classée en forêt-galerie non inondée et inondée. Dans les forêts non inondées, la nappe phréatique reste proche de la surface et les sols sont majoritairement bien drainés. Dans les forêts inondées, la nappe phréatique est proche ou au-dessus de la surface du sol pendant la majeure partie de l'année, avec une topographie assez plate et un mauvais drainage (Figure I.3.b) (Ribeiro et Walter, 2008).

La **forêt sèche** est formée d'espèces d'arbres à feuilles sempervirentes, semi-décidues et décidues dans des sols mésotrophes fertiles. La hauteur moyenne varie entre 15 et 25 m. Pendant la saison des pluies, le couvert forestier est de 70 à 95 % et diminue pendant la saison sèche à 50-35 %, en réponse à la présence des arbres à feuilles caduques (Ribeiro et Walter, 2008).

Le **cerradão ou savane boisée** est considéré dans la limite du concept cerrado *sensu lato* et caractérise une forêt sclérophylle, avec une canopée continue variant de 50 à 90% entre la saison sèche et la saison humide. La hauteur moyenne des arbres varie entre 8 et 15 m. Bien qu'elle soit principalement à feuilles persistantes, elle partage des espèces avec le cerrado *sensu stricto*

(*Caryocar brasiliense*, *Kielmeyera coriacea*, *Qualea grandiflora*) et avec la forêt sèche (*Dilodendron bippinatum*, *Physocalimma scaberrimum*). Le sol du cerradão est profond et bien drainé, avec une fertilité moyenne à faible, des sols légèrement acides, parfois dystrophiques et parfois mésotrophiques (Ribeiro et Walter, 2008).

Les formations de savane

Le **cerrado sensu stricto** se caractérise par des arbres bas, penchés, tordus, à la ramification irrégulière et marqués par les incendies. Certaines espèces possèdent des xylopodes qui favorisent la repousse après les incendies. Pendant la saison des pluies, la couche herbacée et les buissons se développent rapidement. Les arbres ont une écorce épaisse, des feuilles rigides et coriaces ainsi que des racines profondes adaptées à la longue saison sèche. Les sols sont acides à faible teneur en nutriments et à forte teneur en aluminium. La strate arborée peut couvrir entre 20 et 50 % de surface de la canopée, avec des hauteurs variant de 3 à 8 m (Ribeiro et Walter, 2008).

Les **palmeraies et les veredas** se caractérisent par la dominance des arbres de la famille Arecaceae bien que ceux-ci ne soient pas très abondants et ont entre 8 et 15 mètres de hauteur. Les genres *Acrocomia* (macuaba), *Attalea* (babaçu) et *Syagrus* (gueroba) sont observés dans les zones interfluviales, sur des sols bien drainés. Dans les sols marécageux, c'est l'espèce *Mauritia flexuosa* (buriti) qui domine. Elle est aussi appelée **vereda** lorsqu'elle est accompagnée d'arbustes et d'herbacées avec Poaceae, Cyperaceae, Melastomataceae, Fabaceae et Eriocaulaceae parmi les familles les plus communes (Tableau I.1). La canopée formée par les palmiers peut recouvrir de 60 à 80 % de la surface. A l'intérieur de la **vereda**, différentes zones liées à la topographie du drainage sont distinguées : la bordure qui est formée d'un sol sec avec des arbres isolés, le centre avec un sol modérément humide, le bas-fond au sol saturé d'eau et marécageux avec les *Mauritia flexuosa* (Figure I.3b) (Ribeiro et Walter, 2008).

Les formations de savane ouverte

Le **campo sujo**, que l'on pourrait traduire par la prairie « sale » est constituée d'herbacées et d'arbustes sur des sols peu profonds et pauvres pouvant varier en fonction de la disponibilité en eau. Lorsque le couvert arboré est présent, il est inférieur à 5 % (Ribeiro et Walter, 2008).

Le **campo limpo**, la prairie « propre » en portugais, est principalement herbacée avec des variations dans le degré d'humidité. Dans les zones périodiquement inondées situées à proximité des rivières, le campo limpo est appelé *brejo* ou *campo de varzea*. Lorsque le couvert arboré est présent, il est inférieur à 5 % (Ribeiro et Walter, 2008).

Le **campo rochoso** ou prairie d'altitude, est dominé par les herbacées avec la présence occasionnelle d'arbustes pouvant atteindre 2 m de hauteur. Cette formation est observée sur les affleurements rocheux à des altitudes supérieures à 900 m pouvant être soumises au vent ainsi qu'à des variations extrêmes de température entre le jour et la nuit. La disponibilité en eau est limitée car les sols sont mal drainés et la pluie s'écoule directement vers les rivières. Cette formation est fortement dépendante des conditions du sol et de nombreuses espèces présentent des caractéristiques xéromorphes. Le genre *Vellozia* est un indicateur de ce type de physionomie. Lorsque le couvert arboré est présent, il est inférieur à 5 % (Ribeiro et Walter, 2008).

Tableau I.1. Les espèces les plus communément observées classées par physionomie dans les trois types de formation supérieure selon Walter & Ribeiro (2008).

Formation	Physionomie	Espèces végétales les plus communes
Forêt	forêt ciliaire	<i>Anadenanthera</i> spp., <i>Apeiba tibourbou</i> , <i>Aspidosperma</i> spp., <i>Casearia</i> spp., <i>Cecropia pachystachya</i> , <i>Celtis iguanaea</i> , <i>Enterolobium contortisiliquum</i> , <i>Inga</i> spp., <i>Lonchocarpus Cultratus</i> , <i>Sterculia striata</i> , <i>Tabebuia</i> spp., <i>Tapirira guianensis</i> , <i>Trema micrantha</i> , <i>Trichilia pallida</i> , <i>Tripalis gardneriana</i>
	forêt galerie	Non inondable : Apocynaceae (<i>Aspidosperma</i> spp.), Fabaceae (<i>Apauleia leiocarpa</i> , <i>Copaifera longsdorffii</i> , <i>Hymenea courbaril</i> , <i>Ormosia</i> spp., <i>Sclerobium</i> spp.), Lauraceae (<i>Nectandra</i> spp...), <i>Ocotea</i> spp., <i>Ocotea</i> spp.), Myrtaceae (<i>Gomidesia lindeniana</i> , <i>Myrcia</i> spp.) et Rubiaceae (<i>Alibertia</i> spp., <i>Amaioua</i> spp., <i>Ixora</i> spp., <i>Guettarda viburnoides</i> et <i>Psychotria</i> spp.). Inondable : Annonaceae (<i>Xylopa emarginata</i>), Burseraceae (<i>Protium</i> spp.), Clusiaceae (<i>Calophyllum brasiliense</i> , <i>Clusia</i> spp.), Euphorbiaceae (<i>Rickeria grandis</i>), Magnoliaceae (<i>Talauma ovata</i>) et Rubiaceae (<i>Ferdinandusa speciosa</i>) et un nombre important de Melastomataceae (<i>Miconia</i> spp. et <i>Tibouchina</i> spp.), Piperaceae (<i>Piper</i> spp.) et Rubiaceae (<i>Coccocypselum guianense</i> , <i>Palicourea</i> spp.), <i>Posoqueria latifolia</i> et <i>Psychotria</i> spp.). On trouve également des espèces de <i>Cedrela odorata</i> , <i>Croton urucurana</i> , <i>Dendropanax cuneatum</i> , <i>Euplassa inaequalis</i> , <i>Euterpe edulis</i> , <i>Hedyosmum brasiliense</i> , <i>Mauritia flexuosa</i> , <i>Guarea macrophylla</i> , <i>Prunus</i> spp.
	forêt sèche	<i>Acacia polyphylla</i> , <i>Amburana cearensis</i> , <i>Anadenanthera colubrina</i> , <i>A. peregrina</i> , <i>Apuleia leiocarpa</i> , <i>Aspidosperma subincanum</i> , <i>Cabralea canjerana</i> , <i>Cariniana estrellensis</i> , <i>Cass8ormosa88anea</i> , <i>Cedrela fissilis</i> , <i>Centrolobium tomentosum</i> , <i>Chloroleucon temniflorum</i> , <i>Dilodendron bippinatum</i> , <i>Guazuma ulmifolia</i> , <i>Jacaranda brasiliiana</i> , <i>J. caroba</i> , <i>Lithraea molleoides</i> , <i>Lonchocarpus montanus</i> , <i>L. sericeus</i> , <i>Machaerium villosum</i> , <i>Myracrodruon urundeuva</i> , <i>Physocalymma scaberrimum</i> , <i>Platycyamus regnellii</i> , <i>Tabebuia</i> spp., <i>Tapirira guianensis</i> , <i>Terminalia</i> spp., <i>Trichilia elegans antoxylum rhoifolium</i>
	Cerradão ou savane boisée	<i>Caryocar brasiliense</i> , <i>Copaifera langsdorffii</i> , <i>Emmotum nitens</i> , <i>Hirtella gladiolosa</i> , <i>Lafoensia pacari</i> , <i>Siphoneugena densiflora</i> , <i>Vochysia haenkeana</i> , <i>Xylopa aromatica</i> . mésotrophes : <i>Callisthene fasiculata</i> , <i>Dilodendron bippinatum</i> , <i>Guazuma ulmifolia</i> , <i>Helicteres brevispira</i> , <i>Luehea candidans</i> , <i>L. paniculata</i> , <i>Magonia pubescens</i> et <i>Platypodium elegans</i> . Les espèces fréquentes sont <i>Alibertia edulis</i> , <i>A. sessilis</i> , <i>Brosimum gaudichaudii</i> , <i>Bahuiña brevipes</i> , <i>Casearia sylvestris</i> , <i>Copaifera oblongifolia</i> , <i>Duguetia furfuracea</i> , <i>Miconia albicans</i> , <i>M. macrothyrsa</i> , <i>Rudgea virburnoides</i> et des espèces herbacées des genres <i>Aristida</i> , <i>Axonopus</i> , <i>Paspalum</i> et <i>Trachypogon</i> .
savane	fermé sensu stricto	<i>Acosmium dasycarpum</i> , <i>Anno ormosa</i> , <i>Aspidosperma tomentosum</i> , <i>Astronium fraxinifolium</i> , <i>Brosimum gaudichaudii</i> , <i>Bowdichia virginiooides</i> , <i>Byrsinima coccobilifolia</i> , <i>B. crassa</i> , <i>B. verbascifolia</i> , <i>Caryocar brasiliense</i> , <i>Casearia sylvestris</i> , <i>Connarus suberosus</i> , <i>Curatella americana</i> , <i>Davilla elliptica</i> , <i>Dimorphandra mollis</i> , <i>Diospyros hispida</i> , <i>Eriotheca gracilipes</i> , <i>Erythroxylum suberosum</i> , <i>Hancornia speciosa</i> , <i>Himatanthus obovatus</i> , <i>Hymenaea stigonocarpa</i> , <i>Kielmeye ormosa</i> , <i>Lafoensia pacari</i> , <i>Machaerium acutifolium</i> , <i>Ouratea hexasperma</i> , <i>Pouteria ramiflora</i> , <i>Plathymenia reticulata</i> , <i>Qualea grandiflora</i> , <i>Q. multiflora</i> , <i>Q. parviflora</i> , <i>Roupala montana</i> , <i>Salvertia convallariæodora</i> , <i>Sclerolobium aureum</i> , <i>Tabebuia aurea</i> , <i>T. ochracea</i> , <i>Tocoyea ormosa</i> , <i>Vatairea macrocarpa</i> et <i>Xylopia aromaticae</i> .
	Palmeraie vereda et	Poaceae, Cyperaceae, Asteraceae, Melastomataceae, Fabaceae, Eriocaulaceae, et les genres <i>Chamaecrista</i> , <i>Echinodorus</i> , <i>Habenaria</i> , <i>Hyptis</i> , <i>Ludwigia</i> , <i>Lycopodiella</i> , <i>Mimosa</i> , <i>Polygala</i> , <i>Utricularia</i> et <i>Xyris</i> . <i>Muritia flexuosa</i> , <i>Acrocomia</i> (macuaba), <i>Attalea</i> (babacu) et <i>Syagrus</i>
Savane ouvert	camp sujo	Poaceae, Cyperaceae, Leguminosae (<i>Andira</i> , <i>Mimosa</i>), Lamiaceae (<i>Hyptis</i>), Myrtaceae et Rubiaceae. Après un incendie sont observées sont <i>Altroemeria</i> spp., <i>Gomphrena officinalis</i> , <i>Griffinia</i> spp., <i>Hippeastrum</i> spp et <i>Paepalanthus</i> spp. ainsi que <i>Crumenaria</i> , <i>Cuphea</i> , <i>Deianira</i> , <i>Diplusodon</i> , <i>Eryngium</i> , <i>Habenaria</i> , <i>Lippia</i> , <i>Polygala</i> , <i>Piqueta</i> , <i>Syagrus</i> et <i>Xyris</i> .
	campo limpo	Burmanniaceae (<i>Burmannia</i>), Cyperaceae (<i>Rhynchospora</i>), Droseraceae (<i>Drosera</i>), Iridaceae (<i>Cipura</i> , <i>Sysinchium</i>), Lentibulariaceae (<i>Utricularia</i>), Lythraceae (<i>Cuphea</i>), Orchidaceae (<i>Cleistes</i> , <i>Habenaria</i> , <i>Sarcoglottis</i>), Poaceae (<i>Aristida</i> , <i>Axonopus</i> , <i>Mesosetum</i> , <i>Panicum</i> , <i>Paspalum</i> , <i>Trachypogon</i>) et Polygalaceae (<i>Polygala</i>), ainsi que plusieurs Asteraceae, Eriocaulaceae et Xyridaceae.
	campo rochoso ou prairie d'altitude	Asteraceae (<i>Baccharis</i> , <i>Calea</i> , <i>Lychnophora</i> , <i>Wunderlichia</i> , <i>Vernonia</i>), Bromeliaceae (<i>Dyckia</i> , <i>Tillandsia</i>), Cactaceae (<i>Melocactus</i> , <i>Pilosocereus</i>), Cyperaceae (<i>Bulbostylis</i> , <i>Rhynchospora</i>), Eriocaulaceae (<i>Eriocaulon</i> , <i>Leiothrix</i> , <i>Paepalanthus</i> , <i>Syngonanthus</i>), Gentianaceae (<i>Curtia</i> , <i>Irlbachia</i>), Iridaceae (<i>Sisyrinchium</i> , <i>Trimezia</i>), Lamiaceae (<i>Eriope</i> , <i>Hyptis</i>), Leguminosae (<i>Calliandra</i> , <i>Chamaecrista</i> , <i>Galactia</i> , <i>Mimosa</i>), Lentibulariaceae (<i>Genlisea</i> , <i>Utricularia</i>), Lythraceae (<i>Cuphea</i> , <i>Diplusodon</i>), Melastomataceae (<i>Cambessedesia</i> , <i>Miconia</i> , <i>Microlicia</i>), Myrtaceae (<i>Myrcia</i>), Orchidaceae (<i>Cleistes</i> , <i>Cyrtopodium</i> , <i>Epidendrum</i> , <i>Habenaria</i> , <i>Koellensteinia</i> , <i>Pelezia</i>), Poaceae (<i>Aristida</i> , <i>Axonopus</i> , <i>Panicum</i> , <i>Mesosetum</i> , <i>Paspalum</i> , <i>Trachypogon</i>), Rubiaceae (<i>Chiococca</i> , <i>Declieuxia</i>), Velloziaceae (<i>Barbacenia</i> , <i>Vellozia</i>), Vochysiaceae (<i>Qualea</i>) et Xyridaceae (<i>Xyris</i>).

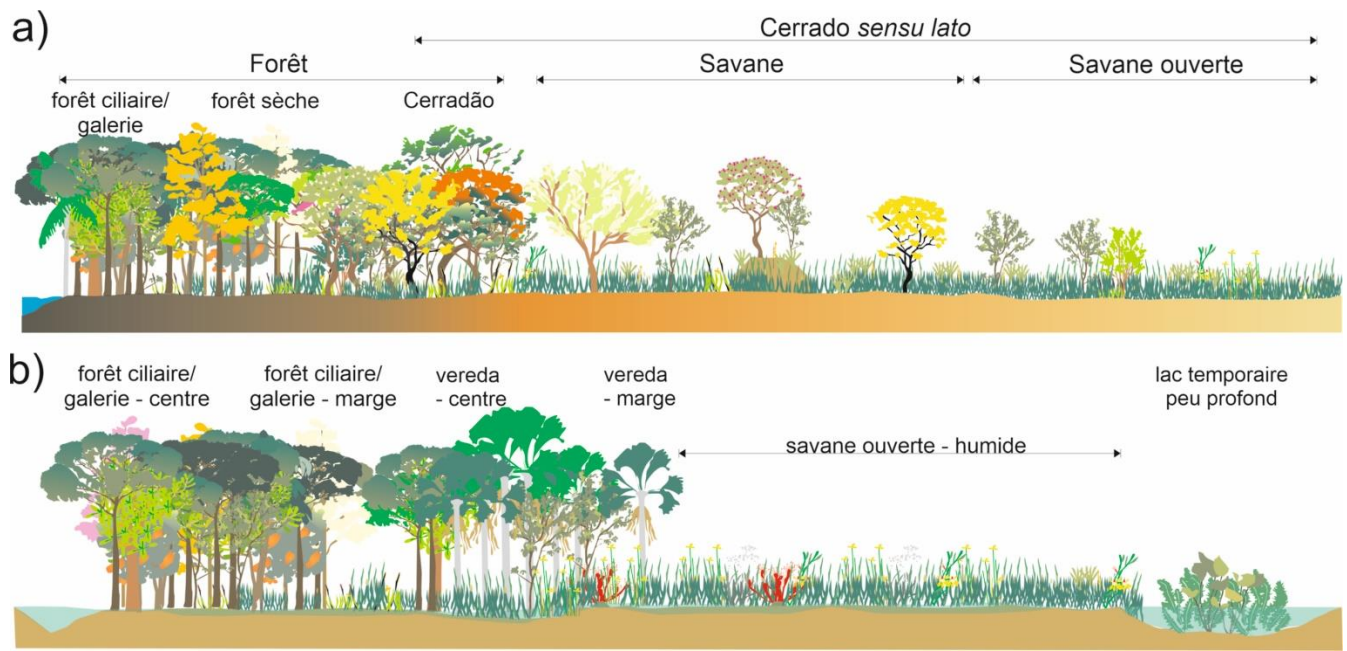


Figure I.3. Les phytophysiognomies du biome Cerrado en fonction a) des sols bien drainés et b) des sols inondés en permanence ou de façon saisonnière, avec les trois formations, forêt, savane et prairie (d'après Cassino et al., 2021).

1.4.2 Facteurs environnementaux

La relation climat végétation

Furley (2006) et Murphy & Bowman (2012) suggèrent que le climat, principalement les précipitations moyennes annuelles et leur distribution saisonnière, serait le principal facteur de répartition de la végétation dans le Cerrado. D'autres facteurs locaux, tels que les caractéristiques du sol et le feu sont également mis en avant. Bueno et al. (2018) ont proposé un gradient dynamique entre le climat (disponibilité en eau), le sol (nutriments et fertilité du sol) et le feu (inflammabilité accrue) permettant de caractériser les différentes physionomies du Cerrado.

Le climat

La large distribution des physionomies du Cerrado répond à plusieurs types de gradient, le gradient de précipitation, les gradients latitudinaux et altitudinaux, ainsi qu'aux caractéristiques édaphiques (Françoso et al., 2019). Des précipitations moyennes annuelles supérieures à 1400 mm sont observées dans le nord-ouest du cerrado, plus proche de l'Amazonie, tandis qu'au sud, les précipitations moyennes annuelles sont inférieures à 1400 mm (Sano et al., 2019). Françoso et al. (2019) suggèrent l'apparition de gelées jusqu'à la latitude de 20°S (basses températures) dans le sud avec une température moyenne annuelle de 18 °C tandis que dans le nord la moyenne est autour de 24°C. L'augmentation de la sécheresse est observée d'Ouest en Est, avec moins de précipitation dans le nord-est (à proximité du biome Caatinga).

Un autre facteur important est la saisonnalité qui modifie la teneur en eau du sol et réduit à environ 50% la couverture arborée pendant la saison sèche (Ribeiro et Walter, 2008). Une saisonnalité prolongée peut entraîner une mortalité accrue des espèces conditionnées à des caractéristiques particulières dans le Cerrado (Furley, 2006; Bueno et al., 2017). Les précipitations sont ainsi le facteur principal du contrôle de la répartition des forêts et des savanes dans le Cerrado. En fait, il a été démontré qu'une augmentation des précipitations moyennes annuelles au-dessus de 1500 mm favoriserait l'expansion des formations forestières tandis que des précipitations inférieures à 1500 mm favoriserait l'expansion des formations de savane plus ouvertes (Furley, 2006).

Le sol

La végétation typique du Cerrado se développe généralement sur des sols acides, dystrophiques et riches en aluminium (Mendoça et al., 2008) (Fig. I.4). Parmi les autres nutriments, les sols riches en matière organique et en azote (mésotrophes) facilitent l'expansion des formations forestières. En revanche, les sols pauvres en nutriments (dystrophiques) tendent à favoriser les formations plus ouvertes. Dans les sols pauvres, les plantes développent des systèmes adaptés comme, par exemple des racines épaisses et très profondes (jusqu'à 20 m de profondeur) ou bien des stratégies végétales de type C₄ (Furley, 1999 ; Lehmann et al., 2014). Les plantes C₄ sont des plantes adaptées à une faible humidité et à des températures chaudes grâce à un contrôle stomatique qui réduit l'évapotranspiration et augmente la capacité de stocker efficacement le carbone (Osborne et Sack, 2012). La fertilité du sol contribue à l'augmentation de la couverture arborée en diminuant la lumière et la température, réduisant ainsi les herbacées et par conséquent l'inflammabilité, tout en augmentant l'humidité *in situ* (Furley, 2006). Dans les transitions écotonales entre la forêt sèche et la savane boisée ou cerradão, la transition d'une physionomie à l'autre se traduit par un changement de la fertilité du sol, avec des sols plus fertiles et des quantités plus élevées de nutriments dans la forêt sèche (Martins et al., 2018). Dans les physionomies ouvertes du Cerrado, par exemple dans les *campo limpo*, les graminées développent des racines superficielles ne permettant pas l'accumulation de nutriments, entraînant un cycle ouvert dans le flux de nutriments dans le sol. En relation avec les caractéristiques du sol, la topographie doit également être prise en compte, par exemple sur les plus hautes altitudes où l'eau est moins abondante que dans les basse altitudes (plaines) (Coutinho et al., 2021).

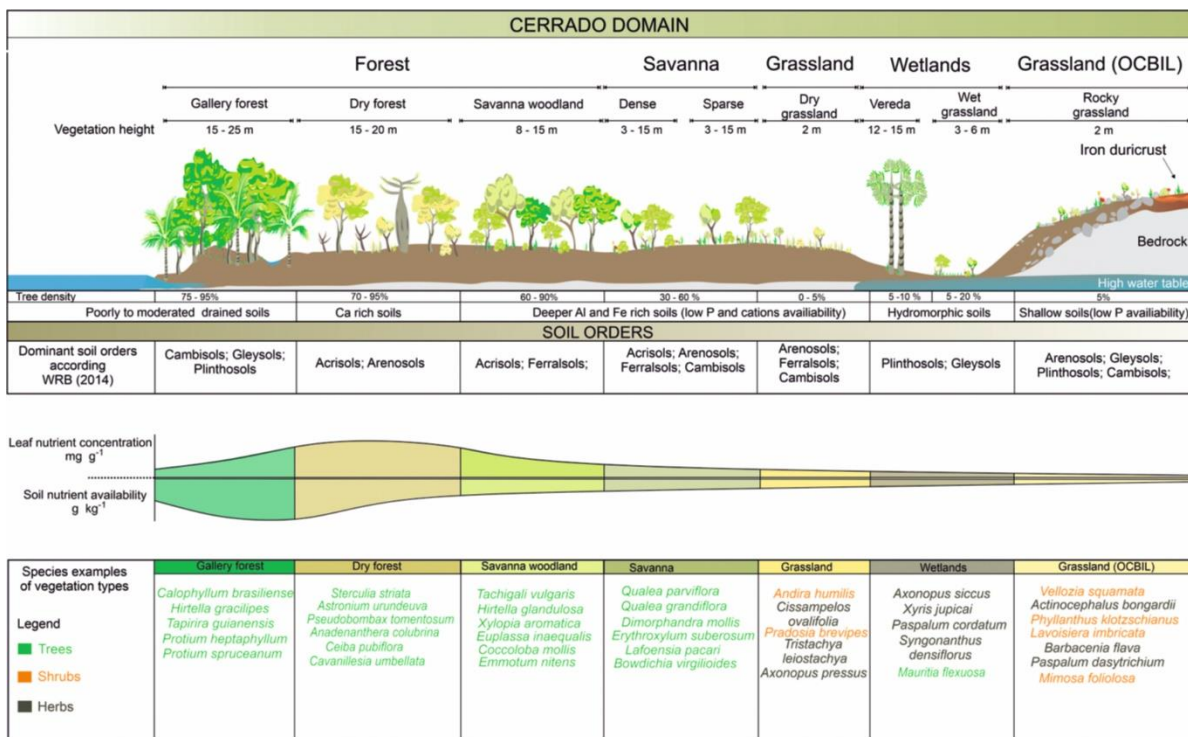


Figure I.4. Les types de sol du Cerrado et leurs phytophysionomies correspondantes (d'après Lira-Martins et al., 2022).

Le feu

Le biome Cerrado est caractérisé comme étant un écosystème sujet aux incendies (Furley, 1999), avec 8 % du Cerrado brûlé chaque année, ce qui représente 17 Mha (Klink et al., 2020). Entre 2000 et 2010 les foyers d'incendie sont passés de ~10 000 à ~160 000 par an (Pivello et al., 2011).

La fréquence des incendies favorise l'expansion des graminées et des autres herbacées alors qu'en leur absence, une expansion de la végétation arborescente est possible (Mistry, 1998 ; Murphy & Bowman, 2012).

Hoffman et al. (2009) ont montré plus précisément qu'il existe un taux de mortalité différencié après le feu entre les arbres du Cerrado et les autres types de forêt. La mortalité aérienne serait plus fréquente chez les arbres de la forêt humide que chez ceux du Cerrado (Hoffman et al., 2009). L'augmentation de l'humidité associée à la réduction ou à l'absence de feu favorise l'expansion des formations forestières dans le Cerrado (Hoffman et al., 2009). Hirota et al. (2011) ont testé cette affirmation dans une étude mettant en relation les précipitations, les couverts arboré et herbacé et les incendies et ont montré que l'expansion des formations forestières est favorisée grâce à une humidité accrue (précipitations plus élevées) qui réduit la fréquence des incendies. Inversement, en période sèche, l'augmentation des incendies favorise l'expansion des herbes et des graminées inflammables et réduit l'étendue des forêts (Hirota et al., 2011). Le feu est donc un facteur important de modification du paysage (Murphy & Bowman, 2012).

La fréquence et l'intensité des incendies dépendent de la disponibilité en matériel combustible, de la nature de la biomasse, de la température et de la durée de la saison des pluies. Lorsque le feu est moins fort, il endommage moins la structure du sol (feu de surface) tout en maintenant la

structure de la végétation. Par exemple, avec une fréquence de feu de 3 ans dans les zones naturelles de formations de savane (Furley, 1999 ; Pereira Júnior et al., 2014), l'augmentation des formations forestières pourrait conduire à une diminution de la fréquence des feux pouvant aller jusqu'à 7 ans (Pereira Júnior et al., 2014) (Fig. I.5). Dans le Cerrado, la saison la plus fréquente des incendies est la saison sèche. Les feux sont aussi plus intenses entre août et septembre lorsque la biomasse inflammable (graminées, herbes, branches) se dessèche, que l'humidité relative atteint 20 % et que les journées sont plus chaudes (20-25 °C) (Mistry, 1998 ; Oliveira et al, 2021). Lorsque les incendies se produisent au début de la saison sèche ou lors de la transition de la saison humide vers la saison sèche, ils sont de plus courte durée, moins étendus, de plus faible intensité et n'agissent pas au-delà de 3 cm de profondeur (Feidler et al., 2006). Si le sol est humide, le feu est plus court en durée et moins profond (1 cm) (Dargien & Fidelis, 2021),

Le feu est naturel dans le Cerrado et peut contribuer à son maintien lorsque le régime de feu reste modéré en fréquence et en intensité (Klink et al., 2020). Le feu affecte également la composition du sol en augmentant l'énergie absorbée par le sol dans la végétation ouverte (Mistry, 1998) mais il peut également avoir l'effet inverse en enrichissant le sol et en diminuant la quantité d'aluminium (Mistry, 1998). Le rôle du feu présente donc des effets variables sur les écosystèmes (Giorgis et al., 2021). En effet, bien que la végétation du Cerrado soit adaptée au feu, une variation dans l'augmentation de la fréquence et/ou de l'intensité pourrait être délétère pour les plantes (Fidelis & Zirondi, 2021). Par exemple, il a été observé que les graines de graminées réagissent aux chocs thermiques provoqués par le feu, avec un seuil inférieur (100 °C) et supérieur (200°C) pouvant entraîner soit leur germination soit la mortalité des graines (Zupo et al, 2020).

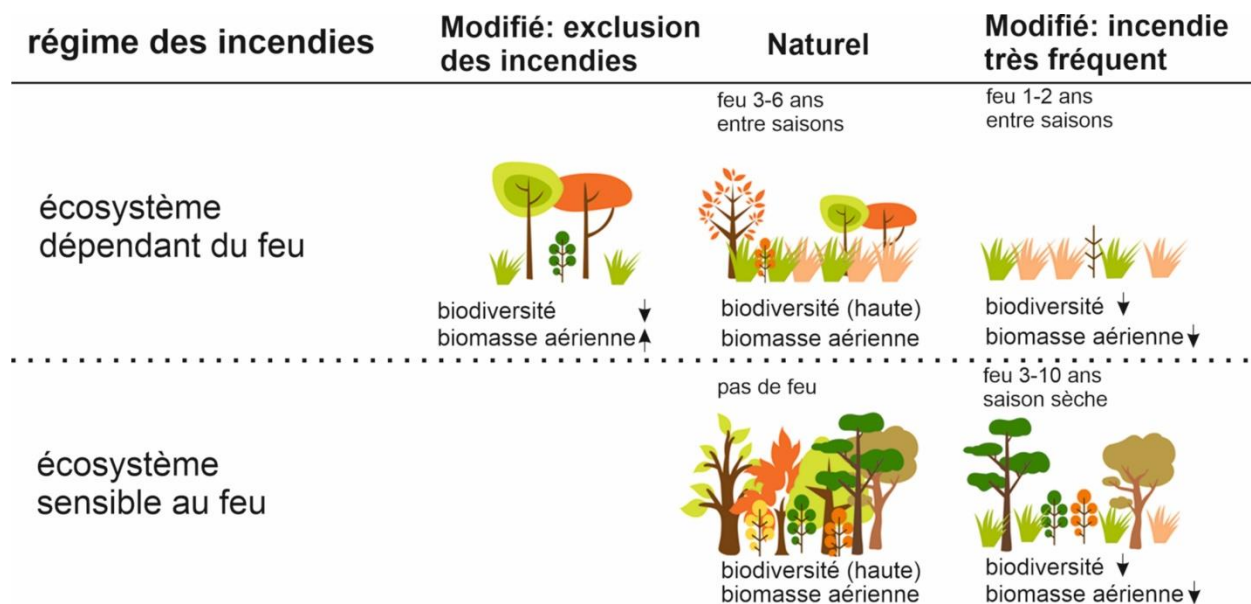


Figure I.5. Représentation graphique montrant les différents régimes de feu observés dans les savanes et les forêts (d'après Pivello et al., 2021)

Les autres facteurs

Parmi les facteurs les plus courants, le CO₂ est à l'origine de la présence de plantes de type C₄. Une augmentation de la teneur en CO₂ peut contribuer à augmenter le nombre et la taille des arbres (plantes de type C₃), en permettant une récupération plus rapide après un incendie.

La composition floristique du Cerrado est influencée par les espèces des biomes voisins qui peuvent se retrouver sur sa périphérie (Furley, 1999 ; Vieira et al., 2022). Aussi, la géologie et géomorphologie de la région permettent de définir d'autres caractéristiques (Lira-Martins et al., 2021)

L'activité humaine : Les études paléoécologiques montrent une augmentation importante des incendies entre 4000 et 5000 ans avant le présent (Rodrigues et al., 2021). Aujourd'hui, les populations indigènes l'utilisent traditionnellement pour diverses activités quotidiennes comme par exemple les Krahô. Sa gestion est pensée dans la protection et l'entretien de l'écosystème afin de maintenir la mosaïque de la végétation et la disponibilité des ressources ainsi que pour l'agriculture. Les Amérindiens considèrent qu'il est bénéfique de brûler certaines zones dans le Cerrado tous les 2 à 3 ans (Mistry et al., 2005). La région du Cerrado est une zone idéale pour l'agriculture intensive de la canne à sucre, de l'eucalyptus, du soja, du coton et du maïs en augmentant ainsi la perte de végétation native du Cerrado (Schmidt et Eloy, 2020). Entre 2002 et 2011, le taux de déforestation est de 1 % par an, soit 2,5 de plus qu'en Amazonie. De plus, lorsque l'humidité est réduite, l'augmentation des incendies à la fin de la saison sèche, qu'ils soient d'origine naturelle ou anthropique, se transforme en méga-incendies qui se propagent sur plus de 50 000 ha (Fidelis et al., 2018). Selon les projections, les perturbations humaines d'ici à 2050 provoqueraient la disparition d'au moins 480 espèces de plantes endémiques alors que la culture du soja et de la canne à sucre devrait atteindre respectivement 13,4 et 1,9 Mha (Strassburg et al., 2017).

L'**herbivorie** limiterait la quantité de biomasse inflammable/non inflammable et favoriserait l'augmentation ou la réduction de la fréquence des incendies. Toutefois une augmentation de la surface des pâturages (déforestation) peut entraîner un appauvrissement accéléré des surfaces cultivées (Furley, 2006 ; Murphy & Bowman, 2012 ; Strassburg et al., 2017). Cependant, Durigan et al. (2022a) suggèrent qu'une bonne gestion du pâturage, lorsque la densité du bétail est faible, serait positive pour le maintien des écosystèmes du Cerrado dans les zones déjà perturbées, en réduisant l'invasion d'espèces exotiques et de biomasse inflammable (Durigan et al., 2022a).

Les **organismes du sol**, tels que les termites qui forment des termitières avec une aération et des quantités de carbone suffisantes favorisent le développement d'une végétation arborescente. En outre, la présence d'organismes qui fixent l'azote ou le phosphore sont aussi importants. Par exemple, les associations fongiques mycorhiziennes avec les légumineuses favorisent la fixation du phosphore (P) dans les plantes présentes dans les sols pauvres en nutriments du Cerrado (Furley, 2006).

1.5 Problèmes actuels dans le Cerrado

Depuis la fin du siècle dernier le Cerrado connaît une grande perte de ses zones naturelles avec ~50% de la végétation naturelle transformée à des fins commerciales (agriculture, élevage de

bovins, déforestation). Aujourd’hui seuls 20% de la surface du Cerrado serait naturelle avec seulement 8% de la superficie qui serait protégée (Françoso et al., 2015), loin des 17% proposés par la Convention sur la diversité biologique (Françoso et al., 2019).

Pour comprendre comment le Cerrado a changé au cours de ces dernières années afin d’évaluer son futur, une étude menée par Souza et al. (2020) a montré qu’entre 1985 et 2017, 71 millions d’hectares utilisés pour le pâturage (46%) et l’agriculture (172%) ont été perdus sur la végétation native du territoire Brésilien. Cependant, c’est aussi le biome brésilien qui a eu la plus grande récupération de végétation avec 25,8 % avec la création d’aires de conservation. Cela indique une capacité de récupération légèrement supérieure à celle de l’Amazonie où seulement 21 % de la végétation est récupérée (Souza et al., 2020). D’autres facteurs ont été explorés comme le changement climatique. Une étude menée par Hoffman et al. (2020) sur l’augmentation des températures et la réduction de l’humidité, entre 1961 et 2019 montre une augmentation de la température de 2,2 à 4 °C pendant la journée et de 2,4 à 2,8 °C pendant la nuit, avec une diminution de 15 % de l’humidité relative. Les auteurs soulignent que ce changement, bien que minime, pourrait éventuellement être contre-productif pour la flore et la faune du Cerrado pendant la saison sèche, de sorte que des paramètres tels que la température et l’humidité devraient être étudiés et pris en compte pour les projections futures (Hoffman et al., 2009). En outre, la modélisation de la survie des amphibiens montre que les végétations d’altitude (*campos rochosos*) sont aussi importantes pour le maintien des espèces que les zones de transition entre les différents écotones. Avec une perte de 50 % de la végétation naturelle d’ici 2050, on peut s’attendre à ce que les anoures perdent leur niche écologique (Alves-Ferreira et al., 2022). Aujourd’hui, la perte de la végétation naturelle est de 0,6 % par an, soit 1700 hectares (Françoso et al., 2019).

De plus, le processus de transformation du Cerrado affecte la dynamique du système dont l’un des éléments les plus courants, le feu, est utilisé de manière inappropriée. Schmidt & Eloy (2020) montrent qu’au cours des 50 dernières années, la fréquence et l’intensité des incendies ont changé, avec une augmentation de l’intensité des incendies se produisant plus fréquemment (2-3 ans) et affectant également la végétation sensible au feu en réponse à la modification du paysage. Le feu est couramment utilisé pour l’expansion des monocultures et il existe peu de plans de gestion des incendies dans les zones naturelles. La diminution des espèces de la végétation d’origine associée à une politique de zéro feu entraînent une modification de la fréquence et de l’intensité des incendies en raison de l’augmentation de la biomasse inflammable et de la multiplication des zones d’ignition (Schmidt & Eloy, 2022). En fait, l’augmentation de la température et de la durée de l’incendie affecterait la résilience des plantes et pourrait éliminer la couverture végétale lorsque le feu pénètre dans des couches plus profondes du sol (Rodrigues et al., 2021).

Au Brésil, les forêts tropicales humides (forêt amazonienne et forêt atlantique) font l’objet d’une plus grande attention de la part des scientifiques et des politiques publiques. En effet 80 % des forêts humides sont protégées (Fig. I.6), alors que l’utilisation des terres pour l’agriculture et l’élevage est accentuée dans le Cerrado (Pennington et al., 2014). Une étude menée dans le parc naturel d’Emas montre que la majorité des incendies naturels (91 %), causés par la foudre sur 45 événements enregistrés entre 1995 et 1999, se produisent pendant la saison des pluies ou pendant la transition vers la saison sèche, et sont de plus courte durée que les incendies anthropiques qui

se produisent généralement pendant la saison sèche, et qui sont plus étendus (Pivello et al. 2011, 2021).

Selon le code forestier brésilien, seulement 20 % des terres privées doivent être préservées dans le Cerrado, ce qui fait que 40 % de la végétation naturelle est menacée de conversion légale (Strassburg et al., 2017). Un processus de réduction, de déclassification et de reclassification des zones protégées est actuellement en cours au Brésil (Françoso et al., 2019). Bien que des progrès aient été réalisés grâce à des programmes tels que l'intégration de la gestion des incendies dans les zones protégées, les coupes budgétaires ont réduit les possibilités d'une gestion adéquate des incendies dans le Cerrado nécessaire pour le maintien de la biodiversité (Schmidt & Eloy, 2020). Ainsi, la nécessité de démontrer l'importance du Cerrado et de sa conservation devrait être priorisée conjointement à l'intégration des études scientifiques dans les programmes de gestion et les politiques publiques (Françoso et al., 2019 ; Schmidt & Eloy, 2020), D'ici à 2050, en raison de l'augmentation de l'expansion démographique, le Cerrado devrait perdre 31 à 34 % de végétation native actuelle (Strassburg et al., 2017). Dans un scénario de pression constante et d'efforts de conservation limités, un processus de « savanisation » (modification sévère du paysage par l'activité humaine) pourrait accroître le déficit hydrique dans la région (Furley, 2006).

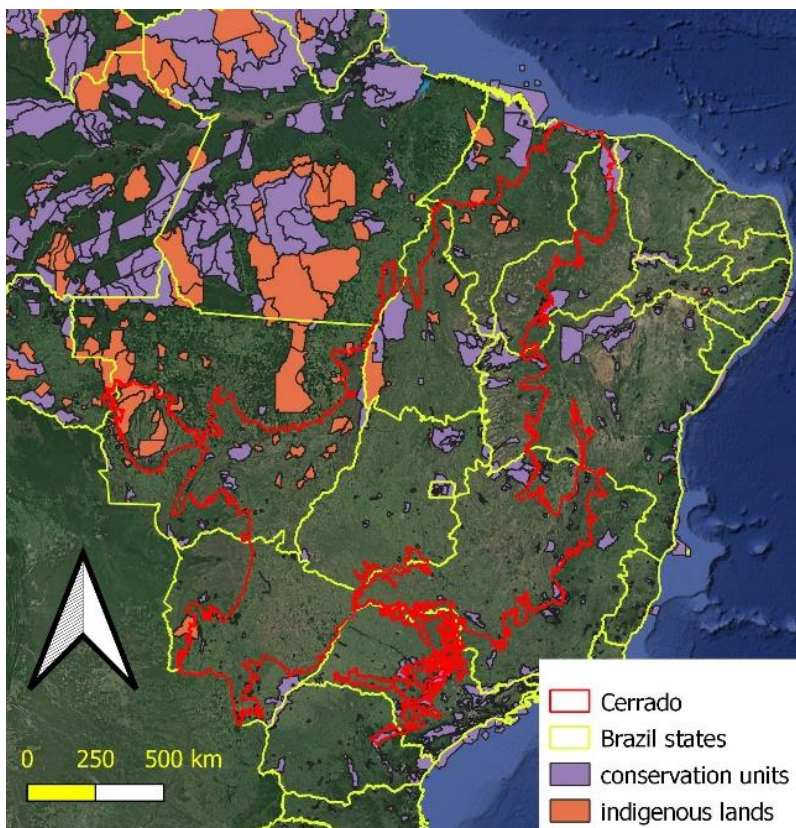


Figure I.6. Carte du Brésil montrant la répartition des zones protégées (principalement en Amazonie et dans la région nord-est du Cerrado) et des territoires indigènes au Brésil (peu nombreux dans le nord-est du Cerrado) (MAPBIOMAS, 2023)

2 Etat de l'art – paléoenvironnement dans le Cerrado

2.1 Études palynologiques

Le *Pléistocène* – avant 32 à 11,6 kyr BP

Les données paléoécologiques du Cerrado central suggèrent qu'à la fin du Pléistocène la physionomie de la végétation est dominée par une savane ouverte, principalement composée de graminées. Au nord-ouest (NO) et au sud-est (SE) avec respectivement les enregistrements des lacs Caço, de Salitre et de Rio Preto (Figure I.6 a), montrent l'augmentation des arbres de la savane et la forêt de galerie était formée d'espèces froides (*Araucaria*, *Drymis*, *Hedyosmum*, *Ilex*, *Myrsine*, *Podocarpus*) (Ledru, 1993; Ledru et al., 2006 ; Costa et al., 2022). Climatiquement ces enregistrements suggèrent qu'un changement de la vegetation s'est produit en réponse à la fin de la période glaciaire (Figure I.6 b). Ils mettent en évidence un gradient d'humidité qui est préservé dans le NO et le SE du biome et une tendance à la sécheresse dans la région centrale (Ferraz-Vincentini & Salgado-Labouriau, 1996; Horák-Terra et al. 2020). Cette tendance n'est pas observée dans l'enregistrement du Lac Feia (15°S) où l'expansion des arbres vers la fin de la période glaciaire est associée à une plus grande humidité (Cassino et al., 2020). De manière générale, à la fin du Pléistocène, l'expansion d'une savane est associée à l'augmentation progressive des températures et de l'humidité avec la migration des arbres du nord-ouest vers le centre et le sud du Cerrado.

Holocène – de 11,6 kyr BP au présent

Les enregistrements palynologiques montrent des réponses de la végétation variées au cours de l'Holocène. L'établissement de savanes arborées (*Astronium*, *Byrsonima*, *Caryocar*, *Casearia*) et de forêts sèches (*Schefflera*, *Myrtaceae*, *Piper*, *Eryngium*) est enregistré du début de l'Holocène jusqu'à l'Holocène moyen (Figure I.7 a) (Ledru, 1993 ; Belhing, 2002). Au cours de cette première phase, on observe également un changement dans la composition de la forêt-galerie, où les taxons froids sont remplacés par des taxons plus chauds (*Alchornea*, Melastomataceae-Combretaceae, Moraceae-Urticaceae et Myrtaceae) dans la région NO (Ledru et al., 2006; Belhing, 2002 ; Cassino et al., 2020) et dans quelques sites de la région SE (Ledru, 1993 ; Horák-Terra et al., 2015). Dans la région centrale, une savane ouverte reste dominante (Ferraz-Vincentini & Salgado-Labouriau, 1996 ; Lorente et al., 2010; Cassino et al., 2018 ; Costa et al., 2022).

Ensuite, à partir de la fin de l'Holocène moyen et pendant l'Holocène récent, un changement majeur s'est produit avec l'expansion d'une savane arborée, probablement due à la présence de conditions environnementales humides dans l'extrême NO (Belhing, 2002; Ledru et al., 2006) et le SE (Ledru et al., 1993; Parizzi et al., 1998), et d'une savane ouverte en réponse à une diminution de l'humidité vers la région centrale (Cassino et Meyer, 2013; Cassino et al., 2018; Horák-Terra et al., 2020; Lima-Sabino et al., 2021). Notons que cette tendance n'est pas observée à Aguas Emendadas où la persistance d'un environnement plus humide est observée, peut être à cause de conditions plus locales (Figure I.7 a,b) (Barberi et al., 2000).

De manière générale, un gradient d'une physionomie plus arborée vers une physionomie plus ouverte est attesté dans les enregistrements palynologiques en fonction de la latitude et de l'altitude.

Entre les époques glaciaire et interglaciaire et au cours de chaque époque, les enregistrements plaéoécologiques montrent une tendance à la présence d'une végétation ouverte avec des taxons frois dans les sites d'altitude supérieure à 900 m, où un changement de température ne semble pas avoir provoqué de changements majeurs dans la physionomie et des changements plus importants dans la composition floristique aux altitudes plus basses (Figure I.7 a,b).

Néamoins, la résolution d'analyse diffère entre les études palynologiques ainsi que le processus de sédimentation avec la présence de hiatus qui interrompent dans les enregistrements sédimentaires. Les enregistrements continus sont rares et la résolution est supérieure ou égale à 200 ans pendant le Pléistocène et le début de l'Holocène precoce, et inférieure ou égale à 200 ans pendant l'Holocène moyen. Pour l'Holocène récent, la plupart des études se situent dans le sud-est du Cerrado. Nous manquons donc d'information pour comprendre la réponse de la végétation aux conditions environnementales entre les époques glaciaires et interglaciaires dans les autres régions du Cerrado.

2.2 Études sur les charbons

La reconstitution des incendies passés est basée sur l'analyse des particules de charbon déposées dans les sédiments. Dans le Cerrado, seules cinq études montrent la relation entre la végétation et le feu, dont deux sont basées sur l'analyse des microcharbons c'est-à-dire les particules de charbon observées sur les lames microscopiques. Les résultats montrent une concentration de particules de l'ordre de $17\ 000 \times 10^3$ à $2\ 000 \times 10^3$ particules/cm³. Elles sont interprétées comme des incendies fréquents associés à des mosaïques de forêt (Cerrado et forêts galerie) et de prairie (Poaceae). Ces incendies ont été enregistrés vers 32 000 ans BP à Crominia, et entre 25 700 et 21 450 ans BP à Aguas Emendadas (Ferraz-Vincentini & Salgado-Labouriau, 1996 ; Barberi et al., 2000) (Figure I.7 a).

Pendant la transition du Pléistocène à l'Holocène, vers 12 000 ans BP, la fréquence et l'intensité des incendies ont fortement augmenté (Ledru et al., 2002; Cassino et al., 2018, 2020). Cette augmentation des incendies est associée à une augmentation de l'humidité et de la température qui ont pu favoriser l'augmentation de la biomasse combustible (herbes).

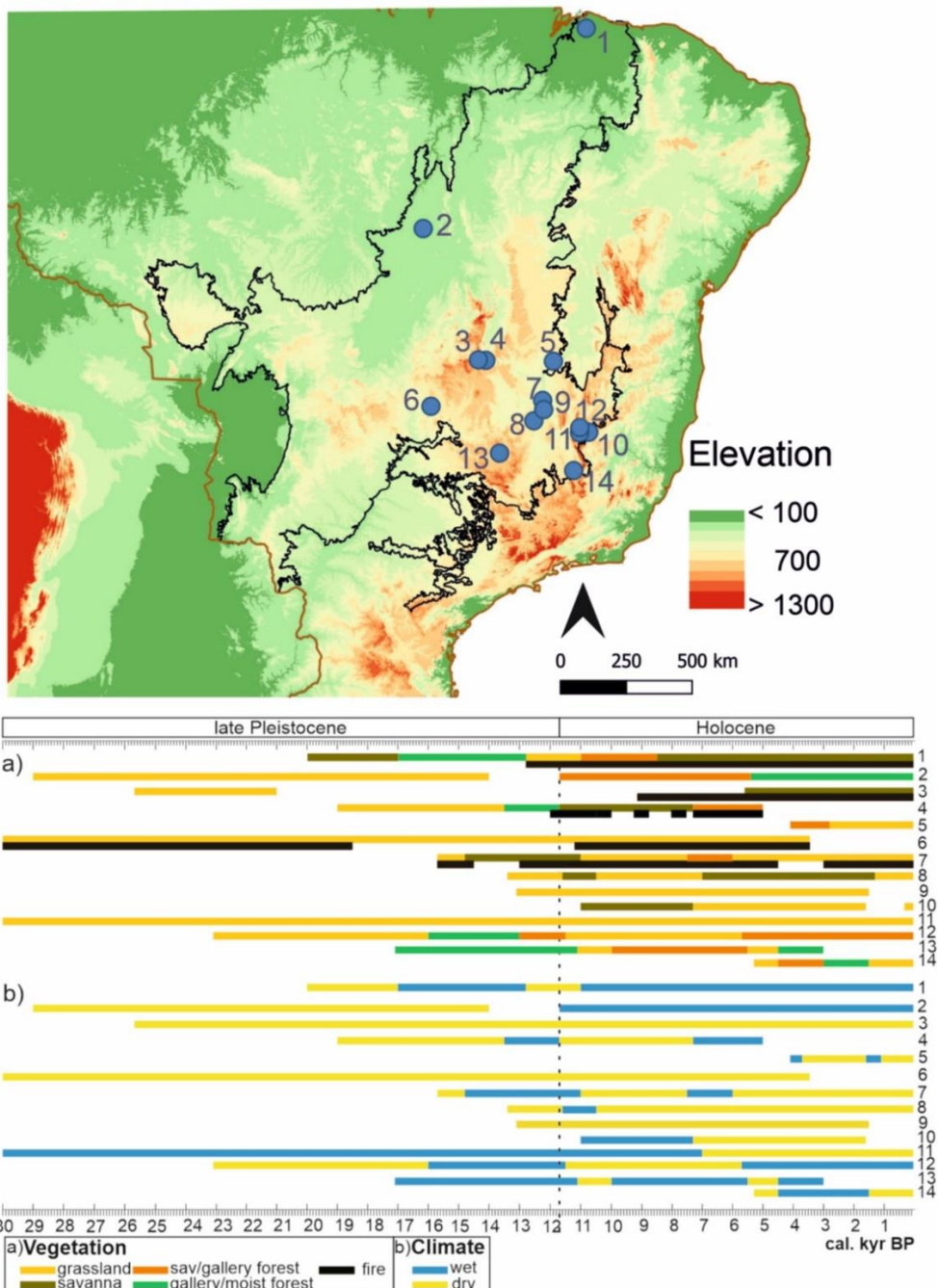


Figure I.7.A. Carte topographique montrant la localisation des enregistrements palynologiques (point bleu) (d'après Fick and Hijmans, 2017) où le biome Cerrado est délimité par une ligne noire. I.7B. Reconstruction (a) des changements de physionomie du Cerrado à partir des analyses palynologiques et des macrocharbons (b). et du climat qui leur est associé. a) wet=humide (barre bleu claire), dry=sec (barre jaune) ; grassland=savane ouverte (barre jaune), savanna=savane (barre marron), sav/gallery forest= savanna/forêt galerie (barre orange), gallery/moist forest= forêt galerie/humide (barre verte), fire = incendie (barre noire). 1 Caço, 2 Confusão, 3 Aguas Emendadas, 4 Lagoa Feia, 5 Pandeiros, 6 Cromínia, 7 São Jose, 8 Laçador, 9 Fazenda Urbano, 10 Pau de fruta, 11 Pinheiro, 12 Rio Preto, 13 Salitre, 14 Lagoa Santa.

2.3 Études paléoclimatiques du Cerrado

Les enregistrements paléoclimatiques à haute résolution sont obtenus à partir des analyses géochimiques réalisées sur les spéléothèmes. Ils couvrent les 16 000 dernières années et sont peu nombreux, avec quatre enregistrements. Le spéléothème de Lapa Sem Fim (12°S , 41°W) (Strikis et al., 2018 ; Azevedo et al., 2021) montre une augmentation des précipitations pendant l'événement de Heinrich 1 (19 000-14 600 yr BP) et le Dryas récent (12 800-11 600 yr BP). Ces changements abrupts du climat sont associés à une méga-mousson sud-américaine provoquée par la fonte des glaces dans l'hémisphère nord. Le début de l'Holocène est caractérisé par un régime de précipitation continu (Stríkis et al., 2011 ; Azevedo et al., 2021), interrompu par des événements plus secs ou plus humides (Figure I.8). Stríkis et al. (2011) suggèrent que certains événements ponctuels sont couplés à des événements Bond (9200, 8200, 7400, 6600, 5200, 4000, 3200, 2700, 2300 et 2200 ans avant le présent). Les événements de Bond sont observés dans l'Atlantique Nord où ils sont liés à des changements de la température de surface de l'Atlantique qui modifient le régime des précipitations dans les zones de mousson. Il s'agit d'événements froids qui produisent un déficit de précipitations dans l'hémisphère nord et qui sont également enregistrés dans le nord de l'Amérique du Sud (Haug et al., 2001).

Au contraire, dans l'hémisphère Sud, une augmentation de la température et des précipitations a été enregistrée, en particulier dans la mousson sud-américaine. Ceci serait dû à la fonte rapide des dernières calottes glaciaires des Laurentides qui auraient modifié la circulation océanique (Cheng et al. 2009 ; Stríkis et al., 2011). Les spéléothèmes de la grotte d'Angelica (13°S , 46°W) montrent des précipitations continues avec des valeurs plus élevées du $\delta^{18}\text{O}$ ($\sim -3\text{‰}$) (Wong et al., 2021) qu'au nord (-4 et $-6,5\text{‰}$) (Wortham et al., 2017) (Figure I.8).

En résumé, les spéléothèmes montrent une forte variabilité de la mousson en intensité et/ou en amplitude au cours des derniers 16 000 ans sur la région centrale du Cerrado.

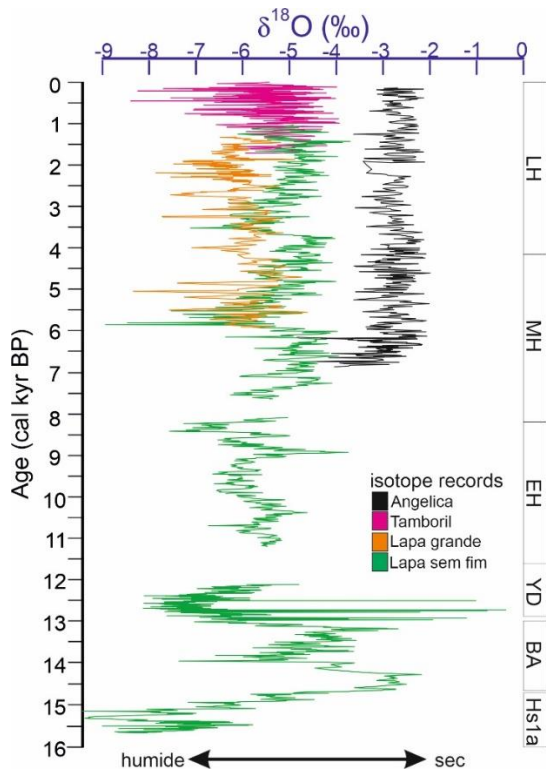


Figure I.8. Variations du $\delta^{18}\text{O}$ mesurées dans les spéléothèmes localisés dans le Cerrado (d'après Strikis et al., 2011, 2018; Wortham et al., 2017; Azevedo et al., 2021; Wong et al., 2021).

3 Objectifs de l'étude

Au cours des dernières années, le Cerrado a suscité l'intérêt de nombreux scientifiques. Entre 2001 et 2014, 28 nouvelles publications sur les dynamiques de la végétation du Cerrado sont enregistrées (Nogueira, 2015). Entre 2014 et 2021, autour de 30 études prennent en considération les incendies (Barradas et Ribeiro, 2021). Ces travaux ont montré une dynamique complexe entre la végétation, le climat, le feu et le sol (Figure I.9). En condition naturelle, sans intervention humaine, une relation bidirectionnelle entre toutes les composantes (végétation, précipitations, feu et sol) est observée (Bueno et al., 2018; Pivello et al., 2021; Lira-Martins et al., 2022). Lorsque l'activité humaine est prise en compte, elle a une influence directe à tous les niveaux.

Une attention croissante est accordée aux études sur l'effet du feu dans le Cerrado. En effet, la fréquence et l'intensité des incendies s'est modifiée en passant de 3-7 ans à 2-3 ans dans des sites peu perturbés par l'activité humaine et avec une végétation native (zones protégées). D'autre part, la surveillance des zones cultivées récupérées montrent un temps de récupération de la végétation native de moins de 50 ans. Cependant, avec plus de 50 % de la surface du Cerrado détruite, il est aujourd'hui nécessaire de comprendre l'effet de ces interactions sur des périodes plus longues en intégrant divers scénarios comme le degré de préservation de la végétation native et le degré de l'impact humain sur l'écosystème.

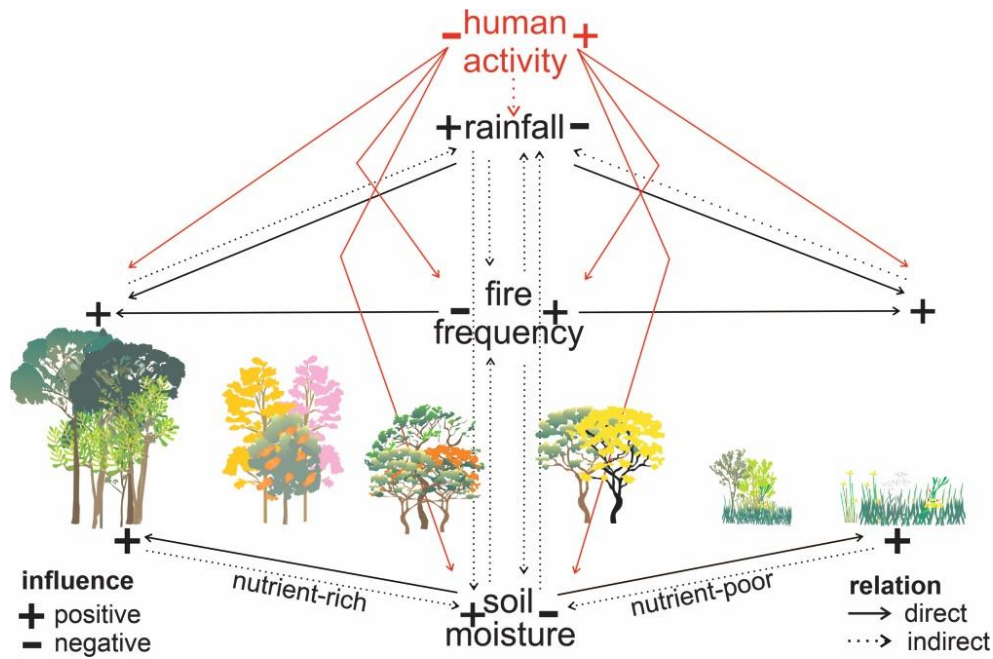


Figure I.9: Interaction des différents forçages (climat, homme, sol, feu) montrant des réponses favorables (positives) ou défavorables (négatives) entre les différentes composantes.

Les études paléoécologiques nous permettent de comprendre les processus écologiques sur de longues périodes de temps (de la centaine à plusieurs milliers d'années). Dans le Cerrado, de telles études sont encore peu nombreuses et surtout concentrées dans la région sud-est (Fig. I.7). De plus lorsqu'elles existent, leur faible résolution temporelle ne permet pas d'atteindre une grande précision d'analyse, ou bien les derniers millénaires sont souvent absents et les études s'arrêtent à la fin de l'Holocène moyen vers 4 000 ans BP.

Notre étude sur le lac Feia et le marais de Getulio va donc nous permettre de compléter les informations sur les derniers millénaires dans la région centrale du biome. Nous explorerons une nouvelle région située sur la transition entre la région centrale et le nord-est. Ces recherches viennent en complément de celles menées dernièrement par Raquel Cassino (post doctorat ISEM), Sergio Xavier (PhD ISEM -UFC) dans le cerrado du Nordeste et Daniely Guerra (post doctorat ISEM) dans une enclave de cerrado du semiaride.

Nous nous attacherons plus particulièrement à examiner :

- l'interaction entre le climat et la végétation dans la zone centrale du Cerrado;
- la réponse de la biodiversité aux différents forçages climatiques et anthropiques;
- l'expression des incendies en fonction du climat et de la biomasse.

La Partie II :

L'article 1 est consacré à la caractérisation de la morphologie et à la description de l'écologie des taxons polliniques représentatifs de nos deux sites d'étude, ainsi qu'à la délimitation de

l'importance de la relation entre les assemblages polliniques et les taxons indicateurs pour les interprétations palynologiques.

L'**article 2** est consacré à l'étude des derniers 5 000 ans dans le Cerrado central.

L'**article 3** est dédié à l'analyse des derniers 15 000 ans dans le Cerrado du nord-ouest.

La **Partie III**, détaille les conclusions finales de notre étude et propose des orientations futures.

4 Région d'étude

Dans le Cerrado, la plupart des études paléoécologiques sont concentrées sur les régions périphériques (sud-est du Cerrado) par rapport au cœur du biome (figure I.7). La définition de notre zone d'étude a pour objectif de compléter les informations en direction du centre du Cerrado avec l'étude de deux nouveaux sites situés dans les zones centrale et nord-ouest du Cerrado (Figure I.10a). Selon Françoso et al. (2020), ce sont des zones relativement préservées de l'influence humaine qui constituent des centres de biodiversité. Les deux sites sont influencés par le régime de précipitations saisonnières contrôlées par la mousson sud-américaine avec quelques différences locales (Figure I.10 a,b).

Le Lac Feia se situe dans la région centrale, près de la ville de Formosa dans l'état du Goiás. Le lac est de forme allongée suivant une orientation NE-SO et une profondeur ne dépassant pas 5 m. Il est entouré d'une forêt-galerie dominée par les arbres pionniers *Cecropia*. Bien que la végétation naturelle ait été profondément modifiée, il est possible d'observer le cerrado *sensu stricto* au nord-est du lac et une zone d'écotone entre le cerrado et les forêts de galerie au sud-ouest (Figure I.10 a,c). La chronologie réalisée sur une carotte prélevée en 2015 a permis de dater l'origine du lac à ~19 000 ans cal BP (Cassino et al., 2020).

Le marécage de Getulio (*Varjão de Getulio* en portugais) se situe à l'intérieur du parc écologique EESGT (*Estação Ecológica Serra Geral do Tocantins* en portugais) sur la limite orientale du district nord-ouest du Cerrado (Figure I.10 a,d), dans une plaine associée au réseau de drainage du bassin fluvial du fleuve Tocantins, un affluent de l'Amazone. La végétation est dominée par des graminées formant un cerrado de type *campo limpo*) et un cerrado *sensu stricto*, avec la présence de forêt-galerie et de *veredas* associés au drainage de la rivière (Figure I.10d). Cette région est relativement peu impactée par les activités agricoles. Toutefois les gestionnaires du parc pratiquent régulièrement des mises à feu contrôlées afin d'éviter la formation de feux plus destructeurs et ainsi protéger les habitants (Schmidt et Eloy, 2020).

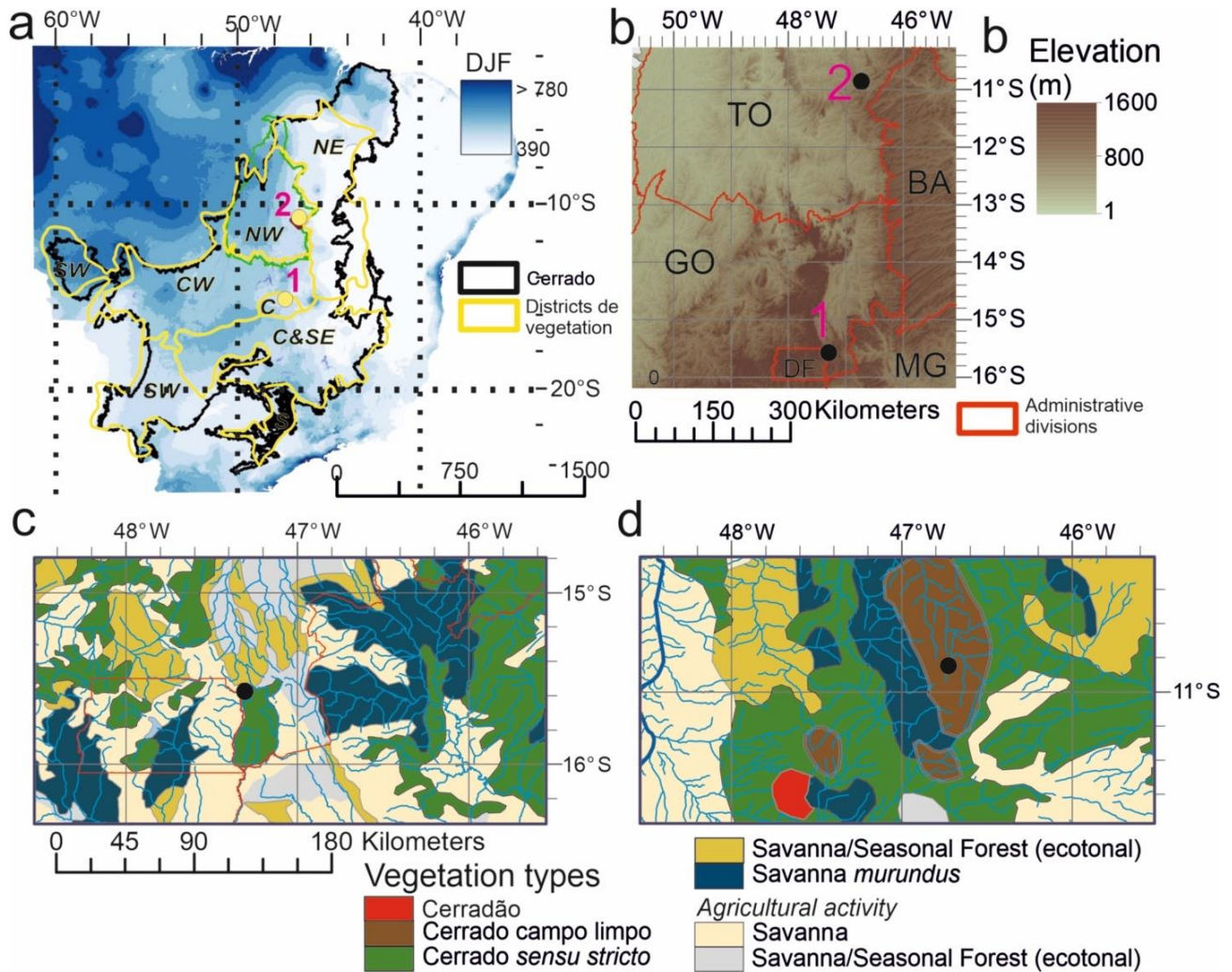


Figure I.10. Cartes (a) de la distribution des précipitations pendant l'été austral (DJF) au Brésil et (b) de la topographie de la zone d'étude montrant l'emplacement des sites d'étude 1) Lagoa Feia et 2) Varjão do Getulio. Détail des types de végétation observés autour de Lagoa Feia (c) et Varjão do Getulio (d) représentés par un point noir. *Fick and Hijmans, 2017; MapBiomass, 2023.*

5 Matériel et méthodes

5.1 Echantillonnage et cadre chronologique

Nos recherches portent sur deux carottes sédimentaires, le lac Feia d'origine lacustre (LFB1) et le marécage de Getulio (*Varjão do Getulio*) (VGE-17).

La carotte LFB1 d'une longueur de 6 m a été extraite du lac Feia en 1990 à l'aide d'un carottier à vibration adapté de Martin et al. (1995). LFB1 ($15^{\circ}34'S$; $47^{\circ}18'W$; 850 m asl) a été prélevé en eau libre dans la partie nord-est du lac à une profondeur de 1,5 m (Fig. I.9 a,b,c) (Turcq et al., 2002). Cette carotte avait été déposée à l'Université de Brasilia (DF, Brésil) où nous l'avons retrouvée intacte en 2018. Pour la présente étude, nous avons analysé les 310 cm supérieurs qui couvrent les

5 000 dernières années afin de compléter les résultats obtenus sur une autre carotte prélevée en 2015 (LF15-2) où les derniers millénaires étaient absents de la séquence (Cassino et al 2020).

La deuxième carotte sédimentaire a été extraite en octobre 2017 du marécage *Getulio* ($10^{\circ}50'41.55''S$; $46^{\circ}43'32.17''W$; 485 m asl) à l'aide d'un carottier russe de 100 cm de long et 5 cm de diamètre. Le marécage est situé à proximité d'une plaine inondable qui fait partie du système de drainage du bassin de la rivière Sono. La carotte VGE-17 a 3 m de profondeur.

Pour dater ces enregistrements, huit échantillons pour LFB1 et douze échantillons pour VGE-17 (Tableau I.1 - LFB1 ; Tableau I.2 - VGE-17) ont été datés au radiocarbone par spectrométrie de masse par accélérateur (AMS) et mesure au *Laboratoire de Mesure du Carbone14* (LMC14)-UMS 2572 (CEA/DSM -CNRS-IRD-IRSN-Ministère de la Culture et de la Communication, Saclay, France). Les dates « radiocarbone » ont été calibrées avec la courbe SHcal20 (Hogg et al., 2020) dans Calib 7.0 (Stuiver et Reimer, 1993). La relation âge-profondeur a été modélisée à l'aide de statistiques bayésiennes avec le package Bacon dans R (Blaauw et Christen, 2011). Pour LFB1, une date supplémentaire de -40 à BP a été ajoutée à 0 cm, correspondant à l'année du carottage, c'est-à-dire 1990 AD. Les paramètres ont été ajustés à SHCal20 (Southern Hemisphere Terrestrial) avec un intervalle de confiance de 0,95. Pour VGE-17, les 20 cm au sommet de la carotte étaient composés d'herbe et de racines non décomposés et ont été éliminés. A partir du modèle d'âge, nous avons calculé le taux de sédimentation (cm/an) et la résolution d'analyse (an/cm) pour les deux enregistrements.

Tableau I.2. Résultats des datations radiocarbone pour la carotte LFB1.

Code du laboratoire	Matériau daté	Profondeur (cm)	$\delta^{13}\text{C}$	^{14}C âge (an BP)
SacA 53907	argile lacustre	14-15	-32.4	220 ± 30
SacA 60352	argile lacustre	40-41	-27.5	910 ± 30
SacA 53908	argile lacustre	60-61	-29.8	870 ± 30
SacA 60353	argile lacustre	102-103	-25.6	1280 ± 30
SacA 60354	argile lacustre	164-165	-30.2	2160 ± 30
SacA 60355	argile lacustre	218-219	-23.8	2925 ± 30
SacA 60356	argile lacustre	270-271	-25.9	3520 ± 30
SacA 53909	argile lacustre	313-314	-33.3	4405 ± 30

Tableau I.3. Résultats des datations radiocarbone pour la carotte VGE-17.

Code du laboratoire	Matériau daté	Profondeur (cm)	Âge ^{14}C (an BP)
SacA53912	sédiment organique	20	75 ± 30
SacA57442	sédiment organique	40	1630 ± 30
SacA53913	sédiment organique	74	4370 ± 30
SacA53914	sédiment organique	96	4705 ± 30
SacA57443	sédiment organique	106	4630 ± 30
SacA64079	sédiment organique	110	5405 ± 30
SacA53915	sédiment organique	125	5920 ± 35
SacA57444	sédiment organique	140	6455 ± 30
SacA53916	sédiment organique	160	7875 ± 40
SacA53918	sédiment organique	220	10085 ± 50

SacA57446	sédiment organique	228	10735 ± 50
SacA57448	sédiment organique	265	11400 ± 60

5.2 Reconstruction de la végétation

Analyses palynologiques

149 échantillons de LFB1 et 140 échantillons de VGE-17 ont été analysés pour ce travail de doctorat, soit un total de 289 échantillons. Chaque échantillon consiste en un volume de 0,25 cm³, 0,5 cm³ ou 1 cm³ prélevée sur 1 cm d'épaisseur et chaque 2 cm, en fonction de la disponibilité du matériel sédimentaire pour chaque niveau. Le contenu pollinique a été extrait au laboratoire de palynologie de l'ISEM. Deux comprimés de spores de *Lycopodium clavatum* (36814 spores par comprimé) ont été ajoutés dans chaque échantillon pour le calcul de la concentration de pollen. Les échantillons ont d'abord été nettoyés des acides humiques et fulviques dans de l'hydroxyde de potassium (KOH) à 10% au bain-marie puis extraits par densité avec du ZnCl₂ (Kummel & Raup, 1965). Pour les échantillons de LFB1 situés entre 309 et 201 cm et VGE-17 entre 298 et 200 cm de profondeur, un traitement supplémentaire avec 5 ml d'acide fluorhydrique à 75% pendant une heure dû être effectué afin d'éliminer les particules de silicate (Faegri & Iversen, 1989). Le pollen, les spores et les non-palynomorphes (algues) ont été identifiés et comptés au microscope optique au grossissement de 600x. Au total, 175 types de pollen ont été identifiés pour LFB1 et 112 types de pollen pour VGE-17 à l'aide de la collection de pollens de référence de l'ISEM ainsi que les clés d'identification et les catalogues des types de pollen du Brésil (Salgado-Labouriau, 1973, Cassino & Meyer, 2011, Bush & Weng, 2007, RCPol, 2021).

Présentation des résultats

Pour les deux enregistrements, les fréquences de pollen sont calculées sur la base de la somme totale des grains de pollen terrestres. L'influx de pollen est exprimé en grains/cm²/an pour chaque taxon identifié. Les zones polliniques sont définies à l'aide de la méthode CONISS (restricted cluster analysis by sum of squares) proposée par Bennett (1996).

Les analyses statistiques et l'élaboration des figures ont été réalisées à l'aide du programme R. Les diagrammes palynologiques ont été produits à l'aide du progiciel *rioja* (Juggins, 2022), les zones ont été définies à l'aide de CONISS dans le progiciel *vegan*. L'analyse en composantes principales (ACP) a été réalisée à l'aide de la fonction ACP du progiciel *FactoMineR* (Lê et al., 2008), toutes les données polliniques ayant été préalablement normalisées par la méthode de la racine carrée. L'ACP réduit la dimensionnalité en explorant l'association linéaire entre les variables.

Le regroupement des taxons sous forme d'assemblages a été établi selon trois critères. 1) tous les taxons polliniques identifiés ont été classés en fonction de leur type de croissance (arbre, herbacée) et de leur phytophysionomie, cerrado arboré ou forêt galerie. Les Poaceae ont été utilisées pour caractériser la phytophysionomie ouverte du cerrado (Gosling et al., (2005 ; 2009). Dans le cas de LFB1, il s'agit du seul taxon représentant la végétation ouverte, tandis que dans le cas de VGE-17, certains taxons supplémentaires ont été sélectionnés sur la base de leur représentativité dans l'enregistrement. 2) les taxons polliniques dont la contribution est inférieure à 1 % n'ont pas été

pris en compte puis nous avons appliqué une Analyse en Composante Principale (ACP) à l'ensemble des taxons sélectionnés. 3) Pour chaque taxon pollinique sélectionné dans la première ACP, nous avons pris en compte à la fois la fréquence (pourcentage élevé ou faible) et le schéma d'apparition (constant ou variable) dans la base de données, deux paramètres qui nous ont aidés à réduire notre sélection au nombre le plus représentatif de taxons polliniques. Dans les deux enregistrements les taxons polliniques sans tendance ou moins fréquents n'ont pas été utilisés.

Enfin, pour LFB1, une ACP a été réalisée sur les 22 taxons polliniques sélectionnés afin d'évaluer la variabilité de la végétation en fonction du temps. L'interprétation palynologique de LFB1 est basée sur la combinaison de ces analyses fondées principalement sur la fréquence de pollen et l'"influx de pollen. En outre, les caractéristiques écologiques, telles que la forme de vie, la strate, l'exposition à la lumière, le syndrome de pollinisation et l'habitat (principalement les exigences du sol) de la plante associée au taxon de pollen défini précédemment dans le premier critère, ont été prises en compte (voir l'**article 1** pour une information plus détaillée).

Pour les 31 taxons sélectionnés de VGE-17, nous avons appliqué la classification des trois types de physionomie (Cerrado ouvert, Cerrado arboré et forêt galerie) ainsi que trois formes de croissance de la végétation (herbe, arbuste, arbre). Cette catégorisation a été évaluée à l'aide d'une ACP. Finalement, une troisième analyse a été réalisée sur le total de taxons du pollen pour reconstruire la température et les précipitations de l'enregistrement à l'aide du programme *crestr* (Chevalier, 2020). Les paramètres climatiques obtenus ont été comparés aux interprétations palynologiques. L'exclusion des taxons polliniques a été basée sur trois critères. 1) les espèces dont la distribution est définie de manière significative par la variable climatique, 3) la définition d'une zone d'étude climatique cohérente pour tirer parti de la pondération de l'abondance climatique 2) la tendance et le pourcentage de chaque taxon pollinique tout au long de l'enregistrement.

5.3 Reconstruction des incendies

Analyse des macrocharbons

Afin de caractériser les incendies, 310 échantillons de 0,5 cm³ ont été analysés sur des intervalles de 1 cm pour LFB1. L'analyse des macrocharbons de VGE-17 a été réalisée en 2018 le cadre d'un stage à l'ISEM sur 148 échantillons de 5 cm³ prélevés chaque 2 cm pour VGE-17. Les échantillons ont été défloculés et blanchis avec 10% d'hydroxyde de potassium ((KOH) et d'hypochlorite de sodium (NaClO) (2,6%), puis tamisés sous l'eau à travers une maille de 160 µm (Genries et al., 2012). Les résidus sont déposés sur une plaque de porcelaine blanche afin de faciliter l'identification et le comptage des particules de charbon. Le matériel a été analysé au grossissement de 600 x 10 sur une loupe reliée à une caméra connectée à un analyseur d'images. Le logiciel d'analyse d'images Winseedle (Regent Instruments Canada Inc., 2009) permet de mesurer la longueur (L) et la largeur (W) de chaque particule ainsi que de calculer la concentration totale des particules de charbon par cm² et par an, la surface de chaque particule de macrocharbon puis la somme cumulative des surfaces de particules de macrocharbon, c'est-à-dire la surface totale de macrocharbon par cm² et par an pour chaque échantillon.

Analyse des incendies

Differentes méthodes analytiques ont été utilisées pour évaluer les incendies. Tout d'abord, le taux d'accumulation des particules de charbon a été calculé en multipliant le nombre total de particules par unité de volume par le taux d'accumulation de sédiments exprimé par CHAR# (particules $\text{cm}^{-2} \text{ an}^{-1}$) et le taux d'accumulation des surfaces de chaque particule par le taux d'accumulation de sédiments et la somme totale des surfaces de chaque particule par unité de volume exprimé par CHARarea ($\text{mm}^2 \text{ cm}^{-2} \text{ an}^{-1}$). Le degré de fragmentation des particules de charbon est évalué en comparant CHAR# et CHARarea. Ainsi, plus CHAR# et CHARarea diffèrent l'un de l'autre plus le taux de fragmentation est élevé. Au contraire, si CHAR# et CHARarea sont similaires, la fragmentation est négligeable et nous pouvons utiliser CHARarea, qui est recommandé pour l'analyse de détection des pics d'incendie (Leys et al., 2013).

Une fois le taux de fragmentation défini, les fréquences des incendies sont évaluées en divisant la série CHAR en CHARbackground et CHARpeak avec une résolution temporelle de 19 ans et 100 ans, basses en la moyenne de resolution de LFB1 et VGE-17 respectivement, et une régression polynomiale localement pondérée (LOWESS) avec une largeur de fenêtre mobile de 500 ans, conseillée comme un minima pour les analyses de résolution décanale et centennale (Higuera et al., 2007). La valeur seuil de 3 est conseillée par Kelly et al (2011) pour l'évaluation de l'indice signal-bruit (SNI). CHARpeak est défini par les pics enregistrés au-dessus du seuil et représente la contribution du charbon provenant d'un ou plusieurs incendies dans l'intervalle de temps représenté par le pic (Whitlock & Larsen, 2001). CHARbackground représente les pics enregistrés en dessous du seuil et représente la variation de la production globale de charbon, en réponse aux processus de sédimentation, de mélange et d'échantillonnage pour la série CHAR (Whitlock & Larsen, 2001). Les CHARpeak obtenus ont été évalués à l'aide d'un modèle mixte gaussien qui sépare les incendies réels du bruit ambiant dans la série des CHARpeak. Le modèle gaussien a été appliqué à une fenêtre de 500 ans et au percentile 95 (Higuera et al., 2007). Une analyse secondaire a également été réalisée à l'aide du GAM (modèle additif généralisé) recommandé par Simpson (2018) pour évaluer les pics, sur la base de modèles de régression. Les mêmes paramètres ont été utilisés pour comparer les résultats. Toutes les analyses de données ont été effectuées à l'aide du paquet *Tapas* dans RStudio (Finsinger et Bonnici, 2022).

Enfin, pour chaque particule, le rapport entre la largeur (W) et la longueur (L) (W:L) et L:W a été calculé. Les valeurs individuelles obtenues ont été intégrées dans un diagramme de densité afin de définir une valeur moyenne pour W:L et L:W. Cette analyse permet d'évaluer la présence et la prévalence des particules carbonisées en distinguant les particules d'origine herbacée des particules d'origine ligneuse. Dans le cas de W:L, les valeurs supérieures à 0,5 sont associées à des particules carbonisées ligneuses peu transportées du lieu de combustion et celles inférieures à 0,5 aux herbacées pouvant être transportées sur une plus grande distance depuis le lieu de combustion (Aleman et al., 2013). Dans le cas de L:W, les valeurs inférieures à 2,5 suggèrent la présence et la dominance de bois carbonisé, les valeurs supérieures à 3,5 la présence d'herbacée carbonisé (Umbanhower & McGrath, 1998 ; Vachula et al., 2021). Les deux calculs ont été utilisés afin de renforcer l'analyse des provenances des particules de charbon.

Dans notre étude, seuls le taux d'accumulation de surface (CHARarea en mm²/cm²/an) le rapport W:L ont été utilisés suivant la recommandation de Leys et al. (2013). L:W nous donne la même information que W/L dans les 2 enregistrements et n'a pas été utilisée (Vachula et al., 2021). D'autre part, le calcul du SNI permettant d'évaluer la fréquence des pics d'incendie ne nous a pas semblé suffisamment fiable pour être utilisé. Toutefois, tous les résultats obtenus à partir de ces analyses sont reportés dans l'annexe 1.

5.4 Les autres indicateurs

Analyse des éléments trace de la carotte LFB1

Les analyses des éléments trace (XRF) de LFB1 ont été réalisées à l'Institut de Geociências de l'université de Brasília au Brésil sous la direction de Elder Yokohama. 81 échantillons de sédiments ont été séchés dans un four de laboratoire à 50 °C pendant 24 heures. Ensuite, les sédiments ont été broyés sur des mortier en agate et les fractions inférieures à 0,180 mm ont été séparées à l'aide d'un tamis 8×2 "INOX ASTM 80 MESH / TYLER 80 by Bertrand". Un volume de 1 cm³ de sédiment de chaque sous-échantillon a été placé dans le récipient de support X-Ray Fluorescence (XRF). Les échantillons ont été analysés dans un XRF DELTA portable (Olympus), en mode sol avec trois répétitions de deux minutes pour chaque échantillon et en utilisant la moyenne des trois répétitions pour l'interprétation des données obtenues. Enfin, les éléments ayant une importance représentative ont été sélectionnés. Ti et Ti/K ont été choisis comme indicateurs de l'érosion (Marshal et al., 2011 ; Davies et al., 2015). Ti/K a été normalisé afin d'observer clairement la variation des données sur une échelle homogène.

Analyse des isotopes et des éléments trace de la carotte VGE-17

Ces analyses ont été réalisées au laboratoire intégré de recherche multi-utilisateurs de l'université des vallées de Jequitinhonha et de Mucuri) - LIPEMVALE situé à Diamantina, état du Minas Gerais au Brésil et dirigées par Ingrid Horak-Terra. 122 échantillons de sédiments avec un volume compris entre 0,5 et 2 cm³ par échantillon en fonction de la quantité de sédiment disponible. Les mesures de la composition isotopique ($\delta^{13}\text{C}$ et $\delta^{15}\text{N}$) du carbone organique total (TOC) et de le Nitrogene total (NT), de l'oxygène (O), de l'hydrogène (H) et des éléments majeurs et traces (Si, S, Cu, Br, V, Rb, Al, Ti, Sr, Nb, Y, Fe) ont été réalisées chaque 2 cm tout le long de la carotte. Les échantillons ont été séchés, broyés et homogénéisés et seuls les niveaux avec suffisamment de sédiment ont été analysés. Les échantillons préparés pour l'analyse isotopique ont été prétraités physiquement et chimiquement selon Pessenda et al. (1996). Les teneurs en COT, TN, O et H ont été obtenues par combustion sèche, dans un analyseur élémentaire LECO CHNS/O, modèle TruSpec Micro, et les gaz générés ont été quantifiés dans un détecteur infrarouge. Deux étalons de composition connue ont été utilisés pour calibrer l'équipement : le sol (C% = 2,35, N% = 0,183 et S% = 0,028) et la feuille d'orchidée (C% = 50,40, H% = 6,22, N% = 2,28 et S% = 0,156). Les éléments majeurs et traces ont été déterminés par fluorescence X à dispersion d'énergie, modèle Shimadzu EDX-720, dans LIPEMVALE. L'étalon A-720 de composition connue a été utilisé pour l'étalonnage de l'équipement. Les résultats ont également été exprimés en pourcentage de poids sec.

Pour évaluer la composition isotopique et élémentaire ($\delta^{13}\text{C}$ et $\delta^{15}\text{N}$ TOC, TN, O, H ; et éléments majeurs et traces), une analyse en composantes principales (ACP) a été réalisée pour identifier les principaux facteurs contrôlant la distribution élémentaire (Muller et al., 2008 ; Sjöström et al., 2020) dans les échantillons. Tout d'abord, les données ont été log-transformées et standardisées pour le mode de corrélation. Ensuite, la méthode de rotation orthogonale Varimax a été appliquée pour maximiser la charge des variables sur les composantes (Eriksson et al., 1999; Reimann et al., 2008). L'analyse a été réalisée avec SPSS 20.0. Des rapports supplémentaires Si/Ti, log(Ti/Ca) et Ti/Al ont été utilisés pour compléter l'analyse statistique (Davies et al., 2015).

Partie II

Article 1

Relationships between pollination syndromes, pollen morphology and plant ecology in Quaternary deposits of the Cerrado

Soumis à Palynology le 26 juin 2023 – doi : 10.1080/01916122.2023.2252871

Katerine Escobar-Torrez^{1, 2}, Raquel Franco Cassino², Marie-Pierre Ledru¹

1. Institut des Sciences de l'Evolution de Montpellier (ISEM), Université de Montpellier-CNRS-IRD-EPHE, France

2. Departamento de Geologia, Universidade Federal de Ouro Preto, Brazil

Corresponding autor: Katerine Escobar-Torrez

email: katerine.escobartorrez@ird.fr

postal address: Institut des Sciences de l'Evolution, ISEM (UMR 226 – IRD/ CNRS/UM2), 34095 Montpellier, cedex 05, France.

Abstract

This study presents the morphological description and ecological information of 58 terrestrial pollen taxa and seven water-related pollen taxa from the Cerrado, obtained from two sediment cores, lake Feia (LFB1) and *Varjão do Getúlio* swamp (VGE-17). We analyze the relationships of ecological and morphological traits (pollination syndrome, vegetation strata, and pollen size) within the two different types of depositional environment. In the LFB1 core, the pollen assemblages were dominated by arboreal pollen from closed physiognomies and lower storey trees (<10 m in height), while a combination of closed to open physiognomies were observed in the pollen assemblages of the VGE-17 core. Regarding pollination syndromes, a large majority of the pollen taxa described in the records presents the entomophilous syndrome and a higher influx of entomophilous pollen was observed on both cores. Anemophilous and anemophilous/entomophilous syndromes of dispersion were less abundant. Small and medium pollen classes were the most abundant, while large pollen was rare. The influx of small pollen was slightly predominant in the lake record, while in the swamp record medium pollen was more abundant. Our results show that swamps and lakes differ in the representation of local versus regional pollen and in their sensitivity and responses to water-level changes. The physiognomy also influences pollen dispersion: a closed physiognomy will increase the local pollen signal while a more open physiognomy results in a better representation of local and regional signals.

Keywords: Tropical forest, plant trait, pollen, sediment core, Brazil, landscape physiognomy

1. Introduction

Palynological studies are largely used as a technique for the reconstruction of vegetation and of its short-to-long term dynamics (Seppä, 2007), providing information about environmental conditions and inferences on climate changes and on ecological patterns and processes (Brewer, 2007). The interpretation of palynological data is, however, highly dependent on the accurate identification of pollen types and on the assessment of deposition biases. In the Neotropics, the high diversity of plant species is a challenge for pollen identification. In the Cerrado, more particularly, the high diversity of ecosystems complicates the interpretation of fossil pollen assemblages, mainly because plant species are often not restricted to one type of physiognomy, but are instead part of a *continuum* vegetation mosaic. In the Cerrado, arboreal vegetation related to water availability is present, with gallery/ciliary forests generally associated to adjacent water bodies, with high soil humidity and nutrients. As the availability of water decreases, dry forest and woody cerrado (cerradão), which are common on fertile and well-drained soils, develop (Ribeiro and Walter, 2008). Then, in less/or poor nutrient and dry soils, sparse woody cerrado (cerrado *sensu stricto*) to open cerrado (herbaceous species dominance) are present, with plants adapted to dryness and fire events (*Byrsonima*, *Curatella*, *Caryocar*), non-adapted to waterlogging (Ribeiro and Walter, 2008; Durigan et al. 2022). Two other physiognomies are strongly influenced by ground water levels, the wetlands, composed of the tree palm *Mauritia*, forming palm swamps - also called “*vereda*”- and composed of common hygrophilous plants of the Cyperaceae, Eriocaulaceae, and Alismataceae families, and the wet grassland (“*campo umido*”) dominated by herbs of gramineae and other herbs dependent or adapted to moist soils (*Drosera*, *Eryngium*, *Polygalaceae*, *Xyris*) (Ribeiro and Walter, 2008; Durigan et al. 2022)

A few studies have dealt with the challenge of interpreting pollen assemblages in the Cerrado complex vegetation, including guides for the identification of Cerrado pollen taxa that also contain information on plant ecology (i.e., Labouriau, 1973; Lorente and Meyer, 2010; Cassino and Meyer, 2011; Freitas et al., 2020; Lorente et al., 2017), and studies that discuss the pollen assemblages of the different vegetation physiognomies (Cassino et al., 2015; Cassino et al., 2021). If these studies have contributed to our knowledge of the pollen representation of this biome, they also highlighted the need for more investigation. Specially, the large territorial extension of the Cerrado - 2 million km² from 2° to 24°S of latitude - and the fact that the vegetation physiognomies are composed of a wide range of plant species according to the region (Vieira et al., 2022; Sano et al., 2019; Bridgewater et al., 2004) which means that the interpretation of pollen assemblages can vary greatly from site to site.

In this study, we present fossil pollen taxa from two different sites located within the Cerrado and discuss how morphological and ecological traits relate to the type of depositional site and varies through time. The analysed traits include pollen size (mall, medium, big), pollination syndromes (biotic, abiotic, both types), plant life-form (herb, shrub, tree), and vegetation stratum (field, shrubby, lower and medium storey) and were defined for each taxa based on botanical studies.

The paleoecological and paleoclimatic interpretations of these two pollen records were presented elsewhere (Escobar-Torrez et al., 2023a; Escobar-Torrez et al., 2023b *in prep.*) and here we focus solely on the depositional aspects of the pollen assemblages. This discussion aims to increase the

information on the ecological significance of fossil pollen in the Cerrado and substantiate inferences on landscape changes in palaeoecological studies.

2. Material and Methods

2.1 Study area and core sampling

Two sediment cores were taken in two different waterbodies. First, in the Lake *Feia* a six meter depth sediment core (LFB1) ($15^{\circ}34'20"S$, $47^{\circ}18'20"W$, altitude 871 m asl) (Fig. II.1a, II.1b) in the vicinity of Formosa city, Goias State, in the central Cerrado. Currently, the lake maximum water column is of 2-3 m and macrophytes (*Nymphaea*, *Sagittaria*, *Eichhornia*) are observed starting from the shore and continuing towards the center of the lake. The pollen record of the first three meters of the LFB1 core was evaluated, representing pollen taxa assemblages of the last 5000 cal yr BP (Escobar-Torrez *et al.*, 2023a).

Second, in the Getulio swamp, located at $10^{\circ}50'41.55"S$, $46^{\circ}43'32.17"W$ (485 m asl) (Fig. IV.1a, II.1b), a sediment core (VGE-17) of 3 meter depth was collected at 100 meters from the drainage network. The swamp is located in the “*Estação Ecologica Serra Geral do Tocantins*” (EESGT), on the *Patamares das Mangabeiras* Plateau (500-700 m of altitude), that separates the basins of the São Francisco and Tocantins rivers. In this Plateau, drainage networks densely occupy the opened wide and flat valleys forming humid areas subject to periodic flooding. The pollen content of the three meter sediment core is covering the last ~15,000 years BP (Escobar-Torrez *et al.*, 2023b *in prep*).

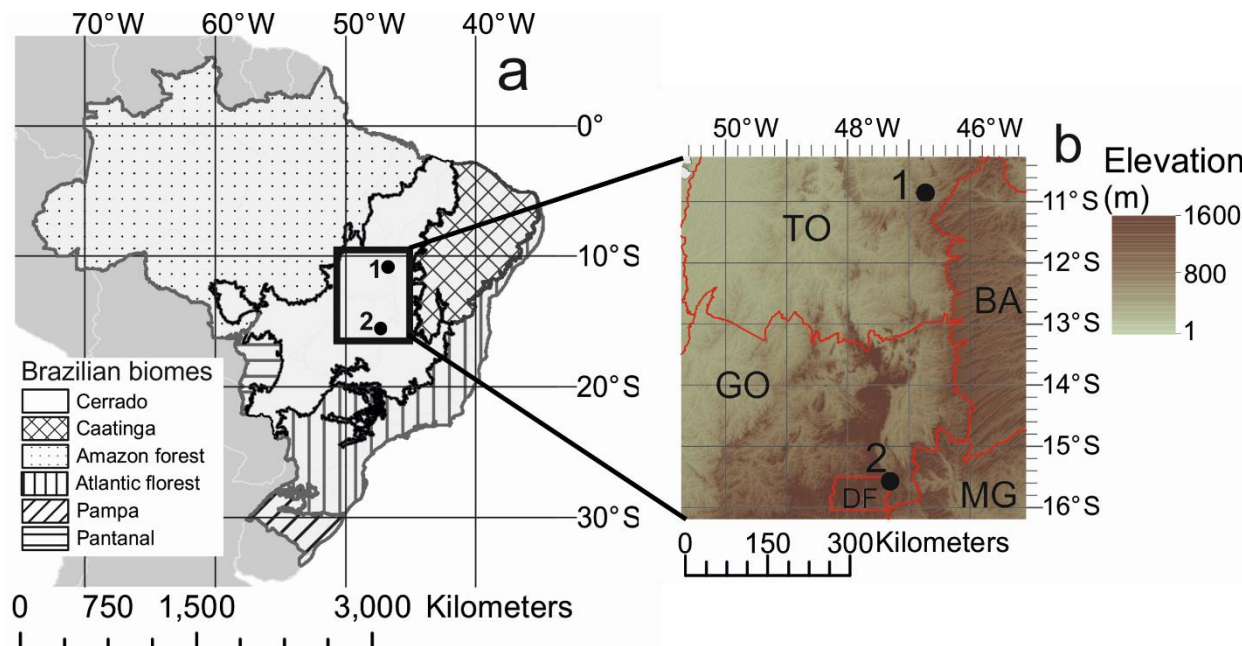


Figure II.1. a) Brazilian biomes showing the location of VGE-17 (1) and LFB1 (2) sediment cores in the Cerrado area, and the b) elevation in which the two sites are emplaced, with the division territory division (red line).

2.2 Climate and vegetation

In the Köppen classification, both LFB1 and VGE-17 sites are classified as Aw type, with dry winter and wet summer (Alvares et al., 2013). For both sites, climate conditions are affected by the same major drivers of precipitation regime. Precipitation is mainly modulated by the South American Convergence Zone (SACZ) band that influences the amplitude of the South American Monsoon System (SAMS), and by the seasonal movement of the Intertropical Convergence Zone (ITCZ), which moves across the equator following the insolation cycle. These systems form an antiphase pattern with high rainfall in Amazonia and central Brazil and low rainfall in northeastern Brazil during the austral summer (DJF) and the opposite pattern during austral winter (JJA) (Reboitia et al., 2012; Marengo et al., 2012).

At lake Feia (core LFB1), mean monthly temperature oscillates between 18 to 24 °C and mean annual precipitation varies from 1450 to 1850 mm. The Getulio swamp (core VGE-17), warmer conditions are observed with temperature ranging from 23 to 33 °C and mean annual rainfall around 1400 mm. Although both sites are under the influence of the same major climatic features, differences are observed related to their latitudinal position. While the lake Feia is mostly affected by the SACZ and the SAMS, the climate at Getulio swamp is characterized by a northwest-southeast precipitation dipole, influenced by the climate of the adjacent biomes, the Amazon to the northwest and the Caatinga to the southeast, a high evapotranspiration during the rainy season (90-70%) which decreases during the dry season, to 40-80% and 50-60% respectively (Assad et al., 1993; Silva et al. 2008).

The landscape around lake Feia is composed of both open cerrado and woody cerrado physiognomies with a gallery forest growing from the lakeshore to 5 m above the lake level on the northeastern side of the lake. A botanical survey performed 7 km from Lake Feia revealed the dominance of the following families: Anacardiaceae, Araliaceae, Malvaceae, Asteraceae, Cyperaceae, Eriocaulaceae, Poaceae, Lamiaceae, Fabaceae, Lentibulariaceae, Malpighiaceae, Melastomataceae, Myrtaceae, Onagraceae, Orchidaceae, Polygalaceae, Pontederiaceae, Verbenaceae and Xyridaceae (Ferraz-Vicentini, 1998). The Getulio swamp is located in a seasonally flooded river valley in which the formation of *veredas* (palm swamps) is favored (Villela and Nogueira, 2011). The vegetation is characterized by the predominance of grassland and open cerrado on sandy soils, dense woody cerrado in rocky areas with colluvial deposition, and *vereda* and gallery forests near the river banks. Common species in this region are represented by *Hirtella ciliata* (Chrysobalanaceae), *Caryocar cuneatum* (Caryocaraceae), and *Parkia platycephala* (Fabaceae - Mimosaceae) (Bridgewater et al., 2004).

2.3 Laboratory work

Sediment samples were processed at intervals of 2 cm for each core totaling 140 samples for VGE-17 and 149 samples for LFB1. A volume of 0.5 - 0.25 cm³ of sediment was used for pollen extraction. Chemical treatments were carried out at the ISEM laboratory in France. A spike of two *Lycopodium* tablets per sample was added to calculate the concentration of pollen. Samples were first washed in 10% KOH in a hot water bath before density separation with ZnCl₂ (Kummel & Raup, 1965). Samples between 309 and 200 cm of depth for LFB1 and 298 to 200 cm of depth for VGE-17, an additional step, that consisted in a 5 ml 75% HF treatment for one hour (Faegri & Iversen, 1989), was performed to remove silica. Pollen, spores, and other non-pollen palynomorphs

were counted and identified at 600x magnification. Photographical record with the microscope camera was taken at the moment of the identification.

2.4 Pollen taxa morphology and ecology

The identification of pollen types was based on the ISEM pollen reference collection for Cerrado taxa (Bremont et al., 2018), and on identification keys and catalogs of pollen types from Brazil (Salgado-Labouriau, 1973; Cassino & Meyer, 2011; Bush & Weng, 2007; RCPol, 2022). For each pollen type, morphological features used for pollen identification were described, including: dispersal form, polarity, symmetry, size class (small <15 µm; medium = 15 to 25 µm; big = 26 to 49 µm), number and aperture type, shape in polar view (amb), shape in equatorial view, surface pattern, and aperture shape. The terminology used for the morphological description followed Punt et al. (2007).

For each pollen taxa, ecological information including pollination syndrome, plant life-form, vegetation physiognomies and stratum were obtained from botanical studies performed in the Cerrado phytophysiognomies, with focus on vegetation composition close to our study areas (Felfili, 1997 and 1997b; Felfili et al., 2007 and 2007b; Lombardo, 1996; Lorenzi, 2002; Martinelli and Moraes, 2013; Martins and Batalha, 2006; Matias et al., 2021; Moreira et al., 2011; Santos and Munhoz, 2012; van der Berg and Oliveira-Filho, 2000; Vieira, 2020; Vieira et al., 2022; Wersal, 2010).

3. Results

3.1 Pollen morphology and ecological information

The pollen analysis of LFB1 and VGE-17 cores resulted in the identification of 175 and 112 terrestrial pollen types, 8 and 4 water level-related pollen types, 6 and 2 types of spores and 15 and 2 non-pollen palynomorphs, respectively. From these, 65 pollen types - 58 corresponding to terrestrial pollen and 7 to water level-related taxa - constituted the most frequent and abundant types which are described here. 51 terrestrial pollen taxa were identified at the genus level, 7 to family level, and 7 pollen water level-related pollen taxa to genus level, which pollen description and ecology are described below.

Amaranthaceae

Gomphrena (Plate II.1, figure 1)

Pollen description: grain monad, apolar, radially symmetric, small size, pantoporate, spheric, reticulate-homobrochate, circular pores located inside the lumen of the reticulum. Size: 10-12 µm.

Ecological information: herbaceous plant, C4 photosynthesis type, distributed mainly in high-altitude in the Cerrado biome (Fank-de-Carvalho et al, 2012). They are drought tolerant plants adapted to a long dry season; some species, like *G. macrocephala*, have tuberous roots allowing them to survive dryness by increasing their storage reserve (de Moraes et al, 2016). Common in

open Cerrado physiognomies (open cerrado, cerrado *sensu stricto*, woody cerrado or cerradão) and less common at the edge of gallery forest or swamp (*vereda*) (Sano et al., 2008)

Anacardiaceae

Astronium (Plate II.1, figure 2 a,b)

Pollen description: grain monad, isopolar, radially symmetric, medium size, tricolporate, amb subtriangular, exine finely striato-reticulate homobrochate, striae longitudinally oriented, subprolate to prolate spheroidal. Pore rectangular (2a) or lalongate (2b) traversing the colpus. Size: 15 - 22 µm (2a) and <20 (2b).

Ecological information: tree, xerophytic and helophytic pioneer species (Lorenzi, 2002) that are commonly found in rocky and dry terrains widespread in the Cerrado of central Brazil. They also occur in the Amazon and Atlantic forests and are also associated to semideciduous tree and some species are present in the Caatinga biome. Felfili et al. (2007b) classified it as a lower storey tree, with ~13 m in height. In the Cerrado biome *Astronium* can be found in cerrado *sensu lato*, cerradão, dry and gallery forests (Sano et al., 2008).

Tapirira (Plate II.1, figure 3)

Pollen description: grain monad, isopolar, radially symmetric, medium size, tricolporate, amb subtriangular, exine markedly striate striae longitudinally oriented, subprolate to prolate-spheroidal, pore rectangular - lalongate traversing the colpus. Size: 18 - 20 µm.

Ecological information: perennial tree, widely distributed and commonly found in humid soils. The most common species in the Cerrado biome is *T. guianensis*. This specie has an average height of 13 m, sometimes growing to more than 20 m. It is considered an emergent plant (above the forest canopy) (Felfili, 1997). In the Cerrado biome is recorded in woody Cerrado or cerradão, and dry and gallery forests (Sano et al., 2008).

Apiaceae

Eryngium (Plate II.1, figure 4)

Pollen description: grain monad, isopolar, radially symmetric, medium size, tricolporate, prolate, amb trilobate, exine psilate, pore lalongate traversing the colpus. Size 18 - 20 µm.

Ecological information: perennial or biennial herb for which growth varies from 0.5 to 1-3 m in height. Usually observed in open cerado, high-altitude grassland to rocky area of montane rainforest, marshes or river banks, and sometimes in degraded areas (Cardozo et al., 2021). Although it can be found in lower precipitation conditions, this plant prefers humid areas. In the Cerrado, *Eryngium* is observed in cerrado *sensu lato*, marshes, *vereda* (swamp) and sometimes on the edge of gallery forests (Flora do Brasil, 2020).

Aquifoliaceae

Ilex (Plate II.1, figure 5)

Pollen description: grain monad, isopolar, radially symmetric, medium size, tricolporate, prolate spheroidal, amb subtriangular, exine clavate. Size 20 - 25 µm.

Ecological information: Tree of no more than ~9 m, usually between 4-8 m height (van der Berg and Oliveira-Filho, 2000). It is a lower storey tree commonly found in gallery forest, in well-drained soils to seasonally or permanently flooded forest (Araujo et al., 2002; da Silva et al, 2018). Its distribution is usually restricted to an altitudinal range, where low temperature (<24 °C) and annual precipitation of at least 1000 mm prevail. In pollen studies, it is an indicator of low temperatures and moister conditions when associated with *Podocarpus*, *Weinmannia*, *Lamanonia*, *Hedyosmum* and *Araucaria* (Ledru et al, 2007). In the Cerrado biome, it is generally observed in gallery forest and less commonly in open cerrado, cerradão and dry forest (Sano et al., 2008).

Arecaceae

Euterpe type (Plate II.1, figure 6)

Pollen description: grain monad, heteropolar, bilaterally symmetric, medium size, exine psilate, monosulcate. Size 25 - 30µm.

Ecological information: a common shade-tolerant tree palm, restricted to forest. *Euterpe edulis* (common species in the Cerrado) is restricted to well preserved forest patches (Martinelli and Moraes, 2013) and requires high moisture, with low tolerance to both dry condition and low temperature (Gatti et al., 2014). In the Cerrado biome, it is generally observed in gallery forest, at the edge of lake, and in floodplain gallery forest (Sano et al. Flora do Brasil, 2008).

Asteraceae

Baccharis type (Plate II.1, figure 7)

Pollen description: grain monad, isopolar, radially symmetric, small size, tricolporate, amb trilobate, oblate spheroidal, exine echinate. Size 10 - 13 µm.

Ecological information: herbaceous or shrubby plant, with C4 photosynthesis type, widely distributed in the Cerrado biome, from lower to high altitude, occupying well-drained soils (Fank-de-Carvalho et al, 2012). Commonly found in open cerrado, cerrado *stricto sensu* and less frequently at the edge of gallery forest and palm swamp (*vereda*) (Sano et al., 2008).

Boraginaceae

Cordia (Plate II.1, figure 8)

Pollen description: grain monad, apolar, radially symmetric , medium size, triporate, amb circular, exine echinate (short echini <1 µm), pore circular annulate. Size 25-28 µm.

Ecological information: tree or shrubby plant, growing up to ~8-14 m in lower storey forest, considered a short-lived pioneer and gap-colonizer (Felfili, 1995). In the Cerrado biome, it is observed in gallery forest, dry forests, cerradão and cerrado *sensu stricto* (Sano et al., 2008).

Brassicaceae – type (Plate II.1, figure 9)

Pollen description: grain monad, isopolar, radially symmetric, small size, tricolporate, subprolate, amb trilobate, exine scabrate. Size ~13 µm.

Ecological information: large family represented by herbs, shrubs and trees. In Quaternary paleoecological studies, it is considered a pioneer herb of successional stage vegetation. It can be used to identify natural or anthropic disturbances associated to the transition from closed to open forest canopy, especially when associated with *Cecropia* (Lorente et al., 2017). In the Cerrado biome, this family occurs as herbs, and is naturally found in open cerrado and in disturbed areas (anthropogenic) (Sano et al., 2008).

Burseraceae

Protium (Plate II.1, figure 10)

Pollen description: grain monad, isopolar, radially symmetric, medium size, tricolporate, subprolate, amb triangular-convex, exine psilate with homogeneous wall, pore rectangular. Size 16-25 µm.

Ecological information: evergreen, shade tolerant, tree with a large and dense crown, usually up to 6-9 m in height, but it can grow up to 10-20 m (Felfili, 1997; Lorenzi, 2002). It grows in dry forests located near riverbanks and in swampy areas (Felfili, 1995). In the Cerrado biome, it is usually found in gallery or riparian forest, dry forest and cerrado *sensu stricto* (Sano et al., 2008).

Cannabaceae

Celtis (Plate II.1, figure 11)

Pollen description: grain monad, apolar, radially symmetric, medium size, triporate, amb subtriangular, exine psilate, endopore. Size ~20 µm.

Ecological information: pioneer tree of up to 6-8 m in height, light-demanding, with fast growth, usually observed in gallery forests that are subject to periodic floods (Lorenzi, 2002). In the Cerrado biome, it occurs mainly in riparian or gallery forest, dry forest and cerradão (Sano et al., 2008).

Trema (Plate II.1, figure 12)

Pollen description: grain monad, apolar, asymmetric, medium size, diporate, amb circular, exine finely scabrate, endopore circular. Size ≤15 µm.

Ecological information: lower storey and light-demanding tree of up to 6-15 m height, usually observed in humid soils. *Trema* is a pioneer tree (Lorenzi, 2002) and can also grow in the swampy area of the *veredas* (Araujo et al, 2012). In the Cerrado biome, it grows in gallery forests, lake margins, *veredas* and cerrado *sensu lato* (Flora do Brasil, 2008).

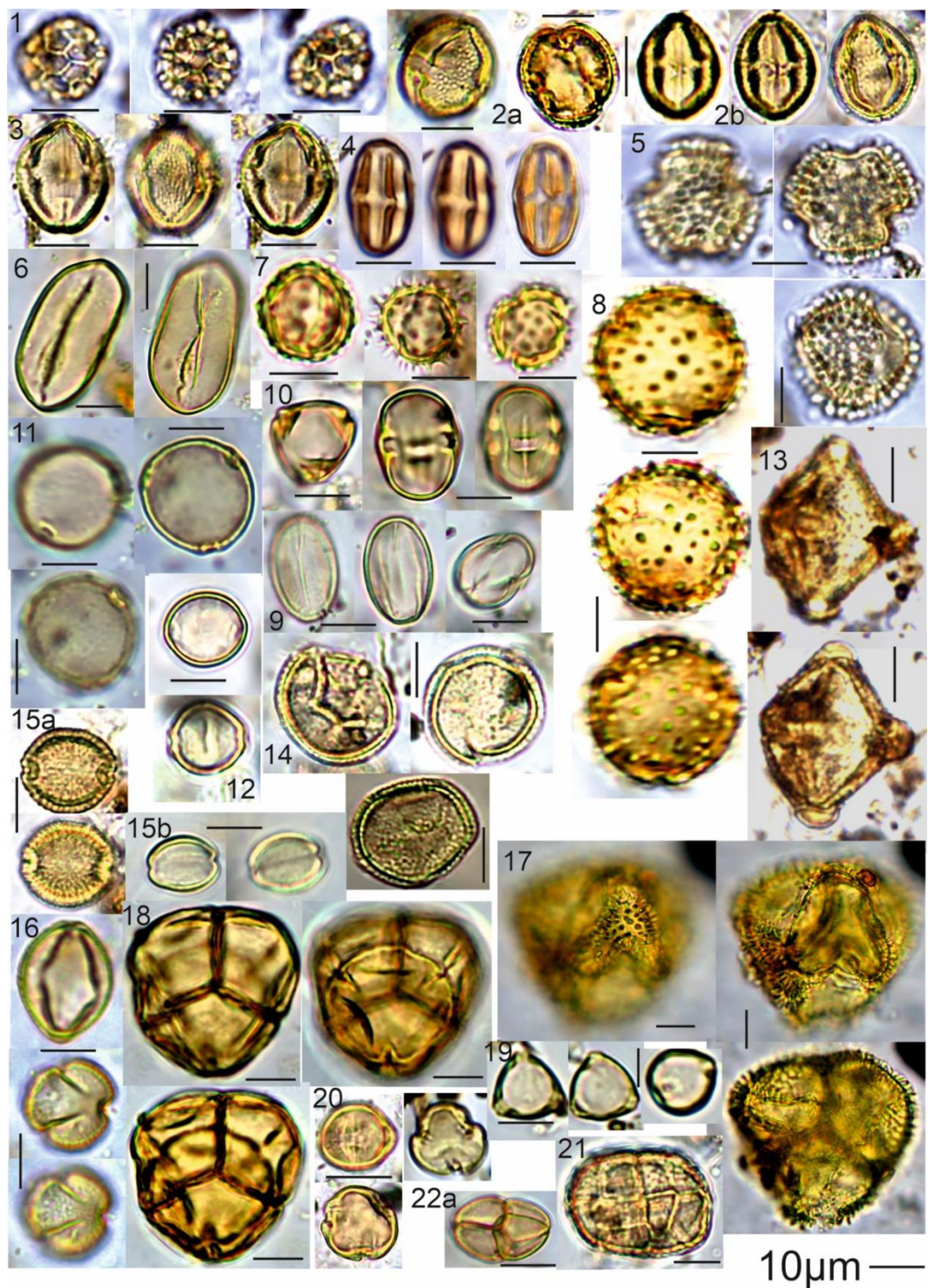


Plate II.1. Photomicrographs of pollen taxa identified in LFB1 and VGE-17 cores: Amaranthaceae – 1) Gomphrena, Anacardiaceae – 2) Astronium, 3) Tapirira, Apiaceae – 4) Eryngium, Aquifoliaceae – 5) Ilex, Arecaceae – 6) Euterpe type, Asteraceae – 7) Baccharis type, Boraginaceae – 8) Cordia, 9) Brassicaceae type, Burseraceae – 10) Protium, Cannabaceae – 11) Celtis, 12) Trema, Caryocaraceae – 13) Caryocar, Chloranthaceae – 14) Hedyosmum, Cunnoniaceae – 15) Lamanonia, Dillenaceae – 16) Curatella, Droseraceae – 17) Drosera, 18) Ericaceae type, Euphorbiaceae – 19) Acalypha, 20) Alchornea, Fabaceae (mim) – 21) Anadenanthera, 22) Mimosa.

Caryocaraceae

Caryocar (Plate II.1, figure 13)

Pollen description: grain monad, isopolar, radially symmetric, big size, tricolporate, subprolate, amb circular-convex, reticulate (in mesocolpium) and regulate exine (in apocolpium), wall thick in the poles and the equator, pore elliptic. Size: 30-35 μm .

Ecological information: tree, 5-15 m in height, that grows in the cerrado *sensu stricto*, on aluminized leached soils (Araujo, 1995; Almeida-Bezerra et al, 2022). It can be perennial or deciduous, present in the Cerrado biome from open cerrado to dense woody cerrado (cerradão) (Araujo, 1995). Frost sensitive, with the death of many sprouts.

Chloranthaceae

Hedyosmum (Plate II.1, figure 14)

Pollen description: grain monad, apolar, asymmetric, spheroidal, medium size, aperture area in form of a five-pointed star, sexine thicker than nexine - sexine clavate. Size 18-20 μm .

Ecological information: lower storey tree commonly found in gallery forest and *vereda*, on well drained soils to seasonally or permanent flooded forests (Araujo et al., 2002). In pollen studies, it relates to low temperature and moist condition when associated with *Podocarpus*, *Weinmannia*, *Lamanonia*, *Ilex* and *Araucaria* (Ledru et al, 2007). In the Cerrado biome, it is usually found in gallery forest, swamp (*vereda*) and marsh (Sano et al., 2008).

Cunoniaceae

Lamanonia (Plate II.1, figure 15)

Pollen description: grain monad, apolar, asymmetric, small to medium size, dicolporate, amb circular, exine finely reticulate (15a) or psilate (15b), endopore circular. Size $\sim 16 \mu\text{m}$ (15a) or $\sim 12 \mu\text{m}$ (15b).

Ecological information: a light-demanding tree of lower storey ($\sim 11 \text{ m}$) (van der Berg and Oliveira-Filho, 2000; Lorenzi, 2002). In the Cerrado biome, it is observed in gallery forest and cerradão (Sano et al., 2008).

Dillenaceae

Curatella (Plate II.1, figure 16)

Pollen description: grain monad, isopolar, radially symmetric, medium size, tricolporate, amb trilobate, subprolate, exine microreticulate, inconspicuous small pores. Size $\sim 20 \mu\text{m}$.

Ecological information: semideciduous tree with a dense rounded crown, up to 6-10 m in height. It is drought-tolerant, slow growing tree, that thrives in dry soil (Lorenzi, 2002). In the Cerrado biome, it is found in open cerrado, cerrado *sensu stricto*, cerradão (Sano et al., 2008).

Droseraceae

Drosera (Plate II.1, figure 17)

Pollen description: tetrad, big size, individual grains isopolar, radially symmetric, big size, amb circular, exine finely clavate. Size entire tetrad ~40 µm.

Ecological information: herbaceous plant, growing no more than 30 cm, usually found in moist grassland, swamps (*vereda*), or flooded soil (Flora do Brasil, 2020). In the Cerrado biome, it occurs in moist grassland cerrado and *vereda* (Sano et al., 2008; Flora do Brasil, 2020).

Ericaceae type (Plate II.1, figure 18)

Pollen description: tetrad, big size, individual grains isopolar, radially symmetric, big size, tricolporate, amb circular, grain suboblate, exine finely scabrate, pores circular and small. Size of the tetrad ~30 µm.

Ecological information: shrub to treelet form, common in gallery forest subject to permanent or periodic flooding, and in marsh or humid soil at the edge of the gallery forest. The most common species in the Cerrado biome of Goiás, Federal District and Tocantins states is *Gaylussacia brasiliensis* (Sano et al., 2008).

Euphorbiaceae

Acalypha (Plate II.1, figure 19)

Pollen description: grain monad, isopolar, radially symmetric, small size, stephanocolporate (tri-tetra-colporate), exine psilate, amb circular to tetra-angular, oblate-spheroidal, pore circular. Size 10-12 µm.

Ecological information: herb to subshrub growing no more than 2 m in height, in the Cerrado biome is associated to dry semideciduous forests, cerradão and gallery forest (Sano et al., 2008; Flora do Brasil, 2020)

Alchornea (Plate II.1, figure 20)

Pollen description: grain monad, isopolar, radially symmetric, small size, tricolporate, suboblate spheroidal, amb subtriangular, exine thick finely scabrate, lalongate pores with operculum. Size 12 - 10 µm.

Ecological information: light-demanding and dominant tree present on lower storey forests, ~3-8 m in height (Felfili, 1997). In the Cerrado biome, it is mainly associated to gallery forest (sometimes flooded) or to semideciduous riparian forest, and occasionally to cerradão (Sano et al., 2008).

Fabaceae (mim)

Anadenanthera (Plate II.1, figure 21)

Pollen description: polyad, composed by more than ten grains, apolar, asymmetric, medium size, exine finely scabrate. Size ~25 µm.

Ecological information: emergent and light-demanding tree of 2 to 24 m in height (Felfili, 1997b), commonly associated to fertile soils although it can resist to low moisture condition (Felfili et al., 2007b). In the Cerrado biome, it is observed in gallery forest, dry forest and cerradão (Sano et al., 2008).

Mimosa (Plate II.1, figure 22)

Pollen description: uniplanar tetrad (22a,b) and triad (22c), apolar, asymmetric, medium size (22a,b) and small size (22c), exine psilate (22a,c) to finely scabrate (22b). Size ~15-20 µm (22a,b) and ~10 µm (22c).

Ecological information: herb to shrub growing no more than ~1m in height, common in the Cerrado, generally observed in cerrado *sensu stricto* and open cerrado (Sano et al., 2008).

Piptadenia (Plate II.2, figure 23)

Pollen description: polyad composed of 10 or more grains, apolar, asymmetric, medium size, exine psilate. Size ~15 - 20 µm.

Ecological information: treelet of the lower storey, 3-6 m in height, in the Cerrado biome, it is generally observed in gallery forest, dry forest and in the transition from open cerrado to woody cerrado. It is also a common plant in dry forest and Caatinga (Felfili et al, 2007b; Sano et al., 2008).

Fabaceae (pap) Plate II.2, figure - 24)

Pollen description: grain monad, isopolar, radially symmetric, small size, tricolporate, subprolate or oblate-spheroidal, amb trilobate, exine psilate, pores elliptic to rectangular. Size ~10 µm.

Ecological information: lower storey, shade tolerant tree, 10 m or more in height (Felfili, 1997b). In the Cerrado biome, it is observed in cerrado *sensu stricto*, cerradão, dry forest and sometimes in gallery forest (Sano et al., 2008).

Dialium (Plate II.2, figure 25)

Pollen description: grain monad, isopolar, radially symmetric, small size, tricolporate, subprolate or oblate-spheroidal, amb circular, exine psilate. Size ~10 µm.

Ecological information: tree of 1 to 12 m height, usually observed in dry or woody cerrado (Flora do Brasil, 2020). In the Cerrado biome, few specimens have been collected in dry forest (Sano et al., 2008; Flora do Brasil, 2020).

Machaerium (Plate II.2, figure 26)

Pollen description: grain monad, isopolar, radially symmetric, medium size, tricolporate, subprolate, amb trilobate, exine psilate, pore circular traversing the pore. Size ~16 µm.

Ecological information: straight tree of upper and middle storey, ~15 m in height, light-demanding (Felfili, 1997b). Usually recorded in dry forest, Atlantic forest, Caatinga and cerradão (Felfili et al., 2007b). In the Cerrado biome, it is found in gallery forest, cerradão or in the transition to the Atlantic forest (Sano et al., 2008).

Iacuminaceae

Emmotum (Plate II.2, figure 27)

Pollen description: grain monad, isopolar, radially symmetric, medium size, tricolporate, subprolate, amb subtriangular, exine psilate, pore lalongate-ellipsoidal traversing the colpus. Size ~16 µm.

Ecological information: dominant and heliophilous tree, of ~15 m in height (Felfili, 1997b). In the Cerrado biome, it is generally observed in gallery forest and cerradão (Sano et al., 2008).

Lythraceae

Cuphea (Plate II.2, figure 28)

Pollen description: grain monad, asymmetric, small size, tricolporate - syncolpate, amb triangular convex, oblate, exine psilate, pore elliptic. Size 10-13 µm.

Ecological information: herbaceous or subshrub heliophyte plant that grows in open vegetation, scrubby or secondary vegetation, over generally deep and sandy substrates, resprouting after fire event (Cavalcanti, 1991). The genus sometimes presents a woody underground system (xylopodium) which enables them to survive when vegetation above ground is burnt (e.g. *C. glareosa*, Cavalcanti, 1991). Usually found in cerrado *sensu lato*, mainly in open physiognomies, wet or dry grasslands and cerrado *sensu stricto*, it can also grow at the forest edge and in *veredas* (Sano et al., 2008; Flora do Brasil, 2020).

Malvaceae

Apeiba (Plate II.2, figure 29)

Pollen description: grain monad, isopolar, radially symmetric, big size, tricolporate, spheroidal, amb triangular convex, exine thick scabrate, pore lalongate traversing the colpus, colpi short. Size ~30 – 25 µm.

Ecological information: evergreen tree of ~15 m in height, the most common species is *A. tibourbou* (Flora do Brasil, 2020). Commonly found in gallery and riparian forests and in dry forest (Sano et al., 2008; Flora do Brasil, 2020).



Plate II.2. Photomicrographs of pollen taxa LFB1 and VGE-17 cores: Fabaceae (mim) - 23) *Piptadenia*, Fabaceae (pap) - 24) *Dalbergia*, 25) *Dialium*, 26) *Machaerium*, Icacinaceae - 27) *Emmotum*, Lythraceae - 28) Cuphea, Malvaceae - 29) *Apeiba*, 32) *Eriotheca*, Malpighiaceae - 30) *Banisteropsis*, 31) *Byrsonima*, 33) Melastomataceae/Combretaceae, Meliaceae - 34) *Guarea*, Menispermaceae - 35) *Abuta*, 36) Menispermaceae type, 37) Moraceae, 38) Myrtaceae, Ochnaceae - 39) *Ouratea*, Pentaphylaceae - 40) *Ternstroemia*, Phyllantaceae - 41) *Hieronima*, Piperaceae - 42) *Peperomia*, 43) Poaceae, Polygalaceae - 44) *Polygala*, Primulaceae - 45) *Cybianthus*, 46) Myrsine.

Eriotheca (Plate II.2, figure 32)

Pollen description: grain monade, big size, tricolporate, suboblate, amb triangular with rounded angle, exine reticulate, circular pores, short colpi. Size 25 - 30 μm .

Ecological information: lower storey tree of ~9 m in height, usually found in gallery forests (van der Berg et al, 2000; Sano et al., 2008), and in cerradão or cerrado *sensu stricto* (Sano et al., 2008).

Malpighiaceae

Banisteropsis (Plate II.2, figure 30)

Pollen description: grain monad, asymmetric, medium size, periporate, spheroidal, exine thick well-defined and psilate, circular pores without annulus. Size ~25 μm .

Ecological information: common plant growing as vine inside gallery or deciduous forests. Most commonly found in gallery forest and secondarily in cerrado *sensu stricto*, cerradão, and open cerrado (Sano et al, 2008 ; Flora do Brasil, 2020).

Byrsonima (Plate II.2, figure 31)

Pollen description: grain monad, isopolar, radially symmetric, small size, tricolporate, subprolate, exine thin psilate or finely scabrate, elliptic or rectangular pore. Size ~10 μm .

Ecological information: tree of the lower storey, height ranging from 2.5 to 6 m, commonly observed in well-drained soils of the cerrado *sensu stricto* and cerradão, and less commonly on gallery forest margin (Sano et al., 2008 ; Flora do Brasil, 2020).

Melastomataceae – Combretaceae (Plate II.2, figure 33)

Pollen description: grain monad, isopolar, radially symmetric, small to medium size, heteroaperturate tricolporate-tricolpate, amb hexalobate, exine psilate, pore circular. Size ~10 to ~13-20 μm .

Ecological information: Marchant et al. (2002) suggest that pollen morphology of this two families are similar being usually combined. The common genus in our study sites were, *Miconia* and *Tibouchina* (Melatomataceae), and *Combretum* and *Terminalia* (Combretaceae) (speciesLink's, 2013-2023). Widely distributed lower storey trees and/or shrub-treelet. In the Cerrado biome, Melastomataceae and Combretaceae are present in cerrado *sensu lato*, in open and woody cerrado, and also to gallery/ciliary forest (Sano et al., 2008). When associated to edaphic moisture or vereda, it can colonize rapidly (Araujo et al, 2002).

Meliaceae

Guarea (Plate II.2, figure 34)

Pollen description: grain monad, isopolar, radially symmetric, medium size, tetracolporate, amb quadrangular convex, exine psilate and well defined, pore circular traversing the colpus. Size ~23 μm .

Ecological information: lower storey tree ~6 m height (van der Berg and Oliveira-Filho, 2000), found in gallery and riparian forests, and occasionally in dry forest and *veredas* (Sano et al., 2008).

Menispermaceae

Abuta (Plate II.2, figure 35)

Pollen description: grain monad, isopolar, radially symmetric, small size, tricolporate, amb circular, spheroidal, exine reticulate homobrochate, pore circular traversing the colpus. Size ~14 µm.

Ecological information: shrub to treelet of 2-4 m in height, it is commonly observed in the Cerrado preferentially in the cerrado *sensu stricto* (Sano et al., 2008; Flora do Brasil, 2020).

Menispermaceae type (Plate IV.2, figure 36)

Pollen description: grain monad, isopolar, radially symmetric, small size, tricolporate, amb triangular-circular convex, exine reticulate homobrochate, pore circular traversing the colpus. Size ~12 µm.

Ecological information: vines, shrub, or treelet forms, this family is commonly found in cerrado *sensu lato*, gallery forest, dry forest, and occasionally in *veredas* (Sano et al., 2008; Flora do Brasil 2020).

Moraceae (Plate II.2, figure 37)

Pollen description: grain monad, isopolar, bilaterally or radially symmetric, small size, di-triporate, amb circular, exine psilate or finely scabrate, pore circular. Size ~12 µm.

Ecological information: widespread family of moist forests trees. This family has been widely used in pollen studies as a indicator of rain forest indicator (Gosling et al., 2005; 2009) due to its easy anemophilous syndrome (Gosling et al, 2005). *Sorocea* and *Naucleopsis* are common genera of the lower storey (< 10 m in height) (van der Berg and Oliveira-Filho, 2000). In the Cerrado usually is observed in gallery forest and less common in woody cerrado (cerradão) (Flora do Brasil, 2020).

Myrtaceae (Plate II.2, figure 38)

Pollen description: grain monad, radially asymmetric, small size, tricolporate, amb triangular, oblate, exine psilate to finely scabrate. Size ~13 µm.

Ecological information: lower storey trees present in areas where the groundwater is close to the surface, and associated to humid environment. It is observed at swamp periphery (Araujo et al, 2002). In the Cerrado biome, the most common genera are *Psidium*, *Eugenia* and *Myrcia*, all trees that grow up to ~ 4-6 m height (Flora do Brasil, 2020). It is commonly observed in gallery forest and woody Cerrado (Flora do Brasil, 2020).

Ochnaceae

Ouratea (Plate II.2, figure 39)

Pollen description: grain monad, isopolar, radially symmetric, small size, tricolporate, subprolate, amb circular-triangular convex, exine psilate, pore elliptic traversing the colpus. Size ~16 µm.

Ecological information: light-demanding and codominant trees with low density that grow up to ~15 m height (Felfili, 1997). In the Cerrado biome, it is generally observed in cerrado *sensu stricto* and cerradão as treelets of up to 2-6 m height (Sano et al., 2008; Flora do Brasil 2020).

Pentaphylacaceae

Ternstroemia (Plate II.2, figure 40)

Pollen description: grain monad, , radially symmetric, small size, spheroidal, amb trilobate-triangular, circular pores, exine thin and psilate. Size ~10 µm.

Ecological information: tree, ~9 m height, widely distributed in Brazil with 22 species, usually observed in open Cerrado, woody cerrado,dry forest (Vieira, 2020). These plants grow in places with high biological diversity and landscape value, sensitive to disturbances and not adapted to fire (Vieira, 2020; Allende, 2021). In the Cerrado biome, it is commonly observed in open cerrado, cerrado *sensu lato*, dry forest and gallery forest (Sano et al., 2008; Allende, 2021)

Phyllantaceae

Hyeronima (Plate II.2, figure 41)

Pollen description: grain monad, isopolar, radially symmetric, medium size, tricolporate, prolate or subprolate, amb trilobate, exine microreticulate homobrochate, pore elliptic - lalongate dividing the colpus. Size ~25 µm.

Ecological information: lower storey tree of ~6 m height, commonly observed in cerrado *sensu stricto*, gallery forest and vereda (Sano et al., 2008; Flora do Brasil, 2020).

Piperaceae

Peperomia (Plate II.2, figure 42)

Pollen description: grain monad, heteropolar, radially symmetric, small size, inaperturate, spheroidal, amb circular, exine verrucate. Size ~10 µm.

Ecological information: heliophyte herb generally obseerved in gallery forest (Sano et al, 2008).

Poaceae (Plate II.2, figure 43)

Pollen description: grain monad, heteropolar, radially symmetric, medium size, monoporate, espheroidal, amb circular, exine psilate, pore circular with annulus. Size 12 - 32 µm, average size ~25 µm.

Ecological information: herbaceous plants, including 13 subfamilies of local grasses. Panicoideae dominates in northern Brazil (*Paspalum* is the most diverse genus) and Pooideae dominates in southern Brazil (Longhi-Wagner et al, 2012). Most of the Panicoidae show C₄ photosynthetic pathway (Longhi-Wagner et al., 2012) and are dominant in the open cerrado and in rocky grassland, less common in swamp and at the edge of the gallery forest (Flora do Brasil, 2008).

Polygalaceae

Polygala (Plate II.2, figure 44)

Pollen description: grain monad, radially symmetric, medium size, stephanocolporate (8-10 colpi), subprolate, amb circular, exine psilate, pore zonoporate and lalongate. Size ~20-22 µm (44a,d), ~16 µm (44b) and ~13 µm (44c).

Ecological information: heliophyte herb dependent on water availability (Matias et al, 2021), commonly observed in cerrado *sensu stricto*, moist open cerrado, and when associated to *vereda* on the edge or in intermediate areas such as (water table near the soil surface) (Araujo et al, 2002; Sano et al., 2008).

Primulaceae

Cybianthus (Plate II.2, figure 45)

Pollen description: grain monad, isopolar, radially symmetric, small size, tricolporate, subprolate, amb trilobate, exine psilate, pore lalongate traversing the colpus. Size ~16 µm.

Ecological information: lower storey tree, ~ 2-9 m in height; in the Cerrado, it is commonly observed in gallery and riparian forests, and occasionally in dry forests and cerrado *sensu lato* (Sano et al., 2008).

Myrsine (Plate II.2, figure 46)

Pollen description: grain monad, isopolar, radially symmetric, small size, tetracolporate, suboblate, amb quadrangular-tetralobate, exine psilate to finely scabrate. Size ~16 µm.

Ecological information: lower storey and light-demanding tree, ~ 5-15 m height (Felfili, 1997; van der Berg and Oliveira-Filho, 2000). In the Cerrado biome, it is observed in gallery forest and secondarily in dry forest, cerradão, cerrado *sensu stricto* and open cerrado (Sano et al., 200; Flora do Brasil 2020).

Rubiaceae

Guettarda (Plate II.3, figure 47)

Pollen description: grain monad, bilaterally symmetric, medium size, dicolporate, oblate, amb circular, exine psilate and thick, pore circular. Size ~20 µm.

Ecological information: lower storey trees, 4-7 m height, that usually grow in woody cerrado, preferring fertile and well-drained soil; once the plant is established, it is tolerant to drought

(Lorenzi, 2002). In the Cerrado biome, it is observed in cerrado *sensu lato* and gallery forest (Sano et al., 2008).

Sabicea type (Plate II.3, figure 48)

Pollen description: grain monad, isopolar, radially symmetric, medium size, tricolporate, oblate or suboblate, amb triangular-circular, exine reticulate homobrochate, pore elliptic and lalongate. Size 25 - 30 μm .

Ecological information: shrub of 0.5 to 1 m in height, generally observed on rocky soil of open cerrado, it is also observed in cerrado *sensu lato*, vereda and gallery forest (Sano et al., 2008; Flora do Brasil, 2020).

Simira (Plate II.3, figure 49)

Pollen description: grain monad, isopolar, radially symmetric, medium size, tricolporate, suboblate or oblate spheroidal, amb circular, pore circular with margin. Size $\sim 25 \mu\text{m}$.

Ecological information: lower storey tree, ~ 4 -10 m height. In the Cerrado biome, this genus is observed in dry forest and gallery forest, and sometimes in floodplain forest (Sano et al., 2008; Flora do Brasil, 2020).

Salicaceae

Casearia (Plate II.3, figure 50)

Pollen description: grain monad, isopolar, radially symmetric, medium size, tricolporate, subprolate, amb trilobate, exine reticulate homobrochate, pore circular traversing and dividing the colpus. Size ~ 20 -25 μm .

Ecological information: lower storey tree, 5-7 m in height (van der Berg and Oliveira-Filho, 2002), natural pioneer of rapid growth, it is observed in cerrado *sensu stricto*, cerradão, and dry and gallery forest (Sano et al., 2008).

Sapindaceae

Matayba (Plate II.3, figure 52)

Pollen description: grain monad, asymmetric, medium size, syncolpate, amb triangular convex (52a) or concave (52b), oblate, exine psilate (52a) or finely scabrate (52b). Size ~ 20 -25 μm .

Ecological information: lower storey tree, height varying from 4 to 10 m (Flora do Brasil, 2020), heliophylous (Felfili, 1997). In the Cerrado biome, it is generally observed in gallery forest, adapted to flood, also observed in cerrado *sensu stricto* (Sano et al., 2008 and Flora do Brasil, 2020).



10 μm —

Plate II.3. Photomicrographs of pollen taxa identified in LFB1 and VGE-17 cores: Rubiaceae – 47) Guettarda, 48) Sabicea type, 49) Simira, Salicaceae – 50) Casearia, Vitaceae – 51) Cissus, Sapindaceae – 52) Matayba, 53) Paullinia, Smilaceae – 54) Smilax, Solanaceae – 55) Solanum, Urticaceae – 56) Cecropia, Verbenaceae – 57) Lippia, Xyridaceae – 58) Xyris, Arecaceae – 59) Mauritia, 60) Cyperaceae, Alismataceae – 61) Echinodorus, 62) Sagittaria, Eriocaulaceae – 63) Eriocaulon, Haloragaceae – 64) Myriophyllum, Nymphaeaceae – 65) Nymphaea.

Paullinia (Plate II.3, figure 53)

Pollen description: grain monad, asymmetric, medium size, tricolporate syncolpate, amb triangular convex, oblate, exine reticulate homobrochate, pore circular. Size ~25-30 µm.

Ecological information: vine of 0.5 to 5 m height, usually found in occasionally flooded gallery forest, also associated with the edge of *vereda*, and secondarily in grassland/forest transition (Sano et al., 2008; Flora do Brasil 2020).

Smilaceae

Smilax (Plate II.3, figure 54)

Pollen description: grain monad, heteropolar, radially symmetric, small size, inaperturate, spheroidal, amb circular, exine verrucate. Size ~16 µm.

Ecological information: woody vine growing from 0.5 to 5 meters in height. This vine is generally observed in cerrado *sensu lato*, *vereda*, and gallery forest (Sano et al., 2008 and Flora do Brasil 2020).

Solanaceae

Solanum (Plate II.3, figure 55)

Pollen description: grain monad, isopolar, radially symmetric, small size, tricolporate, suboblanceolate or spheroidal, amb subtriangular, exine psilate, pore lalongate- zonoporate. The pores form a ring projection around the grain. Size ~16 µm.

Ecological information: herbaceous or shrub plant typical of the Cerrado and sometimes growing on the edge of swamp when the water table is below ~30 - 85 cm deep (Santos and Munhoz, 2012). It grows in open cerrado, cerrado *sensu stricto*, cerradão and gallery forest (Sano et al., 2008).

Urticaceae

Cecropia (Plate II.3, figure 56)

Pollen description: grain monad, apolar, asymmetric, small size, diporate, subprolate, amb circular, exine psilate, pore circular. Size 8-10 µm.

Ecological information: lower storey and light-demanding trees, 6-9 m height, that grows on moist and well-drained soils (Felfili, 1995; van der Berg and Oliveira-Filho, 2000). It is generally observed in riparian and gallery forest, and in cerrado *sensu lato* (Sano et al., 2008). It is a pioneer that stabilizes the woodland (Felfili, 1997).

Verbenaceae

Lippia (Plate II.3, figure 57)

Pollen description: grain monad, isopolar, radially symmetric, medium size, tricolporate, sub-prolate, amb subtriangular, exine thick and psilate, pore lalongate slightly rectangular. The pores form a ring projection around the grain. Size ~25 µm.

Ecological information: shrub to subshrub, 0.5 to 2 m in height, usually growing in cerrado *sensu lato* (moist open cerrado, cerrado *sensu stricto*, cerradão), and at the edge of *veredas* (swamp) (Sano et al., 2008; Flora do Brasil 2020).

Vitaceae

Cissus (Plate II.3, figure 51)

Pollen description: grain monad, isopolar, symmetric, medium size, tricolporate, sub-prolate or prolate, amb trilobate, exine microreticulate homobrochate, pore circular traversing and dividing the colpus, colpi with constriction and costa. Size ~25 µm.

Ecological information: vine plant (Araujo et al, 2002) usually growing in primary and secondary *terra firme* forests, sometimes in humid soil forest, at the edge of the forest/savanna transition (Lombardo, 1996). It is observed in cerrado *sensu lato*, cerradão, and in riverine and dry forests (Sano et al., 2008; Flora do Brasil, 2020).

Xyridaceae

Xyris (Plate II.3, figure 58)

Pollen description: grain monad, bilaterally symmetric, big size, monosulcate, ellipsoidal, exine microreticulate. Size ~32 µm.

Ecological information: herbaceous heliophyte usually growing in places with high edaphic moisture. It is observed in moist open cerrado (Munhoz and Felfili, 2008) and swamps (*veredas*) (Matias et al, 2021). Common in moist open cerrado, marsh, *vereda* and less common in gallery forest (Felfili et al, 2007; Sano et al., 2008).

Water-level related taxa

Arecaceae

Mauritia (Plate II.3, figure 59)

Pollen description: grain monad, heteropolar, radially symmetric, big size, monoporate, amb circular, exine echinate, pore circular. Size ~32 µm (59a) and ~35 µm (59b).

Ecological information: palm tree with 5 to 20 m height. It is a hydromorphic taxa that grows in humid or flooded soils, usually forming the *vereda* (palm swamp), and in gallery forest (Sano et al., 2008; Flora do Brasil, 2020).

Cyperaceae (Plate II.3, figure 60)

Pollen description: grain monad, heteropolar, bilaterally symmetric, medium size, porate (3 to 4 pores), irregular grains, scabrate to microreticulate. Size ~30 µm (60a) or ~20µm (60b).

Ecological information: herbaceous taxa associated with humid soil and swampy areas, close to lake. Their presence suggests that the groundwater table is close to the soil surface (Araujo et al, 2002). In the Cerrado biome, it is observed in cerrado *sensu lato*, humid open cerrado, vereda and marsh (Sano et al., 2008).

Alismataceae

Echinodorus (Plate II.3, figure 61)

Pollen description: grain monad, apolar, asymmetric, medium size, periporate, spherical, exine scabrate to finely microreticulate, pore circular inconspicuous. Size ~20 µm

Ecological information: rooted floating and amphibious life forms. They grow at 20 to 30 cm water depth; during the dry season, they are sensitive to changes of the water-table and become reduced or lacking when the water-table reduces (Moreira et al., 2011).

Sagittaria (Plate II.3, figure 62)

Pollen description: grain monad, apolar, asymmetric, medium size, periporate, spherical, exine echinate, pore circular inconspicuous. Size ~25 µm.

Ecological information: rooted floating and amphibious life forms, growing at 20 to 30 cm water depth. *Sagittaria* is less sensitive to changes of the water-table, reporting continuous presence in dry or wet seasons (Moreira et al., 2011).

Eriocaulaceae

Eriocaulon (Plate II.3, figure 63)

Pollen description: grain monad, apolar, asymmetric, medium size, colporate, espiraperturate, spheroidal, exine echinate. Size ~25 µm

Ecological information: emergent and rooted floating plant, present only during the flooded season (Moreira et al., 2011).

Haloragaceae

Myriophyllum (Plate II.3, figure 64)

Pollen description: grain monad, medium size, stephanoporate (5-pores), circular, suboblate, exine psilate, circular pore with annulus. Size ~25 µm.

Ecological information: submerged rooted-plant that grows at 1 to 2 m of water depth and relates to light availability to survive. It is sensitive to environmental changes as, for instance an increase in shadowiness or the competition with other macrophytes which can threaten its subsistence (Wersal, 2010).

Nymphaeaceae

Nymphaea (Plate II.3, figure 65)

Pollen description: grain monad, medium size, zonosulcate, circular, suboblate, exine psilate. Size ~25 µm.

Ecological information: rooted floating hydrophyte that grows at 1 to 2 m water depth. It presents low sensitivity to flooding and can survive to changes in water depth (Brock et al., 1987; Bernhardt and Willard, 2009).

3.2. Ecological and morphological traits of pollen taxa

Of the 58 terrestrial pollen taxa, the great majority - 42 taxa - are characterized by the entomophilous pollination syndrome (Table II.1). Seven taxa present other types of biotic pollination syndrome (chiropterophilous, ornithophilous, psychophilous, zoophilous, and cantharophyloous). Of the remaining nine taxa, four have exclusive anemophilous syndrome - the Euphorbiaceae genera *Acalypha* and *Alchornea*, the Rubiaceae genus *Simira*, and the family Poaceae, and five have both anemophilous and entomophilous syndromes. In the lake Feia record, the influx of entomophilous pollen is dominant in most samples (Fig. II.2), while in the Getulio swamp record, entomophilous pollen predominates in the bottom part of the core and anemophilous pollen is dominant in the upper part, from 150 cm-depth to the top. The Poaceae family is the largest contributor to the accumulation rate of anemophilous pollen, with lower contributions of the grass *Acalypha*, and of the trees *Alchornea* and *Simira*, in the case of VGE-17 (Table II.1).

From the 58 terrestrial pollen taxa, the great majority, 38 taxa, are produced by lower storey trees, eight taxa are produced by plants of the shrubby stratum, seven from the field stratum and five from medium storey forest trees. Regarding pollen influx variations, in the case of LFB1, pollen influx from lower canopy forest (2-10 m), composed of cerrado trees (*Astronium*, *Byrsonima* *Casearia*, *Curatella* and *Ternstroemia*), and gallery forest (*Alchornea*, *Anadenanthera*, *Banisteropsis*, *Dalbergia*, *Euterpe*, *Ilex*, Menispermaceae, Moraceae, Myrtaceae, *Myrsine* and *Tapirira*) and pioneer forest trees (*Cecropia*, *Celtis*, *Trema*), were dominant throughout the core, followed by pollen from the ground stratum (<50 cm) (Poaceae dominates), which increases at the top, between 37 and 85 cm depth. In the case of VGE-17, pollen deposition from field taxa was the most abundant, except between 170 and 154 cm, when pollen from low canopy forest dominates, mainly represented by cerrado tree *Cissus* and *Eriotheca*, and moist forest *Dialium*, *Melastomataceae-Combretaceae*, *Ilex*, *Hedyosmum* (Fig. II.2). Pollen from the middle stratum (≥ 15 m) were less abundant in both records (represented by *Apeiba* and *Ouratea* for LFB1, and *Emmotum*, *Machaerium*, and *Protium* for VGE-17). In VGE-17, a fourth stratum (shrubs, <2m) was observed, represented by the taxa *Acalypha*, *Baccharis*, Ericaceae, *Eryngium*, *Lippia*, *Mimosa*, *Sabicea*, and *Solanum*, and increased between 192 and 160 cm of depth which is coupled by an increase in pollen from lower and medium storey. Generally, when lower storey pollen are abundant the field stratum signal reduces (Fig. II.2A), contrary when field is abundant the lower storey influx reduces (Fig. II.2B). This pattern is observed principally in VGE-17, meanwhile in LFB1, near the top of the core (37-85 cm of depth) both are present although lower storey dominates.

Regarding pollen size, 30 of the terrestrial pollen taxa and six of the water-level related taxa classified as medium, 22 of the terrestrial pollen taxa classified as small, and only six terrestrial pollen and one water-level taxa classified as big (large size) (Fig. II.2). In the LFB1 core, the influx of small pollen was slightly higher than medium pollen in most samples, while for VGE-17, medium size pollen were more abundant throughout the core (Fig. II.2A and Table II.1). Influx of large pollen was very low in LFB1 (represented only by *Apeiba*) and low in VGE-17 (represented by *Caryocar*, *Drosera*, *Ericaceae*, *Eriotheca* and *Sabicea*) (Fig. II.2B and II.Table 1).

Regarding the influx of water-level related taxa, in the case of LFB1 (total aquatic – Fig. II.2A), higher influxes were observed between depths 37-91 cm, 109-127 cm, 161-197 cm, and 241-285 cm of depth, when they decreased between 37 and 285 cm, they were replaced by an increase in terrestrial pollen, also, at the top and bottom of the core a general reduction in terrestrial and aquatic pollen influx. In the case of VGE-17, the influx of water level-related taxa (represented only by *Mauritia* – Fig. II.2B) follows the terrestrial pollen deposition, increases from 298 to 150 cm and then decreases towards the top, suggesting a drying out of the depositional environment.

Table II.1. pollen taxa classification in response to their pollination syndrome, life form, and physiognomy and strata vegetation from the Cerrado cores LFB1 and VGE-17. PS – pollination syndrome; LF – life form; P – physiognomy; S – stratum; an – anemophilous; en – entomophilous; chi – chiropterophilous; orn – ornitophilous; psy – psychophilous; zoo – zoophilous; can – cantharophyloous ; hyd – hydrophilous; op – open (grassland cerrado); in – intermediate (scrubby cerrado, cerrado sensu stricto); clo – closed (cerradão, gallery forest); la – lake; fi – field (< 1 m)); sh – shrubby (1 – 2 m); lo – lower storey (< 10 m); me – medium storey (~15 m).

Family	taxon	PS	LF	P	S	LFB1	VGE-17
Amaranthaceae	<i>Gomphrena</i>	en	herb, subshrub	in	fi		X
Anacardiaceae	<i>Astronium</i>	en	tree	clo	lo	X	
Anacardiaceae	<i>Tapirira</i>	en	tree	clo	lo	X	
Apiaceae	<i>Eryngium</i>	en	herb	in	sh		X
Aquifoliaceae	<i>Ilex</i>	en	tree	clo	lo	X	X
Arecaceae	<i>Euterpe</i> type	en	tree	clo	lo	X	X
Asteraceae	<i>Baccharis</i> type	en	herb, shrub	in	sh		X
Boraginaceae	<i>Cordia</i>	chi, orn	tree, shrub	clo	lo		X
Brassicaceae	Brassicaceae type	en	herb	in	fi		X
Burseraceae	<i>Protium</i>	en	tree	clo	me		X
Cannabaceae	<i>Celtis</i>	an, en	tree	clo	lo	X	X
	<i>Trema</i>	an, en	tree	clo	lo	X	
Caryocaraceae	<i>Caryocar</i>	chi	tree	in	lo		X
Chloranthaceae	<i>Hedyosmum</i>	en	tree	clo	lo		X
Cunoniaceae	<i>Lamanonia</i>	en	tree	clo	lo		X
Dillenaceae	<i>Curatella</i>	en	tree	in	lo	X	
Droseraceae	<i>Drosera</i>	zoo	herb	op	fi		X
Ericaceae	Ericaceae type	en, orn	shrub	in	sh		X
Euphorbiaceae	<i>Acalypha</i>	an	herb, shrub	clo	sh		X
	<i>Alchornea</i>	an	tree	clo	lo	X	
Fabaceae (mim)	<i>Anadenanthera</i>	en	tree	clo	lo	X	X
	<i>Mimosa</i>	en	subshrub	in	sh		X
	<i>Piptadenia</i>	en	tree	clo	lo		X
Fabaceae (pap)	<i>Dalbergia</i>	en	tree	in	lo	X	
	<i>Dialium</i>	en	tree	clo	lo		X
	<i>Machaerium</i>	en	tree	clo	me		X
Icacinaceae	<i>Emmotum</i>	en	tree	clo	me		X
Lythraceae	<i>Cuphea</i>	en	herb, shrub	op	fi		X
Malvaceae	<i>Apeiba</i>	en	tree	clo	me	X	
	<i>Eriotheca</i>	en	tree	clo	lo		X

Malpighiaceae	<i>Banisteropsis</i>	en	vine	clo	lo	X	
	<i>Byrsinima</i>	en	tree	in	lo	X	X
Melastomataceae	Melastomataceae-Combretaceae	en	tree	clo	lo		X
Meliaceae	<i>Guarea</i>	en, psy	tree	clo	lo		X
Menispermaceae	<i>Abuta</i>	en	shrub	in	lo		X
	Menispermaceae	en	herb, shrub, tree	in	lo	X	X
Moraceae	Moraceae	an, en	tree	clo	lo	X	X
Myrtaceae	Myrtaceae	en	tree	clo	lo	X	X
Ochnaceae	<i>Ouratea</i>	en	tree	in	me	X	
Pentaphylacacées	<i>Ternstroemia</i>	en	tree	clo	lo	X	
Phyllantaceae	<i>Hyeronima</i>	en	tree	in	lo		X
Piperaceae	<i>Peperomia</i>	an, en	herb, shrub	clo	lo		X
Poaceae	Poaceae	an	herb	op	fi	X	X
Polygalaceae	<i>Polygala</i>	en	herb	op	fi		X
Primuliaceae	<i>Cybianthus</i>	en	tree	clo	lo		X
	<i>Myrsine</i>	en	tree	clo	lo	X	
Rubiaceae	<i>Guettarda</i>	orn	tree	in	lo		X
	<i>Sabicea</i> type	en	shrub	in	sh		X
	<i>Simira</i>	an	tree	clo	lo		X
Salicaceae	<i>Casearia</i>	en	tree	in	lo	X	X
Sapindaceae	<i>Matayba</i>	en	tree	clo	lo		X
	<i>Paullinia</i>	en	vine	clo	lo		X
Smilaceae	<i>Smilax</i>	en	vine	in	lo		X
Solanaceae	<i>Solanum</i>	en	shrub	in	sh		X
Urticaceae	<i>Cecropia</i>	an, en	tree	clo	lo	X	
Verbenaceae	<i>Lippia</i>	en	subshrub	in	sh		X
Vitaceae	<i>Cissus</i>	en	vine	in	lo		X
Xyridaceae	<i>Xyris</i>	zoo	herb	op	fi		X
Watrep level-related							
Arecaceae	<i>Mauritia</i>	can	tree palm	op	me		X
Cyperaceae	Cyperaceae	an	herb	op	fi	X	X
Alismataceae	<i>Echinodorus</i>	hyd	herb	la	fi	X	
	<i>Sagittaria</i>	hyd	herb	la	fi	X	X
Eriocaulaceae	<i>Eriocaulon</i>	hyd	herb	la	fi	X	X
Haloragaceae	<i>Myriophyllum</i>	hyd	herb	la	fi	X	
Nymphaeaceae	<i>Nymphaea</i>	hyd	herb	la	fi	X	

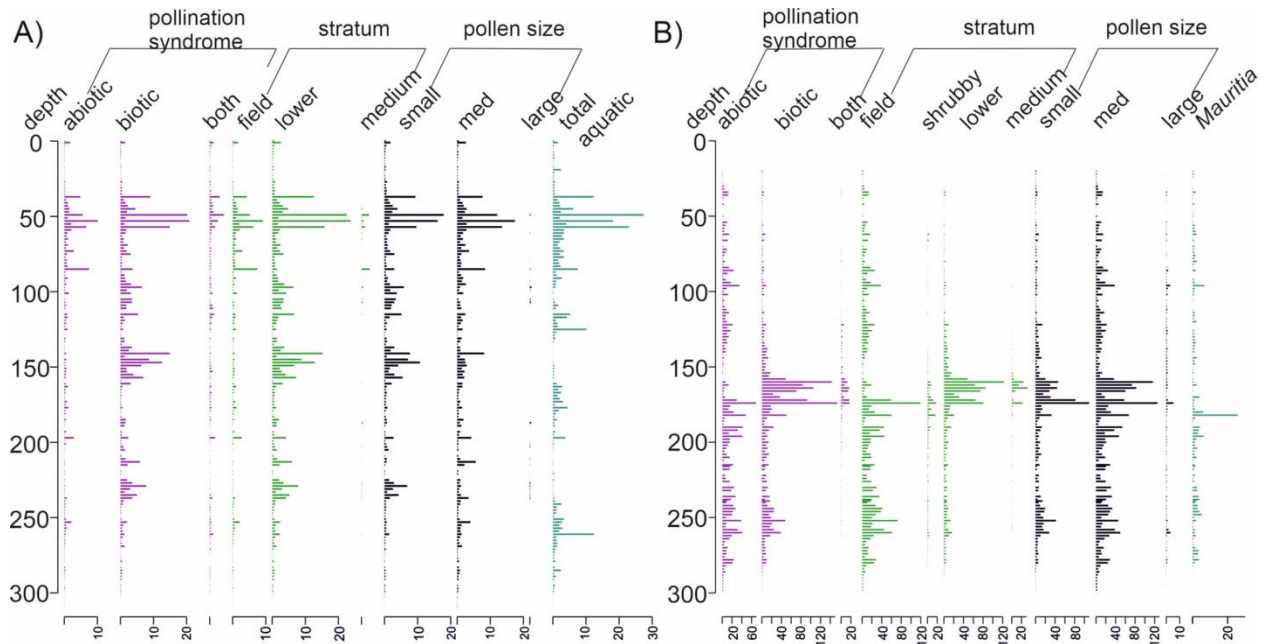


Figure II.2. Synthetic diagram of pollen influx ($\text{mm}^2/\text{cm}^2/\text{yr} \times 1000$) from LFB1 (A) and VGE-17 (B) sediment cores, were we showed the pollen depositions sums in relation to their pollination syndrome (purple color), the stratum from which they come (green color), and their pollen size (dark color). Additionally it has been added the pollen taxa water level-related (green-blue color), for of LFB1 (total aquatic taxa) and for VGE-17 (Mauritia). The diagram was represented in a scale of depth (cm). abiotic=anemophilous, both=biotic/abiotic, field=<50cm, shrubby=<2m, lower=2-10m, medium=>15m, small=<15 μm , med=15-25 μm , large=26-49 μm .

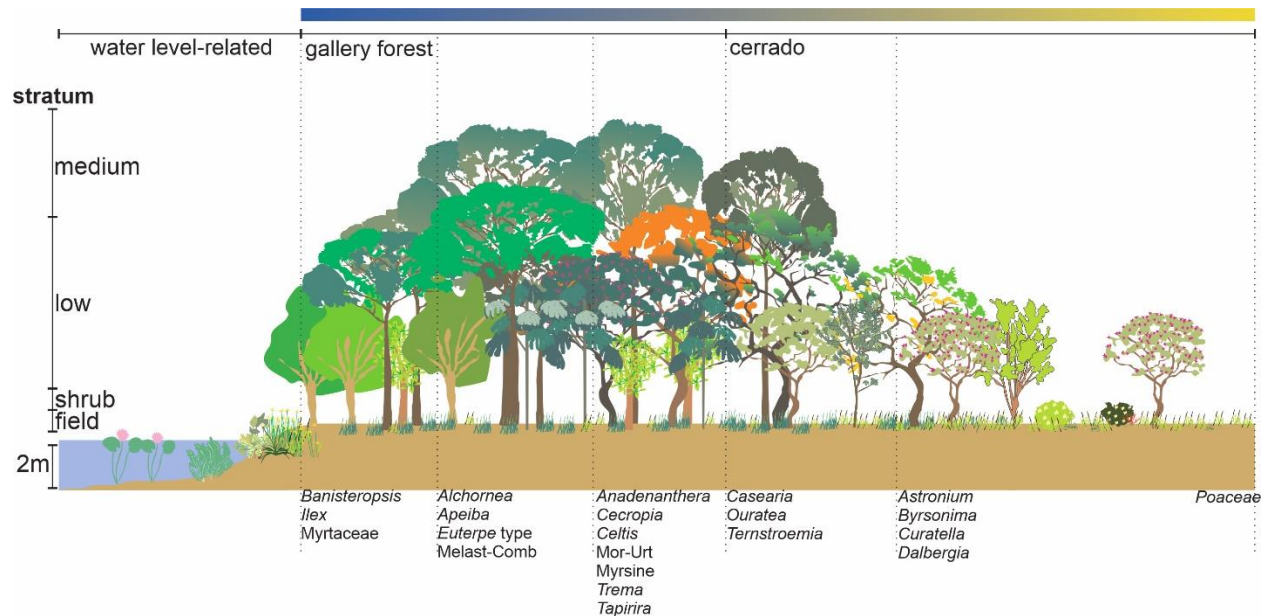


Figure II.3. Schematic representation of the principal phytophysiognomies in lake Feia, showing the list of main pollen taxa identified in the LFB1 core related to the determined classification based in table 1. The band on the top of the schema shows water availability on the soil, from high (blue) to low (yellow).

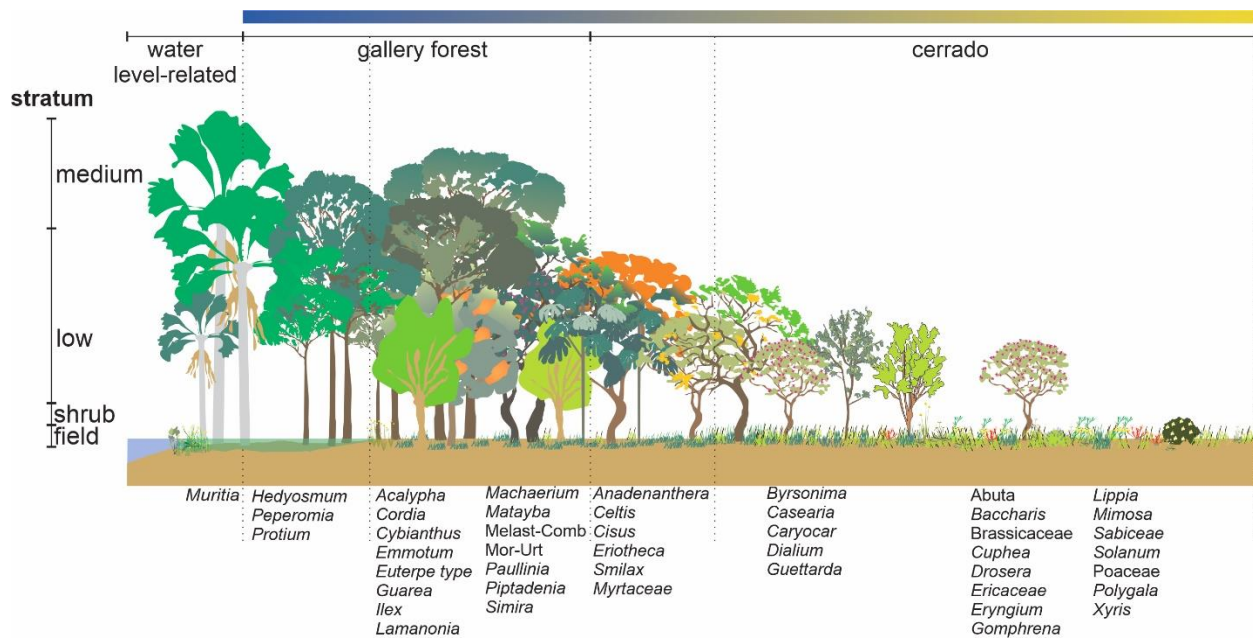


Figure II.4. Schematic representation of the principal phytophysiognomies in “Varjão do Getulio” swamp, showing the list of main pollen taxa identified in the VGE-17 core related to the determined classification based in table 1. The band on the top of the schema shows water availability on the soil, from high (blue) to low (yellow).

4. Discussion

Our results showed that a large majority of taxa that occur on the pollen deposits are characterized by biotic pollination syndromes, with predominance of the entomophilous dispersion. This is in agreement with botanical studies, which have shown that in the Cerrado vegetation, 50 to 80 % of plant species have the entomophilous syndrome, with bees as the main pollinators, while the other types of biotic syndromes concern less than 20 % of plant species (Martins and Batalha, 2006; Gottsberger and Silberbauer-Gottsbeger, 2018). Anemophilous dispersion has been observed in ≤ 20 % of plant species, in majority grasses and sedges (Freitas and Sazima, 2006; Jacobi and do Carmo, 2011). In our records, the accumulation rate of anemophilous dispersed pollen is mainly dictated by the influx of grasses (field stratum) and is only dominant in the upper part of the VGE-17 core in which forest trees and shrubs are very low. In the case of LFB1 arboreal pollen recorded higher values than grasses, suggesting that forest form are dominant throughout the core (Fig. II.3), while pollen assemblages for the VGE-17 core suggest a change of closed to open physiognomies (Fig. II.4). Despite the biotic syndrome, other characteristics from pollen and the environment should be considered.

The LFB1 and VGE-17 are located in flat areas, then the influence of pollen coming from highlands is assumed to be very low. In both cores, pollen deposition changed according to water availability, however, in different ways. In the case of LFB1, increases in the accumulation of terrestrial pollen were linked to reductions in aquatic plant deposition, indicating that the reduction of the lake water-level allowed terrestrial vegetation to advance towards the coring site increasing terrestrial pollen deposition (Escobar Torrez et al., 2023). On the other hand, VGE-17 showed a

different response to changes in water availability, with a reduction in terrestrial pollen deposition when the water level-related pollen taxa reduced (*Mauritia* palm swamp dried) towards the top of the core, and conversely, when the availability of water increases (the drainage was probably wider) the swamp was replaced by arboreal elements (gallery forest) towards the bottom of the core (Escobar-Torrez et al., 2023b *in prep.*). Pollen preservation is mostly affected when there is a succession of dry/wet intervals that affect the sedimentary environment by increasing the oxidation process (Tweddle and Edwards, 2010; Xu et al., 2016), these changes highlight the susceptibility and rapid response to disturbances (e.g. climate change) of swamp areas since the water table in the swamp is more readily affected than lakes when subject to prolonged reduction in water availability. An assessment of differences in pollen preservation in peat-soils showed that an increase or decrease in water availability, in addition to responding to local factors, is also capable of showing variations in response to climatic events (Xu et al., 2016). On the other hand, pollen transport seems to be affected by the type of stratum adjacent to the sediment environment, where a higher rate of recorded pollen accumulation and reduction in pollen taxa diversity suggests a direct deposition by gravitation (Jacobson and Bradshaw, 1981) compared to the other types of transport (like rain), which would be in agreement with an increase of the forest canopy in areas close to the study site, previously suggested in both studies (Escobar-Torrez et al., 2023a; 2023b *in prep*), and indirectly imply a change in precipitation patterns, less or more rain.

Regarding pollen size, small pollen tended to be the most abundant type in LFB1 while in VGE-17 medium pollen tended to dominate. Large pollen grains were also more consistently present in VGE-17 than in LFB1. These differences regarding pollen sizes reflect differences in pollen deposition on lakes and swamps. Although concentration difference between small and medium pollen sizes aren't stronger, they seem to indicate that in wetter periods both sites increased the concentration of medium pollen, more evident at VGE-17 (Escobar-Torrez et al., 2023b *in prep*), while at LFB1 this variation is less evident, although the concentration of small pollen appears to be above that of medium pollen in the three dry periods (Escobar-Torrez et al., 2023a). The fact that LFB1 has a lower pollen concentration in wet periods is expected, especially when river influence is minimal or non-existent (Xu et al., 2016), in Lake Feia the river originates less than 5km away which reduces the possibility of a higher accumulation coming from water transport. In the case of VGE-17 the presence and dominance of medium pollen over small pollen also seems to be directly influenced by precipitation, between 154-298 cm depth. Both cores show an increase of medium pollen when periods of higher precipitation are suggested. Few studies have been conducted on the effect of climate on pollen size. For example, Ejsmond et al (2011; 2015) have made measurements on the size of pollen types and attempted to compare them with temperature gradient, showing a positive relationship with temperature, arguing for an increase in pollen size when conditions changes to drier and warmer (positive relation between temperature and pollen grain size) favoring the conservation in moisture and ensures longer pollen viability. A recent study looking at variations in fossil pollen suggests that the same pollen type may increase (decrease) in size at higher (lower) temperatures between glacial and interglacial periods (McCulloch et al., 2022). However, in our sites, the presence of the cerrado physiognomy suggests that temperature was mostly warm, so detecting temperature related size patterns would be difficult to distinguish. On the other hand, although little evidence for variation on pollen size in function of precipitation variability has been found (Jardine and Lomax, 2017), a study assessing pollen size along a

precipitation gradient shows a positive relationship between increased precipitation and increased pollen size (Zhang et al., 2017), in agreement with our interpretations. Thus both records show that for paleoclimatic reconstructions more than one factor must be taken into account in heterogeneous environments such as the Cerrado.

5. Conclusion

The morphological and ecological characteristics of the Cerrado pollen grains suggest that entomophilous taxa dominate in the biome since the last 15,000 years, with a dominance of pollen assemblages from arboreal physiognomies at lake Feia, and a range of open to closed physiognomies for Getulio swamp. Despite the evidence of local signal in both cores, the presence of regional pollen taxa was also observed, although it is related to the degree of opening of the physiognomies near the coring site (stratum).

On the other hand, the depositional environment depends on wet/dry phases, and will be able to reflect variations in pollen concentration in relation to water availability. Thus, at lake Feia the pollen deposition may be inversely related to the depth of the lake, therefore, when the lake is deeper the stored pollen deposition reduces while as the lake reduces in depth the pollen deposition increases. This pattern continues to be observed at VGE-17, which is more susceptible to this change in water availability, with a change from wet to dry phase that increases the process of oxidation and aerial exposure of pollen (soils reduce in humidity) reducing the concentration of pollen from the bottom to the top of the core.

In relation to the depositional environment and stratum, as long as there is a relationship of increased pollen concentration coupled with a decrease in diversity, pollen deposition is direct (by gravitation), and the opposite is to be expected in more open stratum environments, when the composition of arboreal elements reduces and produces an heterogeneous landscape the vegetation allows the depositional environment to receive transported pollen from other sources (wind, rain). Finally, pollen size, although not reflecting a direct response to changes in temperature likely relates to periods of higher rainfall in our records, with larger pollen size during wetter climatic conditions.

6. Acknowledgements and Funding

We thank the ISEM and DEGEO-UFOP laboratories for allowing the use of their facilities and providing the space and equipment for the development of the research. Financial support was provided by IRD and FAPDF (0193.001374/2016). Katerine Escobar-Torrez benefited from a PhD position funded by the IRD ARTS program and the French Embassy in Bolivia.

Article 2

Long- and short-term vegetation change and inferred climate dynamics and anthropogenic activity in central Cerrado during the Holocene

Soumis à Journal of Quaternary Science, doi: 10.1002/jqs.3567

Katerine Escobar-Torrez^{1, 2}, Marie-Pierre Ledru¹, Raquel Franco Cassino², Paula Ribeiro Bianchini³, Elder Yokoyama³

1. Institut des Sciences de l'Evolution de Montpellier (ISEM), Université de Montpellier-CNRS-IRD-EPHE, France
2. Departamento de Geologia-Universidade Federal de Ouro Preto, Brazil
3. Instituto de Geociências, Universidade de Brasília, Brazil

Correspondence: Katerine Escobar-Torrez

Institut des Sciences de l'Evolution, ISEM (UMR 226 – IRD/ CNRS/UM2), 34095 Montpellier cedex 05, France. E-mail: katerine.escobartorrez@ird.fr

Abstract

A paleoecologic analysis of pollen, macrocharcoal and trace elements from a lacustrine sediment core located at Lake Feia, central Cerrado (Goiás State, Brazil), was used to evaluate the relationship between vegetation, fire and climate during the Holocene. The development of cerrado vegetation appears to have begun 6000 years ago, initially with the establishment of an open cerrado, followed from 4800 cal a BP by a change to a woody cerrado driven by summer insolation. The increases in precipitation levels in central Cerrado during the last 5000 years are related to the increased influence of the Amazon in central Brazil, which has facilitated biomass burning and anthropogenic activities in the region of Lake Feia. Multi-centennial-scale changes in water level-related and gallery forest pollen assemblages indicate three main dry episodes, at 3440–2760, 2700–1690 and 1330–1150 cal a BP, linked to regional shifts between northern and southern South American summer monsoon boundaries. The presence of low continuous fire activity did not appear to affect vegetation recovery, whereas two intervals with increased fire activity, at ~3300 and ~1300 cal a BP, indicated a slower recovery.

Keywords: Tropics, pollen, insolation, fire, South American summer monsoon

1. Introduction

The Cerrado biome in central Brazil covers about 2 million km². It represents a diverse ecosystem, harboring 4800 endemic plant and vertebrate species (Strassburg et al., 2017), and, as most of the Brazilian basins originate in central Brazil, is an important source of freshwater (Lima et al., 2011). However, despite its high biodiversity and socioeconomic importance, the destruction of this ecosystem is continuing at an accelerated rate (Vieira et al., 2022). Intensive human disturbance, including deforestation and the use of fire, has destabilized natural processes within the ecosystem, thereby increasing hydric stress (Hofmann et al., 2020) and the frequency and severity of fire events (Colli et al., 2020). Future projections for the Cerrado indicate a loss of plant diversity (Velazco et al., 2019), underlining the importance of implementing integrated fire management practices, and combining scientific research with traditional knowledge to address fire management problems (Schmidt and Eloy, 2020).

Floral distribution patterns vary widely across the Cerrado domain (Vieira et al., 2022), the landscape being characterized by vegetation physiognomies ranging from open grassland to dense woodland (Ribeiro and Walter, 2008), with close relationships between vegetation, climate, soil condition and fire frequency (Henriques, 2005; Bueno et al., 2018). Today, two main climatic features, the seasonal South American summer monsoon (SASM) and the spatial shifts of the inter-tropical convergence zone (ITCZ), result in bimodal rainfall seasonality, with high rainfall from October to March and low rainfall from April to August (Reboita et al., 2010; Marengo et al., 2012).

In the tropical lowlands of South America, paleoclimatic studies indicate a trend toward more wet conditions during the Last Glacial Maximum (21,000 cal a BP) and the Younger Dryas (12,700–11,000 cal a BP) in western Amazonia, north-eastern Brazil (NEB), and central and south-eastern Brazil (SEB) (Cruz et al., 2009; Deininger et al., 2019). During the early and mid-Holocene, the presence of a precipitation dipole between NEB and SEB in response to north/south hemisphere summer insolation was characterized by longer wet and dry seasons, respectively (Cruz et al., 2009). However, speleothem records have also revealed that central Cerrado underwent numerous fluctuations in wet and dry episodes between 11,000 and 4000 cal a BP (Ward et al., 2019; Azevedo et al., 2021; Wong et al., 2021), with longer wetter episodes in the last 4000 cal a BP (Strikis et al., 2011; Campos et al., 2019), implying both regional and local influences on seasonality. Paleoecologic studies of the Cerrado are rare and discontinuous in space and time. They also show a wide range of responses depending on location, with cerrado vegetation undergoing several episodes of expansion and retreat from 11,000 cal a BP, in response to the variability of local climatic conditions from east to west, and north to south (Ferraz-Vicentini and Salgado-Labouriau, 1996; Behling, 2002; Ledru et al., 2006; Horák-Terra et al., 2020). In northern and central Cerrado, floristic changes from cooler to warmer assemblages characterize the transition from the last glacial to the Holocene (Cassino et al., 2018 and 2020; Horák-Terra et al., 2020; Ledru et al., 2006). More contrasted responses have been observed during the early Holocene, with centennial-scale fluctuations in wet and dry conditions in the central region until 6000 cal a BP (Cassino et al., 2018

and 2020), the full expansion of the Cerrado in northern Brazil from 11,000 cal a BP (Ledru et al., 2006), and the persistence of wet and cold conditions in the northeastern region of central Cerrado (Horák-Terra et al., 2020; Lima Sabino et al., 2021). During the mid-Holocene the vegetation became drier (Salgado-Labouriau et al., 1998; Barberi et al., 2000; Cassino et al., 2020), responding to a weaker SASM influence over eastern Brazil (Prado et al., 2013a and 2013b). During the late Holocene, multi-centennial fluctuations between wet and dry conditions in northern Minas-Gerais indicate the expansion of a drier Cerrado after 4000 cal a BP (Cassino et al., 2018), and two drier episodes at 2900 and 900 cal a BP (Lima Sabino et al., 2021). However, the low resolution of the analyses (e.g., Barberi et al., 2000), the absence of macrocharcoal analyses (e.g., Horák-Terra et al., 2020), and the loss of sediment from the upper levels (e.g., Ledru et al., 2006) have prevented a reconstruction of the relationship between vegetation, fire and climate for the last 5000 years, as well as the process of cerrado vegetation recovery after the mid-Holocene dry episode. Moreover, the Cerrado region has been inhabited for at least 15,000 years (Prous and Fogaça, 1999), with archeological sites indicating a decrease in human occupation during the early–mid-Holocene in southern Cerrado (Araújo et al., 2005), followed by an increase in the late Holocene (Barbosa et al., 2020). Human occupation in the Cerrado is associated with fire activity (Pivello et al., 2021), and deciphering wild from anthropogenic fire is critical to understanding the relationship between fire and climate, and its role in the distribution and composition of cerrado vegetation (Schmidt and Eloy, 2020).

Lake Feia is located in central Cerrado, where pollen analyses have revealed a high sensitivity to climate change between 19,000 and 5000 cal a BP (Ferraz-Vicentini, 1999; Cassino et al., 2020). The LFB1 and LFB2 sediment cores were collected in 1990 (Turcq et al., 2002), while the LF 15-2 core was collected in 2015. Pollen and microchacoal analyses have been conducted on 20 samples covering the upper part of core LFB2 (375 cm deep,) representing the last 6000 years, with a resolution of approximately 260 years between samples (Ferraz-Vicentini, 1999). Pollen and macrocharcoal analyses have been conducted on core LF15-2 (500 cm deep), dating from 19,000 to 5000 cal a BP (Cassino et al., 2020). Core LFB2 has revealed the expansion of a woody cerrado, with two drier intervals, from 5280 to 4850 and 3010 to 2100 cal a BP, and a gradual reduction in more humid conditions until the present (1990 AD) (Ferraz-Vicentini, 1999). Abundant charred particles have been observed throughout the record until 770 a BP (Ferraz-Vicentini, 1999). However, the low sampling resolution does not allow a comparison of the vegetation changes with other paleoclimatic studies based on, for example, speleothems. Thus, to improve our knowledge of the Cerrado biome during the late Holocene, and more particularly our understanding of the relationships between fire, climate, biodiversity and human activity, we performed high-resolution pollen, charcoal and geochemical analyses on the upper 310 cm of core LFB1, representing the last 5000 years. We then compared the results with other sediment and speleothem records, and reconstructed a synthetic framework for the responses of central Cerrado to climatic and anthropogenic effects during the late Holocene.

2. Material and methods

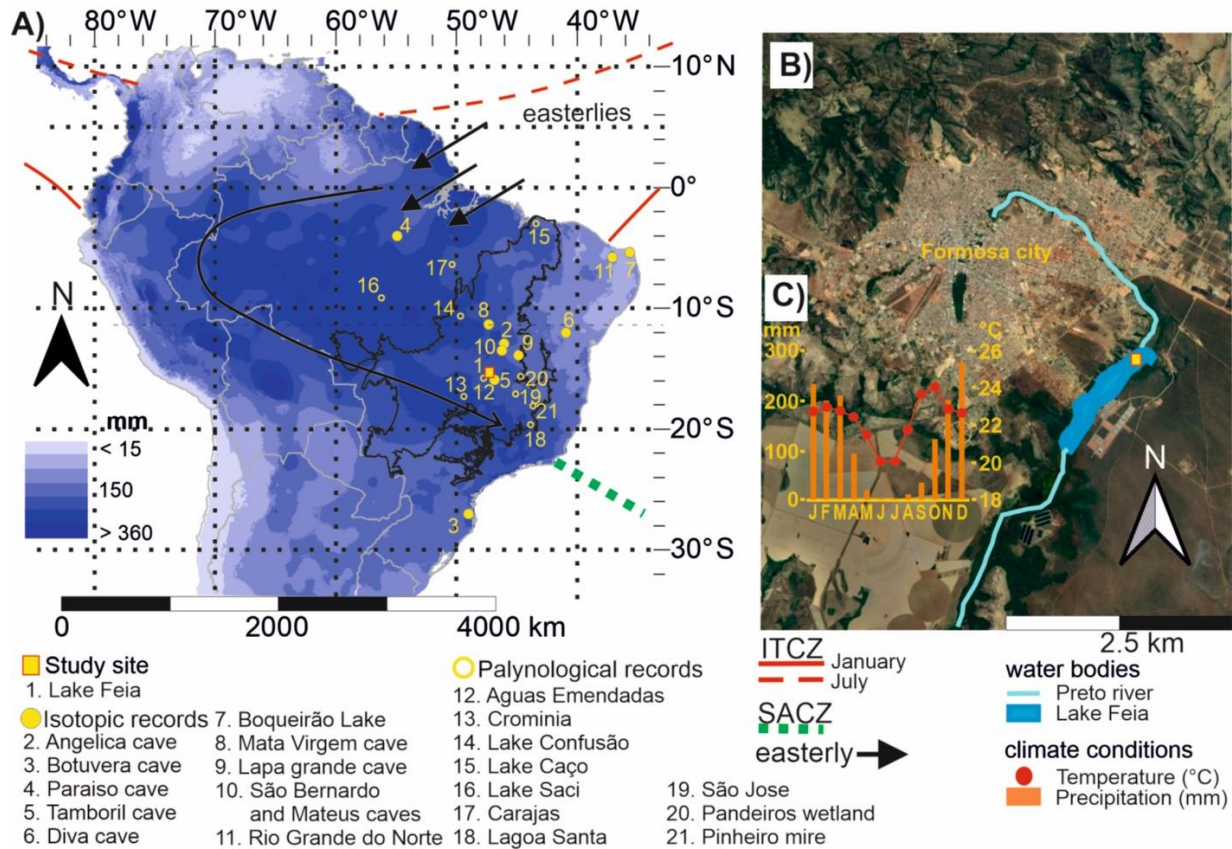


Figure III.1. (A) A map of the mean austral summer precipitation levels, showing the position of the ITCZ, the core region of the summer monsoon today (dark blue), the limit of the Cerrado biome (black line), and the location of Lake Feia and the pollen and isotopic records discussed in the text. (B) A satellite view of Lake Feia (source Google Earth) showing its location relative to Formosa and Preto River. (C) A climate diagram for the city of Formosa (INMET, 2022).

2.1 Study area

Lake Feia ($15^{\circ}34'20"S$, $47^{\circ}18'20"W$, altitude 871 m) is located in the vicinity of the city of Formosa, Goiás State, in central Cerrado (Fig. III.1A), Brazil. It is 3.5 km long, elongated in a northeast (NE)–southwest (SW) direction, 5 m deep (Fig. III.1B), and probably of tectonic origin (Ferraz-Vicentini, 1999). Preto River crosses Lake Feia, entering in the NE and exiting in the SW (Fig. III.1B). Currently, macrophytes (*Nymphaea*, *Sagittaria* and *Eichornia*) can be observed from the shore and continuing toward the center of the lake, in a water column of 2–3 m.

The mean annual temperature at Lake Feia is 18–20°C, while the mean annual precipitation ranges from 1450 to 1850 mm; 50–70% of the rain falls between November and March, exceeding 400–600 mm from December to February, with a 150–250 mm hydric deficit during the other five

months (May to September) characterizing the dry season (Fig. III.1C). The rainfall regime in central Brazil is modulated by the position of the South American convergence zone (SACZ) in the southern Atlantic, which influences the intensity of the SASM. The SASM is also influenced by the ITCZ, which moves across the equator following the seasonal insolation cycle (Fig. III.1A) (Garreaud et al., 2008). The rainfall in Brazil therefore presents an anti-phased pattern, with high rainfall over Amazonia and central Brazil and low rainfall over north-eastern Brazil in austral summer (December to February), and the opposite pattern in austral winter (June to August) (Reboita et al., 2010; Marengo et al., 2012). During the austral summer, when the ITCZ is in its southernmost position, the incursion of North Atlantic Ocean trade winds over the continent is blocked by the Andes (Insel et al., 2010), thus increasing convective moisture over Amazonia. The flux of moist air generated follows a NE–SW trajectory along the southwestern boundary of the Amazon basin, before being redirected toward the Atlantic Ocean at the location where the SACZ activates the SASM (Marengo, 2004). Consequently, in January, when the SACZ reaches its southernmost position (26°S), an increase in precipitation is observed in the core region of the monsoon system, in central and southeastern Brazil (Fig. III.1A) (Marengo et al., 2012; Sulca et al. 2016).

2.2 Modern vegetation

The Cerrado biome comprises diverse types of vegetation and physiognomy, based on plant structure and growth form (Oliveira-Filho & Ratter, 1995; 2002), which are classified according to soil fertility, water availability and fire occurrence (Bueno et al., 2018). Cerrado physiognomies range from open grassland to dense woodlands. The open cerrado is characterized by a grassland physiognomy with a canopy cover of less than 5%; the cerrado sensu stricto by trees and shrubs 3–8 m in height, with the tree species *Astronium fraxinifolium*, *Byrsonima coccolobifolia*, *Caryocar brasiliense* and *Roupala montana* accounting for 30% of the total crown cover (Ribeiro and Walter, 2008); and the woody cerrado by trees 8–12 m or more in height and a crown cover of 50–90% (Oliveira Filho and Ratter, 2002; Durigan et al., 2022). The gallery forest physiognomy of the Cerrado biome is usually related to water bodies, and commonly divided into floodplain and swamp gallery forests, the assemblages varying in response to groundwater level dependance and/or adaptation (Durigan et al., 2022). The physiognomies and floristic compositions overall vary depending on topography, drainage and soil properties (Felfili et al., 1995; Bueno et al., 2018).

The landscape around Lake Feia comprises open cerrado, woody cerrado and gallery forest physiognomies (Cassino et al., 2020). The gallery forest grows from the lake shore to 5 m above the water level on the NE side of the lake. The city of Formosa is located on the western side of the lake (Fig. III.1B). A botanical survey carried out 7 km from Lake Feia revealed the dominance of the following families: Anacardiaceae, Araliaceae, Malvaceae, Asteraceae, Cyperaceae, Eriocaulaceae, Poaceae, Lamiaceae, Fabaceae, Lentibulariaceae, Malpighiaceae, Melastomataceae, Myrtaceae, Onagraceae, Orchidaceae, Polygalaceae, Pontederiaceae, Verbenaceae and Xyridaceae (Table III.1) (Ferraz-Vicentini, 1999).

Table III.1. Key Cerrado species identified near Lake Feia, Brazil (Ferraz-Vicentini, 1999).

Growth form	Common plant list
Trees	<i>Anacardium</i> sp., <i>Schefflera</i> sp., <i>Waltheria</i> sp., <i>Tephrosia leptostachya</i> , <i>Byrsinima</i> sp., <i>Cabralea</i> sp.
Herbs, shrubs and epiphytes	<i>Riencourtia tenifolia</i> , <i>Aristida riparia</i> , <i>Axonofarus</i> sp., <i>Laersia Hexandra</i> , <i>Paspalum gardinerianum</i> , <i>P. polyphyllum</i> , <i>P. stellatum</i> , <i>Thrasya petrosa</i> , <i>Trachypogon</i> sp., <i>T. spicatus</i> , <i>Bauhinia</i> , <i>Galactia</i> , <i>Periandra</i> , <i>Utricularia myriocista</i> , <i>Microlicia</i> , <i>Desmoscelis</i> . Epiphytes are represented by <i>Epidendrum</i> , <i>Phragmidium</i> , sp.
Water level-related	<i>Cyperus haspan</i> , <i>Fivrena</i> sp., <i>Rhynchosphora gigantea</i> , <i>Eriocaulon</i> sp. <i>Hyptis</i> , <i>Polygonum</i> , <i>Pontederia cordata</i> , <i>Xyris jupicæ</i>

2.3 Sampling and chronology

The 6-m long sediment core LFB1 was retrieved from Lake Feia in 1990 AD using vibracoring, adapted from Martin et al. (1995), and stored at the University of Brasília (Federal District, Brazil). For the present study, we analyzed the top 310 cm, corresponding to the last 5000 years. The core was collected in open water in the northeastern part of the lake at a depth of 1.5 m (Fig. III.1B) (Turcq et al., 2002).

Eight bulk sediment samples (Table III.2) were sent to the Laboratoire de Mesure du Carbone14 (LMC14)–UMS 2572 (CEA/DSM –CNRS–IRD–IRSN–Ministère de la Culture et de la Communication, Saclay, France) for analysis and radiocarbon dating by accelerator mass spectrometry (AMS). The radiocarbon dates were calibrated using the Southern Hemisphere Terrestrial SHcal20 curve (Hogg et al., 2020) in Calib 7.0 (Stuiver and Reimer, 1993). The age–depth relationship was modeled using Bayesian statistics with the Bacon package in R (Blaauw and Christen, 2011). An extra date of –40 a BP was added at 0 cm, corresponding to the year of coring, i.e. 1990 AD. The parameters were adjusted to SHCal20 with a confidence interval of 0.95 (Fig. III.2).

Table III.2. Radiocarbon dates for the LFB1 sediment core taken from Lake Feia, Brazil. The ^{14}C dates were calibrated using Calib 7.0 (Stuiver and Reimer, 1993), and values are shown to two standard deviations (2σ).

Laboratory code	Material dated	Depth (cm)	$\delta^{13}\text{C}$	^{14}C age (a BP)	Age range (cal a BP)
SacA 53907	Lake sediment	14–15	–32.4	220 ± 30	136–232
SacA 60352	Lake sediment	40–41	–27.5	910 ± 30	739–789
SacA 53908	Lake sediment	60–61	–29.8	870 ± 30	680–775
SacA 60353	Lake sediment	102–103	–25.6	1280 ± 30	1069–1189
SacA 60354	Lake sediment	164–165	–30.2	2160 ± 30	2007–2159

SacA 60355	Lake sediment	218–219	−23.8	2925 ± 30	2919–3082
SacA 60356	Lake sediment	270–271	−25.9	3520 ± 30	3677–3841
SacA 53909	Lake sediment	313–314	−33.3	4405 ± 30	4851–4983

2.4 Analytical protocols

Pollen was analyzed in 149 sediment subsamples, each measuring 0.5 cm³ long and 1 cm thick, collected at 2-cm intervals. Pollen was extracted at the ISEM laboratory in France. A spike of two Lycopodium tablets (36,814 Lycopodium clavatum spores per tablet) per sample was added to calculate the concentration of pollen. The samples were first washed in 10% KOH in a hot water bath, before density separation with ZnCl₂ (Kummel and Raup, 1965). For samples taken between 309 and 200 cm, a 5-ml 75% HF treatment was performed for 1 hour (Faegri and Iversen, 1989) to remove silica. Pollen, spores and other non-palynomorphs were identified and counted at 600× magnification. A total of 175 pollen types was identified using the ISEM pollen reference collection for Cerrado pollen taxa, identification keys, and catalogs of pollen types from Brazil (Salgado-Labouriau, 1973; Cassino and Meyer, 2011; Bush and Weng, 2007; RCPol, 2021). Pollen percentages were based on the total sum of terrestrial pollen grains. Additionally, the pollen influx, as grains/cm²/a, was calculated for each taxa. Pollen zones were defined by constrained cluster analysis by sum of squares (CONISS), as proposed by Bennett (1996). Diagrams and pollen zones were created using the rioja package in RStudio. For the selection of pollen taxa, we applied the following process. 1) First, we classified the pollen taxa according to their type of growth (arboreal, non-arboreal) and phytobiognomy (woody cerrado, cerrado or gallery forest) (Table S1). The Poaceae were then used to characterize open and closed physiognomies, according to Gosling et al. (2005, 2009). 2) Second, we built a dataset excluding pollen taxa contributing less than 1%, and applied a principal components analysis (PCA) (Table S2). 3) Third, we used both the frequency (high or low) and the representation (constant or variable) of each pollen taxa selected in the first PCA to constrain the most representative pollen taxa.

A second PCA was applied to the most representative pollen taxa to evaluate vegetation variability as a function of time (Table S3). Before each PCA analysis, the dataset was square-root transformed in order to minimize the heterogeneity and reduce over- or under-representation (Becker et al., 1988).

For palynological interpretation, pollen assemblages were characterized by pollen percentage deposition (pollen influx) and the ecological characteristics such as life form, stratum, light exposition, pollination syndrome and habitat (mostly soil requirements) of each taxa (summarized in Table S4).

For the trace element analysis, 81 sediment samples were dried in a laboratory oven at 50°C for 24 hours. Thereafter, sediments were macerated in agate drumsticks, and fractions smaller than 0.180 mm were separated with an 8×2 “INOX ASTM 80 MESH / TYLER 80 by Bertrand sieve”. A sediment volume of 1 cm³ for each subsample was placed in an X-ray fluorescence (XRF) holder cup. The samples were analyzed at the Instituto de Geociências—Universidade de Brasília, using a portable XRF DELTA (Olympus) in soil mode, with three repetitions of 2 minutes for each

sample and using the mean of the three repetitions to interpret the results. Finally, representative elements were selected, using Ti and Ti/K levels as indicators of erosion (Marshal et al., 2011; Davies et al., 2015). Ti/K ratios were normalized in order to view data variation on a homogenized scale.

To reconstruct fire activity, 310 0.5-cm³ subsamples were collected at 1-cm intervals. The subsamples were deflocculated and bleached with KOH (10%) and NaOCl (2.6%), and gently passed through a 160-μm mesh under water. The residues were carefully washed into a porcelain evaporating dish, to aid identification and counting of charcoal particles. The material was analyzed at 60× magnification under a Leica microscope, with a camera connected to an image analyzer and Winseedle image-analysis software (Regent Instruments Canada Inc., 2009), which allowed measurement of total charcoal concentration by number, the area of individual particles, and the cumulative sum of charcoal particle area (i.e. the concentration of charcoal by area). The charcoal accumulation rate was calculated by multiplying the total concentration of charcoal number (area) by the sediment accumulation rate (CHAR) (CHAR#= particles/cm²/a and CHARarea= mm²/cm²/a). In addition, width:length (W:L) was evaluated for each particle. The individual values were then incorporated into a density diagram. The average W:L ratio was used to evaluate the presence and dominance of grass or woody charred particles, for which values above (below) 0.5 suggested charred wooded (grass) particles (Aleman et al., 2013).

3. Results

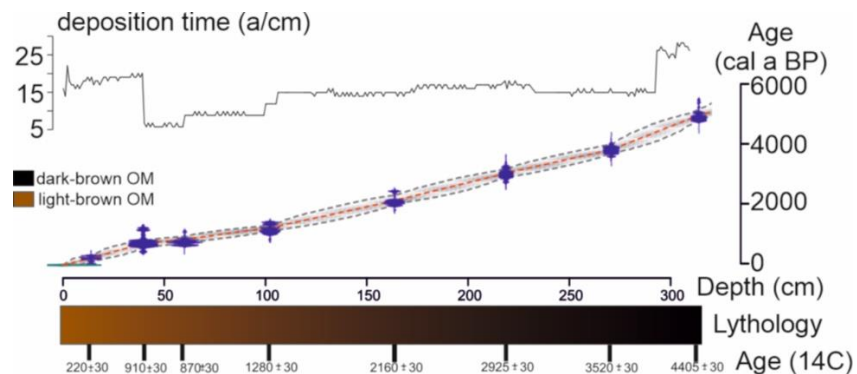


Figure III.2. A calibrated age-depth model for the LFB1 core from Lake Feia, with the accumulation rate curve in a/cm at the top and the position of the radiocarbon dates (Table 1) along the core lithology (in brown) at the bottom. The standardized errors are indicated by the blue boxes. The black dashed lines show the upper and lowest calibrated ages, the gray band the probability of minor or major dates for each depth, and the red dashed line the most probable age.

The age–depth model obtained for the LFB1 core (Fig. III.2) provided a chronology for the last 5000 years of vegetation in the Cerrado. The resolution ranged between 12 and 50 years per sample for pollen analysis, and between 6 and 25 years per sample for macrocharcoal analysis. The lowest deposition rate in the whole section was observed between 310 and 270 cm (4830–3800 cal a BP), with an average of 25 a/cm. Between 269 and 100 cm (3790–1185 cal a BP), the deposition rate was ~15 a/cm. Between 99 and 40 cm (1180–690 cal a BP), the highest deposition rate ranged from 6 to 10 a/cm. From 39 to 0 cm (670 to –40 cal a BP) the sedimentation rate was ~20 a/cm

(Fig. III.2). The top of the core was radiocarbon dated to 220 ± 30 14C a BP, corresponding to the last century (Table III.2); we therefore considered the top of the core to be modern.

3.1 Palynological analyses

Constrained cluster analysis (Bennett, 1996) identified five pollen zones (Fig. S1). From a total of 175 identified pollen taxa, 20 were selected based on the three-step process described in the methods. The PCA for the selected pollen taxa (Fig. S1) separated them into three groups (Fig. S3), providing information about the environment and climatic conditions based on the ecological requirements of each taxa as defined in Table S4. Temporal changes defined by the individual negative z-score values indicated taxa associated with pollen assemblages from gallery forest with seasonal or permanent flooding, while positive values suggested cerrado/gallery forest with well-drained soils (Figs. III.3, S2A and S2B). Thus, the assemblage *Ilex*–*Myrtaceae*–*Banisteropsis* was associated with swampy gallery forest, with *Myrtaceae* at the periphery of the swamp and *Ilex* also present in inundated areas. Both *Myrtaceae* and *Ilex* are small trees, forming lower storey forest, while *Banisteropsis* is a heliophilous woody vine (Araújo et al., 2002). An increase in their pollen frequency/influx associated with a decrease in lake level suggested a forest invasion toward the coring site, as their entomophilous pollen cannot travel long distances. The assemblage *Alchornea*–*Apeiba*–*Casearia*–*Euterpe*–*Melastomataceae*–*Combretaceae*–*Ouratea*–*Ternstroemia* represented plant taxa generally observed in lower storey strata (>10 m) of gallery forest and woody cerrado (Araújo et al., 2002), associated with moist and fertile soils. The assemblage *Poaceae*–*Anadenanthera*–*Astronium*–*Byrsonima*–*Cecropia*–*Celtis*–*Moraceae*–*Urticaceae*–*Myrsine*–*Tapirira*–*Trema* represented cerrado plant taxa generally adapted to dry or reduced water levels (Araújo et al., 2002), with *Celtis* and *Trema* being pioneer taxa. These taxa were not very abundant in the pollen record, suggesting that they did not directly influence the coring site (Araújo et al., 2002).

The presence of *Byrsonima* (<10%), and *Astronium*, *Casearia*, *Ouratea* and *Poaceae* (~20–50%), in pollen surface studies indicated open (>50%) and woody or closed (<20 %) cerrado physiognomies (Ledru, 2002; Jones et al., 2011). However, a decrease in lake level shifted the gallery forest closer to the coring site, which attenuated the deposition of *Poaceae* pollen and thus modified the signature for the expansion of open cerrado (Berrio et al., 2000; Gosling et al., 2009).

The assemblage *Moraceae*–*Urticaceae*, a good pollen producer with an anemophilous syndrome, has been widely used as an indicator of gallery forest when its frequency is more than 40% (Gosling et al., 2005; 2009). However, in the LFB1 record, the frequency of *Moraceae*–*Urticaceae* was less than 40%, and other indicators also inferred local changes in moisture levels, such as the water level-related pollen taxa *Echinodorus*, *Eichhornia*, *Eriocaulon*, *Myriophyllum* and *Nymphaea* (Fig. S3). In addition, non-pollen palynomorphs, including fern and algae, showed similar patterns to water level-related taxa (Fig. S3). Fungi were more or less continuous but, as they were mostly coprophilous (*Sordaria*, *Gelasinospora* and *Ustulina*), while they were associated with continuous fire frequency and dung or organic matter decomposition, their origins could not be defined as natural or anthropic. Finally, the presence of *Sporormiella* was not sufficiently frequent to suggest human activity (pastoralism) in the area (Fig. S3).

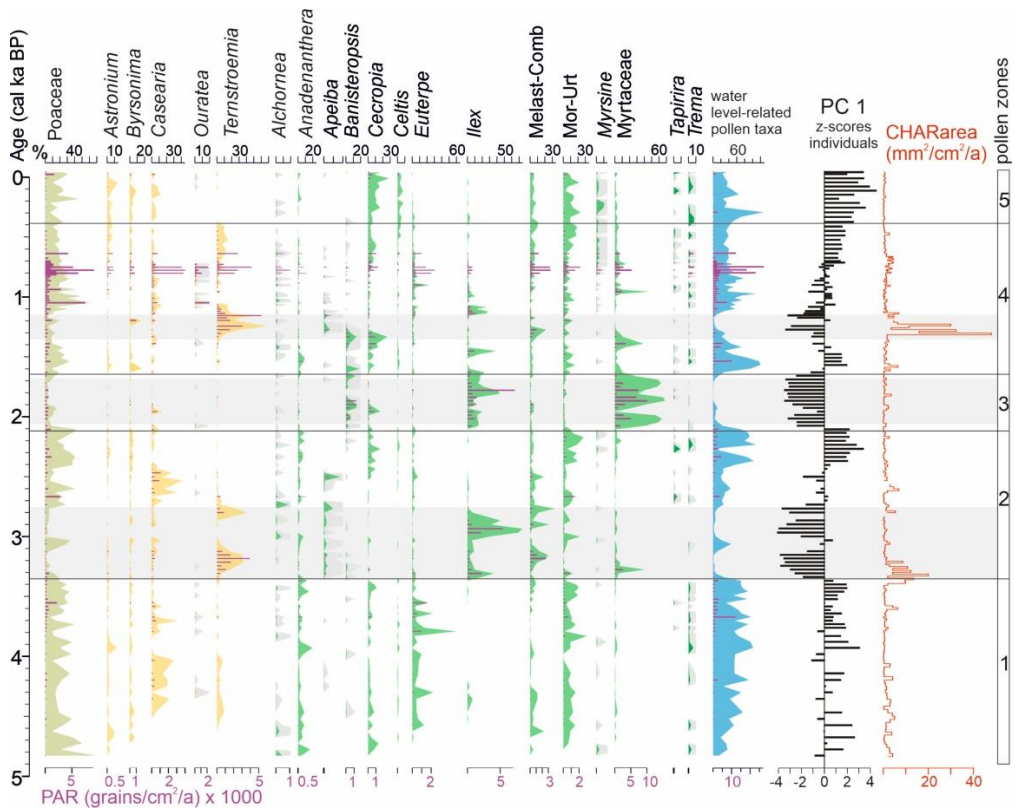


Figure III.3. Synthetic pollen influx (black bars) and frequency (curve) diagram for 20 selected pollen taxa from core LFB1, represented by PC1 scores and macrocharcoal accumulation rate ($\text{mm}^2/\text{cm}^2/\text{a}$), respectively, along a time scale. Woody cerrado taxa are shown in yellow, gallery forest taxa in green, and water level-related taxa in blue. Gray horizontal bands indicate the dry intervals. Exaggeration ($\times 10$) curves are in gray.

Zone 1 (309–241 cm, 4830–3370 cal a BP, 33 samples)

Zone 1 was characterized by arboreal pollen (AP) levels varying between 17% to 82%, including *Moraceae–Urticaceae*, *Euterpe*, *Casearia* and *Cecropia*. High frequencies of *Poaceae* (69%) were seen at the beginning of zone 1 (depth 309–301 cm; 4830–4620 cal a BP), with the presence of the tree taxa *Alchornea* (4–8%) and *Anadenanthera* (4–16%). Above 300 cm *Casearia* (~1–35%) and *Astronium* (~1–8%) were present. Levels of *Ternstroemia* ranged from 3 to 10% between 299 and 279 cm (4570–4030 cal a BP), with *Cecropia* (~0.5–8%), *Anadenanthera* (1–16%), *Euterpe* (~1–61%) and *Moraceae–Urticaceae* (~1–30%) also present. *Moraceae–Urticaceae* showed a decrease concomitant with an increase in *Euterpe*. During this interval, there was a progressive increase in pollen influx from ~ 46 to 6927 grains/ cm^2/a . PC1 values ranged from ~3 to -1.1, with predominantly positive values. The presence of water level-related taxa *Sagittaria* and *Myriophyllum* ranged from 1 to 36% and 1 to 70%, respectively. The percentages increased with the appearance of *Eichhornia* taxa, with a greater frequency at 287 cm (4510 cal a BP). The water level-related taxa followed the same pattern as terrestrial taxa, increasing toward the end of the zone. The pollen influx ranged from 16 to 2893 grains/ cm^2/a , with a peak of 12,355 grains/ cm^2/a .

at 261 cm (3670 cal a BP). Macrocharcoal was observed from the beginning of the zone and increased toward the end of the zone (values ranging from 0.6 to 9.5 mm²/cm²/a).

Zone 2 (239–163 cm, 3340–2100 cal a BP, 36 samples)

AP dominated, with frequencies of ~35–90%, mainly of *Ilex*, *Ternstroemia*, Melatomataceae–Combretaceae, Moraceae–Urticaceae and *Casearia*. Levels of Poaceae (36 to ~1%) and *Byrsonima* (6 to 1%) decreased, while *Casearia*, *Astronium* and *Ouratea* increased (0 to 48%), mostly between 195 and 185 cm (2630–2470 cal a BP). *Ternstroemia* appeared in two phases, the first from 239 to 219 cm (~4–36%) and the second from 205 to 197 cm (~3–41%) (3340–3030 and 2800–2660 cal a BP, respectively). The percentage of gallery forest taxa ranged from ~7 to 70%, with three distinct phases observed at 239–233 cm (3340–3240 cal a BP), 217–209 cm (3000–2860 cal a BP) and 177–163 cm (2330–2100 cal a BP). The two first phases were dominated by *Ilex* (7–75%), *Apeiba* (1–5%) and Moraceae–Urticaceae (1–30%). *Euterpe* decreased to less than 6%, with less than 3% *Myrsine*, *Celtis* and *Banisteropsis* present. In the third phase, the increase in Moraceae–Urticaceae was accompanied by mixed percentages of *Cecropia* (~1–17%), *Euterpe* (1–5%), *Myrsine* (< 2%), *Trema* (~1–6%) and *Celtis* (~1–3%), while *Apeiba* disappeared. The terrestrial pollen frequency ranged from ~900 to 6000 grains/cm²/a. PC1 values varied from ~3.4 to –4.1, with predominantly negative values from a depth of 239–203 cm (3340–2760 cal a BP) and positive values from a depth of 201–163 cm (2730–2100 cal a BP). Macrocharcoal was present throughout the zone from 0.01 to 6 mm²/cm²/a, with high accumulation rates (8–29 mm²/cm²/a) from a depth of 239–231 cm (3330–3210 cal a BP).

Zone 3 (161–131 cm, 2070–1630 cal a BP, 16 samples)

The frequency of AP was high (65%) and included *Ilex* and Myrtaceae. There was less than 2% Poaceae and *Byrsonima*, and *Casearia* (10–2%), *Astronium* and *Ouratea* (less than 2%), *Ternstroemia* (<1%), *Ilex* (~6–44%), *Banisteropsis* (1–13%), *Cecropia* (1–17%), Moraceae–Urticaceae and *Anadenanthera* (1–5%) and *Alchornea*, *Trema*, *Celtis* and *Euterpe* (<1%) were present. Moraceae–Urticaceae levels increased at the end of the zone (10%). The terrestrial pollen influx was between 314 and 17,789 grains/cm²/a. PC1 values ranged from ~–3.4 to –0.6. Water level-related pollen almost disappeared (from 20 to >1%), with the pollen influx decreasing from 1145 to 11 grains/cm²/a. Macrocharcoal was present throughout the zone but accumulation rates were low (0.018–3 mm²/cm²/a).

Zone 4 (129–25 cm, 1600–410 cal a BP, 51 samples)

The frequency of AP ranged from 30 and 85%, including *Ternstroemia*, *Ilex* and Myrtaceae, followed by Moraceae–Urticaceae (~20%), *Cecropia* (~1–26%), Poaceae (5–50%) and *Byrsonima* (~1–19%), with the highest frequencies occurring at the beginning of the zone. *Ternstroemia* (1–55%) was present, with values above 8% from 111 to 87 cm (1330–1060 cal a BP) and 57 to 25 cm (800–400 cal a BP). The two phases with higher AP frequencies (>8–25%), at 89–81 cm (1080–1010 cal a BP) and 71–45 cm (920–720 cal a BP), included *Casearia*, *Astronium* and *Ouratea*. Moraceae–Urticaceae was present at ~20% throughout the zone. *Cecropia* levels (1–26%) increased gradually, while *Euterpe* (1–6%) and *Myrsine* (1–4%) increased toward the end of the zone, and *Alchornea*, *Anadenanthera*, *Apeiba*, *Celtis* and *Trema* levels (~1–5%) remained low. *Ilex*

displayed high frequencies between 121 and 119 cm (1480–1450 cal a BP) and between 95 and 89 cm (1135–1080 cal a BP). The terrestrial pollen influx ranged from 200 to 38,000 grains/cm²/a. PC1 values ranged from –3.4 to 1.9, with negative values from a depth of 121–93 cm (1480–1120 cal a BP) and positive values from a depth of 91 cm (1100 cal a BP) toward the end of the zone. Levels of water level-related taxa *Eichhornia* and *Sagittaria* ranged from 2 to 20% and from 10 to 40% respectively, with a peak of *Sagittaria* at the beginning of the zone at 125 cm (1540 cal a BP) (~50%). *Myriophyllum* increased to ~8% between 73 and 61 cm (930–820 cal a BP). *Nymphaea* was present at ~7% from 31 cm (515 cal a BP) until the end of the zone. All the water level-related taxa decreased between 111 and 97 cm (1330–1150 cal a BP). The water level-related pollen influx ranged from 100 to 24,000 grains/cm²/a. Macrocharcoal was present throughout the zone from 0.1 to 6 mm²/cm²/a, with high accumulation rates (15–47 mm²/cm²/a) from a depth of 111–106 cm (1330–1260 cal a BP).

Zone 5 (23–0 cm, 370 cal a BP–1990 AD, 13 samples)

AP frequencies ranged from ~40 to 78%, including Moraceae–Urticaceae, *Cecropia*, *Astronium*, *Celtis* and *Trema*. *Byrsonima* was present (~10%), while Poaceae was the most frequent taxa (~40–20%). *Astronium* and *Casearia* were present (~1–20%), as were *Cecropia* (5–30%), Moraceae/Urticaceae (5–25%), *Celtis* (~10%), *Trema* (~1–10%) and *Myrsine* (~1–15%). There was less than 5% *Alchornea*, *Anadenanthera*, *Euterpe* and *Ilex*. The pollen influx decreased from 900 to 200 grains/cm²/a. PC1 ranged from ~4.5 to 1.2. Overall, the water level-related taxa frequencies decreased; *Eichhornia* decreased from 60% at the beginning of the zone (19 cm, 295 cal a BP) to ~10%, while *Nymphaea* and *Sagittaria* increased from 1 to ~10% and *Myriophyllum* almost disappeared (0–3%). The pollen influx ranged from 70 to 2416 grains/cm²/a, with the lowest values occurring at a depth of 13–15 cm (180–210 cal a BP). Macrocharcoal was continuously present, although this zone had the lowest accumulation rate, ranging from 0.1 to 2 mm²/cm²/a.

3.2 XRF analyses

The XRF results showed contrasting responses, with four main erosive phases indicated by the normalized Ti/K ratio (Fig. III.4): from 5000 to 4100 cal a BP, 3330 to 2900 cal a BP, 2100 to 1800 cal a BP, and 1100 to 400 cal a BP. The highest Ti/K ratio was observed 400 years ago (Fig. III.4).

3.3 Charcoal analyses

Charcoal analyses showed regular and continuous biomass burning since 5100 cal a BP (Figs. III.4 and Fig. S4), with the charcoal influx ranging from 0 to ~ 40 mm²/cm²/a, mainly below 10 mm²/cm²/a but with two intervals above 10 mm²/cm²/a, from 3330 to 3210 cal a BP and 1330 to 1160 cal a BP (Fig. III.4). The width and length density analysis (W:L mean values ≥ 0.5) suggested that the charred particles originated from woody vegetation until 2900 cal a BP (Fig. S4), and from grass toward the top of the record (Figs. III.4 and S4). The lack of a significant pattern during the two episodes of high charcoal deposition suggested both woody and grass biomass burning.

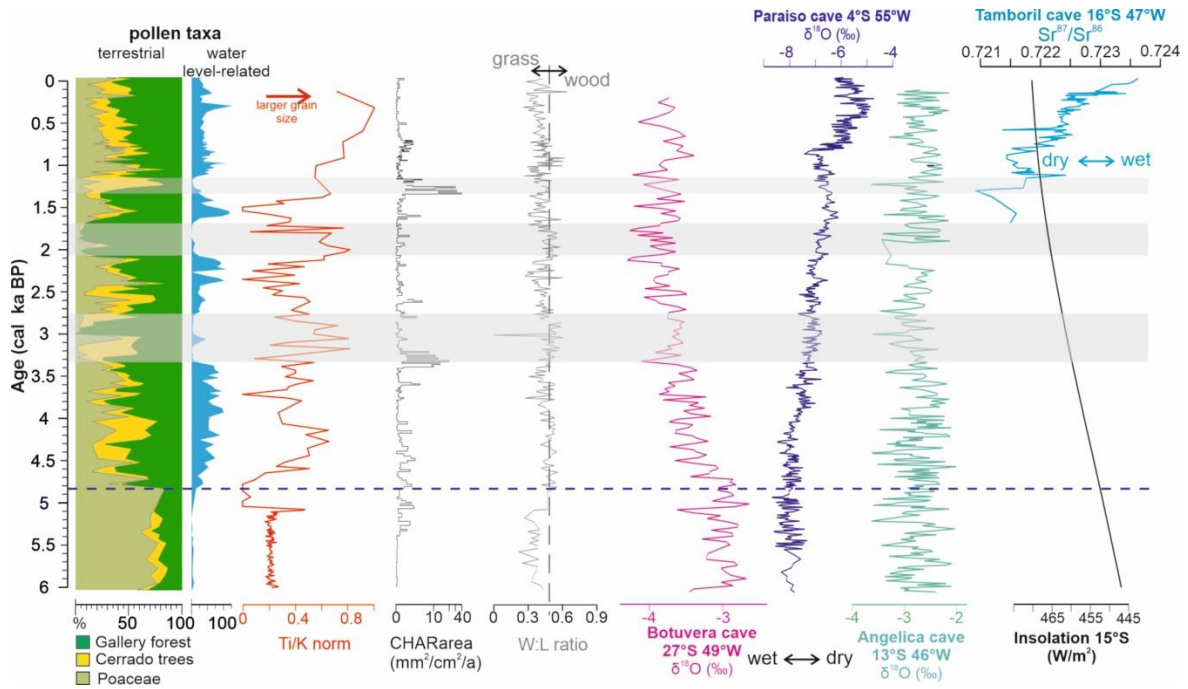


Figure III.4. A representation of the last 6000 years in the central region of the Cerrado biome. A synthetic pollen, charcoal and geochemical diagram is shown for Lake Feia (cores LF-15 and LFB1) (Cassino et al. 2020; present study) along with $\delta^{18}\text{O}$ isotopic ratios from selected speleothem records along a calibrated time scale. The percentages of terrestrial and water level-related taxa, normalized Ti/K ratios and charcoal influxes (CHARarea) are indicated. The speleothem records came from southern (Botuverá cave; Bernal et al., 2016), northern (Paraiso cave; Wang et al., 2017) and central (Angelica cave; Wong et al., 2021; Tamboril; Wortham et al., 2017) Brazil, with an insolation curve at 15°S (Laskar et al., 2011). The blue dotted line shows the main vegetation shift observed in central Cerrado at ~4800 cal yr BP; the gray bands represent the dry intervals.

4. Interpretation

Our results show that, for the last 5000 years, the landscape in the region of Lake Feia has been characterized by a cerrado with Poaceae (< 40%) and the following dominant tree taxa: *Astronium* (1–10%), *Byrsonima* (1–15%), *Casearia* (~1–20%), *Ouratea* (< 5%) and *Ternstroemia* (~2–40%). In the gallery forest, we observed an almost continuous presence of *Anadenanthera* (0–15%), *Euterpe* (0–50%), Melastomataceae–Combretaceae (0–30%), Moraceae–Urticaceae (< 30%) and the three common pioneer taxa *Cecropia* (0–30%), *Celtis* (0–10%) and *Trema* (0–10%). Changes from a closed to open canopy suggested some reorganization within the gallery forest, as shown by fluctuations in *Myrtaceae* (0–60%), *Ilex* (0–70%), *Apeiba* (0–20%), *Banisteropsis* (0–20%), *Alchornea* (0–20%), *Myrsine* (0–10%) and *Tapirira* (0–10%). These changes were related to shifts in the position of the gallery forest in the direction of the coring site, indicating a decrease in the lake water column, from 3340 to 2760, 2070 to 1690, and 1330 to 1150 cal a BP. The two first intervals suggested an invasion of the gallery forest toward the coring site, characterized by a decrease in the aquatic taxa, an abrupt increase in *Ilex* (a tree taxa tolerant of permanent flooding) and an increase in *Myrtaceae* and Melastomataceae–Combretaceae (two tree taxa associated with groundwater). At the beginning of the first interval and during the third, the reduction in gallery

forest elements was accompanied by an increase in the drought-tolerant taxa *Ternstroemia*, and associated with a high fire signal. During the third interval, the disappearance of aquatic taxa suggested a lower lake level. Together, these three intervals suggest drier local climatic conditions. From 4830 to 3370 cal a BP a gradual expansion and stabilization of the arboreal landscape was observed in both gallery forest and woody cerrado.

After each of the dry episodes, the recovery of the arboreal landscape was characterized by an increase in lower storey pioneer tree taxa (*Casearia*, *Cecropia* and *Trema*), while the closure of the canopy was characterized by medium and upper storey tree pollen taxa (*Alchornea*, *Anadenanthera* and *Tapirira*). During the last 400 years, stabilization of the tree cover has been simultaneous with an increase in the aquatic taxa *Nymphaea*, commonly found in deep water (Bernhardt and Willard, 2009). *Ternstroemia* disappeared, while the gallery forest taxa *Cecropia*, *Celtis*, *Trema*, Melastomataceae–Combretaceae and Moraceae–Urticaceae became more frequent, and woody cerrado taxa were well represented by *Astronium*, *Byrsonima* and *Casearia*. Fire activity was low compared with the previous interval.

The two periods of high charcoal influx (deposition) in Lake Feia, at 3350–3200 and 1330–1160 cal a BP, coincided with the observation of two dry intervals in the vegetation, from 3340 to 2760 and from 1330 to 1150 cal a BP. After each event of high fire activity, the recovery of arboreal taxa, mostly gallery forest, took about 30 years. The drier episode from 2070 to 1690 cal a BP showed continuous fire activity and a vegetation recovery of less than 30 years (Figs. III.4 and S4). During the more humid climatic intervals, the charcoal influx was rarely above 1 mm²/cm²/a and no change in the pollen assemblages was observed. Finally, from 813 to 700 cal a BP, the charcoal influx was continuous (~3 mm²/cm²/a), and the tree taxa recovery period was about 12 years (Figs. III.4 and S4).

5. Discussion

5.1 Expansion of the arboreal cerrado in central Brazil

To place the vegetational changes within a wider context, we merged our results with those obtained from core LF15-2, dated to between 19,000 and 6000 cal a BP (Cassino et al., 2020) (Figs. III.4 and III.5). The late Pleistocene is characterized by different assemblages, with a dominance of non-arboreal pollen (Poaceae, Asteraceae) and the presence of a *Myrsine*–*Ilex*–*Hedyosmum* assemblage characteristic of the high-elevation grassland physiognomy of the Cerrado (Ledru et al., 2007). Our study of the last 6000 years suggests a two-step expansion of the Cerrado biome in the region of Lake Feia. First, the interval between 6000 and 5000 cal a BP was characterized by the installation of an open cerrado; second, after 5000 cal a BP, the expansion of a woody cerrado peaked, with the continuous presence of *Astronium* and *Byrsonima*, and fluctuating levels of *Casearia*, *Ouratea* and *Ternstroemia*. Three intervals with low water level-related taxa are attributed to drier episodes, from 3340 to 2760, 2070 to 1690, and 1330 to 1150 cal a BP, with a local expansion of the gallery forest toward the coring site observed during the first and second dry intervals, and a contraction of the gallery forest and expansion of drought-tolerant tree taxa (*Ternstroemia*) coupled with high fire activity during the third interval (Figs. III.3 and III.4).

The two-step installation of open to woody cerrado is in agreement with two other swamp pollen records, Cromínia and Águas Emendadas (with a resolution of 1000 years per sample for Cromínia and 600 years per sample for Águas Emendadas), located in central Cerrado (Fig. III.1A). The Cromínia record ends at 3500 cal a BP, and the Águas Emendadas record at 940 cal a BP (Ferraz-Vicentini and Salgado-Labouriau, 1996; Barberi et al., 2000). The differences in pollen content and Poaceae frequencies (lower at LFB1) can be attributed to the different pollen deposition sites (lake versus swamp).

Two lacustrine pollen records located in northwestern Cerrado (Lake Confusão; Behling, 2002) and northern Cerrado (Lake Caço; Ledru et al., 2006) (Fig. III.1A) suggest that the woody cerrado and the gallery forest were established earlier there than in central Brazil, at ~6000 and 8500 a BP, respectively. Cerrado tree taxa are mainly characterized by *Byrsonima* (5–10%) and Poaceae (less than 50%), but with differences in other pollen indicators, such as a lower frequency of *Curatella* (<5%) at Lake Confusão and of *Mimosa* (10–20%) at Lake Caço. However, the low-resolution analysis at Lake Confusão (~2000 years between samples) and at Caço (~200 years between samples), and the absence of a record after 3000 cal a BP at Caço, makes further detailed comparison impossible.

To the west, in the Amazonia–Cerrado ecotone, the Lake Saci record (Fig. III.1A) initially shows a decrease (from 38 to 20%) in the woody cerrado at 7500 cal a BP, with *Byrsonima* (4%), *Curatella* (~1%), Poaceae (~18–43%) and *Anadenanthera* (5%), followed by expansion of the rainforest after 5000 cal a BP (69–95%) (Fontes et al., 2017). A swamp record located in the eastern Amazonia–Cerrado ecotone (Carajás) shows an open cerrado, with Poaceae (85%), *Byrsonima* (≤ 2%) and *Mimosa* (0–10%) and the dry forest taxa Anacardiaceae (≤10%) and Bignoniaceae and *Zanthoxylum* (<2%) from 10,200 to 3400 cal a BP, after which they are replaced by the rainforest taxa *Alchornea* (30%), *Celtis* (15%), Melatomataceae–Combretaceae (14%), Moraceae–Urticaceae (19%) and *Trema* (<5%) (Hermanowski et al., 2012).

In southeastern Cerrado, the pollen record at Lagoa Santa (Parizzi et al., 1998) (Fig. III.1A) covers the last 5300 cal a BP and shows the presence of the cerrado pollen taxa Poaceae (50%) and *Styphnodendron* (2–4%). Small changes in humidity have occurred during the last 3000 years, and in the Cerrado–Atlantic Forest ecotone (Horák-Terra et al., 2020) a record from Pinheiro mire (located at 1240 m asl and spanning the last 6000 years) indicates an open cerrado, with *Amaranthus* and *Borreria* (5–10%) present until 3100 cal a BP. The frequency of cerrado tree pollen then increased between 3100 and 740 cal a BP, with *Byrsonima*, *Tabebuia* and *Smilax* (< 2%), and grassland has become dominant in the last 740 years (Horák-Terra et al., 2020) at this elevation of the Espinhaço mountain range.

In the northeast, in the Cerrado–Caatinga ecotone, the São José swamp record (at 680 m asl) (Cassino et al., 2018) shows wetter climatic conditions and the expansion of palm swamp until 4400 cal a BP, with *Mauritia flexuosa* (40%), Poaceae (24–60%) and Ericaceae, *Plenckia* and *Roupala* (<3%) present, and an increase in the gallery forest tree taxa *Cecropia* and *Hedyosmum* (>20%). After 3500 cal a BP, the expansion of a drier open cerrado is characterized by a regression of the tree pollen taxa and the palm swamp *Mauritia flexuosa* (<7%), and the expansion of grassland pollen (Poaceae 20%) (Cassino et al., 2018). The Pandeiros wetland record (at 460 m

asl) (Lima Sabino et al., 2021) shows the presence of a woody cerrado [mainly *Astronium* (~5%)] until 2890 cal a BP, when it was replaced by a more open cerrado landscape (Poaceae 18%), with the presence of Asteraceae (5-35%), *Euphorbia* (5-40%) and *Gomphrena* (2-25%), during the last part of the Holocene (Lima Sabino et al., 2021).

Notwithstanding the differences in resolution and chronological controls, our review of published Cerrado pollen records reveals a general trend characterized by the expansion of open cerrado until ~5000 a BP and woody cerrado after 5000 a BP, interrupted by a drier episode at approximately 3500 cal a BP in both central and northeastern regions. An inverse pattern is seen in the southeastern and southern regions, with more humid forest being replaced by a drier and more open cerrado physiognomy between 4000 and 3000 cal a BP and a woody cerrado between ~3100 and

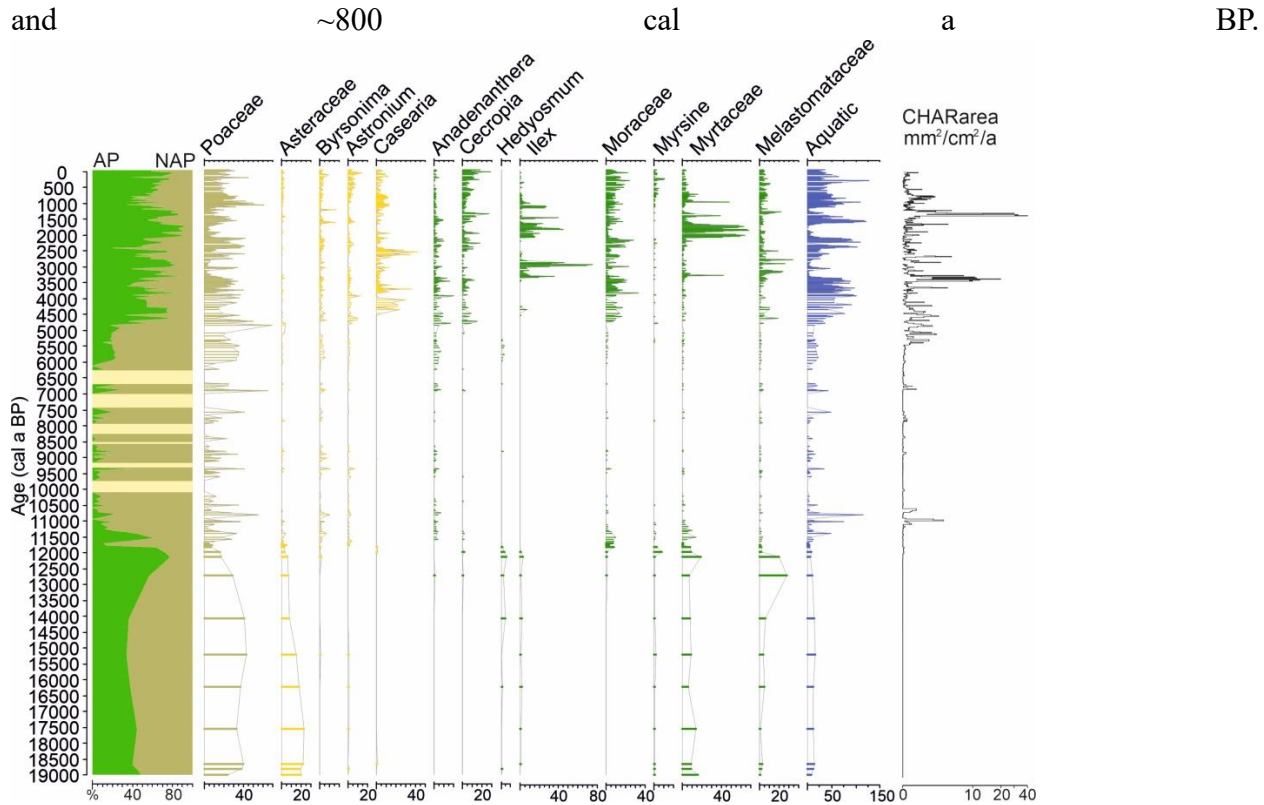


Figure III.5. The last 19,000 years in central Cerrado, as represented by the Lake Feia sediment cores (Cassino et al. 2020; present study). From left to right, a synthetic pollen diagram showing arboreal pollen/non-arboreal pollen frequencies (AP and NAP, respectively), 13 selected pollen taxa, with AP cerrado taxa shown in yellow and gallery forest taxa in green, and water level-related (aquatics) in blue, plus the charcoal influx (CHARarea; mm²/cm²/a). The yellow horizontal bands show the disappearance of Lake Feia during dry episodes (from Cassino et al., 2020).

5.2 Climatic drivers of vegetation changes in central Brazil

The Lake Feia pollen record suggests continuous wet conditions, interrupted by three drier intervals, from 3340 to 2760, 2070 to 1690, and 1330 to 1150 cal a BP (Fig. III.4). Speleothem records in central Brazil (Fig. III.4) show apparently stable climatic conditions during the last 6000 years (Deininger et al., 2019; Wong et al., 2021), compared with southern and northern regions of

Brazil at the margins of the monsoon domain, where the establishment of a SW–NE dipole (Novello et al., 2012 and 2019; Deininger et al., 2019) led to abrupt changes in the extent of the monsoon and consequently in seasonality and precipitation (Campos et al., 2019). At Lake Feia, regular sedimentation and the establishment of the Cerrado started around 6000 cal a BP, suggesting regular regional precipitation. Rainfall stability has also been reported at 7000 a BP in southeastern Brazil (27°S , 49°W) (Bernal et al., 2016), at 6800 a BP in central Brazil (13°S , 46°W) (Wong et al., 2021) and since the mid-Holocene in northern Brazil (4°S , 55°W) (Wang et al., 2017), as a response to the increase in insolation (Deininger et al., 2019). However, regional differences in the expression of drivers have also been observed, such as the strengthening of the SASM system in the south, which increased rainfall, while in the north the increased rainfall was not directly linked to the SASM but driven by humid convection from the eastern Amazonia (Wong et al., 2021). In central Brazil, both speleothem and pollen records suggest that the SACZ has remained stable, thus allowing a regular SASM trajectory between central and eastern Brazil (Fig. III.6). However, pollen records indicating to a more open landscape between 6000 and 4800 cal a BP suggest lower precipitation levels and a weaker SASM than today, decoupled from the SASM core, while stronger rainfall has prevailed at the northernmost boundary of the SASM zone of influence. The location of Lake Feia (15°S , 47°W) was probably too far from the wetter northeast area to be influenced during this period (Fig. III.6A).

Conditions changed after 4800 cal a BP, with the installation of a dipole between southern and northern Brazil, the south became wetter and the northeast drier (Bernal et al., 2016; Wang et al., 2017) (Fig. III.4 and III.6B). At Lake Feia the full expansion of the woody cerrado, the abrupt increase in water level-related pollen taxa and the coarse sediment deposition (Ti/K) suggest that the regional wet levels were related to a strengthening and expansion of the SASM boundary at latitude 15°S , and an increase in summer insolation in the southern tropics (Fig. III.6B) (Cruz et al., 2009; Deininger et al., 2019). However, despite the trend toward a more stable precipitation regime created by an increase in insolation and the establishment of the modern monsoon regime in central Cerrado, three drier episodes are indicated by the Lake Feia pollen record: from 3340 to 2760, 2070 to 1690, and 1330 to 1150 cal a BP. We infer that changes in the hydrological system of Preto River, also characterized by an increase in deposition of coarser sediment, are probably related to a reduction of water input into the lake, and consequently in the amount of precipitation at a centennial scale (Fig. III.4). A southward shift of the ITCZ and SASM boundary has been observed between 3700 to 3400 and \sim 2700 a BP (Bernal et al., 2016; Cruz et al., 2009; Cassino et al., 2018) (Fig. III.6C). The return to wetter conditions at Lake Feia between 2730 and 2100 cal a BP (Fig. III.6D) corresponds to several wet events visible in the speleothem records at Diva cave (Novello et al., 2012) and Lapa Grande cave (Stríkis et al., (2011)). During this interval, the central Cerrado region was wetter because of the expansion of the SASM system (Fig. III.6D). Further north, at 5°S , the higher moisture rates observed between 2450 and 1530 cal a BP (Boqueirão lake, Utida, et al., 2019) have been related to the northward migration of the ITCZ, which increased the tropical South Atlantic winds into the continent, along with more moisture (Utida et al., 2019). At the equator (Paraiso cave; Wang et al., 2017), convective activity was high and the resulting wet wind flow was driven from eastern Amazonia to the central Cerrado region.

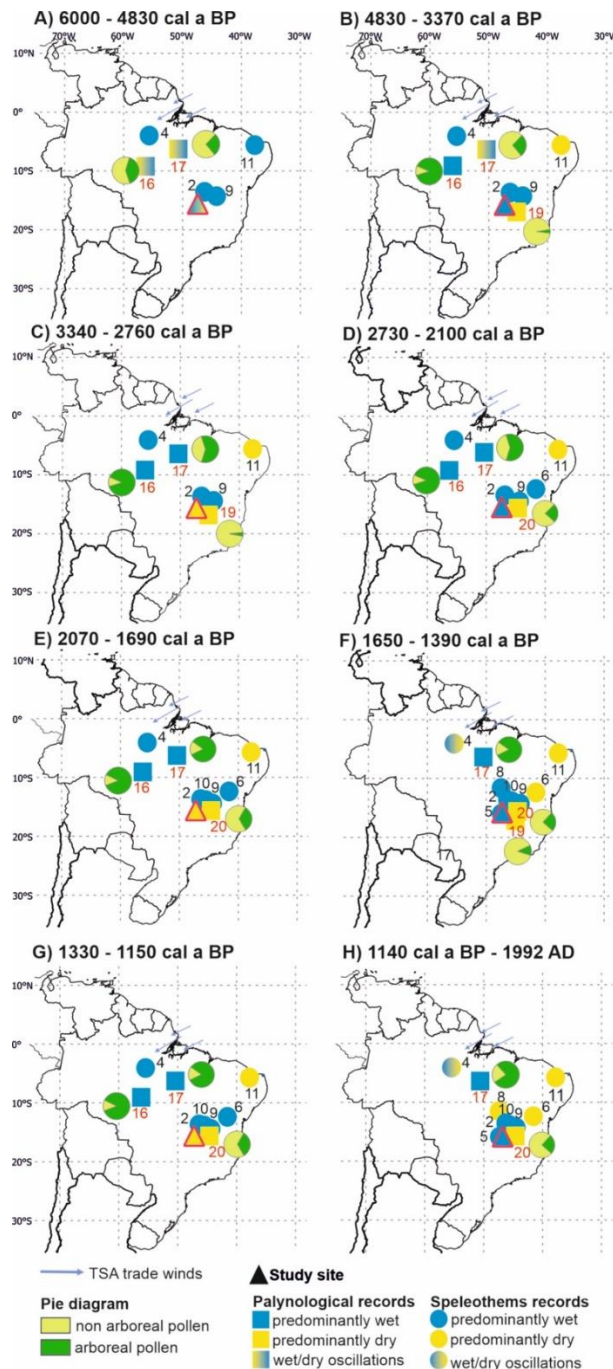


Figure III.6. A schematic representation of the *eight* climate episodes observed during the last 6000 years in the Cerrado biome, with their corresponding latitudinal boundaries. The site numbers are the same as Fig. 1. Arboreal pollen/non-arboreal pollen frequencies available from palynological sites are represented as pie diagrams.

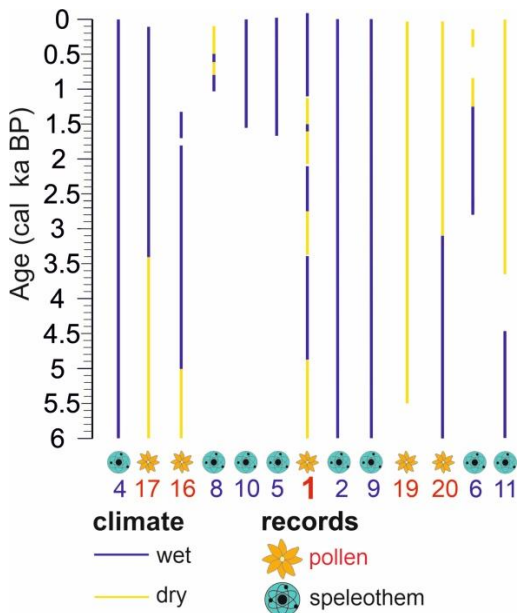


Figure III.7. Summary of the main climate changes (wet/dry events) observed in the last 6000 years between the paleo-records in Figure 6, organized according to their latitude and longitude. From left to right: the age scale in cal ka BP ($ka = 1000$ years), the paleo-records from north to south, and finally a summary of the SASM intensity at $15^{\circ}S$, at lake Feia. The blue lines represent wet climate and the yellow lines represent dry climate. The number below each record indicates the name of the record shown in Figure 1 (in red the pollen records and in blue the speleothem records).

During the second and third drier intervals, at 2070–1690 and 1330–1150 cal a BP, a gradual weakening of the SASM system occurred at Lake Feia, when the ITCZ shifted to a more northerly position (Fig. III.6E and III.6G). The wetter intervals, between 1650 and 1390 cal a BP, and from 1140 cal a BP onwards (Figs. III.6F and III.6H), was probably the result of instability in the ITCZ core area, which expanded and retracted along its northern edge (Utida et al., 2019). At Lake Feia, this was characterized by an abrupt change in erosion (Ti/K norm) at 1100 cal a BP, when conditions were mostly linked to humid wind flow from eastern Amazonia (Fig. III.6F).

Between 1020 and 600 a BP, during the medieval climate anomaly, the ITCZ remained in its northernmost position (Deininger et al., 2019). The northern edge of the SASM core region remained dry (Novello et al., 2012; Utida et al., 2019), while the southern edge received less precipitation as a result of a weaker SAMS trajectory toward the Atlantic Ocean (Bernal et al., 2017; Deininger et al., 2019). In the central region, the rainfall regime remained stable since 1140 cal a BP (as indicated at Tamboril cave at $16^{\circ}S$ and $47^{\circ}W$; Wortham et al., 2017; Wong et al. 2021) (Fig. III.4), suggesting that the rainfall reduction at the northern and southern boundaries of the SASM did not affect the core monsoon region (Fig. III.6H) (Campos et al., 2019). Thus, we infer that, at Lake Feia, a gradual increase in rainfall was mostly linked to its closer position to the core SASM region, with moisture fluxes from eastern Amazonia (Fig III.6H) (Azevedo et al., 2019). In addition, no change in the rainfall regime has been observed at Lake Feia during the last 400 years (corresponding to the Little Ice Age), which is in agreement with a southern shift of the ITCZ, which did not impact the central region (Deininger et al., 2019) but enhanced SASM activity on

the southern edge of the SASM zone of influence, and led to drier conditions in the northern region as a result of the establishment of the SW–NE dipole (Novello et al., 2012; Azevedo et al., 2019).

Overall, the Lake Feia pollen record shows that, during the last 6000 years, the floristic composition of the Cerrado has been highly sensitive to small changes in precipitation and seasonality, which has not been observed in neighboring speleothem records (Figs. III.6 and III.7). The increase in wet climatic conditions was the result of a reduced dry season, as clearly indicated in southern and central Brazil (Azevedo et al., 2019).

5.3 Fire events in central Brazil

Three main phases of fire activity were detected at Lake Feia during the last 19,000 years (Fig. III.4). The late Pleistocene was characterized by no fire activity, the first biomass burning being observed during the glacial–interglacial transition from ~11,000 to 10,500 cal a BP. Between 10,500 and 5100 cal a BP, the low charcoal influx, and the predominance of burned grass particles transported over long distances, suggests a weak, remote and irregular fire activity (Cassino et al 2020; Leys et al., 2017). From 5100 cal a BP onward, a higher charcoal influx and continuous fire activity was observed, with two peaks at ~3330 and ~1330 cal a BP (Figs. III.5, III.4 and Fig. S4). The increase in charred woody particles (W:L ratio > 0.5) (Fig. S4) is in agreement with the dominance of woody cerrado pollen taxa, which started around 4830 cal a BP (Fig. III.5).

The Cerrado is a fire-prone ecosystem where, under natural conditions, fire occurrence varies from 3 to 5–6 years (Pereira et al., 2014; Schmidt et al., 2017). However, limiting factors for fire occurrence are fuel availability and flammability, and heat (Glasspool et al., 2015). Thus, when a cerrado physiognomy becomes more arboreous, the probability of fire episodes decreases because of a reduction in grass biomass, which is more flammable compared to woody plants (Mistry, 1998; Pereira et al., 2014). Consequently, fire is more common in an open cerrado physiognomy, where it favors grass species germination (Oliveira et al., 2021; Fidelis and Zirondi, 2021). At Lake Feia, before 5000 cal a BP, the drier climatic conditions and probably the colder temperatures (indicated by the presence of the mountain taxa *Hedyosmum*) do not appear to have facilitated biomass burning. Experimental studies have shown a positive correlation between charcoal particles and temperature (Leys et al., 2017), suggesting that a reduction in temperature reduces fire activity.

After 5000 cal a BP, an increase in fire events was favored by both an increase in summer insolation and an increase in wet season(Figs. III.4 and III.5). Natural fires in the modern Cerrado are frequent during the wet season or in the transition between seasons, promoted by lightning, with short-lived fires usually extinguished by subsequent rain, burning small areas and with little effect on vegetation (Ramos-Neto and Pivello, 2000). Two short episodes of intense fire activity (CHARa 10–40 mm²/cm²/a) (Fig. III.4 and III.5), from 3330 to 3210 cal a BP and 1330 to 1160 cal a BP, were recorded. Three scenarios are proposed to explain the increased charcoal influx during these time periods: 1) a response to drier climatic conditions and lower lake levels; 2) the presence of fire closer to the study site; 3) human agency. Regarding the first scenario, the two fire events were reported during the first and third dry intervals, characterized by changes in tree taxa and lower lake levels. A drier climate could favor an expansion of grassland and consequently biomass

burning. However, during these two intervals the W:L ratio suggests mixed grass and wood charred particles. Moreover, if a dry climate could promote an intense fire event, the same pattern should be observed in the second dry interval, from 2070 to 1690 cal a BP. The second interval in fact shows lower levels of charred particles and fewer changes in gallery forest and woody cerrado taxa assemblages, with a recovery time of less than 30 years. Consequently, we suggest that drier climatic conditions cannot explain the abrupt increase in fire activity.

For the second scenario, the homogeneous W:L ratio suggests that a strong biomass burning reflects a widely burned area, with the fire occurring near the coring site. An increase in pollen influx is usually associated with an increase in fire intensity and the shorter distance from its source (Tinner et al., 2006; Duffin et al., 2008). Experimental analysis of charcoal particles has shown that the charcoal area increases with local fire (Leys et al., 2015, 2017), especially when charred wood particles are more abundant (Vachula et al., 2023). From 810 to 730 cal a BP, a mid-magnitude fire event (CHARarea <4 mm²/cm²/a) with more charred grass particles (Figs. III.4 and S4) was observed after a short dry episode, and did not prevent the expansion of woody cerrado and gallery forest taxa, with a recovery of about 12 years. Thus, for this shorter drier interval, a more regional fire signal that did not impact the local vegetation cover is inferred. The first and second scenarios could represent peaks in biomass burning reflecting climatic and local fire effects. Finally, regarding the third scenario, human agency cannot be discounted as a cause of localized fire, probably on the lake margin, during drought episodes. In the tropical lowlands, the level of human occupation was low until 5000 a BP (Riris and Arroyo-Kalin, 2019), when the climate was unstable and water resources rare (Cassino et al., 2020). Well-dated archeological studies are missing in the region of Lake Feia, despite its wealth of rock paintings and carvings, which are probably related to year-round abundant freshwater resources. To the west of Lake Feia, and at the same latitude, in the Tocantins–Araguaia river system, an increase in the human population was observed after 4600 cal a BP, as a result of the expansion of the Itaparica civilization (Moreno de Sousa, 2016). During the first and third drier intervals, the higher biomass burning was not concurrent with a gallery forest expansion toward the coring site. Moreover, there was an increase in the tree taxa *Ternstroemia* related to drier environments. After the high fire events, the recovery time for the expansion of the gallery forest toward the coring site was more than 30 years. Considering that forest is less likely to burn, and that gallery forest usually grows over moist and/or waterlogged soils, the presence of human activity on the lake margin cannot be discounted.

Finally, during the last 4800 years, the three intervals characterized by a decrease in water level-related taxa, at 3400–2700, 2100–1700 and 1350–1200 cal a BP, were associated with multi-centennial drought episodes. During these three drought events, the two higher fire activity events, 3330–3210 and 1330–1160 cal a BP, which were not associated with an expansion of the gallery forest toward the coring site, suggest both climatic and anthropogenic influences on vegetation cover and fire activity. No fire was observed during the second dry episode at 2070–1690 cal a BP, thus rejecting a human influence during this short dry interval, and low fire activity with no evidence of drought suggests remote biomass burning of the Cerrado from 810 to 730 cal a BP.

6. Conclusions

Our results show that, since the late Pleistocene, the central Cerrado region has been sensitive to local hydrology and changes in regional climate, driven by latitudinal boundaries of the monsoon convection, with changes in the boundaries toward northern, northeastern and southeastern Cerrado at a millennial scale. The long-term expansion of woody cerrado in central Brazil was precluded by the southward shift of the ITCZ, which was forced by insolation that strengthened the monsoon system and included eastern Amazonia in its zone of influence. Consequently, the development of the Cerrado vegetation started 6000 years ago in central Brazil, with the formation of a bimodal climate and an increase in summer insolation. The expansion of central Cerrado was a two-step process, starting with the establishment of an open cerrado until 4800 cal a BP, which was then replaced by a woody cerrado, perhaps driven by changes in the length of the dry season.

Superimposed on this global trend, multi-centennial short-term wet/dry episodes are reflected in changes in lake level, floristic composition of the gallery forest and biomass burning. These episodes could be related to small-scale enhancement or weakening of the SACZ, linked to changes in the southernmost and northernmost positions of the ITCZ and consequently driving changes in the SASM zone of influence at the latitude of Lake Feia.

Two fire events, at 3330–3210 and 1330–1160 cal a BP, occurred during drier climatic intervals and could be related to anthropogenic activity in the vicinity of the lake. The full vegetation recovery period after these events was more than 30 years.

7. Acknowledgements and funding

This work is part of the “Cerrados & Fogos” program at IRD. Financial support was provided by IRD, FAPDF (0193.001374/2016), ISEM, DEGEO-UFOP and IG-UnB. KET benefited from a PhD position funded by the IRD ARTS program and the French Embassy in Bolivia. RFC benefited from a South-North IRD grant during her stay at ISEM. This work has also benefited from an “Investissement d’Avenir” grant managed by the Agence Nationale de la Recherche (CEBA, ref. ANR-10-LABX-25-01). Radiocarbon dating was performed at LMC14 (LSCE(CNRS-CEA-UVSQ)-IRD-IRSN-MC) with IRD financial support. We thank Ludivine Eloy and Michel Brossard for fruitful discussions.

8. Annex 1. Supporting information

TABLES

Table S1. Ecological classification of pollen taxa identified in the LFB1 core, based on phytosociological surveys (Araújo et al., 2002, 2011; Assunção and Felfili, 2004; Bridgewater et al., 2004; Bueno et al., 2013, 2018; Carvalho and Martins, 2009; Felfili, 1995, 1997; Felfili et al., 2004; Rossi et al., 1998; Silva Junior et al., 1998, Silva and Felfili, 1998).

Family	Taxon	Life form	Ecological classification
Acanthaceae	<i>Justicia</i>	Herb	cerrado
Amaranthaceae	<i>Gomphrena</i>	Herb	cerrado
Amaranthaceae	<i>Althernantera</i>	Herb	cerrado
Amaranthaceae	<i>Am/Cheno</i>	Herb	cerrado
Anacardiaceae	<i>Astronium</i>	Tree	cerrado (cerradão)
Anacardiaceae	<i>Cyrtocarpa</i>	Tree	cerrado (cerradão)
Anacardiaceae	<i>Tapirira</i>	Tree	gallery forest
Anacardiaceae	<i>Thyrsdium type</i>	Tree	gallery forest/cerradão
Apiaceae	<i>Apium</i>	Herb	gallery forest
Apocynaceae	<i>Aspidosperma</i>	Tree	gallery forest/cerradão
Aquifoliaceae	<i>Ilex</i>	Tree	gallery forest
Araceae	<i>Spatiphyllum</i>	Herb	gallery forest
Araliaceae	<i>Schefflera</i>	Tree	cerrado (cerradão)
Arecaceae	<i>Euterpe type</i>	Treepalm	gallery forest/lake margin
Asteraceae	<i>Baccharis</i>	Herb/shrub	cerrado
Asteraceae	<i>Vernonia</i>	Herb	cerrado
Bignoniaceae	<i>Jacaranda</i>	Tree	cerrado (cerradão)
Bignoniaceae	<i>Tabebuia</i>	Tree	cerrado (cerradão)
Boraginaceae	<i>Cordia</i>	Herb	gallery forest/cerradão
Boraginaceae	<i>Echium</i>	Herb	cerrado
Boraginaceae	<i>Heliotropium</i>	Herb	cerrado/antropic
Burseraceae	<i>Protium</i>	Tree	gallery forest/cerradão
Cannabaceae	<i>Celtis</i>	Tree	gallery forest
Cannabaceae	<i>Trema</i>	Tree	gallery forest/lake margin
Caryocaraceae	<i>Caryocar</i>	Tree	cerrado
Celasteraceae	<i>Plenckia</i>	Tree	cerrado
Celasteraceae	<i>Celasteraceae</i>	Tree	gallery forest/cerradão
Chrysobalanaceae	<i>Licania type</i>	Tree	gallery forest/cerradão
Cleomaceae	<i>Cleome</i>	Herb	cerrado
Clethraceae	<i>Clethra</i>	Tree	gallery forest
Connaraceae	<i>Connarus</i>	Tree	gallery forest/cerradão
Convolvulaceae	<i>Evolvulus</i>	Herb	cerrado
Cunnoniaceae	<i>Lamanonia</i>	Tree	gallery forest
Dillenaceae	<i>Curatella</i>	Tree	cerrado
Elaeocarpaceae	<i>Sloanea</i>	Tree	gallery forest
Ericaceae	<i>Ericaceae</i>	Shrub	gallery forest/lake margin

Erythroxilaceae	<i>Erythroxylum</i>	Tree	cerrado (cerradão)
Euphorbiaceae	<i>Chamaesyce</i>	Shrub	cerrado
Euphorbiaceae	<i>Euphorbia</i>	Shrub	cerrado
Euphorbiaceae	<i>Sapium</i>	Shrub	cerrado
Euphorbiaceae	<i>Sebastiana</i>	Shrub	cerrado
Euphorbiaceae	<i>Acalypha</i>	Herb	gallery forest/cerradão
Euphorbiaceae	<i>Alchornea</i>	Tree	gallery forest
Euphorbiaceae	Euphorbiaceae	All	various
Fabaceae	Fabaceae	All	various
Fabaceae (caesalpiniaceae)	<i>Ateleia</i>	Tree	cerrado (cerradão)
Fabaceae (caesalpiniaceae)	<i>Dipteropis</i>	Tree	cerrado (cerradão)
Fabaceae (caesalpiniaceae)	<i>Caesalpinea</i> type	Tree	cerrado (cerradão)
Fabaceae (caesalpiniaceae)	<i>Cassia</i> type	Tree	Gallery forest
Fabaceae (caesalpiniaceae)	<i>Copaifera</i>	Tree	cerrado (cerradão)
Fabaceae (caesalpiniaceae)	<i>Crotalaria</i>	Shrub	cerrado
Fabaceae (caesalpiniaceae)	<i>Senna</i>	Tree	gallery forest/cerradão
Fabaceae (caesalpiniaceae)	<i>Peltogyne</i>	Tree	cerrado
Fabaceae (caesalpiniaceae)	<i>Pterogyne</i>	Tree	cerrado (cerradão)
Fabaceae (mimosaceae)	<i>Anadenanthera</i>	Tree	gallery forest
Fabaceae (mimosaceae)	<i>Mimosa</i>	Shrub	cerrado
Fabaceae (mimosaceae)	<i>Piptadenia</i>	Tree	gallery forest
Fabaceae (papilonaceae)	<i>Andira</i>	Tree	gallery forest/cerradão
Fabaceae (papilonaceae)	<i>Apuleia</i>	Tree	gallery forest
Fabaceae (papilonaceae)	<i>Cratylia</i> type	Shrub	cerrado
Fabaceae (papilonaceae)	<i>Dalbergia</i>	Tree	cerrado
Fabaceae (papilonaceae)	<i>Dipteryx</i> type	Tree	cerrado (cerradão)
Fabaceae (papilonaceae)	<i>Erythrina</i>	Tree	cerrado (cerradão)
Fabaceae (papilonaceae)	<i>Glycyrrhiza</i> type	Subshrub/shrub	cerrado (cerradão)
Fabaceae (papilonaceae)	<i>Machaerium</i>	Tree	cerrado (cerradão)
Fabaceae (papilonaceae)	<i>Macroptilium</i>	Herb	cerrado
Fabaceae (papilonaceae)	<i>Pterodon</i>	Tree	cerrado
Fabaceae (papilonaceae)	Papilionaceae	All	various
Fabaceae	<i>Rhynchosia</i>	Herb	cerrado
Humiricacae	<i>Vantanea</i>	Tree	gallery forest
Icacinaceae	<i>Villarezia</i>	Tree	gallery forest
Lamiaceae	<i>Aegiphila</i>	Tree	gallery forest/cerradão
Lamiaceae	<i>Hyptis</i>	Herb	cerrado
Loranthaceae	<i>Psittacanthus</i>	Herb	cerrado
Lythraceae	<i>Cuphea</i>	Herb	cerrado/lake margin
Lythraceae	<i>Lafoensis</i>	Tree	cerrado
Malvaceae	<i>Apeiba</i>	Tree	gallery forest
Malpighiaceae	<i>Banisteriopsis</i>	Vine	gallery forest
Malpighiaceae	<i>Byrsonima</i>	Tree	cerrado
Malpighiaceae	<i>Malpighia</i> type	Herb/vine	gallery forest

Malvaceae	<i>Ceiba speciosa</i> type	Herb	cerrado
Malvaceae	<i>Byttneria</i>	Herb/subshrub	cerrado
Malvaceae	<i>Helicteres</i> type	Shrub	cerrado
Malvaceae	<i>Eriotheca</i>	Tree	cerrado (cerradão)
Melastomataceae	Melastomataceae	Tree	various
Meliaceae	<i>Cedrela</i>	Tree	gallery forest
Meliaceae	<i>Guarea</i> type	Tree	gallery forest/lake margin
Menispermaceae	<i>Abuta</i> type	Shrub	cerrado
Moraceae	Moraceae	Tree	gallery forest
Myrtaceae	Myrtaceae	Tree	various
Nyctaginaceae	<i>Pisonia</i>	Tree	gallery forest/cerradão
Ochnaceae	<i>Ouratea</i>	Tree	cerrado (cerradão)
Ochnaceae	<i>Sauvagesia</i>	Herb	cerrado/lake margin
Pentaphylacacées	<i>Ternstroemia</i>	Tree	semideciduous forest
Phytolaccaceae	<i>Gallesia</i>	Tree	gallery forest
Piperaceae	<i>Peperomia</i>	Herb	gallery forest
Piperaceae	<i>Piper</i>	Shrub	gallery forest/lake margin
Plumbaginaceae	<i>Plumbago</i> type	Subshrub	gallery forest
Poaceae	Poaceae	Herb	cerrado
Podocarpaceae	<i>Podocarpus</i>	Tree	gallery forest
Portulacaceae	<i>Portulaca</i>	Herb	cerrado
Primulaceae	<i>Cybianthus</i>	Tree	gallery forest/cerradão
Primuliaceae	<i>Myrsine</i>	Tree	gallery forest/lake margin
Rhamnaceae	<i>Ziziphus</i>	Tree	gallery forest
Rhamnaceae	<i>Colubrina</i>	Tree	gallery forest
Rubiaceae	<i>Borreria</i>	Herb	cerrado
Rubiaceae	<i>Didymaea</i> type	Herb	cerrado
Rubiaceae	<i>Alibertia</i>	Shrub	cerrado (cerradão)
Rubiaceae	Sabiceae	Shrub/herb	cerrado (cerradão)
Rubiaceae	<i>Citrus</i>	Tree	cerrado
Rubiaceae	<i>Psychotria</i>	Shrub	gallery forest
Rubiaceae	<i>Amajuoa</i>	Tree	gallery forest
Rubiaceae	<i>Coussarea</i>	Tree	gallery forest/cerradão
Rubiaceae	<i>Guettarda</i>	Tree	gallery forest/cerradão
Rubiaceae	Rubiaceae type	All	various
Rutaceae	<i>Esenbeckia</i>	Shrub	cerrado
Rutaceae	<i>Zanthoxylum</i>	Tree	cerrado (cerradão)
Salicaceae	<i>Casearia</i>	Tree	cerrado (cerradão)
Sapindaceae	<i>Diatenopterix</i>	Shrub	cerrado/gallery forest
Salicaceae	<i>Neosprucea</i>	Tree	cerrado
Sapindaceae	<i>Paullinia</i>	Herb	gallery forest
Sapindaceae	<i>Matayba</i>	Tree	gallery forest/cerradão
Sapotaceae	<i>Chrysophyllum</i>	Treelet	cerrado (cerradão)
Sapotaceae	<i>Diplooon</i>	Tree	gallery forest/cerradão

Sapotaceae	<i>Pouteria</i>	Tree	gallery forest/cerradão
Simaroubaceae	<i>Simaruba</i>	Tree	gallery forest/cerradão
Smilaceae	<i>Smilax</i>	Herb	gallery forest
Solanaceae	<i>Solanum</i>	Shrub	cerrado/gallery forest
Urticaceae	<i>Cecropia</i>	Tree	gallery forest/lake margin
Verbenaceae	<i>Lantana</i>	Shrub	cerrado/gallery forest
Verbenaceae	<i>Lippia</i>	Shrub	cerrado/lake margin
Vochysiaceae	<i>Vochysia</i>	Tree	cerrado/cerradão
Winteraceae	<i>Drimys</i>	Tree	gallery forest
Xyridaceae	<i>Xyris</i>	Herb	cerrado/lake margin
Cyperaceae	Cyperaceae	Herb	various
Alismataceae	<i>Echinodorus</i>	Herb	lake margin
Alismataceae	<i>Sagittaria</i>	Herb	lake margin
Arecaceae	<i>Mauritia</i> type	Treepalm	lake margin/aquatic
Cabombaceae	<i>Cabomba</i>	Herb	lake margin/aquatic
Eriocaulaceae	<i>Eriocaulon</i>	Herb	lake margin
Haloragaceae	<i>Myriophyllum</i>	Herb	aquatic
Lentibulariaceae	<i>Utricularia</i>	Herb	lake margin
Lythraceae	<i>Crenea</i>	Herb	lake margin/aquatic
Nymphaeaceae	<i>Nymphaea</i>	Herb	aquatic
Onagraceae	<i>Ludwigia</i>	Shrub	lake margin
Plantaginaceae	<i>Stemodia</i> type	Herb	lake margin
Polygalaceae	Polygalaceae	Herb	lake margin
Polygonaceae	<i>Polygonum</i>	Herb	lake margin
Pontederiaceae	<i>Eichornia</i>	Herb	aquatic
Potamogetaceae	<i>Potamogeton</i>	Herb	aquatic
Rubiaceae	<i>Diodella</i>	Herb	lake margin
Scrophulariaceae	<i>Bacopa</i>	Herb	lake margin
Typhaceae	<i>Typha</i>	Herb	aquatic

Table S2. Principal component analysis (PCA) of the pollen taxa and their contribution to the temporal variability.

Taxon	PC1	PC2	PC3	PC4	PC5
Myrtaceae	0.0016	4.18E+00	1.53E+01	3.71E-01	1.06E-01
Melastomataceae	1.179555	9.39E-01	4.80E-02	4.28E-01	6.18E+00
<i>Ilex</i>	0.790575	2.14E+00	6.53E+00	4.26E-02	4.08E-01
<i>Trema</i>	1.402998	1.13E-01	5.64E-01	1.94E+00	1.68E+00
<i>Guarea</i>	0.008116	3.25E-01	1.39E-01	1.11E+00	4.05E+00
<i>Myrsine</i>	5.787764	3.21E-01	4.36E-01	1.37E-02	1.81E-01
<i>Cecropia</i>	5.454394	1.11E-01	6.56E-01	2.99E+00	7.49E-01

<i>Euterpe</i>	0.741225	1.25E+00	1.46E+00	4.21E-02	3.14E+00
<i>Tapirira</i>	2.838768	7.98E-02	3.29E-01	3.02E-02	2.84E-01
<i>Celtis</i>	6.514203	1.90E+00	1.89E-03	9.86E-02	3.21E+00
<i>Clethra</i>	0.030433	6.68E-01	3.62E-02	1.38E+00	9.27E-01
<i>Lamanonia</i>	3.87372	1.02E+00	3.69E-02	1.93E+00	1.33E-03
<i>Sloanea</i>	0.511929	3.26E-03	2.72E+00	2.02E-01	2.48E-03
<i>Alchornea</i>	1.795179	3.66E-01	2.77E-01	1.05E-01	7.44E+00
<i>Apuleia</i>	1.789067	2.63E+00	1.65E-01	1.09E+01	7.93E-01
<i>Anadenanthera</i>	1.361225	2.09E-01	4.76E-02	4.27E-01	2.98E-01
<i>Piptadenia</i>	1.383366	1.73E-06	1.14E-02	1.41E-01	1.90E+00
<i>Vantanea</i>	1.456087	3.65E+00	5.69E-02	1.39E+01	1.37E-01
<i>Villarezia</i>	0.00212	6.72E-01	1.63E-01	1.73E-01	1.03E+00
<i>Apeiba</i>	0.664419	1.76E-01	6.34E-01	7.08E-02	7.95E+00
<i>Cedrela</i>	0.053749	2.83E+00	7.97E+00	5.87E-01	6.90E-01
Moraceae	5.905101	7.39E-01	1.18E-02	1.06E+00	8.53E-02
<i>Gallesia</i>	0.370934	9.15E-02	6.24E-01	1.82E-03	4.11E+00
<i>Podocarpus</i>	0.087041	1.09E+00	4.32E-01	1.30E+00	9.35E-03
Rosaceae	0.001568	1.33E+00	5.42E-02	1.41E-05	7.25E-02
<i>Ziziphus</i>	0.432087	3.34E+00	2.85E-01	2.02E-02	9.02E-03
<i>Colubrina</i>	2.372129	7.57E-01	4.17E-03	3.11E+00	2.14E+00
<i>Amaiuaoa</i>	0.001871	4.38E-01	8.29E-05	1.75E-01	6.12E-01
<i>Drymis</i>	0.07726	2.59E-02	1.37E-03	3.45E-02	1.55E+00
<i>Banisteriopsis</i>	0.053486	2.46E+00	1.40E+01	5.23E-01	3.18E-03
<i>Poaceae</i>	5.870007	3.69E-02	1.29E-01	9.43E-01	7.74E-01
<i>Cassia</i> type	0.311777	7.81E-01	2.87E-01	1.54E-01	1.43E-01
<i>Senna</i>	0.720932	3.90E+00	2.07E+00	2.07E+00	1.51E-02
<i>Andira</i> type	0.078293	1.01E-01	7.02E-02	1.46E+01	8.68E-01
<i>Pisonia</i>	0.36167	5.85E-03	7.45E-02	5.60E-01	5.23E-01
<i>Cybianthus</i>	3.035126	4.22E-01	3.75E-01	6.79E-01	3.08E-01
Rhamnaceae	0.043932	3.59E-05	1.02E-03	2.72E-02	1.10E-02
<i>Coussarea</i>	0.603992	5.49E+00	1.83E+00	3.23E-02	8.98E-01
<i>Guettarda</i>	3.281143	2.29E+00	6.99E-01	4.07E-01	1.63E-01
<i>Matayba</i>	2.751269	2.17E+00	2.87E+00	6.16E-01	1.33E-04
<i>Samaba/Simaruba</i>	0.041321	1.39E-02	1.94E-01	1.08E-02	2.03E-01
<i>Protium</i>	0.74764	5.92E-01	2.75E-01	1.30E+00	6.73E-01
<i>Aspidosperma</i> type	0.05617	1.43E+00	7.61E+00	6.67E-01	1.69E-02
<i>Thyrsodium</i> type	0.718029	3.43E+00	6.21E-01	1.33E+00	1.37E-03
<i>Erythrina</i>	0.122823	4.17E-02	4.98E-02	1.48E-01	6.34E-03
<i>Ternstroemia</i>	0.145183	2.11E+00	1.11E+00	3.12E-03	8.27E+00
<i>Pterogyne</i>	0.094572	2.93E+00	3.90E-01	6.00E-03	9.29E-01
<i>Ateleia</i>	0.032263	1.32E-02	2.81E-01	8.44E-01	3.45E+00
<i>Diplotropis</i>	0.086668	1.56E-01	1.31E-02	1.22E-01	6.45E-03
<i>Licania</i> type	0.138436	1.94E+00	1.27E+01	1.58E-01	1.59E-01

<i>Connarus</i> type	0.48735	4.76E-01	3.15E-01	2.35E-01	3.07E-01
<i>Aegiphila</i>	0.123962	5.15E-04	4.68E-03	3.25E-03	7.77E-01
Celasteraceae type	0.163682	3.32E+00	5.24E-01	2.77E+00	1.74E+00
<i>Diplooon</i>	2.40457	4.47E+00	2.20E-01	3.76E+00	2.02E-02
<i>Pouteria</i>	1.792844	1.28E+00	6.30E-01	9.57E-03	2.14E+00
<i>Astronium</i>	4.430871	1.88E-01	3.80E-01	4.56E-01	2.11E+00
<i>Schefflera</i>	5.924555	6.70E-01	6.31E-03	2.65E-01	2.01E-01
<i>Copaifera</i>	3.411755	3.25E-02	1.52E-01	9.01E-01	3.58E-01
<i>Eriotheca</i>	0.966714	2.14E+00	2.56E-03	9.67E-01	2.53E+00
<i>Zanthoxylum</i>	0.04248	1.12E+00	1.24E-01	6.56E-02	2.72E+00
<i>Casearia</i>	1.872353	6.42E-02	1.06E+00	7.22E-03	3.45E+00
<i>Chrysophyllum</i>	0.063083	3.45E-02	1.47E-01	1.68E+00	4.25E-05
<i>Vochysia</i>	0.009194	2.89E-01	7.17E-01	1.12E-01	2.26E-01
Ouratea	0.289571	1.75E-02	1.66E-02	1.33E-01	2.73E+00
<i>Cyrtocarpa</i>	1.467075	5.73E-01	1.21E-01	3.76E-02	1.73E+00
<i>Jacaranda</i>	0.403733	8.87E-01	2.54E+00	1.92E+00	8.58E-03
<i>Tabebuia</i>	1.012926	7.05E+00	1.02E+00	2.99E-01	5.16E-01
<i>Erythroxilum</i>	1.273246	4.04E+00	2.01E+00	4.01E-01	1.15E+00
<i>Caesalpinea</i> type	0.186274	6.28E-01	2.04E-01	1.50E-01	5.10E-02
<i>Dalbergia</i>	0.077493	3.50E-03	1.29E-01	2.71E-01	1.07E-03
<i>Dipteryx</i> type	0.222771	7.62E-01	2.87E+00	5.03E-03	2.28E-01
<i>Machaerium</i>	0.025338	1.29E-01	1.20E-02	1.46E-01	3.05E-01
<i>Byrsinima</i>	3.848225	8.85E-01	3.68E-02	2.17E+00	2.06E-01
<i>Peltogyne</i>	0.032795	5.77E+00	1.01E+00	4.48E-02	8.90E-03
<i>Caryocar</i>	0.123721	4.71E-02	2.08E-01	1.67E-01	4.18E-01
<i>Plenckia</i>	0.187918	7.40E-01	2.16E-01	1.20E+01	1.53E-01
<i>Curatella</i>	1.665836	9.96E-01	2.36E-01	6.00E-02	2.19E+00
<i>Pterodon</i>	0.112336	9.95E-04	6.79E-02	1.67E-01	1.48E+00
<i>Lafoensia</i>	0.008988	9.33E-01	1.72E-02	4.36E-01	1.39E+00
<i>Citrus</i>	0.655789	6.51E-02	1.85E-01	2.41E-02	3.55E+00
<i>Neosprucea</i>	0.529339	6.51E-01	1.78E-01	2.60E+00	1.62E-01

Table S3. Principal component analysis (PCA) results showing the eigenvalues of each component and the significance as a percentage, and the contribution of Poaceae, cerrado tree taxa and gallery forest taxa. Bold numbers show the contribution of important taxa in each component

	PC1	PC2	PC3
Eigenvalue	4.0720421	2.2171906	1.9753245
% of variance	20.360211	11.085953	9.876623
Cumulative % of variance	20.360211	31.44616	41.32279
Variable contribution			
<i>Alchornea</i>	0.015606	0.477148	5.833479
<i>Anadenanthera</i>	3.077405	0.110325	4.029714

<i>Apeiba</i>	5.513804	8.668668	7.532887
<i>Astronium</i>	10.3359	1.096979	6.5464
<i>Banisteropsis</i>	2.953117	14.38045	0.692803
<i>Byrsonima</i>	6.169119	0.42987	0.543156
<i>Casearia</i>	0.199846	14.40314	0.004718
<i>Cecropia</i>	9.185715	2.078618	3.580463
<i>Celtis</i>	11.24933	1.655514	3.258701
<i>Euterpe</i> type	0.160955	11.48573	1.565791
<i>Ilex</i>	10.70556	4.836976	0.10812
Melastomataceae	0.200181	2.718896	25.27243
Moraceae	10.10654	0.001396	2.318473
<i>Myrsine</i>	5.923308	0.195154	13.17908
Myrtaceae	3.90931	23.25632	0.036048
<i>Ouratea</i>	0.023185	2.980759	1.503758
Poaceae	8.930181	1.534874	8.595117
<i>Tapirira</i>	2.372401	1.015388	1.806671
<i>Ternstroemia</i>	3.213703	8.524285	13.55841
<i>Trema</i>	5.754831	0.149508	0.033776

Table S4. Classification of pollen based on their life form (LF), pollination syndromes (PS), ecological needs (S = stratum; L = light exposition) and habitat. t = tree; h = herb; e = entomophilous; a = anemophilous; ls = lower storey (< 10 m); ms = medium storey (~15 m); us = upper storey (>20 m); st = shade tolerant; ld = light demanding. The classification of pollination syndrome was based on Deus *et al.* (2014), Martins and Batalha (2006), Pereira *et al.* (2022) and Rios and Sousa-Silva (2017). The classification of life form and ecological needs was obtained from Rossi *et al.* (1998), Silva Junior *et al.* (1998), Araujo *et al.* (2011), Felfili *et al.* (2007), Oliveira-Filho and Ratter (1995), Assunção and Felfili (2004), Araujo *et al.* (2002), Carvalho and Martins (2009), Felfili *et al.* (2004), Bridgewater (2004), Silva and Felfili (1998), Bueno *et al.* (2013, 2018) and (Durigan *et al.* (2022).

Family	Pollen taxa	LF	PS	S-L	Habitat
Gallery forest					
Anacardiaceae	<i>Tapirira</i>	t	e	ms-st	Commonly found in moist soils that can tolerate a reduction in humidity
Aquifoliaceae	<i>Ilex</i>	t	e	ls-st	When present and well established can support low humidity. Can be present in montane forest and in floodplain or swampy gallery forest
Arecaceae	<i>Euterpe</i>	t	e	ls-st	Moist soils and/or increase in precipitation
Cannabaceae	<i>Celtis</i>	t	e	ls	Moist soils, when present in gallery forest can support periodic flooding
Cannabaceae	<i>Trema</i>	t	ae	ls-ld	Found in humid soils, but can growth in inundated areas. Pioneer tree
Euphorbiaceae	<i>Alchornea</i>	t	a	us-ld	Along river banks and alluvial plains
Fabaceae (mim)	<i>Anadenanthera</i>	t	e	md-ld	Fertile soils with resistance to water deficiency
Malpighiaceae	<i>Banisteropsis</i>	t	e	ls-ld	Inside gallery forest and dry forest
Malvaceae	<i>Apeiba</i>	t	e	ms	Moist soils with low resistance to water deficiency
Melastomataceae	<i>Melast-Comb</i>	t	e	ls	Fertile and moist soils. Can be found associated with the edge of swamps and marshes
Moraceae	<i>Mor-Urt</i>	t	ae	ls	Well-drained soils in moist forest, common in rainforest

Myrtaceae	Myrtaceae	t	e	ls	Moist soils, adapted to reduction in water availability. Can tolerate less humid conditions
Primulaceae	<i>Myrsine</i>	t	e	us-ld	Usually found in forest (gallery forest, dry forest and cerradão), tolerant to reduced water availability
Urticaceae	<i>Cecropia</i>	t	ae	ls-ld	Moist soils. Pioneers with rapid growth: re-establishes woodland physiognomies
Cerrado					
Poaceae	Poaceae	t	a	f	Most species C4 plants, dominant on open cerrado physiognomies
Anacardiaceae	<i>Astronium</i>	t	e	ls	Commonly found in rocky and dry soils, with a preference for fertile soils, and can tolerate reduction in humidity
Dillenaceae	<i>Curatella</i>	t	e	ls	Adapted to dry soils; drought tolerant and slow growth
Fabaceae (pap)	<i>Dalbergia</i>	t	e	ls-st	Fertile soils; adapted to dry conditions and reduced water availability
Malpighiaceae	<i>Byrsonima</i>	t	e	ls	Well-drained soils, adapted to reduced water availability
Ochnaceae	Ouratea	t	e	ls, lm-ld	Well-drained soils, can tolerate dry conditions. Found in transition zones from open to closed physiognomies, usually in Cerrado <i>sensu stricto</i> and cerradão
Pentaphylaceae	<i>Ternstroemia</i>	t	e	ls	Fertile soils; when established can tolerate drought
Salicaceae	<i>Casearia</i>	t	e	ls	Found in moist soils; tolerates reduced water availability. Natural pioneer trees, observed after burn episodes. Commonly found near river banks, in the upper area, and in transition zones from grassland to arboreal vegetation

FIGURES

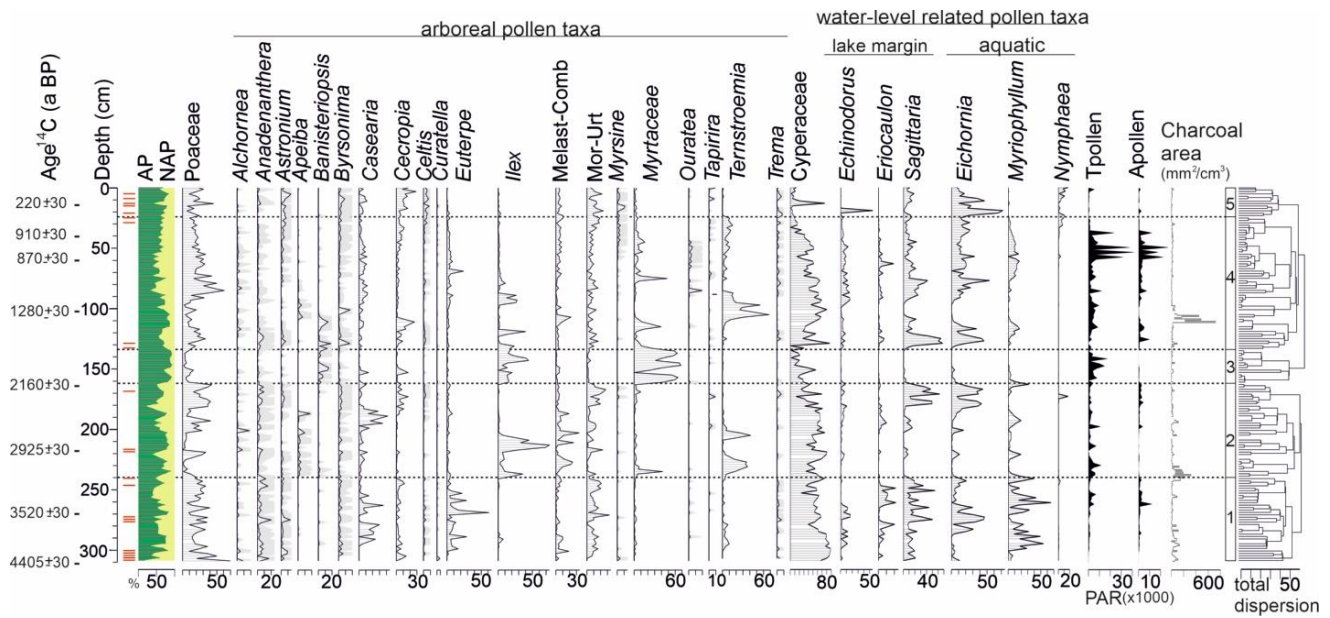
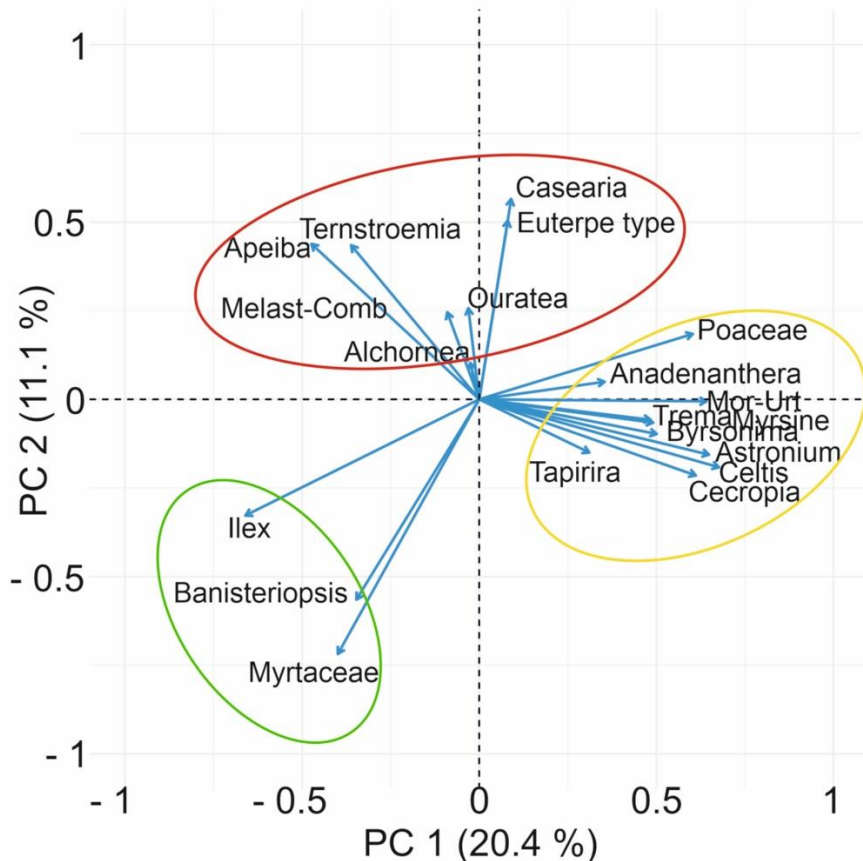


Figure S1. Pollen diagram for core LFB1 showing, from left to right, radiocarbon date, depth scale, arboreal/non-arboreal pollen (AP/NAP) frequency, the frequency of 28 selected pollen taxa, total pollen influx (PAR) for terrestrial (Tpollen) and water level-related (Apollen) taxa, macrocharcoal concentration (mm^2/cm^3) and cluster diagram for five pollen zones. The red bars on the left show the samples with less than 300 pollen grains in the sum of total pollen.

A)



B)

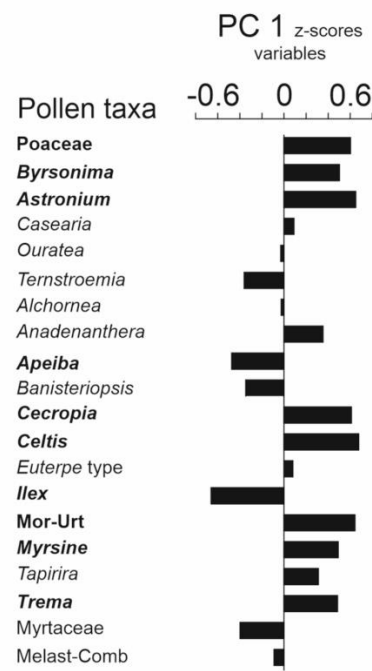


Figure S2. (A) Principal component analysis (PCA) of selected pollen taxa representing the first and second components. The groups suggest a relationship with water availability: high (green), intermediate (red), and low (yellow) dependance. (B) *z*-scores for each variable contributing to PC1; the pollen taxa in bold contributed >5% to the temporal changes for the first component.

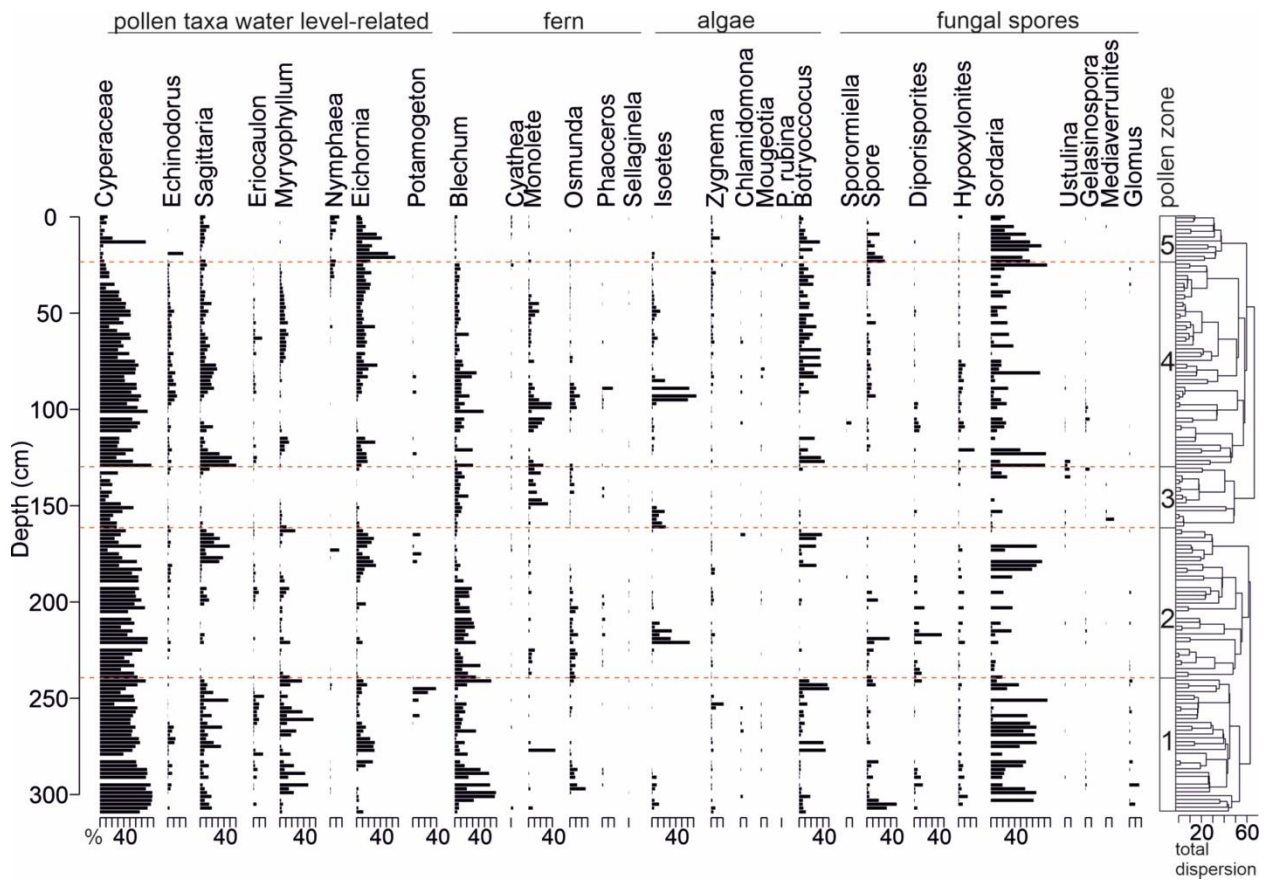


Figure S3. Pollen diagram of the water level-related taxa (8), fern spores (6) and non-palynomorphs (algae and fungal spores) (15) from core LFB1, presented along a depth scale and showing the pollen zones.

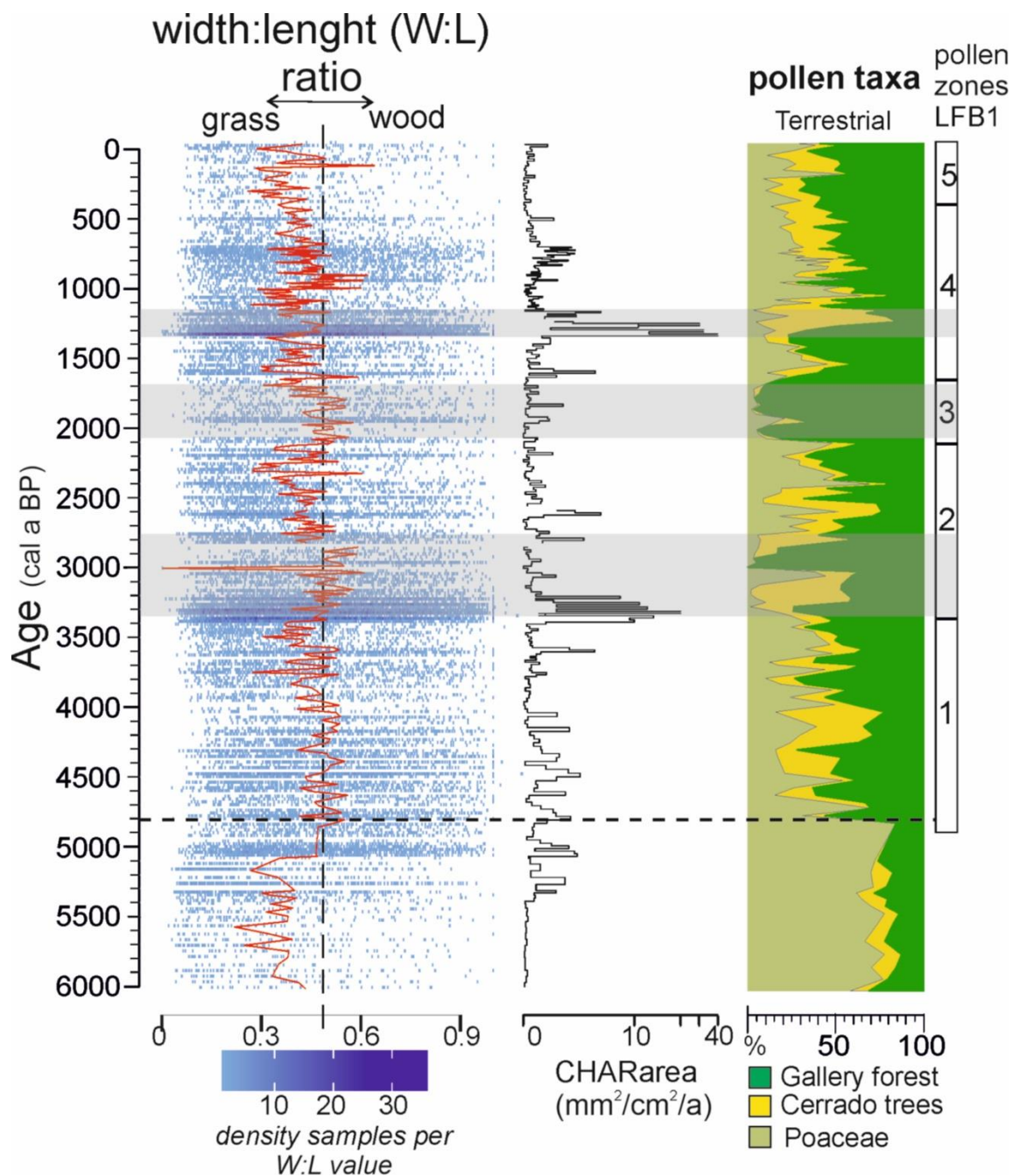


Figure S4. Changes in fire activity at Lake Feia during the last 6000 years, showing, from left to right, the time scale (cal a BP), W:L ratio, charcoal influx (CHARarea; $\text{mm}^2/\text{cm}^2/\text{a}$), a summary pollen diagram for the three main ecological groups, and the pollen zones. The dashed vertical line shows the division between grass/wood origin of the charcoal particles (from Aleman et al., 2013), the dashed horizontal line shows when the vegetation cover changed from an open to a woody cerrado, and the gray bands show the dry intervals as identified by the palynological analysis.

Article 3

Link between northern hemisphere ice melting and Cerrado biodiversity

Article en préparation

Katerine Escobar-Torrez^{1,2}, Marie-Pierre Ledru¹, Raquel Franco Cassino², Ingrid Horák-Terra³, Ilana Wainer⁴, Manuel Chevalier⁵

1. Institut des Sciences de l'Evolution de Montpellier (ISEM), Université de Montpellier-CNRS-IRD-EPHE, France

2. Departamento de Geologia, Universidade Federal de Ouro Preto, Brazil

3. Instituto de Ciências Agrárias, Universidade Federal dos Vales do Jequitinhonha e Mucuri (ICA/UFVJM), Brazil

4. Institute of Oceanography, University of São Paulo (IOUSP)

5. Institute of Geosciences, Sect. Meteorology, Rheinische Friedrich – Wilhelms - Universität Bonn, Germany

Corresponding author: Katerine Escobar Torrez

e-mail address: katerine.escobartorrez@ird.fr

postal address: Institut des Sciences de l'Evolution, ISEM (UMR 226 – IRD/ CNRS/UM2), 34095 Montpellier, cedex 05, France.

Abstract

A multi-proxy study based on pollen, macrocharcoal, isotopes and trace elements was carried out at the ecological station of Serra Geral to Tocantins in Brazil. The sediment core (VGE-17) was taken from the Getulio swamp, at 10°S and 46°W, located in the drainage network of the Sano river. 15,000 years of continuous landscape history was recorded in the VGE-17 core, where the multiproxy analyses was able to differentiate change in vegetation composition related to regional climatic events. The cerrado vegetation was primarily composed of a grassland with sparse trees and a gallery forest which experienced a re-arrangement of tree elements coupled with climate periods in response to south and north hemisphere climatic gradients , recorded two particular events. First, the two phases Younger Dryas event, wet since 12,900 to 12,300 followed by dryness until 11,500. Second, recording for the first time in the region the “8200 event” with a long gradual duration of 1060 years, between 9300 to 8240 cal yr BP. Then, the gradual decrease of arboreal elements and the dominance of open cerrado phygionomies since 7160 cal yr BP marked the onset of drier conditions in the region, with an almost complete retreat of gallery forest by 4370 cal yr BP, encompassed with the dominance of open cerrado vegetation towards the present. Our results show that vegetation changes in VGE-17 were sensitive to global changes as insolation, ocean circulation, South American monsoon system and Inter tropical convergence zone (ITCZ) position and intensity, the extent of the 8200 event, and the linkage of the study area with insolation and ITCZ movements more related to Nort-east of Brazil climate. On the other hand, fire events were less common near our study site suggesting only the presence of regional fires far from Getulio swamp area.

Keywords: gallery forest, pollen, Holocene, insolation, South American Summer Monsoon, fire.

1. Introduction

The Cerrado is the second largest biome in Brazil, covering two million km² (Strassburg et al., 2017), and located in between two major tropical rainforests (Amazon and Atlantic forest) with which it shares plant families and genera although with different species composition (Bridgewater et al., 2004). From North to South differences in floristic composition are linked to climate (precipitation and temperature), soil conditions (hydric deficiency increasing from southeast to the northeast) (Ratter et al., 2003; Silva et al., 2008) and fire (Henriques, 2005; Pereira Júnior, et al., 2014; Bueno et al., 2018). Differences in species composition lead to several classification within the biome Cerrado. Mainly by comparing endemic shrub and tree species (Castro, 1994; Ratter et al. 2003), a phytogeographical division of the biome was achieved, largely explored and re-defined through time (Bridgewater et al., 2004; Ratter et al., 2011), and corroborated in the analysis of herbaceous and shrub species (Amaral et al., 2017). Thus, it has been defined that the highest number of indicator species is found in the north-west, centre and south of the Cerrado (Fransoço et al., 2019), distinguished as three supercenters of biodiversity (Amaral et al., 2017; Vieira et al., 2019) and reflecting its environmental heterogeneity and the influence of the adjacent biomes (Amazon Forest, Caatinga, Atlantic Forest, Pantanal) (Sano et al., 2019).

During the Late Pleistocene, paleoclimatic studies in north, northeastern and central Brazil showed abrupt changes in moisture rates with two wet periods (Heinrich Stadial 1 - HS1 at 19-14.64 ka BP and Younger dryas – YD 12.9 to 11.7 ka BP) and one dry period (Atlantic cold reversal – ACR at 14.67-13 ka BP) (Cruz et al. 2009; Stríkis et al., 2015; Wainer et al., 2021; Custodio et al., 2022). Since the mid-Holocene, anti-correlated climatic response were observed between northeastern and central Brazil induced by changes in the intensity and amplitude of the south american monsoon system (SASM) (Zolitschka et al., 2021; Goresntein et al., 2022) in response to atmospheric and ocean circulation changes primarily driven by insolation changes and secondarily by pCO₂ concentration (Azevedo et al., 2021; Shimizu et al., 2020).

Palynological studies showed that before 17,000 years BP, an open vegetation composed of grasses (C4) prevailed in the Cerrado region (Ledru, 1993; Ferraz-Vincentini & Salgado-Labouriaou, 1996; Barberi et al., 2000; Behling, 2002). The late glacial, from north to south, is characterized by the expansion of the tree taxa *Araucaria*, *Drymis*, *Hedyosmum*, *Ilex*, *Myrsine*, *Podocarpus* associated to cooler and wetter climatic conditions (Ledru et al., 2006; Casino et al., 2018 and 2020; Costa et al., 2022; Horák-Terra et al., 2020). A weaker SASM was observed in eastern Brazil (Prado et al 2013).

Since the last Interglacial (Holocene), differences in landscape evolution are observed according to their location, although a general expansion of the cerrado vegetation (Cassino et al., 2020; Horak-Terra et al., 2015). During the early Holocene (11,600-8,200 yr BP), a change in the vegetation level is observed, with a greater amount of tree pollen taxa in the north (Absy et al 1992; Belhing, 2002) and south of the Cerrado (Horak-Terra et al., 2015, 2020; Ledru, 1993), one influenced by the proximity of Amazonia and the second by the arrival of moist polar fronts allowing the presence of cold-adapted trees. While the centre cerrado vegetation remained dominated by open vegetation (Barberi et al., 2000; Cassino et al., 2020). Meanwhile, fire activity has been constant, due to rises in temperature and humidity, and an increase in combustion material

(grasses), fire activity decreases towards the end of the period probably in response to the change towards dry climate and low material for combustion (Ferraz-Vincentini & Salgado-Labouriaou, 1996; Barberi et al., 2000; Ledru et al., 2002; Cassino et al., 2020).

In the middle Holocene (8200–4200 yr BP), open Cerrado dominated the biome (Ferraz-Vincentini & Salgado-Labouriaou, 1996; Barberi et al., 2000; Ledru et al., 2006; Cassino et al., 2020) except in those areas closest to adjacent biomes (Behling, 2002; Ledru et al., 1993). Throughout this period a recovery of tree vegetation was seen since 6000 yr BP onwards at altitudes below 900 m (Cassino et al., 2020), while in the highlands open vegetation became more widespread (Horak-Terra et al., 2015 and 2020; Costa et al., 2022). During this period, low fire activity was observed (Ferraz-Vincentini & Salgado-Labouriaou, 1996; Barberi et al., 2000; Ledru et al., 2002; Cassino et al., 2020).

In central Brazil, oscillating rainfall events were associated with weakened monsoon activity from the mid Holocene onwards (Prado et al., 2013; Stríkis et al., 2011). Then, at 4200 yr BP, an abrupt decrease in moisture rates over NEB was driven by higher insolation and intensification of ITCZ interhemispheric shifts (Chiessi et al., 2021; Utida et al., 2020; Vásquez et al., 2022), while increased humidity in the western Amazon and southern Brazil resulted from enhanced monsoon activity (van Breukelen et al., 2008).

These last phase showed more difference between the Cerrado districts, where records are located, in the northwestern, the savanna with some trees and shrubs sparse remained with no major changes(Ledru et al., 2006), meanwhile closer to the Amazonia, Behling (2002) reported gallery forest dominance, contrary in the south edge of the northeast district, Pandeiros wetland recorded a change from a mosaic of savanna accompanied by gallery forest at 4300 yr BP, to open cerrado dominated by grassland since 2700 yr BP to present (Lima-Sabino et al., 2021). In the center, at high altitudes, savanna with open landscape remained although humid soils allowed *Mauritia* swamp persistence (Barberi et al., 2000), at low altitude, increase in arboreal cerrado vegetation was abrupt and persistent towards the present, although three dry phases (from 3340 to 2760, 2070 to 1690, and 1330 to 1150 cal yr BP) have been observed suggesting arboreal cerrado and gallery forest retraction (Escobar-Torrez et al., 2023a). In the central-southeastern, palynological records suggested open cerrado landscape as a general trend, dominating highlands and intermediate altitudes (> 500m) (Lorente et al., 2010; Cassino et al., 2018; Horak-Terra et al., 2015 and 2020; Costa et al., 2022) in with respect to climatic conditions that gradually dried. Meanwhile fire activity remained low in the northeast and central-southeastern districts (Ledru et al., 2002; Cassino et al. 2018 and 2020). In the center district, continuous fire activity were observed (Barberi et al., 2000; Escobar-Torrez et al., 2023a), two higher peaks of fire activity were recorded suggesting higher perturbations (natural and/or anthropic origin) which strongly modified vegetation composition of gallery forest with probably less impact in the cerrado vegetation (Escobar-Torrez et al., 2023a)

A clear relation between the south-southeastern Cerrado and the centre Cerrado became more stronger towards the present, meanwhile the north of the Cerrado, only with two palynological studies recorded, need more attention to get a complete frame of the Cerrado landscape changes, which prevent us on delimitating the boundaries of the monsoon zone of influence and associated

environmental gradients throughout the Holocene. Here we present a new high resolution paleoecological record located between the central and northern region of the Cerrado. We analyzed pollen macrocharcoal, stable isotopes and trace elements to reconstruct the changes in vegetation and fire activity during the last 15,000 years and we included our results along a latitudinal gradient to improve our understanding of the contrasted responses between northern and central region and how they relate to monsoon activity. In addition, our record is located in a remote area allowing to discuss the issue of long-term fire activity in the biome Cerrado in the light of human inference.

2. Materials and methods

2.1 Study area

The Getulio swamp is located in the ecological station “Serra Geral do Tocantins” (EESGT), on the southeastern edge of Tocantins’ state (Fig. IV.1a). The swamp is part of the drainage network of the Sono river within the Tocantins river basin (Figs. IV.1a and IV.1b) and is located on a Plateau at 485 m of altitude. The Plateau is characterized by fluvial plains which are periodically inundated allowing the formation of palm swamp (*veredas* in Português) (Villela and Nogueira, 2011). The different cerrado physiognomies represented at EESGT are open grassland, dense arboreal cerrado or cerradão in well drained soils, and *veredas* and gallery forest in the inundated areas (Fig. IV.1b).

The climatic conditions in the Cerrado are controlled by two main factors, the Intertropical Convergence Zone (ITCZ) and the South American Summer Monsoon (SASM) (Reboitia et al., 2010). The climate of the Tocantins is bimodal, classified according to Köppen as Aw (Alvares et al., 2013) with an average annual precipitation of 1400 mm, with 50-70% of rainfall during the austral summer (December to February), 30% evapotranspiration mainly between December and March (Silva et al., 2008) and a dry season of 4-5 months duration during the austral winter (April to September) that represents approximately 10% of the annual precipitation (less than 50 mm) (Silva et al., 2008), the mean annual temperature is ~25°C. At a detailed scale, Tocantins state shows a west-east gradient of precipitation varying from >500 to less than 100 mm per month during the wet season with some days without precipitation in the southeast of the state (Assad et al., 1993; Silva et al. 2008) (Fig. IV.1c).

The EESGT history of fire management is divided by three periods, the suppression period, when any use of fire was forbidden, with the governmental managers neglecting traditional knowledge of local traditional communities (e.g. *Quilombos*) in 2001. After, increases in social conflicts and when large wildfires became recurrent affecting fire-sensitive vegetation, they initiated in 2010 the paradigm shift period, putting more efforts in understand fire patterns (fire seasonality, common fire areas, fire return interval (FRI), potential areas of ignition, allowing the use of fire for traditional communities, prescribed burning in early dry season (Barradas and Ribeiro, 2021).

Lately in 2015, consistent implementation of Integrated Fire Management (IFM) was established with improvements in firefighting and prescribed burning activities (Barradas and Ribeiro, 2021). Since the instauration, savanna landscape has increase in heterogeneity in the parc, where, also homogenized fire (causing mega-wildfires) became heterogeneous in the landscape (increase in

pyrodiversity) in the period from 2014 to 2019 (Barradas and Ribeiro, 2021). With regard to the evolution of practices, since 2017 the main objectives of the IFM have been related to the conservation and maintenance of socio-biodiversity and ecological processes, including the appreciation of the culture of fire (as social right, cultural heritage and knowledge for conservation purposes) (Barradas and Ribeiro, 2021).

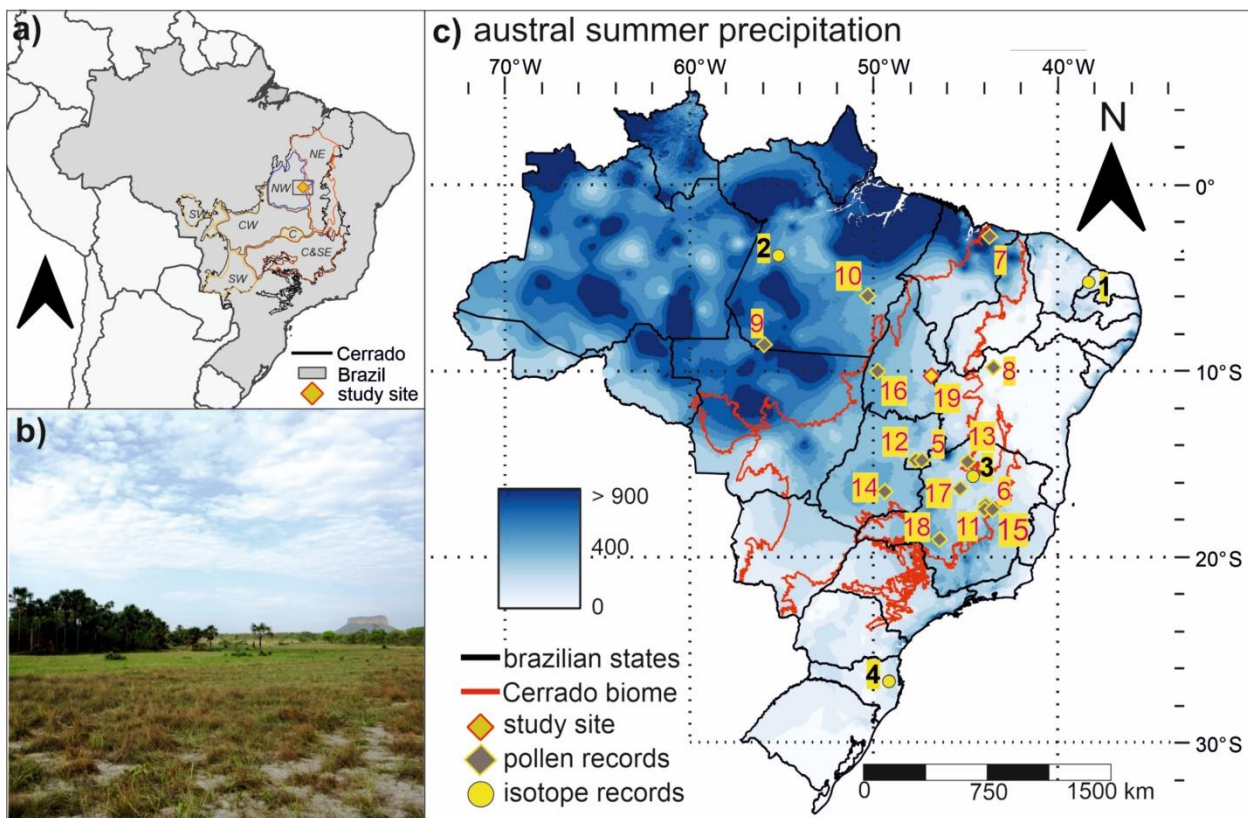


Figure IV.1. a) Map of northern South America showing the Cerrado biome location (dark line) inside the Brazilian territory (filled in gray) and the limits of Tocantins state (green line), and the Cerrado division of the biome defined by Fraçoso et al. (2019) – NW=northwestern, NE=northeastern, C=center, CW=central western, C&CE=central and southeastern, SW=southwestern. b) Picture of Varjão do Getulio swamp, Tocantins (by M-P Ledru) c) Map of Brazil showing the distribution of the austral summer precipitation, the limits of the biome Cerrado (red line), the states of Brazil (black line), the location of core VGE-17 (yellow rhomb), and the pollen (brown rhomb) and isotope records (yellow circle) from cerrado and adjacent areas. 1. Rahina, 2. Paraíso, 3. Lapa Sem Fim, 4. Botuverá, 5. Feia, 6. Rio Preto, 7. Caço, 8. Saquino, 9. Saci, 10. Carajas, 11. Pau de Fruta, 12. Aguas Emendadas, 13. Pandeiros, 14. Crôminia, 15. Pinheiro, 16. Confusão, 17. São Jose, 18. Salitre, 19. Getulio swamp (this study).

2.2 Modern vegetation

The Getulio swamp is located in the center of the Cerrado at 10°S (Figure IV.1a), at the southeastern limit of the northwestern Cerrado district (Françoso et al., 2019). The vegetation is characterized by a sparse savanna that includes cerrado *sensu stricto* accompanied by small *veredas*, and grassland (open cerrado) (Figure IV.1b) (Table IV.1) (Medeiros et al, 2012; Antar and Sano, 2019) with mosaics of seasonal dry forest, woody cerrado, and gallery forest (Table IV.1)

(Medeiros et al, 2012). Eight main plant families were observed in the EESGT, the Fabaceae with 91 species, followed by Poaceae (31), Lamiaceae (25), Rubiaceae (22), Myrtaceae (20), Malpighiaceae (19) and Euphorbiaceae (18) (Antar and Sano, 2019). The landscape is characterized by an open cerrado physiognomy with *Chamaecrista*, *Bauhinia* and *Mimosa*, endemic species of *Varronia* sp. (Boraginaceae), *Eriope* sp. (Laamiaceae), *Eugenia* sp. (Myrtaceae), *Piriqueta* sp. (Turneraceae), *Lippia* sp. (Verbenaceae), *Xyris* sp. (Xyridaceae), *Bonamia campestris* (Convolvulaceae), *Dioscorea compacta* (Dioscoreaceae), *Homalolepis tocantina* (Simaroubaceae), *Ouratea acicularis* (Ochnaceae) and *Senna biglandularis* (Caesalpiniaceae), and sparse tree as *Andira*, *Byrsonima*, *Caryocar*, *Casearia*, *Curatella*, *Hirtella*, *Pouteria*, *Qualea* and *Vochysia* (Antar and Sano, 2019).

However, when comparing the composition of the center and central-southeastern district with the northwestern district botanical studies, a same genus or species can be part of several different types of physiognomy. Although the composition of plants is not always the same, highlighting the difference between regions, with at least the presence of some species of the common genera (Table IV.1). Lemos et al. (2013) have suggested that the influence of adjacent biomes (Caatinga and Amazon Forest) in the Tocantins state reinforces the floristic and structural particularity with the presence of common species like *Dimorphandra gardneriana* and *Cenostigma tocantinum*.

Table IV.1. Classification of modern vegetation in the Cerrado region in comparison with the northeast Cerrado. (based upon: Felfili et al., 2007; Ribeiro and Walter, 2008; Medeiros et al., 2012; Medeiros and Walter, 2012; Lemos et al., 2013; Silva et al., 2016; Antar and Sano, 2019)

Vegetation physiognomy	Vegetation description	Common Family, genera or species	northwestern Cerrado
Open Cerrado (cerrado campo limpo (úmido) (open fields), campo sujo (dense fields), campo rupestre)	Continuous ground cover of graminoids, herbs and shrubs can be present and 5% to 10% are cover by treelets or trees if they are present.	Campo limpo: Burmanniaceae, Cyperaceae, Droseraceae, Iridaceae, Lythraceae, Orchidaceae, Poaceae, Polygalaceae, complemented by Asteraceae, Eriocaulaceae and Xyridaceae. Campo sujo: Poaceae and Cyperaceae dominates, the some families of Leguminosa (<i>Andira</i> , <i>Mimosa</i>), Lamiaceae (<i>Hyptis</i>), Myrtaceae and Rubiaceae. Genus of <i>Gomphrena</i> , <i>Cuphea</i> , <i>Diplusodon</i> , <i>Eryngium</i> , <i>Lippia</i> , <i>Polygala</i> , <i>Syagrus</i> and <i>Xyris</i> .	When campo limpo dominates the predominance of Poaceae, Cyperaceae, Eriocaulaceae and Xyridaceae, they constitute the 54%. Then can be found <i>Hirtella ciliata</i> and <i>Pouteria ramiflora</i> , as some tree, with <i>Mimosa sericantha</i> and <i>Mouriri elliptica</i> (Melastomataceae) in middle stratum. <i>Mimosa sericantha</i> is present in Campo sujo. Shrub species where <i>Toulisia</i> sp., <i>Ouratea macrantos</i> , <i>Simaba trichilioides</i> , <i>Krameria tomentosa</i> , <i>Jacaranda ulei</i> , <i>Manihot tripartite</i> and <i>Davilla elliptica</i> .
Arboreal Cerrado (cerrado sensu, <i>stricto</i> cerradão, dry forest)	dry forest: They are not associated to water courses. In rich of nutrient soils, with semideciduous forest, they have 15-25 m height covering the 74-90% of the canopy during rainy season. cerradão: 50-90% of arboreal cover, with trees 8-15 m tall they can be present from mid to low fertile soils to dystrophic soils the vegetation is mostly sclerophyllous. cerrado ss: moderately acid soils, covering the 20 to the 50% with components arboreal-arbuscute, of 3-6 m tall.	cerrado ss: <i>Astronium</i> , <i>Brosimum</i> , <i>Casearia</i> , <i>Byrsonima</i> , <i>Caryocar</i> , <i>Curatella</i> , <i>Davilla</i> , <i>Eriotheca</i> , <i>Hancornia</i> , <i>Kilmeyera</i> , <i>Pouteria</i> , <i>Ouratea</i> , <i>Qualea</i> , <i>Roupala</i> , <i>Tabebuia</i> , <i>Alibertia</i> , <i>Andira</i> , <i>Copaifera</i> , <i>Emmotum</i> , <i>Schefflera</i> , <i>Simarouba</i> , among others. cerradão: common genus are <i>Caryocar</i> , <i>Kilmeyera</i> and <i>Qualea</i> . And others like Fabaceae (<i>Dalbergia</i> , <i>Machaerium</i> , <i>Pterodon</i>), <i>Astronium</i> , <i>Hirtella</i> , <i>Brosimum</i> , <i>Casearia</i> , <i>Copaifera</i> , <i>Alibertia</i> , <i>Bauhinia</i> , among others. dry forest: common family are Fabaceae (<i>Acacia</i> , <i>Anadenanthera</i> , <i>Cassia</i>), Bignoniacaeae (<i>Jacaranda</i> , <i>Tabebuia</i>) and Anacardiaceae (<i>Tapirira</i>), Rutaceae (<i>Zanthoxylum</i>), and others.	cerrado ss: <i>Qualea parviflora</i> , <i>Anacardium occidentale</i> , <i>Hirtella ciliata</i> and <i>Caryocar coriaceum</i> (cerrado-caatinga transition), and <i>Vochysia cinnamomea</i> , <i>Curatella americana</i> , <i>Dimorphandra gardneriana</i> , <i>Cenostigma tocantinum</i> , and <i>Astronium fraxinifolium</i> and <i>Magonia pubescens</i> in more fertiles soils. cerradão: Principal species are <i>Parkia platycephala</i> , <i>Sclerobium paniculatum</i> , <i>Byrsonima sericea</i> , <i>Agonandra brasiliensis</i> , <i>Caryocar coriaceum</i> , <i>Celtis iguanea</i> and others. dry forest: <i>Dilodendron bipinnatum</i> , <i>Acacia tenuifolia</i> ,

			<i>Pseudobombax tomentosum</i> , <i>Combretum duarteanaum</i> and <i>Myrracrodruon urundeuva</i> representing the 56.4%, and <i>Cavanillesia arborea</i> , <i>Tabebuia impetiginosa</i> , <i>Sterculia striata</i> , <i>Aspidosperma subincanum</i> and <i>Astronium fraxinifolium</i> .
Forest (gallery/ciliary forest)	Canopy cover >70%, generally associated to water bodies, shrubby and herbaceous understory and usually present surrounded by wet (shrubby) grasslands, the transition is sharp when open Cerrado (grasslands) dominates. When ciliary forest (possess deciduous elements), sometimes there is a transition towards other arboreal physiognomies like dry forest or Cerradão.	Gallery Forest: when they are non-flooded Apocynaceae (<i>Aspidosperma</i>), Leguminosae, Lauraceae (<i>Nectandra</i> , <i>Ocotea</i>), Myrtaceae, Rubiaceae (<i>Alibertia</i> , <i>Psychotria</i> , <i>Guettarda</i>). In flooded, the common families are Annonaceae (<i>Xylopa</i>), Burseraceae (<i>Protium</i>), Clusiaceae (<i>Clusia</i>), Euphorbiaceae (<i>Richeria</i>), and an excessive number of species of Melastomataceae (<i>Miconia</i>), Piperaceae (<i>Piper</i>), Rubiaceae (<i>Palicourea</i> , <i>Posoqueria</i> , <i>Psychotria</i>), also can be observed <i>Croton</i> , <i>Cedrela</i> , <i>Euterpe</i> , <i>Hedyosmum</i> , <i>Mauritia</i> , among others. Ciliary Forest: common genus are <i>Anadenanthera</i> , <i>Casearia</i> , <i>Aipeiba</i> , <i>Aspidosperma</i> , <i>Celtis</i> , <i>Tapirira</i> , <i>Trema</i> , <i>Syagrus</i> and <i>Athalea</i> tree palms. <i>Protium</i> and <i>Tapirira</i> are present in both types of physiognomies.	<i>Licania egleri</i> , <i>Protium heptaphyllum</i> , <i>Sclerobium paniculatum</i> , <i>Brosimum rubescens</i> , <i>Tapirira guianensis</i> , <i>Trattinickia rhoifolia</i> , <i>Oenocarpus distichus</i> , <i>Physocalymma scaberrimum</i> , Myrtaceae and <i>Emmotum nitens</i> . Also, <i>Ocotea</i> sp., <i>Heisteria</i> sp., and <i>Richeria grandis</i> .
Palm swamp Vereda	Continuous layer of graminoids, forbs and shrubs, with palm trees (12-15 m tall), scattered or clumped, and few tree and shrub species (canopy cover 5-10%). When <i>Mauritia</i> is present, canopy cover increases to 40-70%, herbs and shrubs are scarce or absent, connected with the gallery Forest.	Common families are, Poaceae, Cyperaceae, Melastomataceae, Fabaceae and Eriocaulaceae, with the genus of <i>Chamaecrista</i> , <i>Echinodorus</i> , <i>Habenaria</i> , <i>Hyptis</i> , <i>Ludwigia</i> , <i>Lycopodiella</i> , <i>Mimosa</i> , <i>Polygala</i> , <i>Utricularia</i> and <i>Xyris</i> . For the establishment of Buritizal (<i>Mauritia flexuosa</i>) the presence of other genus like <i>Cecropia</i> , <i>Euplassa</i> , <i>Hedyosmum</i> , <i>Miconia</i> , <i>Myrsine</i> , as the arboreal component from adjacent gallery Forest.	The richest families are Poaceae and Cyperaceae, and genera <i>Rhynchospora</i> and <i>Xyris</i> . Common species: <i>Andropogon bicornis</i> , <i>Anthoxanthum lanata</i> , <i>Ascolepis brasiliensis</i> , <i>Ludwigia nervosa</i> , <i>Mauritia flexuosa</i> and <i>Rhynchospora globosa</i> .

2.3 Sampling and Chronology

A 3-m deep sediment core was retrieved in 2017 from Getulio swamp ($10^{\circ}50'41.55''S$; $46^{\circ}43'32.17''W$; 485 m asl) with a Russian-type corer (100 cm long, 5 cm in diameter). Twelve sediment samples were sent for radiocarbon dating by Accelerator Mass Spectrometry (AMS) and measurement to the *Laboratoire de Mesure du Carbone14* (LMC14)–UMS 2572 (CEA/DSM – CNRS–IRD–IRSN–Ministère de la Culture et de la Communication, Saclay, France). Radiocarbon dates have been calibrated with the SHcal20 curve (Hogg et al., 2020), with a confidence interval of 0.95 (see Table IV.2) in Calib 7.0 (Stuiver and Reimer, 1993). Age-depth relationship was modeled by means of Bayesian statistics with the Bacon package in R (Blaauw and Christen, 2011). The first 20 cm from the top of the core were composed of grass and roots and considered as modern material.

Table IV.2. Radiocarbon dates of VGE-17 core. Calibrated ages (2σ) were obtained from Calib 8.0 (Stuiver and Reimer, 1993)

Laboratory code	Depth (cm)	14C age (yr BP)	Age range (cal yr BP)	Mean cal age
SacA53912	20	75 ± 30	3-251	212
SacA57442	40	1630 ± 30	1406-1539	1463
SacA53913	74	4370 ± 30	4837-4977	4816
SacA53914	96	4705 ± 30	5312-5477	5349
SacA57443	106	4630 ± 30	5270-5333	5644
VGE-110	110	5405 ± 30	6165-6281	6074
SacA53915	125	5920 ± 35	6662-6799	6695
SacA57444	140	6455 ± 30	7270-7422	7342
SacA53916	160	7875 ± 40	8516-8777	8626
SacA53918	220	10085 ± 50	11284-11764	11604
SacA57446	228	10735 ± 50	12622-12744	12157
SacA57448	265	11400 ± 60	13158-13360	13285

2.4 Analytical methods

Geochemical analysis, isotopic compositions ($\delta^{13}\text{C}$ and $\delta^{15}\text{N}$) of total organic carbon (TOC) and total nitrogen (TN), oxygen (O), hydrogen (H), and the major and trace elements (Si, S, Cu, Br, V, Rb, Al, Ti, Sr, Nb, Y, Fe), were performed each 2 cm on previously dried, ground and homogenized samples. The TOC, TN, O and H contents were obtained by means of dry combustion, in a LECO CHNS/O elemental analyzer, TruSpec Micro model following Pessenda et al. (1996). The generated gases were quantified in an infrared detector at the Laboratório Integrado de Pesquisa Multiusuário dos Vales do Jequitinhonha e Mucuri (Integrated Laboratory of Multiuser Research of the Jequitinhonha and Mucuri Valleys) – LIPEMVALE (Diamantina, MG, Brazil). For equipment calibration, two standards of known composition were used: soil (C% = 2.35, N% = 0.183 and S% = 0.028) and orchid leaf (C% = 50.40, H% = 6.22, N% = 2.28 and S% = 0.156). The major and trace elements were determined using dispersive energy X-ray fluorescence, Shimadzu EDX-720 model, at LIPEMVALE. The standard A-720 of known composition was used for equipment calibration. Results were also expressed as dry weight percentages. A PCA was performed on all the geochemical elements to identify the main factors that control the elemental distribution (Muller et al., 2008; Sjöström et al., 2020) in the samples. First, the data were log-transformed and standardized for the correlation mode. Subsequently, the Varimax orthogonal rotation method was applied in order to maximize the variable loads on the components (Eriksson et al., 1999; Reimann et al., 2008). Analysis was performed using SPSS 20.0 software. Additional ratios (Si/Ti, log(Ti/Ca), and Ti/Al) were used to complement the analysis.

Pollen was analyzed in 140 sediment subsamples measuring 0.5 – 0.25 cm³ and 1 cm thick collected at 2 cm intervals. Pollen was extracted at the ISEM laboratory in France. A spike of two *Lycopodium* tablets per sample was added to calculate the concentration of pollen. The samples were first washed in 10% KOH in a hot water bath before density separation with ZnCl₂ (Kummel & Raup, 1965). For samples taken between 298 and 200 cm, a 5 ml 75% HF treatment was performed for one hour (Faegri & Iversen, 1989) to remove silica. Pollen, spores, and other non-palynomorphs were identified and counted at 600x magnification. Pollen types were identified using the ISEM pollen reference collection for Cerrado taxa, identification keys and catalogs of pollen types from Brazil (Salgado-Labouriau, 1973; Bush & Weng, 2007; Cassino & Meyer, 2011;

Lorente et al., 2017; Antonio-Dominguez et al., 2018; Freitas et al., 2020; Soares et al., 2020). Pollen taxa were classified in agreement with botanical studies from Cerrado phytobiogeographies, with focus on vegetation composition near our study area (for details see Table S.1).

Palynological diagrams were elaborated with *rioja* package (Juggins, 2022), zones were defined by CONISS (*vegan* package); for zone definition only terrestrial pollen taxa were considered. Principal component analysis was performed using the function PCA in *FactoMineR* package (Lê et al., 2008), all pollen data were prior standardized by square-root method. PCA reduces dimensionality by exploring the linear association between variables.

For the palynological interpretation, two types of approach were used for the pollen taxa selection. We first evaluate the change in the distribution of the pollen taxa, a first Principal Component Analysis (PCA) was performed to select the order of importance of pollen taxa contributing in more than 1 % in samples (Table S.2). Therefore, those taxa were organised in three ecological groups (open cerrado, closed cerrado and gallery/ciliary forest) and different forms of vegetation growth (herb, shrub, tree) (Table S.3), based on previous classification of modern vegetation (Table IV.1 and Table S.1). Poaceae was evaluated as a taxa representative of grassland presence/absence and/or dominance. Then, a second selection was based on the patterns of occurrence of each taxa, so those without a specific pattern were excluded. The Palynological interpretation was carried out with this final selection.

Reconstruction of temperature and precipitation based on the pollen taxa assemblage was performed using the *crestr* package (Chevalier, 2022), which uses a method based on probability density functions (PDF) that compares pollen taxa with the actual distribution of plants at different levels (family, genus or species) in a determined region. The pollen taxa was compared with the plant species distribution from database of the Global Diversity Information Facility (GBIF). Taxa were considered for reconstruction if were present at least in 20 distinct sites for each plant species present on the climate space. For climate space we defined the analysis for Cerrado biome and extended to the Brazilian territory. Then, the trend and climate distribution of each taxa was evaluated, independently, to select those which have a good signal for the reconstruction, where the exclusion of pollen taxa was based in two criteria: 1) define a coherent climate study area to take advantage of the climate abundance weighting, 2) select species whose distribution are significantly defined by the climate variable. Finally, with the pollen taxa selected the climate reconstruction was modeled for the four variables. All statistical analysis were performed in R program. Climate reconstruction was obtained for four climatic variables: mean annual temperature (MAT), minimum temperature of the coldest month (Tmin coldest month), mean annual precipitation (MAP) and precipitation during the driest quarter (Pdq).

For macrocharcoal analysis, a total of 148 subsamples measuring 5 cm³ were collected at 2 cm intervals. The subsamples were deflocculated and bleached in 10% KOH and 2.6% NaOCl, and gently sieved through a 160 µm mesh under water (Genries et al., 2012). The residues were carefully washed into a porcelain evaporating-dish to aid identification and counting of charcoal particles. The material was analyzed at x60 magnification with a camera connected to an image analyzer using WinSEEDLE image-analysis software (Regent Instruments Canada Inc., 2009). Total number of particles, total area and particles size were measured. Charcoal data is presented

as charcoal influx (charcoal total area/cm²/year). Also, for each particle, the ratio of width (W) vs. length (L) (W:L) was evaluated. The individual values obtained were incorporated into a density plot, and the mean W:L ratio was calculated. This analysis was used to assess the presence and predominance of charred particles, distinguishing between herbaceous and woody. Values above (below) 0.5 suggest woody (herbaceous) charred particles (Aleman et al., 2013).

3. Results

3.1 Age-depth model and sedimentation rates

The age-depth model (Table IV.2) shows a continuous sediment deposition with an age of 15,020 cal yr at the base of core VGE-17 (Fig. IV.2). Mean sedimentation rates are ~ 50 years per centimeter (~0.02 cm/yr) with periods of slow sedimentation between 109-105 cm (5970-5540 cal yr BP) and 69-40 cm (4482-1436 cal yr BP) (Table S.5).

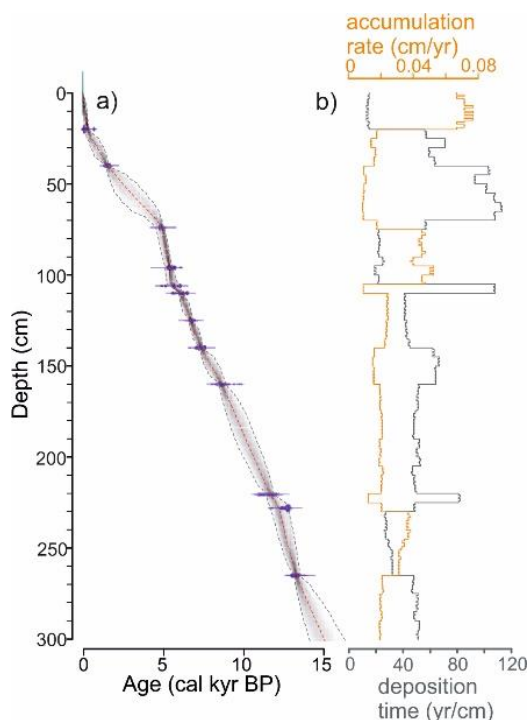


Figure IV.2. a) Age-depth model for the core VGE-17 based on linear interpolation between calibrated ages (Blaauw and Christen, 2011) b) sediment-accumulation rate (cm/yr) and deposition time (yr/cm) for VGE-17 core.

3.2 Elemental and isotopic proxies

The first four components of the Principal component analysis explain 78% of the elemental and isotopic variation (Fig. IV.3). The first component, explained the 35.7%, was represented by C, H, N, O and Br with positive scores (>0.7) and S with middle positive value, and by negative scores for Si and Zr (Table S.5). The variation of these elements recorded changes in the core composition from inorganic to organic material. Si and Zr dominated until ~ 13,500 cal yr BP, which suggests higher input of silicates and inorganic minerals (coarser grain-sand), respectively (Fig. IV.3) (Cuven et al., 2010). Then, from 13,000 cal yr BP onwards, more positive PC1 values reflect the increase in C, H, N, O, and Br and indicate higher organic matter (OM) content (Davies et al.,

2015). PC1 scores reached their highest values between 12,800 to 11,900 cal yr BP (values ~1) and remained positive throughout the rest of the core, except from 4940 to 3060 cal yr BP (Figs. IV.3 and S.1). Additionally, Si/Ti ratio recorded, from about 8933 cal yr BP, a progressive augmentation in the deposition of biogenic silica (Davies et al., 2015) with the highest deposition at 1463 and 325 cal yr BP (Fig. S.1). Si/Ti ratio could suggest accumulation of either terrestrial/aquatic local origin in response to long water residence in soil which allow the retention of Si, they are probably coming from grass and sedge (Gramineae and Cyperaceae) vegetation, as they are present in wetland vegetation (Struyf and Conley, 2009).

The second component explained ~19 % of the variance and is characterized by high positive scores of the lithogenic elements Fe, Sr, K, Ti, and Al (Table S.6), which are associated to finer mineral material respect to previous coarser grains (Davies et al., 2015). More positive PC2 values, which indicates the dominance of clay/silt deposition, occurred from 13,910 to 8935 cal yr BP, although with some fluctuations (Fig. IV.3). Afterwards, PC2 values remained low suggesting a reduction of the deposition of these lithogenic elements (Fig. IV.3). By 1335 cal yr BP, a slight increase was recorded (Fig. IV.3). Additionally, the variation of the Ti/Al ratio, which also reflects changes in terrigenous input, corroborates the reduction in the deposition of fine materials after 8935 cal yr BP (Fig. S.1).

The third component explained 15% of the variance with $\delta^{15}\text{N}$ high positive scores (Fig. IV.3), Ca mid positive scores and C/N with mid negative scores. Fluctuation of $\delta^{15}\text{N}$, with depleted values between 14,920 and 9438 cal yr BP (<1-2) and C/N values ~40 with some fluctuations, suggest the dominance of organic material from terrestrial plants in an environment with slight increase in water availability. Then between ~9300 to 7300 cal yr BP, the C/N and $\delta^{15}\text{N}$ values reached to 60 and ~3, respectively, to gradually decrease to 30 and 2 (Fig. S.2), suggesting the period of maximum increase in local moisture which after this period get gradually drier. The fluctuation on the amount of $\delta^{15}\text{N}$ (Fig. S.2) are linked to a change in local moisture with high values usually related to increase in C₃ plant presence and to low temperatures in denser forest (Martinelli et al., 1999; 2021). Meanwhile the C/N ratio suggest a change in organic material origin (Sifeddine et al., 2004; Aranibar et al., 2008), where low (high) ratio suggest increase in aquatic(terrestrial) organic matter. However, low values of C/N can be also the result of terrestrial organic matter that reduced the ratio in response to nitrogen mineralization at higher temperatures when water availability in soil reduces (Aranibar et al., 2008; Zhao et al., 2015). Then after these period, principally since 6000 cal yr BP, $\delta^{15}\text{N}$ increased until the present (1 to 4), and after 3500 cal yr BP became out of phase with C/N ratios which reduced gradually from 40 to 20 (Fig. S.2). These trends suggest that first organic terrestrial input increased and thus precluded the enrichment of $\delta^{15}\text{N}$, and that after 3500 cal yr BP, the input was still present but probably with plants with low C/N values, thus, $\delta^{15}\text{N}$ was no longer reflecting the variation in water availability, but the deposition of 15N-rich organic matter (Fig. S.2).

The fourth component explains ~11% of the variance, dominated by $\delta^{13}\text{C}$ with a high negative score related to a $\delta^{13}\text{C}$ enrichment and increase in C₄ plants, while positive scores relate to depleted $\delta^{13}\text{C}$ and increase in C₃ plants (Fig. IV.3) and Vanadium with mostly permanent positive values. The interval from 9340 to 7165 cal yr BP stands out for its predominant negative values, indicating predominance of C₃ plants with fluctuations by 8115 cal yr BP that suggest events of changes from C₃ towards C₄ plants. Vanadium (V), which is commonly associated to organic rich-soils and peats,

with a strong signal when OM increases (Marshall et al., 2017), presented higher values from 13,000 to 4705 cal yr BP (Fig. S.2). This suggests that water table was close to the soil surface from ~13,000 to 5000 cal yr BP (Fig. S.2); before and after this interval where more variability in the water-level table was observed.

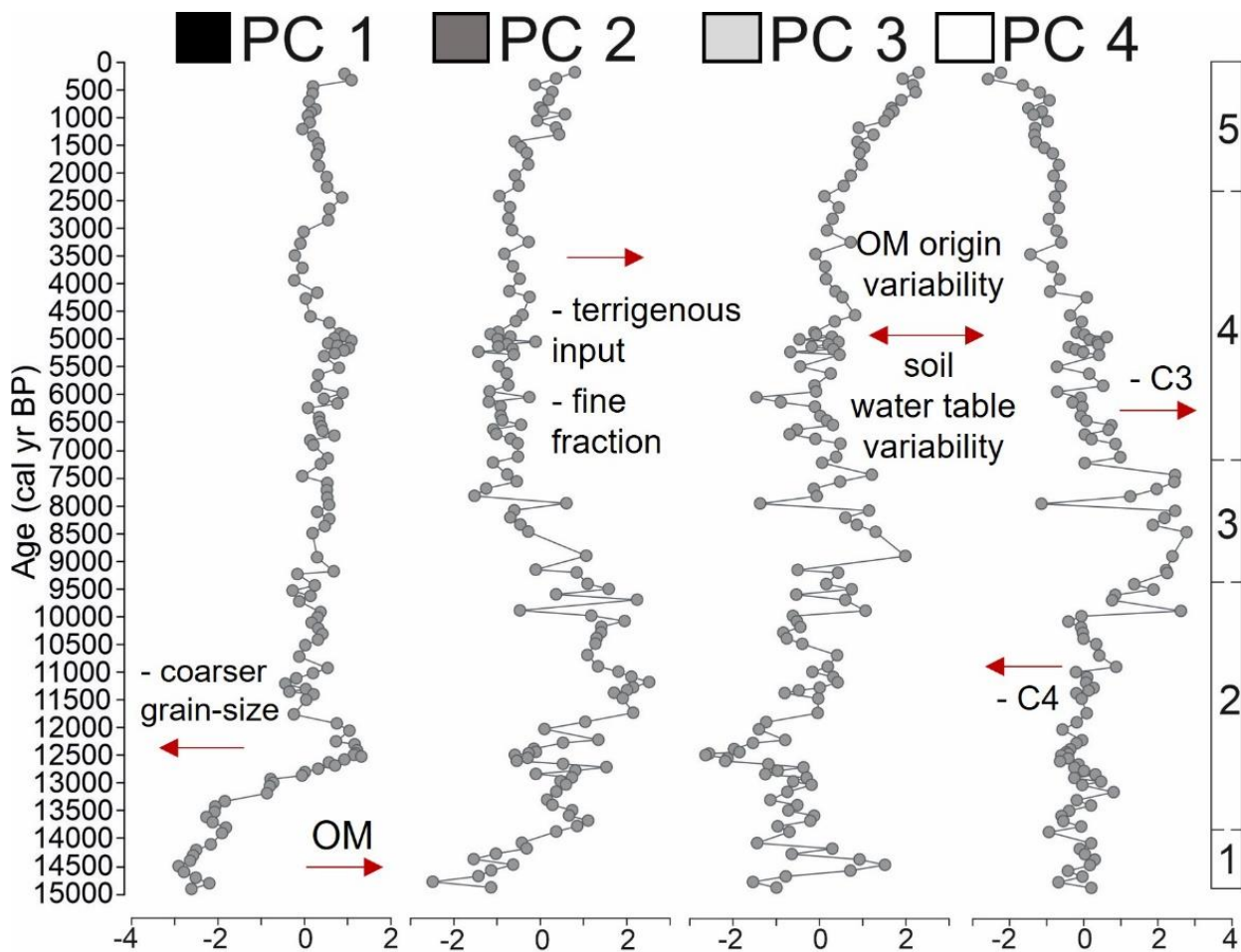


Figure IV.3. Principal component analysis from Isotopic and XRF elements from VGE-17 core. Z-scores' curves from first fourth principal components.

3.3 Pollen analysis

Based on pollen zonation (CONNIS) the VGE-17 core has been divided in five zones. Temporal resolution ranges from ~50 to 200 years between each sample with the lowest resolution observed after ~4500 cal yr BP. A total of 112 terrestrial pollen taxa with four water level-related pollen taxa, two ferns, and two non-pollen palynomorphs (*Pseudoschizaea rubina* and *Zignema*) were identified, among them we selected 31 terrestrial pollen taxa (Fig. IV.4). Water level related pollen taxa and non-pollen palynomorph are discussed for each pollen zone (Fig. S.3).

Zone 1 (298 – 278 cm; 14,920 – 13,910 cal yr BP; 11 samples) was characterized by Non-Arboreal pollen (NAP) varying between 60 to 70 % mainly with Poaceae (~60 %) and other shrubs and herbs with frequencies below 5 % such as *Baccharis*, *Gomphrena*, *Xyris*, *Peperomia* and *Cuphea*, the later increased to 10 % at the end of the zone. Arboreal pollen (AP) was characterized by low frequency of Cerrado trees (<5 %) represented by *Byrsonima* and *Casearia*, a continuous presence of Melastomataceae-Combretaceae, with less frequent *Celtis*, *Eriotheca*, and *Smilax* vine. Gallery forest presented higher values ~ 10 %, with *Ilex* (5-10%), Myrtaceae (~ 2 %) and other taxa with less than 2% (*Cordia*, *Cybianthus*, *Emmotum*, *Hedyosmum*, *Lamanonia*, *Machaerium*, Moraceae-Urticaceae and *Protium*). Pollen accumulation rate (PAR) increased from 240 grains/cm²/yr at the base to 3400 grains/cm²/yr at the end of the zone.

Water level-related pollen taxa were represented by Cyperaceae and *Sagittaria*, with less than 2%, similarly, *Mauritia* pollen increased from 2 to 5 % at the end of the zone.

Zone 2 (276 – 176 cm; 13,810 – 9440 cal yr BP ; 49 samples). NAP pollen was still dominant, varying between 85 to 55 %, mainly composed of Poaceae (60 to 30%), an increase in *Cuphea* (5 – 40 %) peaking between 264 and 239 cm (13,250 to 12,500 cal yr BP), and *Baccharis* that increased continuously from the beginning to the end of the zone (3 – 15 %). Other herbs and shrubs taxa, *Gomphrena*, *Polygala*, *Xyris*, *Lippia* and *Peperomia* below 3%. Cerrado tree frequencies increased mainly with *Casearia* (1 – 10%) and the continuous presence of *Byrsonima* and *Cissus* (<2%). Melastomataceae-Combretaceae, *Smilax* (~5%), *Celtis*, *Eriotheca* and *Anadenanthera*, at lower frequencies (< 2%). Also, *Dialium* a taxa attributed to dry forest was first observed in zone 2 (0 – 8 %). Gallery forest was dominated by *Ilex* (5-10 %) with *Cordia*, *Cybianthus*, *Emmotum*, *Euterpe*, *Machaerium* and Moraceae-Urticaceae (less than 5%). *Protium* (<2%) was observed at 218 cm (11,505 cal yr BP). This period marks a continuous occurrence of ~5% for *Hedyosmum*, between 226-200 cm (12060 - 10620 cal yr BP). Pollen accumulation rate increased from 800 to 11300 grains/cm²/yr, with the highest value at 9727 cal yr BP and decreased towards the end of the zone (~4200 grains/cm²/yr).

Water level-related pollen taxa increased with fluctuating values of *Mauritia* (2-15%) and Cyperaceae (0-10%), and *Eriocaulon* and *Sagittaria* with minor values (<2%). The non-pollen palynomorph *Pseudoschizaea rubina* (0 – 10%) and *Zygema* (0 – 7%) were more continuous during this zone.

Zone 3 (174 – 136 cm; 9340 – 7165 cal yr BP; 20 samples). NAP abruptly decreased from 60 to 15 %, with Poaceae below 32 % and reaching to less than 2% at 156 cm (8370 cal yr BP). The presence of other herb and shrubs remained constant, with *Baccharis* (2-10 %) and *Cuphea* (0-40%), and less frequent (<5%) *Gomphrena*, *Polygala* and *Lippia*. Shrubby pollen taxa *Peperomia* (1-20%) increased. Cerrado tree pollen taxa also increased, mainly with the presence (~10%) of *Casearia*, and less of *Byrsonima*, *Caryocar*, *Cissus*. Also, Melastomataceae-Combretaceae (10 – 35%), *Eriotheca* and *Smilax*, and low frequency of *Anadenanthera*, and *Celtis*. *Dialium* has remained continuous (~2%). The gallery forest was represented by *Hedyosmum* (0 – 50 %) and *Protium* (0 – 25 %), with Myrtaceae, *Machaerium*, *Paullinia*, *Euterpe*, *Simira* (less than 5%), *Ilex* decreased to 2% and disappeared at 7987 cal yr BP (150 cm). Pollen accumulation rate increased

from 800 to 26000 grains/cm²/yr, with the highest value observed between 174-160 cm (9339 to 8626 cal yr BP), reaching ~1200 grains/cm²/yr at the end of the zone.

Water level-related pollen taxa have reduced to values below 3% at the beginning of the zone, for both, *Mauritia* and Cyperaceae frequencies, accompanied by *Eriocaulon* and *Sagittaria* (below 1%). The values of *Mauritia* and Cyperaceae reestablished, reaching to ~10 %, and to 5% for *Eriocaulon* and *Sagittaria* at the end of the zone, after 8000 cal yr BP (148 cm).

Zone 4 (134 – 50 cm; 7075 – 2445 cal yr BP; 44 samples), NAP increased to 70 - 90 % with two phases. First, Poaceae (70 – 50 %) was dominant and remained stable (~60%) until 70 cm (4590 cal yr BP), together with *Gomphrena* (10 to <5%), *Cuphea*, *Polygala*, *Xyris* (< 5%) and the shrubs *Peperomia* (15-1 %). Cerrado tree taxa were present with *Byrsonima*, *Caryocar*, *Casearia* below 5%). Melastomataceae-Combretaceae (0 – 20 %), *Anadenanthera*, *Celtis*, *Eriotheca* and *Smilax* vine (<5%). *Dialium* fluctuated between 5 to 0 %. The gallery forest taxa *Euterpe*, *Hedyosmum*, *Machaerium*, Mor.-Urt.) decreased (< 5 to 0 %), while *Ilex*, *Paullinia*, *Emmotum* were not observed after 4590 cal yr BP (70 cm). Second, from 4370 cal yr BP (68 cm) to the end of the zone, Poaceae fluctuated (80 – 30 %), *Baccharis* (1 - 37%) and *Cuphea* (1-8 %) increased. *Polygala* and *Xyris* were below 1% and shrubbs reduced to < 1% (*Peperomia*). Cerrado trees, *Byrsonima* and *Casearia* (<1%). Melastomataceae-Combretaceae decreased (4-1%) together with *Anadenanthera*, *Smilax* fluctuated (5-1 %). *Dialium* increased to ~13% from 3060-2850 cal yr BP (56-54 cm). Gallery forest pollen taxa decreased with Myrtaceae (0-20%), *Cybianthus*, *Euterpe*, *Machaerium* and Moraceae-Urticaceae (0-2 %). Pollen accumulation rate increased from 70 to ~ 4000 grains/cm²/yr with pollen deposition decreasing towards the end of the zone.

Water level-related pollen taxa showed a replacement, with a progressive increase of *Mauritia* palm tree (0-25 %) and a decrease of Cyperaceae (25-0 %), the presence of *Eriocaulon* and fluctuation of *Sagittaria* (0-5%) which disappeared at the end of zone 4.

Zone 5 (48 – 20 cm; 2260 – 210 cal yr BP; 16 samples). NAP was the same as in previous zone 4 (75-90 %). Two sub-zones are characterized by change in shrubby-herb taxa. First, until 1336 cal yr BP – 38 cm, high frequency of *Cuphea* (45-11 %) when *Gomphrena* decreased (33-3 %). *Polygala*, *Xyris* and *Peperomia* (<5%). Cerrado tree taxa were dominated by *Casearia* (<3 %). Melastomataceae-Combretaceae (8-0 %), *Smilax* (<10 %), *Anadenanthera*, *Celtis* and *Dialium* decreased (0-2 %). Gallery forest taxa decreased with *Euterpe* <2 %) and *Hedyosmum* (<2%) with two peaks of 3% at 28 (700 cal yr BP) and 10% at 24 (440 cal yr BP) cm. *Cybianthus*, *Emmotum* and Mor.-Urt. (<2 to 0%).

The second sub zone, from 36 cm (1210 cal yr BP) to 20 cm (modern) is characterized by Poaceae (70-30 %), *Cuphea* (0-5 %) replaced by *Gomphrena* (0-57 %), *Baccharis* was continuous (0-3 %). A decrease of arboreal pollen *Anadenanthera*, *Celtis* and gallery forest *Machaerium*, Moraceae-Urticaceae and Myrtaceae was observed (< 3%). Pollen accumulation rate increased from 40 to ~

1800 grains/cm²/yr, pollen deposition decreased towards the end of the zone. Water level-related pollen taxa *Mauritia* (0-30 %) Cyperaceae (0-15 %) were present.

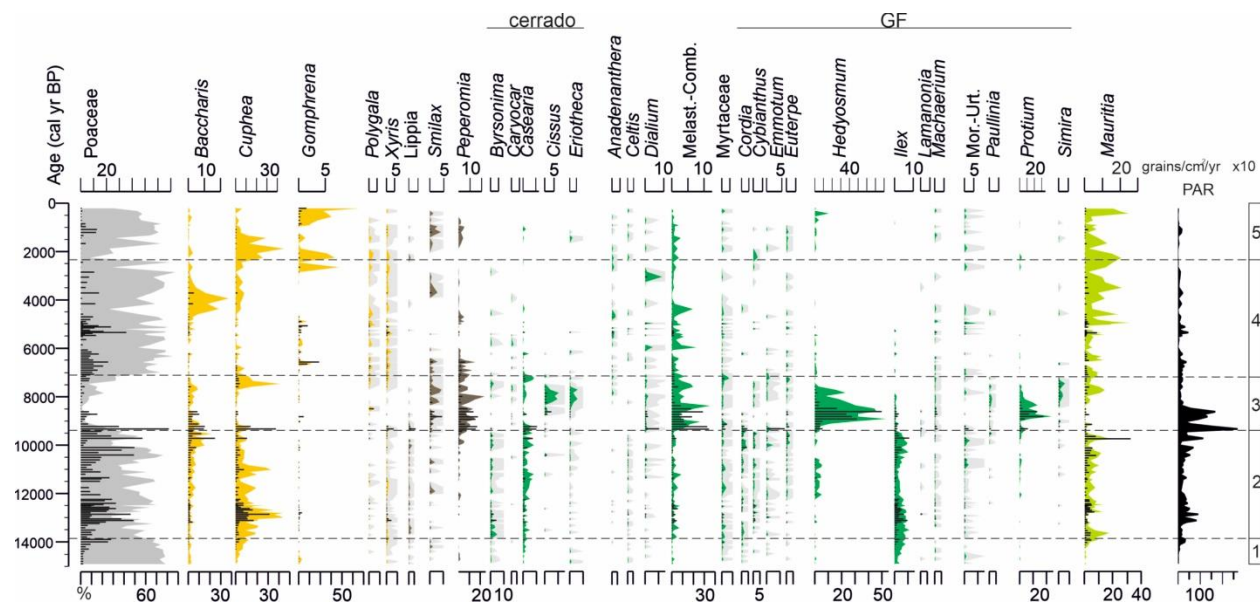


Figure IV.4. Pollen diagram of the 31 most representative terrestrial taxa from VGE-17 core along a time scale. From left to right pollen percentage (colored curves) and concentration (black bars), total of terrestrial pollen accumulation rate (PAR) (area/cm²/yr), and the pollen zones. Herbaceous taxa (yellow), shrub taxa (brown) and tree taxa (green) are presented in front of their corresponding predominant physiognomy [cerrado and gallery forest (GF)]. *Mauritia* % and accumulation rate were added to represent the general trend of water level-related pollen taxa (green-light).

Complementary principal component analysis explains the 58.61 % of variability, and allows to differentiate diverse states of vegetation composition surrounding the swamp. On the first component (PC1 – 38.9%), a tendency to more negative values suggests increase in grassland by Poaceae dominance and a tendency to positive values indicates increase in arboreal physiognomies, with increases in trees from the Cerrado and gallery forest (Table S.4 and Fig. S.4). For the second component (PC2 – 19.7%), negative values are related to gallery forest presence and positive values suggest a trend to herbs adapted to vereda or humid soils, and shrubs and dispersed trees of Cerrado vegetation (Table S.4 and Fig. S.4).

For the first and second zones, a trend from negative to fluctuating positive PC1 values (~ -2 to 2) is observed, while PC2 scores were dominated by negative values (~ -1.8). During the third zone, PC1 recorded permanent positive values (~ 2 to 4), while PC2 had a change from negative (-0.5 to -3) to positive values (0.5 to 3.5), this change occurred between 154 to 152 cm of depth (8242 to 8114 cal yr BP). In the fourth zone, divided in two phases, the first phase was dominated by negative values in PC1 (0 to -2) and positive values in PC2 (0 to 3). Afterwards, during the second phase (from 4370 cal yr BP (68 cm) to the end of the zone) scores are dominated by negative

values in both principal components, 0 to -2 and 0 to 1.5 respectively. Finally, in the fifth zone, the PC1 and PC2 have remained with negative values, 0 to -2 and 0 to -1.5 respectively (Fig. S.5).

3.4 Paleoclimate reconstruction based on pollen

The calibration parameters used for the paleoclimate interpretations were mean annual precipitation (MAP) and precipitation during the driest quarter (values presented in Table S.8). The MAP showed a general stable trend, with ~1400 mm in average, although some variation was observed. These variations include a period of slight increases in precipitation (1413 to 1458 mm) from 13,125 to 12,470 cal yr BP and isolated events (peaks \geq 1450 mm) occurring in centennial to millennial scale (total of eight events at 6150, 5970, 5170, 3710, 3270, 2850, 2070 and 1670 cal yr BP (Fig. S.6).

Similarly, Pdq reconstruction suggest ~27 mm average of precipitation during the dry months, with some events of decrease/increase in the precipitation amount. First, with five isolated events of reduction in precipitation (~19 mm) at 13,330, 13,000, 12,930, 12,520 and 12,410 cal yr BP, then a period of increased amount of precipitation (~50 mm) from 9230 to 8500 cal yr BP and three individual events at 5200 (36 mm), 5160 (39 mm) and 4810 (59 mm) cal yr BP (Fig. S.6).

As the record approached to present, MAP reduces (\sim 1380 mm) closer to present annual precipitation, and Pdq reduced in precipitation to 19 mm (Fig. S.6).

3.5 Macrocharcoal signal

The charcoal signal recorded variable charcoal influx with values below and/or between 0.01 and 0.05 mm²/cm²/yr. Four events were differentiated of which three showed a similar influx of \sim 0.3 mm²/cm²/yr at 241 (12,550 cal yr BP), 99 (5400 cal yr BP) and after 19 (last decades at present) centimeters of depth (Fig. IV.5). The fourth event, with 0.7 mm²/cm²/yr, was observed at 187 cm (10,000 cal yr BP). On the other hand, the W/L ratio was below 0.5 (Fig. IV.5), although the particle pattern in the density diagram suggests that in smaller quantities the presence of particles with values above 0.5 were present too, especially in the last two events recorded at 99 and 19 cm depth (Fig. IV.5). There were also forty punctual events with zero charcoal particles in the record, at 239 (12,498 cal yr BP), 215 (11,358 cal yr BP), 175 (9389 cal yr BP), 171 (9186 cal yr BP), 139 (7297 cal yr BP), 139 (7297 cal yr BP), 135 (7120 cal yr BP), 131 (6949 cal yr BP), 123 (6613 cal yr BP), 97 (5369 cal yr BP), 81 (5005 cal yr BP), 47 (2166), 41 (1566), 31 (910 cal yr BP) centimeters of depth (Fig. IV.5).

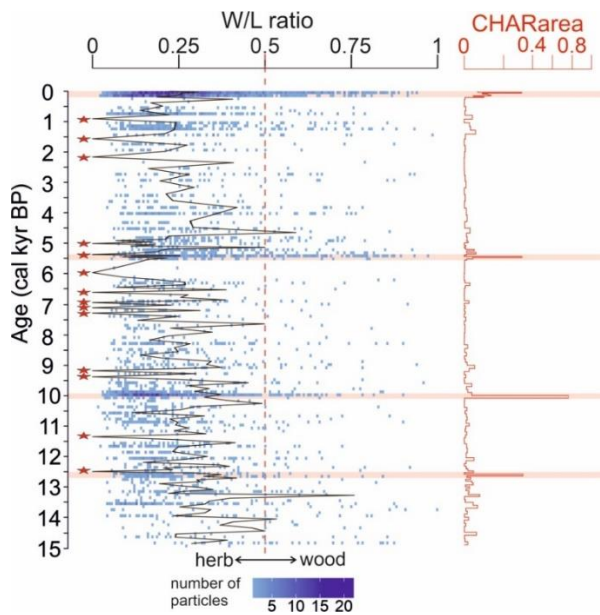


Figure IV.5. Results of the macrocharcoal analyses of core VGE-17 with the distribution of W:L ratios for each particle per sample (blue squares) and the average of W:L ratio per sample (dark line) (red-dotted line suggest the threshold between grass <0.5 and wood particles >0.5; red stars showing the punctual events of zero fire), CHARarea ($\text{mm}^2/\text{cm}^2/\text{yr}$), red bands highlight the four macrocharcoal peaks.

4. Interpretation

During the Late Pleistocene, between 15,000 and 13,800 cal yr BP, the landscape at 10°S latitude was characterized by an open cerrado with shrubs and herbs indicating dry (humid) soil condition. A narrow gallery forest was dominated by *Ilex*, a shade tolerant tree common in temporal/seasonal flooded soils (Araujo et al., 2002; Silva et al., 2019). Indeed, usually *Ilex* pollen deposition suggest local increase in its abundance, as a low pollen producer and low pollen dispersion (insect-pollinated) (Van den Berg, Oliveira-Filho). *Ilex* grows in wet places, found usually in forest when is found in hills is associated to rocky surfaces near water bodies (gallery forest or swamps) (Loizeau et al., 2005; Brotto, 2022). *Ilex* survival is associated to the capacity of water availability in the system (Loizeau et al., 2005; Brotto, 2022). In the present, a few registers locate this genus in the center of Tocantins state were precipitation is around 1600-1800 mm (Medeiros et al., 2012), so we argue that rather than cold temperatures their permanence was mostly due to the soil humidity conditions, which were stable and increasing gradually causing this taxa to rise from 13,800 cal yr BP. The low pollen influx corresponds to the onset of the swamp formation (Fig. IV.6), a weak signal of *Mauritia* and Cyperaceae (Fig. IV.6 and S.3) with low edaphic moisture (Si and Zr from PC1 and PC3 elements in Fig. IV.3 and Fig. S.1 and S.2) and high erosive conditions (see grain size on PC1) (Figs. IV.3 and IV.6). Precipitation reconstruction shows that the mean annual value was not different from today (Fig. S.6).

Then, from 13,800 cal yr BP, an increase in the transition from glacial to interglacial is characterized by the progressive expansion of soil moisture-related herbs (*Eryngium*, *Polygala*, and *Xyris*, and the persistence of *Eriocaulon* and *Sagittaria*), the expansion of the *Mauritia* swamp and of the gallery forest formation (*Ilex* and Melast.-Combret.) within an open Cerrado landscape

(*Baccharis* and *Cuphea*) with some Cerrado trees increases (*Byrsonima* and *Casearia*). Less erosive conditions also were established after 13,300 cal yr BP (Figure IV.6 and S.3), with pollen accumulation rapidly increasing until 12,300 at the same time when the *Mauritia* palm tree was increasing along with the gallery forest tree *Ilex*, and Poaceae and *Cuphea*. Increase in humid soil conditions with expansion of wet grasslands is supported by the OM increases between ~13,000 and 12,000 cal yr BP (Figs. IV.3, IV.4 and IV.5). Then, from ~12,300 to 11,500 cal yr BP, a reduction in pollen influx and in the previously cited taxa indicators suggests a period of reduction in soil moisture.

From 12,060 to 10,620 cal yr BP the expansion of *Hedyosmum* suggests the installation of a cool and wet forest (Ledru and Araújo, 2023). Today, only the species *Hedyosmum brasiliensis* is observed in Brazil, rare in gallery forest of central Brazil and more abundant in the high elevation physiognomy of the Cerrado or of the Atlantic Forest where it is commonly associated to *Drimys*, *Ilex*, *Podocarpus*, *Weinmannia* (Oliveira-Filho and Fontes, 2000). Pollen records showed that *Hedyosmum* spread over lower elevation in central Cerrado during the late glacial in response to wet and cool climatic conditions (Ledru and Araújo, 2023) (Figs. IV.4 and IV.6). Precipitation reconstruction shows fluctuations in mean annual precipitation and in the amount of rain during the dry season (Pdq) (Fig. S.6). During the early Holocene, a sharp change in the vegetation was observed between 9340 and 8240 cal yr BP, characterized by the expansion of a gallery forest with Melastomataceae-Combretaceae, *Hedyosmum* and *Protium* and the disappearance of the swamp. This assemblage suggests a change towards more humid edaphic conditions under cool climatic conditions, and an increase of the river discharge, indicated by the increase allochthonous coarser particles (Fig. IV.3), with the edge closer to the coring site. This change in floristic composition is in agreement with the stable isotopes (Fig. IV.6). The precipitation reconstruction shows an increase of 40 mm of precipitation during the dry season (Fig. S.6). During the mid-Holocene, a gradual change towards an open cerrado physiognomy associated to a decrease in soil moisture characterized by the expansion of dry-adapted tree taxa *Casearia*, *Cissus*, *Dialium*, *Byrsonima*, and *Caryocar* (Sampaio et al., 2018; Junior et al., 2016; Lombardo, 1996) was observed from 8110 to 7160 cal yr BP (Fig. IV.4). The expansion of a *Mauritia* palm swamp followed the retreat of the river from the coring site (Fig. IV.6). The climate was characterized by a decrease in winter precipitation (Pdq) (Fig. S.6) and warmer temperature. Then, between 7080 to 4600 cal yr BP, the landscape was dominated by an open cerrado physiognomy with sparse Cerrado tree taxa (the grassland re-expansion, the PC2 pollen values, the $\delta^{13}\text{C}$ associated to C4 plants) (Figs. IV.4 and IV.6). The expansion of Cyperaceae-*Mauritia* together with the water level-related plant taxa *Eriocaulon* and *Sagittaria* suggest the establishment of the swamp (Fig. S.3). Climatic reconstruction of MAP (~1400-1500 mm) and Pdq (~25 – 60 mm) show some fluctuations in both the mean annual precipitation and the amount of rainfall during the dry season (Fig. S.6). The late Holocene, from 4370 to 2445 cal yr BP, is characterized by the dominance of an open cerrado (PC1 pollen in Figure IV.6) with mixed shrub and herbs (*Baccharis* and *Cuphea*) and less continuous herbaceous edaphic moisture-related taxa *Polygala* and *Xyris* (Figs. IV.4 and IV.6). The low pollen concentration suggests that the swamp dried up (Fig. IV.6) associated to the installation of warmer and drier conditions.

Finally, between 2260 cal yr BP and 1210 cal yr BP, the expansion of *Cuphea* and *Gomphrena* associated to dry edaphic conditions suggest a continuation toward drier conditions in the open Cerrado with *Mauritia* swamp. Then, from 1210 cal yr BP onward, with the installation of the modern landscape (Fig. IV.1b), an open cerrado with scarce trees in the gallery forest under high erosive conditions. Two peaks of *Hedyosmum*, observed at 709 cal yr BP (3%) and 439 cal yr BP (10%), suggest punctual events of increased precipitations and/or low temperatures. Today, the species *Hedyosmum brasiliense* is poorly distributed in the Tocantins state where it was observed in a gallery forest (Medeiros et al., 2012). The progressive decline of MAP and Pdq suggests a change towards reduction in wet conditions compared to precedent periods, this reduction in precipitation was also suggested by the increase of $\delta^{13}\text{C}$ (C_4 plants dominance). The retreat of the swamp area and the reduction of edaphic moisture availability responded to the precipitation decrease (Fig. S.6). In addition, the disappearance of the tree taxa *Byrsonima* and *Caryocar* which are drought tolerant suggest that the landscape suffered major changes during the last thousand years (Fig. IV.4).

The fire signal was weak in the whole core (below $1 \text{ mm}^2/\text{cm}^2/\text{yr}$) with four marked events at 12,550 cal yr BP, 10,000 cal yr BP, 5400 cal yr BP and during the last century (Figs. IV.5 and IV.6). Less or no fire could be associated to the spatial heterogeneity of fire propagation and the characteristics of the local vegetation and soil moisture (Ouarmim et al., 2016) particularly when dry atmospheric conditions prevent charcoal particle deposition in soil, peat or lake (Conedera et al., 2009). The open landscape and the dry soil likely prevented fire ignition (Fig. IV.6). This hypothesis is consistence with the dominance of grass transported charcoal particles in the entire record (Fig. IV.5).

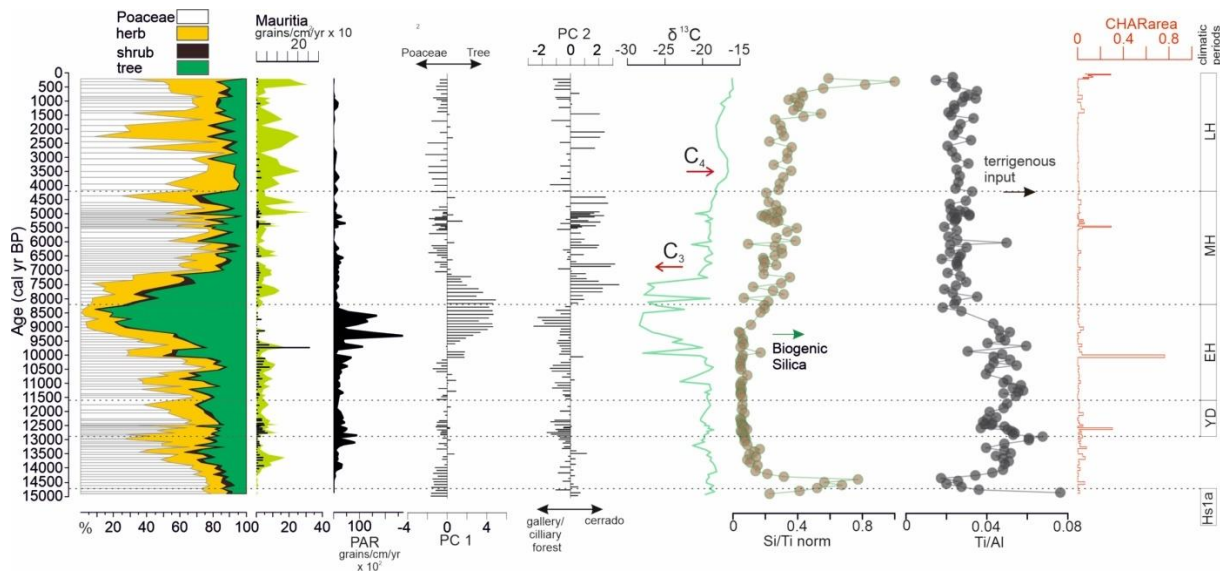


Figure IV.6. Synthetic diagram showing the regional changes in our study area through time. From left to right, pollen frequency according to their growth forms; changes in *Mauritia* frequency (green) and pollen influx (PAR) (black bars); z-scores obtained from PC1 and PC2; $\delta^{13}\text{C}$ signal, Si/Ti and Ti/Al ratio, charcoal influx (area/ cm^2/yr) (red line), and the regional climatic periods. Hs1a = Heinrich stadial 1a (16,110 -14,690 yr BP), YD = Younger Dryas, EH = early Holocene, MH = mid Holocene, LH = late Holocene.

5. Discussion

5.1. 15,000 years of ecological successions in the Cerrado

The Getulio swamp multiproxy record is filling a gap along a north – south latitudinal gradient through the Cerrado (Fig. IV.1c). During the late glacial, the southern region of the Cerrado (Salitre; 19°S - 46°W, 1050 m asl; Ledru, 1993) showed an opposite signal with an open landscape with the cool temperature tree taxa *Podocarpus*, *Ilex*, and *Araucaria*. More to the north, the Rio Preto swamp (18°S - 43°W, 1612 m; Costa et al., 2022) in the southeastern region of the Cerrado, also showed an open landscape with cold elements until 13,400 cal yr BP which was replaced by drought tolerant taxa (*Psychotria* 10%, *Baccharis* ~1-5% and *Mikania* at 1%) during the transition from Pleistocene to Holocene.

In the central region, the lake Feia record (15°S - 47°W, 870 m; Cassino et al., 2020; Escobar-Torrez et al., 2023a) showed the dominance of an open landscape (Poaceae ~53%, Asteraceae 26%) with cool temperature-adapted trees (*Hedyosmum* (5%), *Ilex* (3%), *Myrsine* (1.7%), *Weinmannia*, *Drimys* (<2%) gradually replaced by the expansion of the gallery forest formed of Moraceae, *Annona*, *Anadenanthera*, *Celtis* mixed with cool temperature-adapted taxa (*Hedyosmum* 5%, *Ilex* 3%, *Myrsine* 1.7%) and Cerrado tree taxa (*Astronium* 5%, *Byrsonima* 5%, *Caryocar* <2%) until 13,300 cal yr BP. During the transition to Holocene the expansion of Cerrado tree taxa was associated to warmer climate conditions (Fig. IV.7a). At VGE-17 which is located further north the installation of *Mauritia* associated to warmer temperature was observed 500 years earlier.

Farther north, the lake Caço pollen record (2°58'S - 43°25'W, 120m; Ledru et al., 2006) showed the presence of a cool and moist forest until 12,800 cal yr BP. The transition to Holocene is characterized by the expansion of Poaceae (~ 60%) (Fig. IV.7a) which is very different from *Gétulio*.

During the early Holocene in the central Cerrado, the Lake Feia record showed the dominance of open cerrado with alternate wet and dry phases which lasted until 7000 cal yr BP (Cassino et al., 2020). In the northern Cerrado, at Caço Lake, the development of a dry Cerrado started between 11,800 to 9200 cal yr BP, with *Byrsonima* (~5%), *Mimosa* (0 to 25%) and Poaceae (40-50%) followed by the decrease of the Mimosaceae and the progressive increase in moisture during the Holocene. The cool forest expansion observed at *Getulio* swamp between 9300 and 8200 cal yr BP was not observed elsewhere in Brazil (Fig. IV.7a).

In the mid Holocene (8200 to 4200 cal yr BP), the Getulio swamp recorded a two-step expansion of the open cerrado, first from 8115 to 7165 cal yr BP with the disappearance of the cool taxa *Hedyosmum* and *Ilex* and the re-establishment of *Mauritia* (5-15%); and second, between 7080 to 4590 cal yr BP, the full expansion of the open cerrado . A similar trend was observed in the southeastern (Rio Preto, Costa et al., 2020) and northeastern Cerrado (Saquinho peatland; Oliveira et al., 1999). In the central Cerrado, the lake Feia record showed an opposite change at 6000 cal yr BP, with the expansion of the Cerrado (*Astronium* ~5%, *Byrsnoima* ~2%), gallery forest (Moraceae ~2%, *Hedyosmum* 0-3%), followed from 5000 cal yr BP by the full establishment of

woody cerrado (~20-40%) (*Astronium*, *Byrsonima*, *Casearia*) and gallery forest (10-40%) (*Anadenanthera*, *Cecropia*, *Moraceae*, *Melastomataceae*) (Escobar-Torrez et al., 2023a).

During the Late Holocene (4200 cal yr BP to present), at VGE-17 the tree taxa were replaced by an open vegetation dominated by Poaceae (~70%) by 4370 cal yr BP, becoming drier when shrubby taxa were replaced by *Cuphea* (20-40%) at 2260 cal yr BP and by *Gomphrena* (15-50%) at 1210 cal yr BP. The same trend was observed in southeastern Cerrado at Rio Preto where the grassland was (40-45%) associated to high elevation tree taxa (*Hedyosmum* 30-20%, *Myrsine* 2% and *Podocarpus* 1%) (Costa et al., 2022), and in NEB (Oliveira et al., 1999). In the northwestern Cerrado (edge with the Amazonia), the VDD (7°S - $47^{\circ}26'\text{W}$, 307 m) record suggested synchronicity with a regional arid event from ~4300 to 4000 cal yr BP, when the dewatering of the swamp prevented pollen preservation (Xavier et al., 2023). In the central Cerrado, the regional vegetation was composed of cerrado and gallery forest with three episodes of lower lake level (3340-2760, 2070-1690 and 1330-1150 cal yr BP) (Escobar-Torrez et al., 2023a). Thus, we infer that VGE-17 was more in-phase with the eastern rather than the central Cerrado region during the late Holocene.

5.2 Climate drivers affecting vegetation

The latitudinal changes in vegetation cover described in the previous section relate to changes in the amplitude and intensity of the South American Monsoon System. First, towards the end of the late Pleistocene, between 15,000 and 13,800 cal yr BP, VGE-17 recorded a period of transition to a warm and humid climate, when the presence of *Maurita* and the change in deposition of coarse to fine terrigenous particles (low to high Ti/Al ratio) were observed. Subsequently, as pollen deposition increased (PAR increase) and arboreal elements of Cerrado vegetation appeared and gallery forest became established, a major and prolonged change was observed between ~13,300 to 11,500 cal yr BP. First, forest and wet grasslands increased from ~13,300 to 12,300 cal yr BP followed by a phase of reduced moisture, and slight retreat of gallery forest between ~12,300 to 11,500 cal yr BP, suggesting reduction in wet conditions (Fig. IV.6)

During the end of the Late Pleistocene, two ~1500 yr long climatic episodes - the Heinrich stadial 1 (HS1) between 19,000 and 14,690 cal yr BP and the Younger Dryas (YD) between 12,900 and 11,600 cal yr BP - related to ice meltwater fluxes in the North Atlantic caused a change in the latitudinal temperature gradient: to colder and drier conditions in the northern hemisphere (NH) and to wetter and warmer conditions in the southern hemisphere (SH) (Cheng et al., 2020; Wainer et al., 2021). These two cooler NH events were interrupted by an intermediate period of opposite conditions (warm NH and cold SH) between 14,700 to 13,000 cal yr BP, called the Atlantic cold reversal (ACR) (Fig. IV.7) (Pedro et al., 2015; Wainer et al., 2021).

The base of VGE-17 record coincides with the transition between the end of HS1 and the onset and establishment of the ACR. In the SH, a demise of the precipitation regime in the core of the monsoon system and a regional trend towards drier conditions are observed (Stríkis et al., 2015). In central Brazil, during the late phase of HS1a (16,110 to 14,690 cal yr BP) in the southern border of northeastern Brazil a gradual precipitation reduction was observed (Paixão cave 12°S - Stríkis

et al., 2015) as well as a reduction in SAMS intensity, both in response to a meridional shift of the ITCZ towards its northerly position (10°N) (Wainer et al., 2021).

During the ACR, the southern region of South America at latitudes greater than 40°S remained cold and was influenced by Antarctic meltwater discharge (Fig. IV.7), whereas between 0°S to 20°S the ACR signal weakened and this area was mainly influenced by the NH, with increased subsidence of warm air into the NEB that led to increased temperature and reduced precipitation (Pedro et al., 2015; Custodio et al., 2022). Contrarily, VGE-17 suggests increased wet and warm climate since 13,800 cal yr BP with special second wetter phase from 13,300 to 12,300 cal yr BP. The first wet phase could be related to the effect of the ACR which prevented precipitation in the NEB but did not decline precipitation in the Amazon basin, which remained wet (Paraiso cave – Wang et al., 2017), then arriving until our study site, although subdued due to its remoteness. Similarly, a slight increase in precipitation was recorded in the central Cerrado (Lapa Sem Fim) between 14,000 to 13,500 yr BP, almost synchronous with a first reduction in temperature from the Greenland record (Fig. IV.7) thus signaling that the ACR event was attenuating. This connection may have remained during the second, wetter phase, between the ACR transition and the onset of YD.

Towards the end of the Pleistocene, the YD has marked the last cold phase of the Late Pleistocene in the Northern Hemisphere (NH), between 12,900 to 11,600 cal yr BP (Cheng et al., 2020). A regional study comparing the climatic variations recorded between the Northern and Southern Hemispheres suggest that this period was initiated by an abrupt increase in meltwater (Greenland ice core - Fig. IV.7), whose cooling flow had a directionality of onset from low latitudes in the NH to high latitudes in the Southern Hemisphere (SH), in which the atmospheric circulation was rapid (Cheng et al., 2020) and an increase (reduction) of rainfall in the southern (northern) hemisphere was recorded (Custodio et al., 2022). Conversely, the end of this phase began with its termination first in the Southern Hemisphere (12,300 cal yr BP) and later in the Northern Hemisphere (11,700 cal yr BP), with the re-establishment of the oceanic circulation flow 11,950 cal yr BP (Cheng et al., 2020).

Time transgressive climate circulations is suggested for the YD event, with the Atlantic Meridional Oceanic Circulation (AMOC) weakened first in the NH (cold temperatures) at the same time that enhanced the Monsoon system in SH (warm temperatures), extending to areas of the central Cerrado (Lapa Sem fim wet period from 13,000 to 12,300 yr BP and VGE-17) (Fig. IV.8), increasing in precipitation (Cheng et al., 2022). Meanwhile in the NEB, at $\sim 1^{\circ}\text{S}$, a dry landscape was still present suggesting an inverse precipitation pattern with the Parnaiba river region (Bouimetarhan et al., 2018) and at the lake Caço (Ledru, 2002), where dry conditions are recorded during the whole YD events. Thus signaling the existence of a dipole of precipitation between the NEB and the Monsoon system region. The decoupled relation was confirmed during the second phase of VGE-17, when the reduced precipitation was also recorded in the Amazon basin (12,300 yr BP) and the northern hemisphere (12,200 – 11,700 yr BP), marking the gradual termination of the YD (Cheng et al., 2020; Pigati et al., 2022), meanwhile increases in rainfall was suggested by a change in the ITCZ position towards the area of the Paranaiba river region in the NEB in response

to the weakened AMOC with the lowest activity between 12,300 to 12,100 yr BP (Bouimetarhan et al., 2018).

The spatial comparation of VGE-17 with other records, suggest that the NEB region was the last one receiving the precipitation , with the ITCZ arriving to the latitudinal position of 5°N-5°S proposed by Wainer et al. (2021) by 12,300 cal yr BP, then, during these period an increase in the flow of warm moist temperatures from the northeast region of the South Atlantic Ocean (known as NE-SASD) could increased precipitation in the eastern of NEB and reaching closer areas to VGE-17 (10°S;46°W). Also, despite this period end by 11,600 cal yr BP, our VGE-17 core recorded a continuation in the increased precipitation between 12,000 and 10,500 cal yr BP, with the presence of arboreal elements adapted to continuous cold conditions, the retraction of the *Mauritia* swamp, and the marked rainfall seasonality (MAP and Pdq slow and gradual decrease) (Fig. IV.7b), suggesting a shift towards stable climatic conditions between the end of the YD in the late Pleistocene and the beginning of the Holocene (Fig. IV.7b).

During this transition, the atmospheric temperature gradient was changing, with an increase in insolation in the southern hemisphere and a stop in meltwater discharge in the North Atlantic Ocean (Campos et al., 2022). In this period of restored atmospheric and oceanic circulation, precipitation increased in northern South America and Brazil (Cariaco basin 10°N,65°W - Haug et al., 2001; Paraíso - 4°S,55°W – Wang et al., 2017) and was maintained in the NEB (Rio Grande do Norte caves - 5°S, 37°W - Cruz et al., 2009), while towards southeastern Brazil precipitation was reduced (Botuverá - 27°S,49°W - Wang et al., 2007). Thus, suggesting changes from homogeneous to variable climatic conditions in the monsoon region towards the beginning of the Holocene, with warmer temperatures in the Southern Hemisphere. In VGE-17 the presence and permanence of taxa adapted to cool and humid environments may have been due to this gradual change in environmental conditions, with the effect of polar advection from the North Atlantic being less intense, at 10°S, possibly related not only to its latitudinal position but also to its altitude (450 m asl).

During the present Interglacial period, between 11,600 to 8200 cal yr BP (early Holocene), VGE-17 recorded the expansion of gallery forest composed of cold-adapted elements and a weak signal of Cerrado elements between 9300 to 8240 cal yr BP (~1060 years of duration), suggesting a wet and cold period (Fig. IV.7 and IV.8), which coincides with a new change in atmospheric conditions, more or less similar to those of the YD although with a milder intensity (Thomas et al., 2007), started at 9000 yr BP and lasted ~1000 yr, related to the “8200 event”, a last period in which meltwater flux in the North Atlantic ocean colder the NH and shifted ITCZ position, again, towards the SH enhancing rainfall in the NEB and northern South America (Aguiar et al., 2020; Campos et al., 2022). However, rainfall increase was not observed at latitudes higher than 16°S, with the central region experiencing a fluctuation between dry and wet periods (15°S - Cassino et al., 2020) (Figs. IV.8 and IV.9a and b).

Model reconstructions suggested the formation of the SST dipole in the South Atlantic Ocean (called South Atlantic Subtropical Dipole - SASD) as the principal promotor for increase in precipitation (Wainer et al., 2021; Custodio et al., 2022). This dipole in its positive (negative) phase cools (warms) the northeast pole and warms (cools) the southwest pole of the south Atlantic Ocean

(Wainer et al., 2014). A negative phase of the SASD facilitated increased precipitation in northern South America (latitudes below 15°S) (Wainer et al., 2021) at the same time as reduced insolation in the southern hemisphere weakened the SAMS region reducing precipitation in the western Amazon and increasing it in the NEB (Campos et al., 2022), with weaker trade winds between 9800 to 8000 yr BP (Aguiar et al., 2020) in response to a weak ocean circulation (AMOC) promoted by an increase in meltwater discharge in the Labrador sea (Aguiar et al., 2021). These models suggested a more prolonged period that lead to the 8200 event, with was not recorded by the Greenland ice core (Fig. IV.8), and, for the first time, VGE-17 agreed with this a marked period with enhanced precipitation observed to affect the NEB region up to our study area, while in intermediate areas (Paixão cave - 12°S, 41°W) this event was weakened by the mixed response to insolation, affected by SAMS and ITCZ. Although the duration of our wet period was 300 years earlier than predicted models.

After this event VGE-17 recorded a gradual change in vegetation, between 8110 to 7160 cal yr BP, with a shift towards dry and warm conditions the vegetation became less denser and open cerrado started to expand meanwhile gallery forest retracted, coincides with the onset of the mid-Holocene (8200 to 4200 yr BP). At global scale, these changes were may be in response to ocean circulation gradual reestablishment, the southern hemisphere began to warm and the ITCZ moved to its southernmost position (~4°S) (Jomelli et al., 2022), when the positive mode in SASD is suggested, after 6000 yr BP (Wainer et al., 2014; Custodio et al., 2022), contributing to the east-west antiphase relationship in the SH tropics (Campos et al., 2022). Temperatures increased again in the SH (Fig. IV.9a).

During the mid-Holocene, the discharge of meltwater into the oceans stopped and climatic conditions were mostly controlled by insolation (Fig. IV.7) (Cruz et al., 2009; Wainer et al., 2021). In VGE-17 the middle Holocene continued to record a reduction in humidity towards dry climatic conditions, with a predominantly open landscape between 7080 to 4600 cal yr BP, when insolation reached its “thermal maximum” in the NH and northern South America (Fig. IV.7) (Haug et al., 2001). During the late Holocene from 4370 cal yr BP to the present VGE-17 recorded the continuation of dry climatic conditions with the retraction of gallery forest and swamp demise, this dryer event was also recorded by another palynological record, in synchrony with VGE-17, towards the west of the northern Cerrado region, in *Vereda de Dodó* (Xavier et al., 2023) suggesting a regional response to a strong dry episode. The relation between both cores decoupled after this event, with VGE-17 recording increased dryness with punctual events at 2445 and 1210 cal yr BP. During the late Holocene, the increase in insolation during the austral summer shows a change with increased temperature and the strengthening of SAMS, especially in western Amazonia (Zolitschka et al., 2021), while in this period in the NEB subsidence increases (reducing precipitation in the region), while the ITCZ contracts (Campos et al., 2022), an increase in soil erosion was also recorded in Trapiá cave (5°S-37°W) (Utida et al., 2020). Although the central Cerrado does not show a large variation in the precipitation regime (Fig. IV.7), towards the north of South America can be observed that at the end of the mid Holocene and during the late Holocene the region started to dry out, especially in the beginning of the late Holocene (Fig. IV.7e) (Haug et al., 2001). The VGE-17 record clearly evidences that although the SAMS is one of the main systems in the Cerrado precipitation regime, the northern Cerrado region (mainly at 10°S; 46°W)

was also influenced by similar climate mechanisms from the NEB region, which are linked to changes in the ITCZ and the SST of the Atlantic Ocean. However, some events of increased precipitation in the central Brazil (Lapa Grande cave – Strikís et al., 2011) suggest punctuated events of increased precipitation, related to bond events, which shows that even when the region is primarily related the NEB, some connections remained with the SAMS.

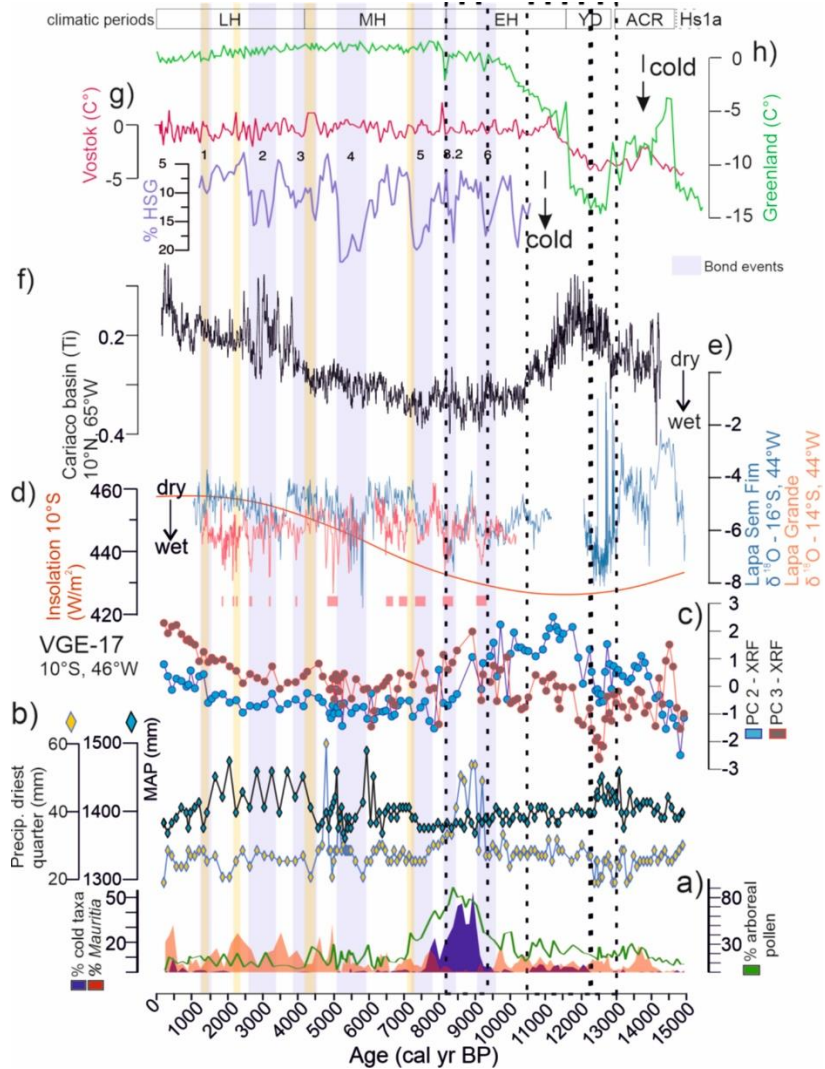


Figure IV.7. a) Synthesis of principal changes observed between 10,000 and 7500 cal yr BP on the VGE-17 core with pollen representation, (b) Mean annual precipitation (MAP) and precipitation of the driest quarter reconstruction made with Crest package (Chevalier et al., 2020), (c) PC2 and PC3 from XRF analyses, (d) the Insolation curve at 10°S (red curve) (Laskar et al., 2011) (e) changes in moisture from the isotopic analyses of the speleothems (Strikis et al 2011, 2015) and (f) Ti signal from Cariaco basin (Haug et al., 2001) (g) temperature reconstruction for Vostok ice core (Petit et al., 1999) and the % HSG (purple curve) representing the ice drift (Bond et al., 2001) and (h) Greenland ice core (Badgley et al., 2020). The yellow band highlights the drier interval and the dotted black lines show the wet intervals observed at VGE-17 (this study). Light purple bands represent the bond events (from Bond et al., 2001).

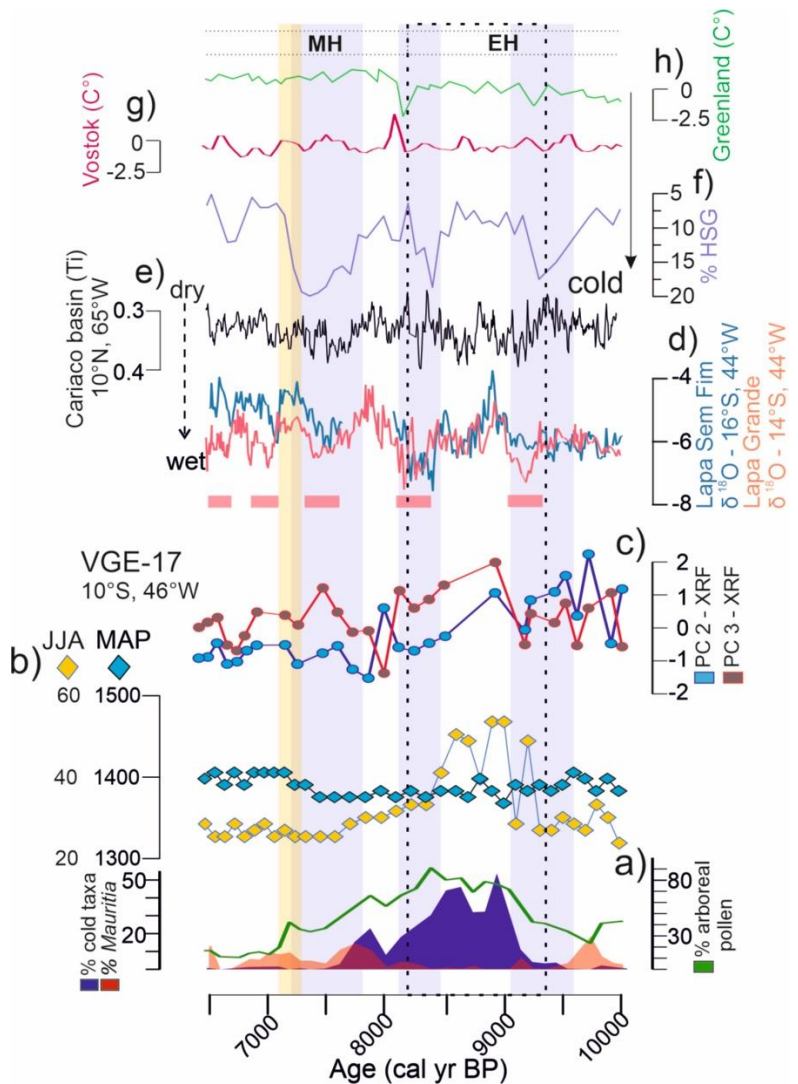


Figure IV.8. a) Synthesis of principal changes observed between 10,000 and 7500 cal yr BP on the VGE-17 core with pollen representation, (b) Mean annual precipitation (MAP) and precipitation of the driest quarter reconstruction made with Crest package (Chevalier et al., 2020) (c) PC2 and PC3 from XRF analyses, (d) changes in moisture from the isotopic analyses of the speleothems (Strikis et al 2011, 2015), (e), Ti signal from Cariaco basin (Haug et al., 2001) (f) temperature reconstruction for Vostok (Petit et al., 1999) and Greenland (Badgley et al., 2020) ice cores. The yellow band highlights the drier interval and the dotted black lines show the wet intervals observed at VGE-17 (this study). Light purple bands represent the bond events (from Bond et al., 2001).

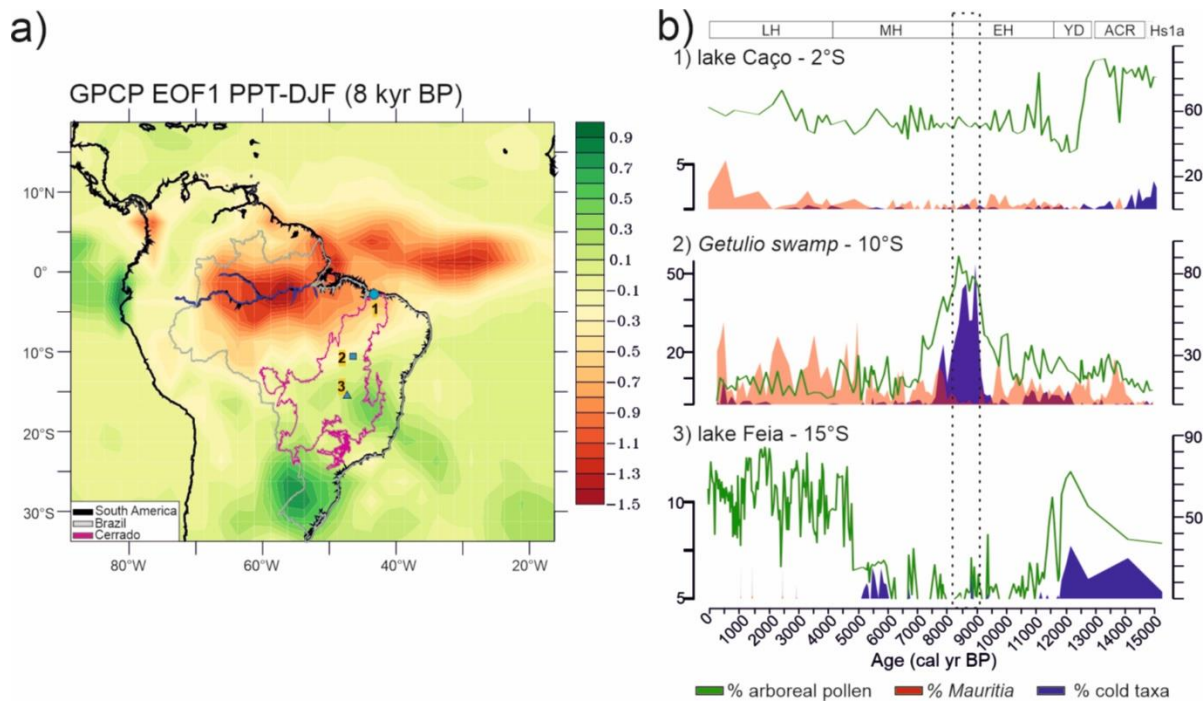


Figure IV.9. a) December-January-February (DJF) precipitation reconstruction (PPT) at 8000 yr BP (from ref). Changes in vegetation along across a latitudinal transect b) Summary graphic showing the indicator pollen taxa used for climate and precipitation changes interpretations, with arboreal pollen (green), *Mauritia* (red) and cold and humid taxa (blue) from three records: Caço Lake (from 15,040 cal yr BP to 1997 AD) (Ledru et al., 2006), Gétulio swamp (this study) and Feia Lake (from 15,210 cal yr BP to 1990 AD) (Cassino et al., 2020; Escobar-Torrez et al., 2023a). The site names are related to the numbers in the pollen diagrams (b) in this figure.

5.3 Fire occurrence in the “Serra Geral do Tocantins”

The influx of charcoal deposition remained low at VGE in the last 15,000 years (Fig. IV.7). The W:L ratio showed continuous fire occurrence dominated by grass particles (< 0.5) (Aleman et al., 2013) with four main fire events at 12,550 cal yr BP, 10,000 cal yr BP, 5400 cal yr BP and the last century. The low and constant fire signal suggests that the biomass burning was not close to the VGE-17 coring site and was rather at a broad regional scale. The fire signal at VGE-17 is very different from Lake Caço and Lake Feia records which showed a high fire activity synchronous of the expansion of the cerrado, at 13,000 cal yr BP and at 5300 cal yr BP respectively. We infer either an absence of human activity in the vicinity of the swamp or continuous high soil moisture due to the numerous streams and rivers (Villela and Nogueira, 2011) which prevented fire propagation (Schmidt et al., 2017) or both.

6. Conclusion

The Getulio swamp multiproxy record showed that the last 15,000 years were characterized by a cerrado landscape dominated by open vegetation with change in the expansion and composition of the gallery forest. Our data showed two abrupt and short climatic changes related to northern hemisphere ice melting, the Younger Dryas (12,700–11,600 cal yr BP) and the 8.2 event which induced strong changes in the vegetation. The first one was characterized by a YD divided into two phases, a first wet period between 13,300 to 12,300 cal yr BP followed by a dry period (12,300

to 11,500 cal yr BP), suggesting a gradual change in SAMS intensity in response to the weakened AMOC, which recovered by the onset of the second phase. The second one, characterized by a period of major precipitation which was prolonged from 9300 to 8240 cal yr BP, suggesting a wider period of meltwater discharge which promoted increased precipitation in VGE-17.

The vegetation responses to both events revealed that the region of Serra Geral do Tocantins (latitude 16°S) relates more to NEB climatic features than central Brazil, with for instance the two-step Younger Dryas and the late Holocene increase of aridity. The strong signal observed between 9300 and 8200 cal yr BP highlight an earlier and longer response of the vegetation than the one observed in NH marine core or in the speleothems. It is also one of the first palynological record that allowed to delimit the spatial influence of the changes in ocean-atmosphere coupling during northern hemisphere ice melting with precision. Today we are facing a similar situation although at a faster velocity. The end of the ice melting induced the installation of drier and warmer conditions at 16°S which strengthened as summer insolation became stronger.

7. Acknowledgments and funding

This work is part of the “Cerrados & Fogos” program at IRD. Financial support was provided by IRD, FAPDF (0193.001374/2016), ISEM, DEGEO-UFPB and ICA/UFVJM. KET benefited from a PhD position funded by the IRD ARTS program and the French Embassy in Bolivia. This work has also benefited from an “Investissement d’Avenir” grant managed by the Agence Nationale de la Recherche (CEBA, ref. ANR-10-LABX-25-01). Radiocarbon dating was performed at LMC14 (LSCE(CNRS-CEA-UVSQ)-IRD-IRSN-MC) with IRD financial support. We thank Ludivine Eloy and Michel Brossard for their advices and fruitful discussion during the development of the work and, Ana Carolina Sena Barradas, Marco Assis Borges, Maximo Menezes Costa of the Instituto Chico Mendes de conservação da Biodiversidade (ICM-Bio), Ludivine Eloy, Silvia Laine Borges Lucio, Christelle Hély-Alleaume for their assistance during fieldwork at the Serra Geral do Tocantins Ecological Station.

8. Annex 1. Supporting Information

Tables

Table S.1. Life form and ecological classification of pollen taxa identified in VGE-17 core. Bolded ecological group suggest that the taxon was mostly reported in that type of ecological group. *sl*= *sensu lato*, *ss* = *Cerrado sensu stricto*, *CR* = *Campo rupestre*, *CLU* = *Campo limpo umido*, *SDTF* = *Semideciduous Tropical forest*, *GF*=*gallery forest*, *CF*=*Cillary forest* (Martins et al., 2008 ; Medeiros et al., 2012, Medeiros and Walter, 2012; Lemos et al., 2013 ; Silva et al., 2016; Silva et al., 2018 ; Antar et al., 2019 ; Matias et al., 2021).

Family	Taxon	Life form	Ecological group
Acanthaceae	<i>Aphelandra</i>	herb subshrub	cerrado sl, dry anf gallery forest
Amaranthaceae	<i>Am/Chenop</i>	herb	cerrado ss
Amaranthaceae	<i>Althernantera</i>	herb	Cerrado ss vereda
Amaranthaceae	<i>Gomphrena</i>	herb subshrub	Cerrado ss
Apiaceae	<i>Eryngium</i>	herb	Cerrado sl, GF, vereda
Asteraceae	<i>Baccharis</i>	herb/shrub	Cerrado ss, CR
Asteraceae	Asteraceae	herb/shrub	Cerrado ss
Boraginaceae	<i>Heliotropium</i>	herb	Cerrado ss
Bromeliaceae	Bromeliaceae	herb	Cerrado sl (CR, ss, CLU), GF
Brassicaceae	Brassicaceae	herb	Cerrado sl (campos brejos)
Cabombaceae	<i>Cabomba</i>	herb	Cerrado vereda
Convolvulaceae	<i>Evolvulus</i>	herb shrub	Cerrado ss vereda
Droseraceae	<i>Drosera</i>	herb	Cerrado sl (CLU, CR) vereda
Euphorbiaceae	<i>Euphorbia</i> type	herb shrub	Cerrado sl (rupestre ss)
Lamiaceae	<i>Hyptis</i>	herb subshrub	Cerrado sl (CLU, CR, s), vereda
Lentibulariaceae	<i>Urticularia</i>	herb	Cerrado sl (CLU, CR, s), vereda
Lythraceae	<i>Cuphea</i>	herb shrub	vereda, Cerrado sl (CLU, rupestre, ss)
Menispermaceae	<i>Cissampelos</i> type	herb subshrub	Cerrado sl (ss, rupestre)
Onagraceae	<i>Ludwigia</i>	herb subshrub	Cerrado sl (ss, CLU), vereda
Poaceae	Poaceae	herb	Cerrado sl
Polygalaceae	<i>Polygala</i>	herb	Cerrado sl (CLU, ss), vereda
Rubiaceae	<i>Borreria</i>	herb shrub	Cerrado sl (ss, CLU), vereda
Xyridaceae	<i>Xyris</i>	herb	Cerrado CLU, vereda
Araceae	<i>Spathiphyllum</i>	herb	GF
Euphorbiaceae	<i>Acalypha</i>	shrub	GF CF, Dry Forest
Piperaceae	<i>Peperomia</i>	shrub	CF GF
Ericaceae	Ericaceae	shrub	Cerrado (rupestre)
Euphorbiaceae	<i>Sebastiania</i>	shrub	Cerrado sl (ss, rupestre, CLU)
Fabaceae (caes)	<i>Chamaecrista</i>	shrub	Cerrado sl (ss, rupestre)
Fabaceae (caes)	<i>Senna/Chamaecrista</i>	shrub	Cerrado sl (ss, rupestre)
Fabaceae (pap)	<i>Copaifera</i>	shrub	Cerrado sl (ss, rupestre, CLU)
Fabaceae (mim)	<i>Mimosa</i>	subshrub	Cerrado sl (ss, rupestre)

Malpighiaceae	<i>Banisteriopsis</i>	shrub vine	Cerrado sl (ss, rupestre), CF SDTF
Malvaceae	<i>Helicteres</i>	shrub	Cerrado sl (ss, rupestre, Cerradão), CF GF
Menispermaceae	<i>Abuta</i>	shrub	Cerrado ss, GF
Piperaceae	<i>Piper</i>	shrub	Cerrado sl (ss, Cerradão), vereda
Rubiaceae	<i>Alibertia</i>	shrub	Cerrado sl (ss, rupestre)
Rubiaceae	<i>Sabiceae</i> type	shrub	Cerrado ss
Rubiaceae	<i>Psychotria</i>	shrub	Cerrado ss, vereda
Sapindaceae	<i>Diatemopterix</i>	shrub	Cerrado sl (rupestre)
Solanaceae	<i>Solanum</i>	shrub	Cerrado ss
Verbenaceae	<i>Lantana</i>	shrub	Cerrado ss
Verbenaceae	<i>Lippia</i>	subshrub	Cerrado sl (ss, Cerradão), vereda
Euphorbiaceae	Euphorbiaceae	variuos	various
Menispermaceae	Menispermaceae	variuos	various
Melastomataceae	Melastomataceae	tree	various
Myrtaceae	Myrtaceae	tree	various
Anacardiaceae	Anacardiaceae	tree	Cerrado sl (ss, rupestre)
Anacardiaceae	<i>Thrysodium</i>	tree	SDTF, CF, cerradão
Bignoniaceae	<i>Tecoma</i>	tree	Cerrado ss Cerradão, GF CF
Bignoniaceae	Bignoniaceae	tree	Cerrado ss
Cannabaceae	<i>Celtis</i>	tree	Cerradão, GF CF SDTF
Caryocaraceae	<i>Caryocar</i>	tree	Cerrado (ss, rupestre cerradão)
Celasteraceae	<i>Plenckia</i>	tree	Cerrado ss , Cerradão
Euphorbiaceae	<i>Sapium</i>	tree	Cerrado ss, SDTF
Fabaceae (pap)	<i>Andira</i>	tree	Cerrado sl (ss, rupestre, Cerradão)
Fabaceae (mim)	<i>Anadenanthera</i>	tree	Cerrado ss
Malpighiaceae	<i>Byrsinima</i>	tree	Cerrado sl (ss, rupestre), vereda GF
Malvaceae	<i>Eriotheca</i>	tree	Cerrado sl (ss, rupestre), CF SDTF
Ochnaceae	<i>Ouratea</i>	tree	Cerrado sl (ss, Cerradão, rupestre)
Pentaphylaceae	<i>Ternstroemia</i>	tree	SDTF, Cerradão CF
Phyllanthaceae	<i>Hyeronymia</i>	tree	Cerrado ss, CF GF
Rubiaceae	<i>Chomelia</i>	tree	Cerrado sl (ss, rupestre), CFGF
Rubiaceae	<i>Guettarda</i>	tree	Cerrado ss, GF CF
Salicaceae	<i>Casearia</i>	tree	Cerrado sl (ss, rupestre, Cerradão)
Salicaceae	<i>Flacourzia</i>	tree	Cerrado sl (ss, rupestre, Cerradão)
Salicaceae	<i>Cissus</i>	tree	Cerrado sl (ss, rupestre, Cerradão)
Sapindaceae	<i>Thinouia</i> type	vine	Cerradão
Sapotaceae	<i>Pouteria</i>	tree	Cerrado sl (ss, Cerradão, rupestre), GF CF
Smilaceae	<i>Smilax</i>	vine	Cerrado sl (ss, rupestre, CLU) vereda , CF GF
Fabaceae	<i>Peltophorum</i>	tree	SDTF
Fabaceae	<i>Dialium</i>	tree	SDTF
Anacardiaceae	<i>Tapirira</i>	tree	CF GF Cerrado vereda
Araliaceae	<i>Schefflera</i>	tree	GF CF, Cerrado ss, rupestre
Arecaceae	<i>Euterpe</i>	treepalm	GF, cerrado

Aquifoliaceae	<i>Ilex</i>	tree	CF GF CR
Bignoniaceae	<i>Tabebuia</i>	tree	GF CF, SDTF Cerradão
Boraginaceae	<i>Cordia</i>	tree shrub	CF GF, Cerrado ss SDTF
Boraginaceae	<i>Thunbergia</i>	vine	forest, antropic
Boraginaceae	<i>Cordia</i>	tree shrub	CF GF, Cerrado ss SDTF
Burseraceae	<i>Protium</i>	tree	CF GF
Cannabaceae	<i>Trema</i>	tree	CF GF
Cecropiaceae	<i>Cecropia</i>	tree	CF GF, Cerrado
Celasteraceae	<i>Clethra</i>	tree	CF GF
Celasteraceae	<i>Maytenus</i> type	tree	CF GF Cerrado sl (ss)
Chloranthaceae	<i>Hedyosmum</i>	tree	GF vereda
Cunoniaceae	<i>Weinmannia</i>	tree	GF, CR CLU
Cunnoniaceae	<i>Lamanonia</i>	tree	CF GF Cerrado sl (Cerradão, CR)
Dillenaceae	<i>Doliocarpus</i>	tree	CF GF Cerrado sl (ss, CR, Cerradão) vereda
Euphorbiaceae	<i>Alchornea</i>	tree	CF GF, Cerrado ss
Euphorbiaceae	<i>Maprounea</i>	tree	CF GF SDTF, Cerrado sl (rupestre, ss)
Fabaceae	<i>Pterocarpus</i>	tree	GF CF, Cerrado sl (rupestre)
Fabaceae	<i>Machaerium</i>	tree	CF GF, Cerrado sl (cerradão, ss)
Fabaceae	<i>Piptadenia</i>	tree	SDTF, CF
Icacinaceae	<i>Emmotum</i>	tree	CF GF, Cerrado sl (Cerradão, ss, rupestre, CLU)
Icacinaceae	<i>Villaresia</i>	tree	CF GF sdft
Lecythidaceae	<i>Eschweilera</i>	tree	CF GF, Cerrado sl (ss, campo sujo)
Meliaceae	<i>Cabralea</i>	tree	CF GF, Cerrado ss
Meliaceae	<i>Guarea</i>	tree	CF GF, Cerrado ss
Moraceae	mor/urt	tree	CF GF
Primulaceae	<i>Myrsine</i>	tree	GF, Cerradão
Primulaceae	<i>Cybianthus</i>	tree	CF GF
Podocarpaceae	<i>Podocarpus</i>	tree	GF, cerrado sl (rupestre)
Rhamnaceae	<i>Zyziphus</i>	tree	GF
Rubiaceae	<i>Amaioua</i>	tree	CF GF
Rubiaceae	<i>Bathysa</i>	tree	CF GF
Rubiaceae	<i>Sisimira</i>	tree	GFCF
Salicaceae	<i>Salix</i>	tree	GF
Sapindaceae	<i>Paullinia</i>	vine	GF
Sapindaceae	<i>Matayba</i>	tree	GF CF, Cerrado ss
Sapotaceae	<i>Chrisophyllum</i>	tree	GF
Winteraceae	<i>Drymis</i>	tree	CF GF
Water-level related taxa			
Arecaceae	<i>Mauritia</i>	tree palm	vereda CLU
Alismataceae	<i>Sagittaria</i>	herb	pond lake
Cyperaceae	Cyperaceae	various	various
Eriocalaceae	<i>Eriocaulon</i>	herb	vereda, CLU pond
Pontederaceae	<i>Eichornia</i>	aquatic herb	vereda, CLU, lake, GF

Table S.2. List of pollen taxa with highest contribution (%) in PC1 and PC2 in VGE-17.

Variables contribution			
PC1	%	PC2	%
Poaceae	8.051061	<i>Ilex</i>	9.93
<i>Hedyosmum</i>	6.554363	<i>Cordia</i>	8.23
<i>Paullinia</i>	6.489554	<i>Byrsinima</i>	7.28
<i>Protium</i>	6.296195	<i>Lippia</i>	5.39
<i>Cissus</i>	5.758149	<i>Cuphea</i>	4.87
<i>Simira</i>	4.884745	<i>Casearia</i>	4.50
<i>Eriotheca</i>	4.802713	<i>Cybianthus</i>	2.85
<i>Peperomia</i>	4.302766	<i>Peperomia</i>	2.60
Melastomataceae/Combretaceae	3.458148	<i>Piptadenia</i>	2.45
Ericaceae	2.901884	<i>Guettarda</i>	2.23
<i>Smilax</i>	2.542688	<i>Sabicea</i>	2.04
<i>Casearia</i>	2.172205	Moraceae/Urticaceae	1.74
<i>Acalypha</i>	2.00691	<i>Smilax</i>	1.74
Myrtaceae	1.888225	<i>Polygala</i>	1.64
<i>Matayba</i>	1.88209	<i>Baccharis</i>	1.63
Brassicaceae	1.775227	<i>Hyeronomia</i>	1.50
<i>Emmotum</i>	1.715407	<i>Emmotum</i>	1.48
<i>Baccharis</i>	1.561464	<i>Hedyosmum</i>	1.47
<i>Guarea</i>	1.529133	Melastomataceae	1.38
<i>Euterpe</i>	1.505984	<i>Solanum</i>	1.37
Menispermaceae	1.455535	<i>Caryocar</i>	1.36
<i>Machaerium</i>	1.392483	<i>Celtis</i>	1.36
<i>Xyris</i>	1.250202	<i>Anadenanthera</i>	1.35
<i>Lamanonia</i>	1.243507	<i>Cissus</i>	1.34
<i>Eryngium</i>	1.208865	<i>Matayba</i>	1.33
<i>Gomphrena</i>	1.204058	<i>Mimosa</i>	1.27
<i>Dialium</i>	1.129362	Ericaceae	1.20
<i>Abuta</i>	1.034028	<i>Drosera</i>	1.11
		Myrtaceae	1.09

Table S.3. Ecological classification of pollen taxa selected in VGE-17 (Martins et al., 2008 ; Medeiros et al., 2012, Medeiros and Walter, 2012; Lemos et al., 2013 ; Silva et al., 2016; Silva et al., 2018 ; Antar et al., 2019 ; Matias et al., 2021).

Ecosystems classification	Pollen taxa indicators
open Cerrado	Herb: Poaceae, <i>Baccharis</i> , Brassicaceae <i>Cuphea</i> , <i>Gomphrena</i> usually present in well-drained soils, meanwhile, <i>Drosera</i> , <i>Eryngium</i> , <i>Polygala</i> , and <i>Xyrys</i> are associated to humid soils or tend to be present in vereda or marsh ecosystems Shrub: common in Cerrado with well-drained soils phygionomes (campo limpo, rupestre and cerrado <i>sensu stricto</i>) <i>Lippia</i> , Ericaceae, <i>Mimosa</i> , <i>Solanum</i> .
arboreal Cerrado	Lower understory (≤ 10 m) Flood soils: <i>Celtis</i> and Melatomataceae/Combretaceae, usually found in humid soils. They can be adapted to flooded areas. Their occurrence in Cerrado phygionomes is related to Cerradão, Campo rupestre, and in transition with Gallery forest. Well-drained soils: <i>Byrsinima</i> and <i>Caryocar</i> are commonly found in well drained soils, however, they can be also associated to denser woodland in association with <i>Casearia</i> , <i>Cissus</i> , <i>Eriotheca</i> , <i>Guettarda</i> , and <i>Smilax</i> vine which in abundance suggest the presence of Cerradão physiognomy. Middle understory (≥ 15 m): <i>Anadenanthera</i> and <i>Dialium</i> both common in fertile soils, and also associated to semideciduous forest, they are rarely founded in savannas, in the South of Tocantins are commonly recorded in cerrado typic with mesotrophic soils.
Gallery forest	Lower understory (≤ 10 m):

	Flood soils: Myrtaceae, <i>Hedyosmum</i> , <i>Ilex</i> , <i>Protium</i> Well drained soils: Moraceae/Urticaceae, <i>Cordia</i> (pioneer), <i>Cybianthus</i> , <i>Emmotum</i> , <i>Euterpe</i> , <i>Lamanonia</i> , <i>Machaerium</i> , (light-demanding), <i>Matayba</i> , <i>Paullinua</i> and <i>Simira</i> . Shrubs-herbs: <i>Acalypha</i> and <i>Peperomia</i> .
Vereda or marsh	<i>Eriocaulon</i> , <i>Sagittaria</i> and <i>Mauritia</i> tree palm, all these taxa are present in flooded soils.

TableS.4. Results of the PCA analysis showing the Eigenvalues of each component and the significance as a percentage, the contribution of each ecological group and their dispersion in the components. herbT= terrestrial herbs, herbTV=terrestrial herbs present near/inside veredas, ShrubC=shrubs from Cerrado sensu lato, ShrubF= shrubs from gallery/ciliary forest, TreeCD= trees from Cerrados sensu lato+*Dialium*+*Melast.*Comb, TFM = tree from gallery:ciliary forest + Myrtaceae.

	PC1	PC2	PC3	PC4	PC5
eigenvalue	2.725969	1.377149	1.124918	0.821707	0.457457
% of variance	38.94241	19.67355	16.07025	11.73868	6.535096
cumulative % of variance	38.94241	58.61596	74.68621	86.42489	92.95998
Variable contribution					
Poaceae	29.96796	0.082008	8.471121	0.279151	3.994738
herbT	0.011491	0.065034	82.92428	5.670112	1.147863
HerbTV	0.778559	48.60633	0.604308	22.39181	18.45691
ShrubC	1.623812	39.60093	0.604641	39.20948	15.9869
ShrubF	17.13087	0.548029	5.374611	31.03858	45.86997
TreeCD	25.23299	2.609593	1.830312	0.427162	11.04968
TFM	25.25432	8.48807	0.190731	0.983705	3.493941
Variable coord					
Poaceae	-0.90383	-0.03361	-0.3087	0.047894	0.135182
herbT	0.017699	0.029927	0.965831	0.215851	0.072464
HerbTV	-0.14568	0.818157	-0.08245	0.428947	-0.29057
ShrubC	0.210392	0.738487	0.082473	-0.56762	0.270431
ShrubF	0.683361	0.086874	-0.24589	0.505021	0.458078
TreeCD	0.829363	0.189573	-0.14349	-0.05925	-0.22483
TFM	0.829714	-0.3419	-0.04632	-0.08991	-0.12642

Table S. 5. Differences in sedimentation rate and deposition time of the VGE-17core.

Depth (cm)	Age (cal yr BP)	Sedimentation rate (cm/yr)	Deposition time (yr/cm)
300 – 265	15,020 – 13,285	~ 0.02	~ 50
264 – 231	13,250 – 12,280	0.031 – 0.037	30 – 25
230 – 160 (224 – 220)	12,250 – 8625 (11,930-11,600)	~ 0.02 (~ 0.012)	~ 50 (~ 80)
159 – 140	8560 – 7340	~0.014	~ 64
130 – 110	7300 - 6070	~ 0.022	~ 42
109 – 105	5970 – 5540	~ 0.009	~108
104 - 75	5515 – 4870	~ 0.045	~ 23
74 – 70	4820 – 4590	~ 0.017	~ 57
69 – 40	4482 – 1436	~ 0.0096	~ 104
39 - 20	1400 - 212	~ 0.017	~ 62
19 – 0	197 cal yr BP to 2017 AD	~ 0.07	~ 14

Table S.6 resume of the results obtained from PCA analysis, showing the first fourth components, for elemental and isotope composition in VEG-17 core samples.

Total Variance Explained				
Component	Initial Eigenvalues		Rotation Sums of Squared Loadings	
	Total		% of Variance	Cumulative %
1	6.429		33.595	33.60
2	4.693		18.75	52.35
3	1.741		14.955	67.30
4	1.185		10.745	78.04

Table S.7 Element and Isotope z-scores and contribution for the first fourth components from VEG-17 core samples. Bold scores signal the representative elements in each component.

Rotated Component Matrix(a)								
	Component scores				Component contribution			
	1	2	3	4	1	2	3	4
C	0.94	0.13	0.10	0.11	0.88	0.02	0.01	0.01
H	0.94	0.04	0.09	0.27	0.88	0.00	0.01	0.07
N	0.90	-0.03	0.36	0.02	0.82	0.00	0.13	0.00
O	0.86	0.01	-0.20	-0.19	0.74	0.00	0.04	0.04
Si	-0.85	-0.14	0.26	-0.29	0.73	0.02	0.07	0.08
Br	0.70	-0.10	0.47	0.06	0.49	0.01	0.22	0.00
Zr	-0.69	0.33	0.01	-0.07	0.48	0.11	0.00	0.01
S	0.60	-0.22	0.09	0.47	0.36	0.05	0.01	0.22
Fe	0.08	0.86	0.07	-0.13	0.01	0.74	0.01	0.02
Sr	0.07	0.79	-0.07	0.15	0.00	0.63	0.01	0.02
K	-0.03	0.78	-0.33	-0.21	0.00	0.61	0.11	0.04
Ti	-0.25	0.73	-0.53	0.24	0.06	0.54	0.28	0.06
Al	-0.21	0.69	-0.53	0.30	0.04	0.47	0.28	0.09
dN15	-0.04	-0.09	0.85	-0.01	0.00	0.01	0.72	0.00
Ca	0.41	-0.25	0.60	-0.03	0.17	0.06	0.36	0.00
C/N	0.50	0.29	-0.53	0.22	0.25	0.08	0.28	0.05
dC13	-0.09	0.01	0.00	-0.91	0.01	0.00	0.00	0.83
V	0.37	0.17	-0.41	0.63	0.14	0.03	0.17	0.40

Table S.8. Temperature and precipitation changes reconstructed from the 46 pollen taxa selected in core VGE-17. MAT = Mean Annual Temperature, Tmin= Minimum Temperature of the coldest month, MAP=Annual Precipitation, Pdq= Precipitation of the driest quarter

Age	MAT	Tmin	MAP	Pdq
212	21.1155779	11.5477387	1383.03518	18.9346734
325	21.2763819	11.7286432	1367.9397	28.4020101
439	20.9547739	11.5477387	1383.03518	26.8241206
567	21.1155779	11.5477387	1390.58291	23.6683417
709	21.1155779	11.7286432	1405.67839	23.6683417
851	21.2763819	11.9095477	1398.13065	23.6683417
910	21.2763819	11.7286432	1375.48744	28.4020101

969	20.9547739	11.7286432	1398.13065	26.8241206
1088	20.9547739	11.7286432	1405.67839	26.8241206
1210	21.1155779	11.9095477	1413.22613	28.4020101
1336	21.1155779	11.7286432	1375.48744	28.4020101
1436	21.1155779	11.7286432	1398.13065	25.2462312
1669	20.9547739	11.7286432	1450.96482	26.8241206
1876	21.2763819	12.2713568	1420.77387	20.5125628
2073	21.1155779	11.9095477	1473.60804	20.5125628
2259	21.2763819	11.7286432	1398.13065	25.2462312
2445	21.2763819	11.7286432	1428.32161	28.4020101
2648	21.2763819	11.7286432	1405.67839	23.6683417
2852	20.9547739	11.7286432	1458.51256	28.4020101
3060	20.9547739	11.7286432	1405.67839	26.8241206
3274	20.9547739	11.5477387	1458.51256	26.8241206
3489	20.9547739	10.281407	1398.13065	25.2462312
3713	20.9547739	11.7286432	1458.51256	25.2462312
3938	21.2763819	11.9095477	1420.77387	25.2462312
4159	20.9547739	11.5477387	1450.96482	26.8241206
4374	21.1155779	11.7286432	1405.67839	20.5125628
4590	21.1155779	11.7286432	1375.48744	28.4020101
4703	21.5979899	11.9095477	1383.03518	29.9798995
4816	20.9547739	11.5477387	1398.13065	59.959799
4895	20.7939698	10.1005025	1375.48744	28.4020101
4938	21.1155779	11.9095477	1398.13065	28.4020101
4982	21.4371859	11.9095477	1405.67839	20.5125628
5028	21.1155779	11.7286432	1413.22613	25.2462312
5073	20.9547739	10.8241206	1420.77387	28.4020101
5117	20.9547739	11.7286432	1458.51256	28.4020101
5160	20.9547739	11.5477387	1375.48744	39.4472362
5204	21.2763819	11.7286432	1390.58291	36.2914573
5254	20.9547739	11.5477387	1405.67839	28.4020101
5305	21.1155779	11.5477387	1367.9397	29.9798995
5349	20.9547739	11.3668342	1360.39196	28.4020101
5388	20.9547739	9.73869347	1390.58291	28.4020101
5427	21.1155779	11.7286432	1375.48744	28.4020101
5471	20.9547739	11.0050251	1390.58291	28.4020101
5515	21.1155779	11.5477387	1375.48744	28.4020101
5644	21.2763819	11.7286432	1390.58291	25.2462312
5859	21.2763819	11.7286432	1413.22613	20.5125628
5966	20.9547739	9.73869347	1488.70352	25.2462312
6074	20.9547739	11.3668342	1383.03518	25.2462312
6157	20.9547739	11.7286432	1450.96482	28.4020101
6239	21.2763819	11.7286432	1383.03518	28.4020101
6322	20.9547739	11.7286432	1398.13065	29.9798995
6406	20.9547739	10.8241206	1367.9397	29.9798995
6489	20.9547739	11.7286432	1398.13065	28.4020101
6572	20.9547739	11.3668342	1405.67839	25.2462312
6654	20.9547739	11.7286432	1390.58291	25.2462312
6738	20.9547739	11.7286432	1405.67839	28.4020101
6822	20.9547739	11.5477387	1390.58291	25.2462312
6907	20.9547739	11.7286432	1405.67839	26.8241206
6992	20.9547739	11.7286432	1405.67839	28.4020101
7077	21.1155779	11.7286432	1405.67839	25.2462312
7164	23.3668342	13.1758794	1405.67839	26.8241206
7253	20.9547739	12.2713568	1390.58291	25.2462312
7342	21.1155779	11.7286432	1390.58291	25.2462312
7467	21.2763819	13.718593	1375.48744	25.2462312
7592	20.9547739	13.5376884	1375.48744	25.2462312
7721	20.9547739	11.5477387	1375.48744	28.4020101
7854	21.4371859	11.7286432	1375.48744	29.9798995
7987	21.1155779	12.2713568	1383.03518	29.9798995
8114	21.1155779	11.9095477	1375.48744	31.5577889
8242	20.9547739	11.7286432	1383.03518	33.1356784
8370	21.1155779	11.5477387	1375.48744	33.1356784
8498	20.9547739	11.3668342	1383.03518	41.0251256
8626	20.9547739	11.1859296	1383.03518	50.4924623

8729	20.9547739	11.0050251	1375.48744	48.9145729
8831	21.1155779	11.5477387	1398.13065	39.4472362
8933	20.7939698	10.6432161	1383.03518	53.6482412
9034	20.7939698	10.1005025	1367.9397	53.6482412
9135	20.7939698	10.4623116	1390.58291	28.4020101
9237	20.7939698	10.281407	1383.03518	48.9145729
9339	21.2763819	11.7286432	1390.58291	26.8241206
9438	20.7939698	11.5477387	1383.03518	26.8241206
9534	20.9547739	11.7286432	1390.58291	29.9798995
9631	20.6331658	12.0904523	1405.67839	28.4020101
9727	21.2763819	11.9095477	1398.13065	26.8241206
9823	21.2763819	11.9095477	1383.03518	33.1356784
9919	21.1155779	11.7286432	1398.13065	29.9798995
10015	21.5979899	12.4522613	1383.03518	23.6683417
10110	21.2763819	11.9095477	1390.58291	26.8241206
10214	21.2763819	11.7286432	1405.67839	28.4020101
10317	21.2763819	11.5477387	1390.58291	26.8241206
10419	21.2763819	12.0904523	1390.58291	28.4020101
10519	21.4371859	11.7286432	1383.03518	26.8241206
10620	21.1155779	11.7286432	1405.67839	28.4020101
10725	20.9547739	11.7286432	1390.58291	28.4020101
10829	21.1155779	11.5477387	1405.67839	26.8241206
10929	21.1155779	11.5477387	1405.67839	26.8241206
11023	21.2763819	12.0904523	1405.67839	26.8241206
11116	21.1155779	11.3668342	1383.03518	31.5577889
11213	21.2763819	11.9095477	1398.13065	25.2462312
11358	21.1155779	11.5477387	1383.03518	31.5577889
11407	21.5979899	12.2713568	1383.03518	28.4020101
11505	21.1155779	11.5477387	1398.13065	28.4020101
11767	21.1155779	11.5477387	1398.13065	25.2462312
11930	21.2763819	11.9095477	1405.67839	26.8241206
12060	20.9547739	11.3668342	1398.13065	29.9798995
12254	21.2763819	11.7286432	1398.13065	26.8241206
12308	21.2763819	11.5477387	1398.13065	26.8241206
12416	21.2763819	12.0904523	1398.13065	18.9346734
12471	21.2763819	11.7286432	1420.77387	25.2462312
12498	21.2763819	11.7286432	1428.32161	25.2462312
12526	21.2763819	11.7286432	1420.77387	18.9346734
12579	20.9547739	11.9095477	1443.41709	20.5125628
12633	21.2763819	11.7286432	1450.96482	20.5125628
12689	21.2763819	12.0904523	1420.77387	25.2462312
12748	21.2763819	11.9095477	1413.22613	25.2462312
12807	21.2763819	11.7286432	1435.86935	26.8241206
12870	20.9547739	11.1859296	1413.22613	23.6683417
12934	21.2763819	11.9095477	1428.32161	18.9346734
12997	21.5979899	12.6331658	1420.77387	18.9346734
13061	21.2763819	11.5477387	1413.22613	25.2462312
13125	21.2763819	11.7286432	1458.51256	23.6683417
13189	21.2763819	11.7286432	1398.13065	28.4020101
13253	21.2763819	11.5477387	1375.48744	28.4020101
13333	21.2763819	11.7286432	1398.13065	18.9346734
13429	21.2763819	11.5477387	1428.32161	20.5125628
13524	21.2763819	11.5477387	1398.13065	26.8241206
13618	21.2763819	11.7286432	1413.22613	23.6683417
13711	21.4371859	12.4522613	1405.67839	25.2462312
13809	21.1155779	11.7286432	1413.22613	25.2462312
13910	21.1155779	11.5477387	1413.22613	25.2462312
14011	21.1155779	11.5477387	1413.22613	25.2462312
14112	21.2763819	11.7286432	1398.13065	28.4020101
14213	21.1155779	11.5477387	1405.67839	25.2462312
14311	21.4371859	11.9095477	1390.58291	26.8241206
14408	21.2763819	11.7286432	1390.58291	28.4020101
14505	21.4371859	11.9095477	1420.77387	25.2462312
14609	21.2763819	11.7286432	1405.67839	25.2462312
14713	21.2763819	11.5477387	1390.58291	26.8241206
14816	21.2763819	11.7286432	1390.58291	28.4020101

Figures

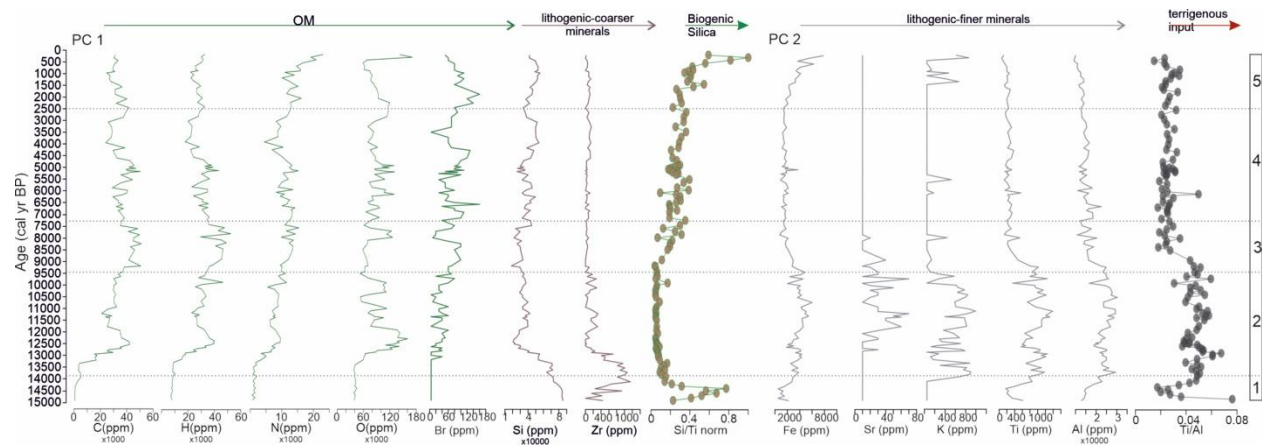


Fig. S. 1. Diagram showing the selected trace elements for the components PC1 (C,H,N,O, Br, Si, Zr) and additional Si/Ti ratio, and PC2 (Fe, Sr, K, Ti, Al) with additional Ti/Al ratio. The scale of age (cal yr BP) in the left side and defined pollen zones on the right side (dark dotted line represent the duration of pollen zones).

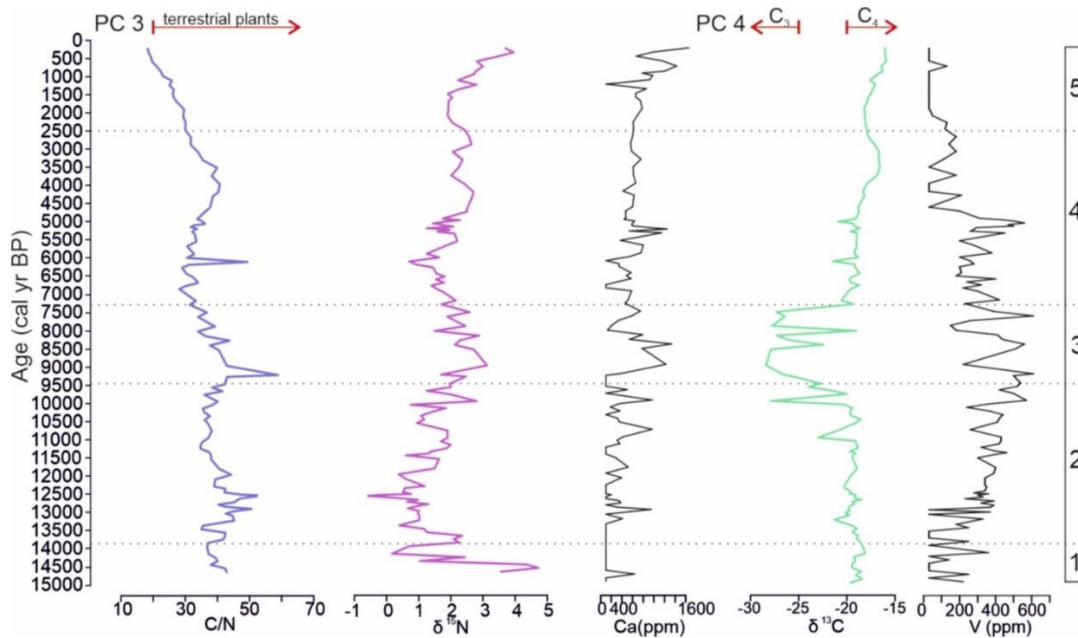


Fig. S. 2. Diagram showing the elements and isotopes selected for PC3 (C/N ratio, $\delta^{15}\text{N}$ and Ca) and PC4 ($\delta^{13}\text{C}$ and V). Curves are represented in a scale of age (cal yr BP) on the left side and accompanied by the pollen zones on the right side (dark dotted line represent the duration of pollen zones).

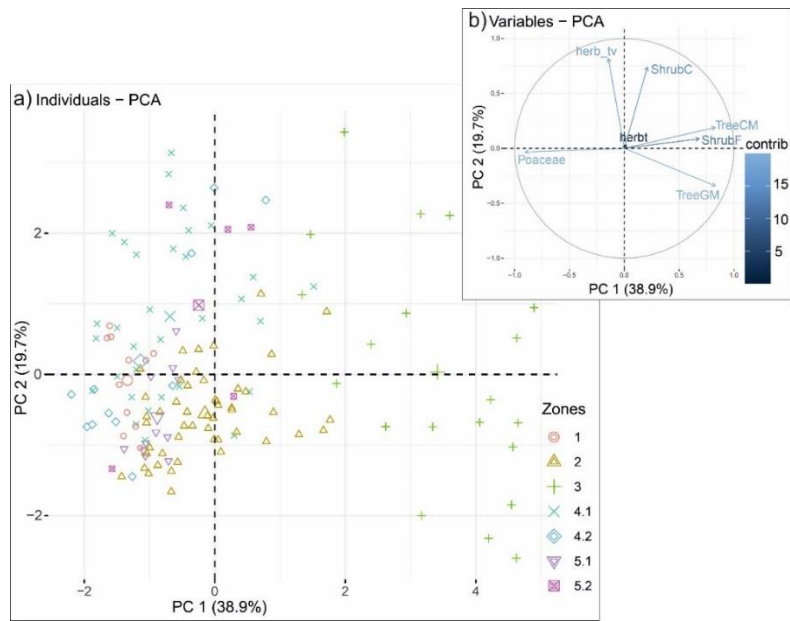


Fig. S.3. a) PCA showing temporal variability (Zones) in response to ecological groups representing the 1 and 2 components. b) ecological groups from 1 and 2 component, with their percentage of significance (intensity of blue color).

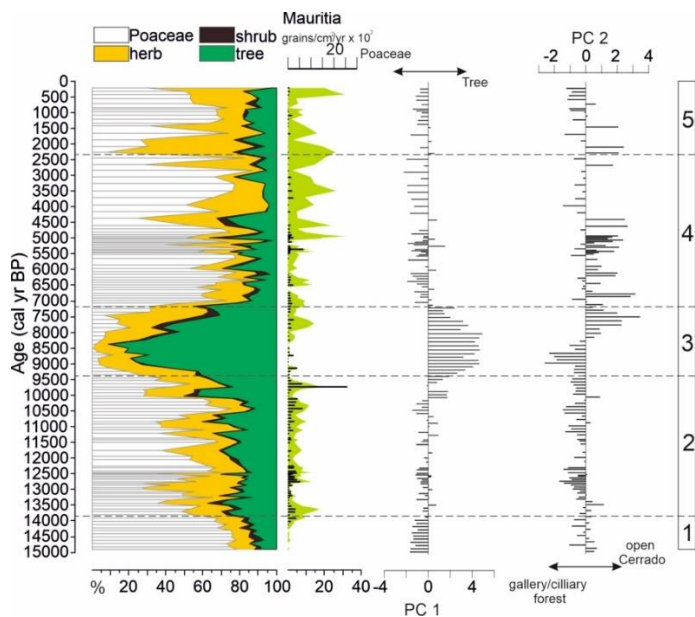


Figure S.4. From left to right, the Age (cal yr BP), a summarized diagram of total pollen taxa respect to their growth forms (%), accompanied with the % (colored curve) and PAR (black bars) of *Mauritia*, the results of PC1 and PC2 of the ecological groups and the pollen zones.

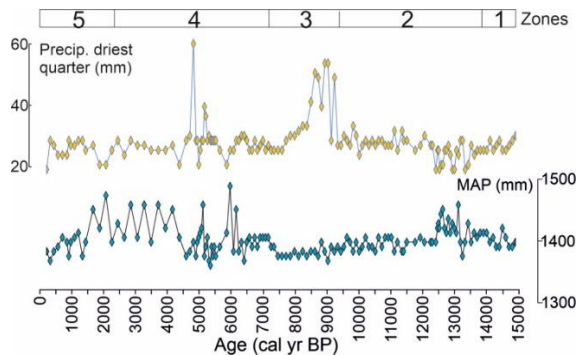


Fig. S5. Mean annual precipitation and precipitation during the driest quarter for VGE-17 core, reconstruction based on pollen taxa probability density function (Chevalier, 2022).

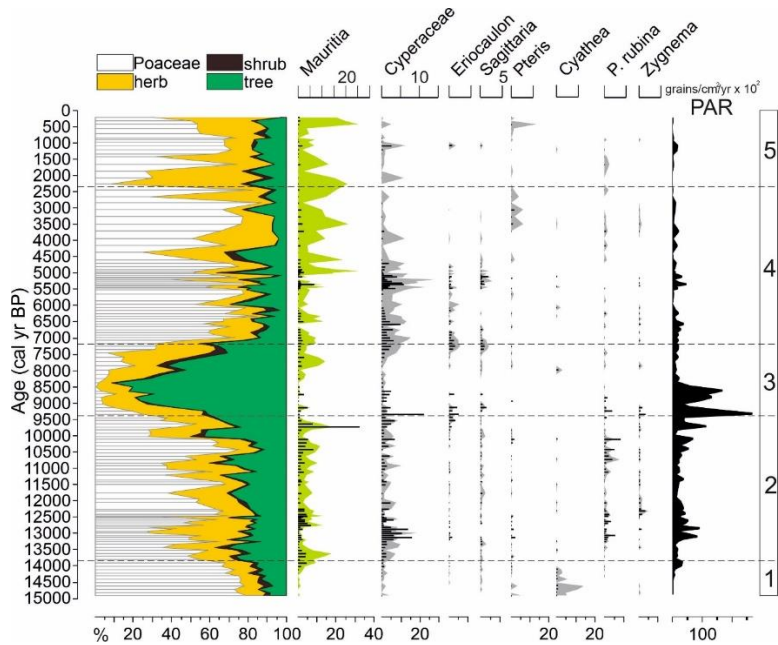


Figure S. 6. From left to right, the Age (cal yr BP), a summarized diagram of total pollen taxa respect to their growth forms (%), accompanied with the % (colored curve) and PAR (black bars) of *Mauritia*, *Cyperaceae*, water-level related pollen taxa (*Eriocaulon*, *Sagittaria*), *Pteris* and *Cyathea* ferns, and Algae (*Pseudoschizaea rubina* and *Zygnuma*), the total PAR of terrestrial pollen and the pollen zones.

Partie III

Synthèse des résultats, conclusions et perspectives

1. Synthèse

Au cours de nos travaux, l'analyse multi-proxy, axée principalement sur le pollen et les particules de charbon et complétée par les mesures des isotopes stables et des éléments traces dans deux profils sédimentaires, nous a permis de reconstruire l'histoire du paysage sur les hauts plateaux du Brésil central. L'**article 1** constitue une application de nos analyses écologiques des taxa polliniques, laissant percevoir une nouvelle voie de recherche sur les changements de traits fonctionnels liés aux grains de pollen. Après, notre analyse palynologique a notamment permis d'accéder à une meilleure compréhension spatio-temporelle des schémas généraux de végétation dans les zones centrales du Cerrado, d'une part entre la dernière période glaciaire et l'interglaciaire, et d'autre part en fonction de la latitude. En effet, la relation végétation-climat et le rôle des incendies (naturels ou anthropiques) ont été étudiés d'un point de vue phytocentrique ce qui nous permet de préciser les zones bioclimatiques à l'intérieur du biome Cerrado. Les résultats obtenus dans les **articles 2** et **3** forment les principaux contributeurs qui nous ont permis d'explorer les objectifs que nous avions définis dans la partie **1**.

L'**article 1**, détaille l'écologie et la physionomie des taxons de pollen que nous avons déterminés dans les deux enregistrements précédents. Notre recherche est axée sur le dépôt de pollen et discute les différents facteurs qui peuvent l'influencer. L'étude souligne que, bien que la dispersion soit principalement biotique (principalement par les insectes), elle ne réduit pas la possibilité d'une dispersion locale et régionale du pollen avec la majorité des grains de pollen déposés présentant des tailles moyennes ou petites (inférieures à 25 µm). Les implications relatives à la strate de végétation et à l'environnement de dépôt (caractéristiques intrinsèques et extrinsèques du système) sont également discutées et sont marqués comme essentielles et à prendre en compte avant les interprétations des résultats des analyses palynologiques et ses implications pour le climat. Par exemple comment à partir du dépôt des grains de pollen il est possible de déduire les caractéristiques de l'environnement ainsi que le lien entre l'augmentation de la taille du pollen et la précipitation que nous avons mis en évidence.

L'**article 2** montre 6000 ans de l'évolution du Cerrado central, en différenciant les variations centennales et décennales grâce à une sédimentation continue et à la haute résolution de nos analyses. Pour la première fois, nos résultats montrent que, il y a environ 5000 ans, le Cerrado central s'est transformé à partir d'une formation ouverte dominée par les graminées vers une formation forestière. Cet enregistrement met aussi en évidence deux faits importants concernant la végétation du Cerrado. Tout d'abord, si le Cerrado est présent en continu pendant toute cette période, montrant ainsi sa résilience à la variation de l'humidité, la composition et la distribution de la végétation se sont modifiées et se sont restructurées en fonction de la disponibilité de l'eau (par exemple le cas de la forêt-galerie). Plus précisément, trois périodes de sécheresse (3340-2760, 2070-1690 et 1330-1150 cal ans BP) marquées par une baisse du niveau du lac ont été identifiées, caractérisées par le changement de structure de la forêt-galerie et les modifications des taxons aquatiques. Deuxièmement, si la présence d'incendies est constante sur la région centrale du Cerrado, fréquence des feux reste très faible, sauf à deux reprises où la végétation du Cerrado semble plus affectée. Cette augmentation des incendies semble due principalement à des facteurs climatiques.

L'**article 3** présente l'évolution du Cerrado au cours des 15 000 dernières années à partir d'une étude localisée environ 500 km plus au nord que l'enregistrement précédent (**article 1**), ce qui nous permet d'analyser les réponses du Cerrado le long d'un transect latitudinal en comparant nos résultats à ceux obtenus sur d'autres enregistrements au nord et au sud de notre site et couvrant le même intervalle de temps. Ce nouveau site d'étude se trouve dans une région inexplorée d'un point de vue de la paléoécologie, où la végétation du cerrado est principalement ouverte, dominée par les graminées et quelques arbres éparses. Cet enregistrement, qui repose sur une approche multi-proxy, montre des états de la végétation et des changements dans la composition du sol détectés à partir des éléments traces et des isotopes stables reliés à des changements locaux et régionaux entre la fin de la période glaciaire (fin du Pléistocène) et l'interglaciaire actuel (Holocène). La végétation arborée (le cerrado et la forêt-galerie) est plus sensible aux perturbations que la végétation herbacée. Nos résultats montrent des changements radicaux dans la composition de la végétation au début de l'Holocène avec l'expansion d'assemblages de taxons humides et froids qui sont rarement rencontrés dans la flore du Cerrado aujourd'hui. Cette période correspond à la succession de deux refroidissements successifs dans l'hémisphère nord, à 9,3 et à 8,2 ka BP qui ont entraîné un refroidissement et une augmentation de l'humidité sur les latitudes tropicales. C'est la première fois que ces événements sont observés de façon détaillée sur les latitudes tropicales ce qui devrait permettre de préciser les modèles de prévision climatique actuelle. En effet, la situation de relargage massif d'icebergs et de fonte de la glace polaire est similaire à celle que nous observons aujourd'hui. L'intensité des incendies est très faible pendant cette période avec quelques particules de charbon probablement transportées dans l'atmosphère depuis des points éloignés de notre site d'étude ce qui nous permet également de réviser le lien entre les Cerrados et les incendies, qui s'ils sont constants, restent faibles et ne se distinguent pas des autres biomes.

2. Conclusion et perspectives

Nos deux enregistrements, le lac Feia et le marais de Getulio, ont montré une grande variabilité temporelle de la composition floristique du Cerrado, allant de la dominance d'une végétation ouverte vers un paysage plus arboré, avec la succession de taxons indicateurs de milieux secs (*Astronium*, *Byrsonima*, *Caryocar*, *Casearia*) ou de milieux humides (*Hedyosmum*, *Ilex*, Moraceae-Urticaceae, Myrtaceae, Melastomataceae-Combretaceae). Ces changements sont liés aux variations spatiales de l'amplitude et de l'intensité de la mousson sud-américaine (SAMS - *South American Monsoon System*), elles-même modulées par les différents gradients interhémisphériques (pole-equateur-pole) observés depuis la fin de la dernière glaciation (Wainer et al., 2021 ; Cheng et al., 2020).

Ainsi, à la fin du dernier glaciaire et au début de l'Holocène le paysage était formé de prairies à graminées avec l'expansion des arbres adaptés aux environnements plus froids (par exemple *Hedyosmum*). Puis, au cours de l'Holocène moyen et récent, le paysage de la région de la Serra Geral do Tocantins, où se trouve le marais de Getulio (10°S), devient plus ouvert avec la présence de forêts-galeries. Parallèlement, dans la région du lac Feia (15°S), est observée l'expansion de la savane arborée et des forêts-galeries. À partir de ~7000 cal ans BP, les deux régions commencent à évoluer différemment avec une barrière géographique située entre 10° et 15° de latitude qui

devient plus marquée après ~5000 cal ans AP. Des études paléoclimatiques ont montré qu'au cours de l'Holocène, en Amérique du Sud tropicale, l'insolation estivale devient l'un des principaux moteurs du changement climatique, accompagné par l'influence d'événements froids à courte échelle provenant de l'hémisphère Nord (Stríkis et al., 2011 ; Deininger et al., 2019), avec une plus grande variabilité spatiale des précipitations se développant, principalement à partir des 5 000 dernières années (Cruz et al., 2009 ; Wang et al., 2017 ; Deininger et al., 2019). Lorsque le nord-est devient sec (Utida et al., 2020) plus au sud- sudouest, la mousson sud-américaine s'intensifie avec une convection humide croissante en provenance de l'Amazonie (Wong et al., 2021). Ainsi, notre étude souligne que le Cerrado pouvait être aussi bien représenté par des physionomies plus froides dont l'analogie actuel serait les prairies d'altitude observées au-dessus de 1200 m que des physionomies caractéristiques de milieux plus chauds ou plus humides, comme les forêts-galeries ou le cerrado arboré (*cerradão* en portugais). De ce fait, la forte variabilité spatiale du climat observée dans le Brésil central depuis la fin du Pléistocène sur des échelles séculaire à millénaire (Strikis et al. 2015; Cassino et al. 2020; cette étude) met en jeu toutes les physionomies qui se succèdent les unes aux autres, de cerrado arboré à prairie, sans atteindre la structure du biome. Par conséquent, l'on peut dire que le Cerrado est peu vulnérable aux changements climatiques et montre une forte capacité d'adaptation et de résilience aux perturbations naturelles.

D'autre part, nos résultats montrent que l'intensité des feux (CHARa) est restée très faible sur les deux sites d'étude distants de ~800 km si l'on excepte les deux pics observés au lac Feia probablement due aux activités humaines sur le pourtour du lac. De manière générale, les incendies sont observés sur des intervalles de 30 ans environ, et lorsqu'ils se produisent plus fréquemment, le temps de récupération de la végétation est de 12 ans environ. Ainsi, au cours de l'Holocène, et plus particulièrement sur les 5000 dernières années, les incendies sont plus faibles que ceux qui sont observés, depuis les derniers siècles (Schmidth et Eloy, 2020) et n'affectent pas la biodiversité du Cerrado.

Toutefois, notre étude a aussi montré que si les incendies sont enregistrés de manière continue pendant 30 ans, alors la composition floristique du Cerrado sera modifiée avec une reduction de la diversité et une changement à des espèces pionnières, et qu'une durée similaire sera nécessaire pour revenir à la composition initiale démontrant ainsi sa résilience aux feux. Aujourd'hui, dans la station écologique du Tocantins (EESGT), les incendies sont provoqués de façon régulière sur des courtes durées par les gardes-forestiers afin de maintenir l'hétérogénéité du paysage et sa pyrodiversité (Barradas et Ribeiro, 2021).

Le Cerrado est un biome très ancien (Simon et al., 2009) qui se maintient grâce à sa très forte capacité d'adaptation aux forces externes tels que le climat ou les incendies (Anjos et Toledo, 1028 ; Neves et al., 2020). Aujourd'hui, le Cerrado est gravement affecté par les brûlis associés à l'expansion démographique et aux surfaces destinées à l'agriculture et à l'élevage (Klink et al., 2022). D'autre part, avec le réchauffement en cours, les modèles de végétation (Hoffman et al., 2009 ; Alves-Ferreira et al., 2022) montrent que la biodiversité du Cerrado risque d'être fortement touchée, en particulier les espèces fragiles qui se trouvent dans les prairies d'altitude (Overbeck et al 2022). En effet, si une ou plusieurs de ces phytophysionomies qui abritent la grande biodiversité du Cerrado disparaissaient, le Cerrado risquerait d'être atteint de façon irréversible.

D'autre part, il serait nécessaire d'étendre les études paléoécologiques vers des régions où l'occupation du Cerrado par les Amérindiens est ancienne, en lien avec des recherches archéologiques, afin de préciser la relation entre la fréquence et l'intensité des incendies et l'activité humaine. Enfin, pour une meilleure compréhension de la dynamique globale du biome Cerrado, il serait également intéressant d'améliorer notre compréhension du mode de dépôt des particules de charbon dans les sédiments et de comparer l'histoire et l'évolution des incendies dans les savanes américaines et dans les savanes africaines.

Références

- Ab'Saber, A. N. 2003. Os domínios de natureza no Brasil: Potencialidades paisajísticas. São Paulo, Brazil: Ateliê Editorial.
- Aguiar W, Meissner KJ, Montenegro A, Prado L, Wainer I, Carlson AE, Mata MM. 2021. Magnitude of the 8.2 ka event freshwater forcing based on stable isotope modelling and comparison to future Greenland meting. *Scientific Reports*, **11**, 5473.
- Aguiar, W., Prado, L.F., Wainer, I., Liu, Z., Montenegro, A., Meissner, K.J., Mata, M.M., 2020. Freshwater forcing control on early-Holocene South American monsoon. *Quaternary Science Review*, **245**, 106498.
- Aleman JC, Blarquez O, Bentaleb I, et al. 2013. Tracking land-cover changes with sedimentary charcoal in the Afrotropics. *The Holocene*, **23**, 1853 – 1862.
- Alvares, C.A., Stape, J.L., Sentelhas, P.C., Gonçalves, J.L.M., Sparovek, G., 2013. Köppen's climate classification map for Brazil. *Meteorol. Z.*, **22** (6), 711-728.
- Alves-Ferreira G, Giné GAF, Fortunato DS, Solé M, Heming NM. 2022. Projected responses of Cerrado anurans to climate change are mediated by biogeographic character. *Perspectives in Ecology and Conservation*, **20**: 126-131.
- Amaral AG, Munhoz CBR, Walter BMT, Aguirre-Gutierrez J, Raes N. 2017. Richness pattern and phytogeography of the Cerrado herb-shrub flora and implication for conservation. *Journal of Vegetation Science*, **28**, 848-858.
- Anjos LJS, Toledo PM. 2018. Measuring resilience and assessing vulnerability of terrestrial ecosystems to climate change in South America. *PlosONE*, 13(3): e0194654
- Antar GM, Sano PT. 2019. Angiosperms of dry grasslands and savannahs of Jalapão the largest conserved Cerrado area in Brazil. *Rodriguésia*, **70**, e04002017
- Antonio-Dominguez H, Corrêa AMS, Queiroz RT, Bitar, NAB. Pollen morphology of some Fabaceae species from Patos de Minas, Minas Gerais State, Brazil. *Hoehnea*, **45**, 103-11.
- Aranibar JN, Anderson IC, Epstein HE, Feral CJW, Swap RJ, Ramontsho J, Macko SA. Nitrogen isotope composition of soils, C₃ and C₄ plants along land use gradients in southern Africa. *Journal of arid environments*, **72**, 326-337.
- Araujo AGM, Neves WA, Piló LB, Atui JPV. 2005. Holocene dryness and human occupation in Brazil during the “Archaic Gap”. *Quaternary Research*, **64**: 298 – 307.
- Araujo GM, Barbosa AAA, Arantes AA, Amaral AF. 2002. Composição florística de veredas no Município de Uberlândia, MG. *Revista Brasil. Bot.*, **25**(4), 475-493.
- Assad ED, Sano EE, Masutono R, Castro LHR, da Silva FAM. 1993. Dry spells in the Brazilian “Cerrados” region/ frequency and probability of occurrence. *Pesq. Agrop. Brasi.*, **28**(9): 993 – 1003.
- Azevedo V, Stríkis NM, Novello VF, Roland CL, Cruz FW, Santos RV, Vuille M, Utida G, de Andrade FRD, Cheng H, Edwwards RL. 2021. Paleovegetation seesaw in Brazil since the Late Pleistocene: A multiproxy study of two biomes. *Earth and Planetary Sciences Letters*, **563**, 116880.
- Azevedo V, Stríkis NM, Santos RA, Souza JG, Ampuero A, Cruz FW, Oliveira P, Iriarte J, Stumpf CF, Vuille M, Mendes VR, Cheng H, Edwards L. 2019. Medieval climate variability in the eastern Amazon-Cerrado regions and its archeological implications. *Nature*, **9**, 20306.
- Badgley JA, Steig EJ, Hakim GJ, Fudge TJ. 2020. Greenland temperature and precipitation over the last 20,000 years using data assimilation. *Climate of the Past*, **16**, 1325-1346.
- Barberi M, Salgado-Labouriau ML, Sugio K. 2000. Paleovegetation and paleoclimate of “Vereda de Águas Emendadas”, central Brazil. *Journal of South American Earth Sciences*, **13**, 241-254.

- Barbosa JB, Afonso MC, Rubin JC. 2020. Estudio micromofologico en ditios alfareros Uru de la cuenca del rio Araguaia, Goiás, Brasil. *Boletin de Arqueología PUCP*, **28**, 31-52.
- Barradas AC, Ribeiro KT. 2021. Integrated Fire Management: Serra Geral do Tocantins Ecological Station's Journey (2001 to 2020). *Biodiversidade Brasileira*, **11**(2), 139-152.
- Becker RA, Chambers JM, Wilks AR. 1988. The New S Language. Wadsworth & Brooks/Cole.
- Behling, H. 2002. Late Quaternary vegetation and climate dynamics in southern Amazonia inferred from Lagoa da Confusão in Tocantins state, northern Brazil. *Amazoniana*, **17** (1/2), 27-39.
- Bennett K. 1996. Determination of the number of zones in a biostratigraphic sequence. *New Phytologist*, **132**, 155-170.
- Bernal JP, Cruz FW, Stríkis NM, Wang X, Deininger M, Catunda MCA, Ortega-Obregón C, Cheng H, Edwards RL, Auler AS. 2016. High-resolution Holocene South American monsoon history recorded by a speleothem from Botuverá Cave, Brazil. *Earth and Planetary Science Letters*, **450**, 186-196.
- Berrio, J.C., Hooghiemstra, H., Behling, H., Van der Borg, K., 2000, Late Holocene history of savanna gallery forest from Carimagua area, Colombia. *Review of Palaeobotany and Palynology*, **111**, 295-308. doi.org/10.1016/S0034-6667(00)00030-0.
- Blaauw M, Christen JA. 2011. Flexible paleoclimate age-depth models using an autoregressive gamma process. *Bayesian Anal.*, **6**, 457-474. doi: 10.1214/11-BA618.
- Bouimetarhan I, Chiessi CM, González-Arango LD, Voigt I, Prange M, Zonneveld K. 2018. Intermittent development of forest corridors in northeastern Brazil during the last deglaciation: Climatic and ecologic evidence. *Quaternary Science Review*, **192**, 86-96.
- Bremond L, Muller S, Rouland S, Favier C. 2018. ISEM reference palynological database. OSU OREME. (Collection). [accessed 2023 February 23]. <https://data.oreme.org/observation/pollen>
- Bridgewater S, Ratter JA, Ribeiro JF. 2004. Biogeographic patterns, β -diversity and dominance in the cerrado biome of Brazil. *Biodiversity and Conservation*, **13**, 2295 – 2318.
- Brotto ML. 2022. Aquifoliaceae no estado do Paraná, Brasil. *Hoehnea*, **49**, e072021.
- Bueno ML, Dexter KG, Pennington RT, Pontara V, Neves DM, Ratter JA, Oliveira-Filho AT. 2018. The environmental triangle of the Cerrado domain: Ecological factors driving shifts in tree species composition between forest and savannas. *Journal of Ecology*, **106**(5), 2109-2120.
- Bueno ML, Pennington RT, Dexter KG, Kamino LHY, Pontara V, Neves DM, Ratter JA, Oliveira-Filho AT. 2017. Effects of Quaternary climatic fluctuations on the distributions of Neotropical savanna tree species. *Ecography*, **40**, 403-414.
- Bueno, L., Isnardis, A., 2018. Peopling Central Brazilian Plateau at the onset of the Holocene: Building territorial histories. *Quaternary International*, **473**, 144 – 160.
- Bush MB, Weng C. 2007. Introducing a new (freeware) tool for palynology. *Journal of Biogeography*, **34**, 377-380.
- Campos JLPS, Cruz FW, Ambrizzi T, Deininger M, Vuille M, Novello VF, Stríkis NM. 2019. Coherent South American Monsoon Variability During the Last Millennium Revealed Through High-Resolution Proxy Records. *Geophysical Research Letters*, **46**, 8261-8270.
- Campos MC, Chiessi CM, Novello VF, Crivellari S, Campos JLPS., Albuquerque ALS, Venancio IM, Santos TP, Melo DB, Cruz FW, Sawakuchi AO, Mendes VR. 2022. South American

- precipitation dipole forced by interhemispheric temperature gradient. *Scientific Report*, **12**, 10527.
- Carmignotto AP, Pardini R, Vivo M. 2022. Habitat heterogeneity and geographical location as major drivers of Cerrado small mammal diversity across multiple spatial scales. *Frontier in Ecology and Evolution*, **9**: 739919.
- Cassino RF, Ledru M-P. 2021. Quantitative reconstruction of vegetation cover from modern pollen rain in the Cerrado biome of Brazil. *Paleogeography, Palaeoclimatology, Palaeoecology*, **547**, 110462.
- Cassino RF, Martinho CT, Caminha SAF. 2015. Modern pollen spectra of the Cerrado vegetation in two national parks of Central Brazil, and implications for interpreting fossil pollen records. *Review of Palaeobotany and Palynology*, **223**: 71 – 86.
- Cassino RF, Martinho CT, Caminha SA. 2018. A Late Quaternary palynological record of a palm swamp in the Cerrado of central Brazil interpreted using modern analog data. *Paleogeography, Palaeoclimatology, Palaeoecology*, **490**, 1-16.
- Cassino RF, Meyer KEB. 2011. Morfologia de grãos de pólen e esporos de níveis holocênicos de uma vereda do Chapadão dos Gerais (Buritizeiro, Minas Gerais), Brasil. *Gaea*, **7**, 41-70.
- Cassino, R.F. and Meyer, K.E.B. 2013. Reconstituição paleoambiental do Chapada dos Gerais (Quaternário tardio) a partir da análise palinológica da vereda Laçador, Minas Gerais, Brasil. *Revista Brasileira de Paleontologia*, **16**(1): 127-146.
- Cassino, R.F., Ledru, M-P., de Almeida Santos, R., Favier, C. 2020. Vegetation and fire variability in the central Cerrados (Brazil) during the Pleistocene-Holocene transition was influenced by oscillations in the SASM boundary belt. *Quaternary Science Reviews*, **232**, 106209.
- Castro AAJF and Martins FR. 1999. Cerrados de Brasil e do Nordeste: caracterização, área de ocupação e considerações sobre a sua fitodiversidade. *PEsq; Foco, São Luis*, **7**, 147 – 178.
- Chamber JC, Allen CR, Cushman SA. 2019. Operationalizing ecological resilience concepts for managing species and ecosystems at risk. *Frontiers in Ecology and Evolution*, **7**, 241.
- Cheng H, Fleitmann D, Edwards LR, Wang X, Cruz FW, Auler AS, Mangini A, Wang Y, Kong X, Burns SJ, Matter A. 2009. Timing and structure of the 8.2 kyr B.P. event inferred from $\delta^{18}\text{O}$ records of stalagmites from China, Oman, and Brazil. *Geology*, **37**, 1007–1010.
- Cheng H, Zhang H, Spötl C, Baker J, et al., 2020. Timing and structure of the Younger Dryas event and its underlying climate dynamics, *PNAS*, **117**, 23408-23417.
- Chevalier, M., 2022, crestr: an R package to perform probabilistic climate reconstructions from palaeoecological datasets, *Climate of the Past*, **18**(4), pp. 821-844, doi:10.5194/cp-18-821-2022
- Colinvaux P, De Oliveira PE, Moreno JE. 1999. Amazon pollen manual and atlas. Amsterdam: Harwood Academic Publishers.
- Colli GR, Vieira CR, Dianese JC. 2020. Biodiversity and conservation of the Cerrado: recent advances and old challenges. *Biodiversity and Conservation*, **29**, 1465-1475.
- Conedera M, Tinner W, Neff C, Meurer M, Dickens AF, Krebs P. 2009. Reconstructing past fire regimes: methods, applications, and relevance to fire management and conservation. *Quat. Sci. Rev.*, **28**, 555-576. <https://doi.org/10.1016/j.quascirev.2008.11.005>.
- Costa CR, da Luz CFP, Horák-Terra I, Camargo PB, Barral UM, Mendoça-Filho CV, Gonçalves TS, Silva AC. 2022. Paleoenvironmental dynamics in central-eastern Brazil during the last 23000 years: Tropical peatland records in the Cerrado biome. *Jounral of Quaternary Science*, **38**, 61-75.

- Coutinho JMCP, Jardim MAG, Castro AAJF, Costa Neto SV, Viana Junior AB. 2021. Environmental drivers organize Wood plant assemblages across a Cerrado vegetation mosaic in Northern Brazil. *Nature and Conservation*, **14**: 1-21.
- Cruz F, Vuille M, Burns S., et al. 2009 Orbitally driven east–west antiphasing of South American precipitation. *Nature Geosci*, **2**, 210–214; doi: 10.1038/ngeo444
- Cruz Jr. FW, et al. 2005. Insolation-driven changes in atmospheric circulation over the past 116,000 years in subtropical Brazil. *Nature*, **434**, 63e66. <https://doi.org/10.1038/nature03365>.
- Custodio IS, Dias PLS, Wainer I, Prado LF. 2022. Changes in the South American Monsoon System since the last Glacial Maximum. *Climate Dynamics*, <https://doi.org/10.21203/rs.3.rs-2106177/v1>
- Cuven S, Francus P, Lamoureux SF. 2010. Estimation of grain size variability with micro X-ray fluorescence in laminated lacustrine sediments, Cape Bounty, Canadian high Artic. *J. Paleolimnol.*, **44** (3): 803 – 817.
- Darien M, Fidelis, A. 2021. How does fire affect germination of grasses in the Cerrado?. *Science Research*, 1 – 9. <https://doi.org/10.1017/S0960258520000094>
- Davies SJ, Lamb HF, Roberts SJ. 2015. Micro-XRF core scanning in Palaeolimnology : recent developments. In: Croudace, I.W. & Rothwell, R.G. (eds.). *MICROXRF studies of sediment cores, developments in Paleoenvironmental research*, 189-225. Cambridge, UK.
- Deininger M, Ward BM, Novello VF, Cruz FW. 2019. Late Quaternary Variations in the South American Monsoon System as Inferred by Speleothems—New Perspectives Using the SISAL Database. *Quaternary*, **2**, 6. doi: [10.3390/quat2010006](https://doi.org/10.3390/quat2010006)
- Duffin KI, Gillson L, Willis KJ. 2008. Testing the sensitivity of charcoal as an indicator of fire events in savanna environments: quantitative predictions of fire proximity, area and intensity. *The Holocene*, **18**, 279 – 291.
- Durigan G, Munhoz, CB, Zakia, MJB, Oliveira RS, Pilon NA, do Valle RST, Walter BMT, Honda EA, Pott A. 2022. Cerrado wetlands: multiple ecosystems deserving legal protection as a unique and irreplaceable treasure. *Perspectives in ecology and conservation*, **20** (3), 185-196.
- Durigan, G, Pilon N, Souza FM, Melo ACG, Ré DS, Souza SCPM. 2022a. Low-intensity cattle grazing is better than cattle exclusion to drive secondary savannas toward the features of native Cerrado vegetation. *Biotropica*, **53**(3), 789-800.
- Edwards EJ, Osborne CP, Strömberg CAE, Smith SA, et al. 2010. The Origins of C₄ grasslands: Integrating evolutionary and ecosystem science. *Science*, **283**: 587-591
- Eiten G. 1978. Delimitation of the Cerrado concept. *Vegetatio*, **36**(3):169-178.
- Ejsmond MJ, Ejsmond A, Banasiak K, Karpinska-Kolaczek M, Kozlowski J, Kolaczek P. 2015. Large pollen at high temperature: an adaptation to increased competition on the stigma?. *Plant Ecology*, **216**, 1407-1417.
- Ejsmond MJ, Wronska-Pilarek D, Ejsmond A, Dragosz-Kluska D, Karpinska-Kolaczek M, Kolaczek P, Kozlowski J. 2011. Does climate affect pollen morphology? Optimal size and shape of pollen grains under various desiccation intensity. *Ecosphere*, **2**, 1-15.
- Eriksson, L., Johansson, E., Kettaneh-Wold, N., et al., 1999. Introduction to Multi- and Megavariate Data Analysis Using Projection Methods (PCA & PLS). Umea: Umetrics.

Escobar-Torrez K, Ledru M-P, Cassino RF, Bianchini PR, Yokoyama E. 2023a. Long- and short vegetation change and inferred climate dynamics and anthropogenic activity in central Cerrado during the Holocene. *Quaternary Science Review*.

Escobar-Torrez K, Ledru M-P, Cassino RF, Horák-Terra I, Wainer I, Chevalier M. 2023b. How northern hemispheric ice melting changed the biodiversity of the Cerrado. (*in prep*)

Evaldt AC, Bauermann SG, Fuchs SCB, Diesel S, Cancelli RR. 2009. Grãos de pólen e esporos do Vale do Rio Caí, nordeste do Rio Grande do Sul, Brasil: descrições morfológicas e implicações paleoecológicas. *GAEA*, **5**(2), 86 – 106.

Faegri K, Iversen J. 1989. Textbook of Pollen Analysis. *Hafner*, New York.

Fank-de-Carvalho SM, Somavilla NS, Marchioretto MS, Bão SN. 2015. Plant structure in the Brazilian Neotropical Savannah Species. In: Biodiversity in Ecosystems – linking structure and functions, chapter 16, pages 407-442.

Feidler NC, Merlo DA, Medeiros MB. 2006. Ocorrência de incêndios florestais no parque nacional da chapada dos Veadeiros, Goiás. *Ciência Florestal*, **16**(2): 153-161.

Felfili J.M. 1995. Diversity, structure and dynamics of a gallery forest in central Brazil. *Vegetatio*, **117**, 1-15.

Felfili JM, da Silva Junior M, Mendoça R, Fagg C, Filgueiras T, Mecenas V. 2007. Composição florística da estação ecológica de Aguas Emendadas no Distrito Federal. *Heringiana*, **1**(2), 25–85.

Felfili JM, Nascimento ART, Fagg CW, Meirelles EM. 2007b. Floristic composition and community structure of a seasonally deciduous forest on limestone outcrops in Central Brazil. *Revista Brasileira de Botânica*, **4**, 611–621.

Felfili JM. 1995. Structure and Dynamics of the gallery forest in central Brazil. *Vegetatio*, **117**, 1-15.

Felfili JM. 1997. Dynamics of the natural regeneration in the Gama gallery forest in central Brazil. *Management Forest Ecology and Management*, **91**, 235–245.

Felfili JM. 1997b. Diameter and height distributions in a gallery forest tree community and some of its main species in central Brazil over a six-year period (1985-1991). *Revista Brasileira de Botânica*, **20**(2), 154–162.

Ferraz-Vicentini KR, Salgado-Labouriau ML. 1996, Palynological analysis of palm swamp in Central Brazil. *Journal of South American Earth Sciences*, **9**, 207-219.

Ferraz-Vicentini KR. 1998. História do fogo no Cerrado: uma análise palinológica. Universidade de Brasília, doctoral thesis, 208 pp.

Fick, S.E. and R.J. Hijmans, 2017. WorldClim 2: new 1km spatial resolution climate surfaces for global land areas. *International Journal of Climatology* 37 (12): 4302-4315.

Fidelis A, Alvarado ST, Barradas ACS, Pivello VR. 2018. He year 2017: megafires and management in the Cerrado. *Fire*, **1**, 49.

Fidelis, A., Zirondi, HL., 2021. And after fire, the Cerrado flowers: A review of post-fire flowering in a tropical savanna. *Flora*, **280**, 151849.

Flora do Brasil. 2020. Under construction. Jardim Botânico do Rio de Janeiro. http://floradobrasil.jbrj.gov.br/reflora/florado_brasil/FB128482; accessed march 2023.

Fontes D, Cordeiro RC, Martins GS, Belhing H, Turcq B, Sifeddine A, Seoane JCS, Moreira LS, Rodrigues RA. 2017. Paleoenvironental dynamics in south America, Brazil, during the last 35,000 years inferred from pollen and geochemical records of Lago do Saci. *Quaternary Sciences Review*, **173**, 161 – 180.

Françoso RD, Dexter KG, Machado RB, Pennington RT, Pinto JRR, Brandão RA, Ratter JA. 2019. Delimiting floristic biogeographic districts in the Cerrado and assessing their conservations status. *Biodiversity and Conservation*, **29**, 1477-1500.

Françoso RD, Haidar RF, Machado RB. 2016. Tree species of South America central savanna: endemism, marginal areas and the relationship with other biomes. *Acta Botanica Brasilica*, **30**: 78-86

Francoso, R.D., Brandaõ, R., Nogueira, C.C., Salmona, Y.R., Machado, R.B. Colli, G.R. 2015. Habitat loss and the effectiveness of protected areas in the Cerrado biodiversity hotspot. *Natureza and Conservacao*, **13**, 35 – 40.

Freitas A, Conçalves-Esteves V, MEndoça CBF, Fernández S, Carrión J. 2020. First quaternary brazilian cave pollen record: Morphological descriptions, taxonomic and ecological data. *Revista Brasileira de Paleontologia*, **23**, 32-47.

Freitas L, Sazima M. 2006. Pollination biology in a tropical, high-altitude grassland in Brazil: interactions at the community level. *Ann. Missouri Bot. Gard.*, **93**, 465-516.

Furley PA. 1999. The nature and diversity of neotropical savanna vegetation with particular reference to the Brazilian cerrados. *Global Ecology and Biogeography*, **8**: 223-241.

Furley PA. 2006. Tropical savannas. *Progress in Physical Geography*, **30**: 105-121.

Garreaud RD, Vuille M, Compagnucci R, Marengo J. 2008. Present-day South American climate. Palaeogeography, Pealaecoclimatology, Palaeoecology. doi:10.1016/j.palaeo.2007.10.032
Gatti MG, Campanello PI, Villagra M, Montii I, Goldstein G. 2014. Hydraulic architecture and photoinhibition influence spatial distribution of the arborescent pal Euterpe edulis in subtropical forest. *Tree Physiology*, **34**, 630-639.

Genries A, Finsinger W, Asnong H, Bergeron Y, Carcaillet C, Garneau M, Hély C, Ali AA. 2012. Local versus regional processes: can soil characteristics overcome climate and fire regimes by modifying vegetation trajectories?. *Journal of Quaternary Science*, **27**, 745-756.

Giorgis MA, Zeballos SR, Carbone L, et al. 2021. A review of fire effects across South American ecosystems: the role of climate and time since fire. *Fire Ecology*, **17**: 11.

Glasspool IJ, Scott AC, Waltham D, Pronina N, Shao L. 2015. The impact of fire on the Late Paleozoic Earth system. *Frontiers in Plant Science*, **6**, 756.

- Gorenstein, I., Prado, L.F., Bianchini, P.R., Wainer, I., Griffiths, M.L., Pausata, F.S.R., Yokoyama, E., 2022. A fully calibrated and update mid-Holocene climate reconstruction for Eastern South America. *Quaternary Science Review*, **292**, 107646.
- Gosling WD, Mayle FE, Tate N, Killeen TJ. 2005. Modern pollen-rain characteristics of tall terra firme moist evergreen forest, southern Amazonia. *Quaternary Research*, **64**, 284–297.
- Gosling WD, Mayle FE, Tate NJ, Killeen TJ. 2009. Differentiation between Neotropical rainforest, dry forest, and savannah ecosystems by their modern pollen spectra and implications for the fossil pollen record. *Review of Palaeobotany and Palynology*, **153**, 70–85.
- Gottsberger G, Silberbauer-Gottsberger I. 2018. How are pollination and seed dispersal modes in Cerrados related to stratification? Trends in a Cerrado *sensu stricto* woodland in southeastern Brazil, and a comparison with Neotropical forests. *Acta Botanica Brasilica*, **32**(3), 434 – 445.
- Haug G, Hughen K, Sigman DM, Peterson LC, Röhl U. 2001, Southward migration of the Intertropical Convergence Zone through the Holocene. *Science*, **293**, 1304–1308.
- Henriques RPB. 2005. Influência da história, solo e fogo na distribuição e dinâmica das fitofisionomias no bioma Cerrado. In: Scariot, A. et al. (Orgs). *Cerrado: ecologia, biodiversidade e conservação* (pp. 73-92) Brasília: Ministério do Meio Ambiente..
- Hermanowski B, da Costa ML, Hermann B. 2012. Environmental changes in southern Amazonia during the last 25,000 a revealed from a paleoecological record. *Quaternary Research*, **77**, 138 – 184.
- Hiraota M, Holgren M, Van Nes EH, Scheffer M. 2011. Global resilience of tropical forest and savanna to critical transitions. *Science*, **334**: 232-235.
- Hoffmann WA, Adasme R, Haridasan M, de Carvalho MT, et al. 2009. Tree topkill, not mortality, governs the dynamics of savanna forest boundaries under frequent fire in central Brazil. *Ecology*, **90**, 1326-1337.
- Hofmann GG, Cardoso MF, Alves RJV, Weber EJ, Barbosa AA, Toledo PM, Pontual FB, Salles LO, Hasenack H, Cordeiro JLP, Aquino FE, Oliveira LFB. 2020. The Brazilian Cerrado is becoming hotter and drier. *Global Change Biology*, **27**, 4060– 4073. <https://doi.org/10.1111/gcb.15712>
- Hogg A, Heaton TJ, Hua Q, Palmer JG, Turney CSM, Sounthorpe J, Bayliss A, Blackwell PG, Boswijk G, Ramsey CB, Pearson C, Petchey F, Reimer P, Reimer R, Wacker L. 2020. SHCal20 southern Hemisphere calibration, 0-50,000 Years cal BP. *Radiocarbon*, **62**, 759-778.
- Horák-Terra I, Cortizas AM, Pinto da Luz CF, López PR, Silva AC, Torrado PV. 2015. Holocene climate change in central-eastern Brazil reconstructed using pollen and geochemical records of Pau de Fruta mire (Serra do Espinhaço Meridional, Mina Gerias). *Palaeogeography, Palaeoclimatology, Palaeoecology*, **437**, 117 – 131.
- Horák-Terra I, Martínez Cortizas A, da Luz CFP, Silva AC, Mighall T, Camargo PB, Mendoça-Filho CV, de Oliveira PE, Cruz WF, Vidal-Torrado P. 2020. Late Quaternary vegetation and climate dynamics in central-eastern Brazil: insights from a ~35k cal a BP peat record in the Cerrado biome. *Journal of Quaternary Science*, **35**, 664-676. <https://doi.org/10.1002/jqs.3209>
- Insel N, Poulsen CJ, Ehlers TA. 2010. Influence of the Andes Mountains on South American moisture transport, convection, and precipitation. *Climate Dynamics*, **35**, 1477-1492. doi: 10.1007/s00382-009-0637-1

- Jacobi CM, do Carmo FF. 2011. Life-forms, pollination and seed dispersal syndromes in plant communities in ironstone outcrops, SE Brazil. *Acta Botanica Brasilica*, **25** (2), 395 – 412.
- Jacobson GL, Bradshaw RHW. 1981. The selection of sites for paleovegetational studies. *Quaternary Research*, **16**, 80–96.
- Jardine PE, Lomax BH. 2017. Is pollen size a robust proxy for moisture availability?. Review of *Palaeobotany and Palynology*, **246**, 161-166.
- Jomelli, V., Swingedouw, D., Vuille, M. et al. In-phase millennial-scale glacier changes in the tropics and North Atlantic regions during the Holocene. *Nat Commun*, **13**, 1419 (2022). <https://doi.org/10.1038/s41467-022-28939-9>
- Jones, HAT, Mayle, FE, Pennington RT, Killeen TJ. 2011. Characterisation of Bolivian savanna ecosystems by their modern pollen rain and implication for fossil pollen records. *Review of Palaeobotany and Palynology*, **164**, 223 – 237.
- Juggins S. 2022. *rioja: Analysis of Quaternary Science Data*. R package version 1.0-5, <https://cran.r-project.org/package=rioja>.
- Junior MJAF, Pinto RB, Mansano VF. 2016. A taxonomic revision of the genus *Dialium* (Leguminosae: Dialiinae) in the Neotropics. *Phytotaxa*, **283**(2). Doi: [10.11646/phytotaxa.283.2.2](https://doi.org/10.11646/phytotaxa.283.2.2)
- Klink CA, Sato MN, Cordeiro GG, Ramos MIM. 2020. The role of vegetation on the dynamics of water and fire in the Cerrado ecosystems: implications for management and conservation. *Plants*, **9**, 1803.
- Klink, C.A., Moreira, A.G., 2002. Past and Current Human Occupation and Land Use. In The Cerrados of Brazil; Press, CU: New York, NY, USA, 2002; pp. 69–88.
- Kummel B, Raup D. 1965. Handbook of Paleontological Techniques. W. H. Freeman, San Francisco, CA.
- Laskar J, Fienga A, Gastineau M, Manche H. 2011. La2010: A new orbital solution for the long-term motion of the Earth. *Astron. Astrophys.*, **532**, A89.
- Lê S, Josse J, Husson F., 2008. “FactoMineR: A Package for Multivariate Analysis.” *Journal of Statistical Software*, **25**(1), 1–18. doi:[10.18637/jss.v025.i01](https://doi.org/10.18637/jss.v025.i01).
- Ledru M-P, Araújo FS. (*in press*). 2023. The Cerrado and restinga pathways: two ancient biotic corridors in the neotropics. *Frontiers of Biogeography*. doi:[10.21425/F5FBG59398s](https://doi.org/10.21425/F5FBG59398s)
- Ledru M-P, Ceccantini G, Gouveia SEM, López-Sáez JA, Pessenda LCR, Ribeiro AS. 2006. Millenial-scale climatic and vegetation changes in a northern Cerrado (Northeast, Brazil) since the Last Glacial Maximum. *Quaternary Science Reviews*, **25**, 1110-1126.
- Ledru M-P, Salatino MLF, Ceccantini G, Salatino A, Pinheiro F, Pintaud J-C. 2007. Regional assessment of the impact of climatic change on the distribution of the tropical conifer in the lowlands of South America. *Diversity and Distributions*, **13**, 761 – 771.
- Ledru M-P. 1993. Late Quaternary Environmental and Climatic Changes in Central Brazil. *Quaternary Research*, **39**, 90-98.
- Ledru, M-P. 2002. Late Quaternary History and Evolution of the Cerrados as revealed by Palynological Recods. In : Oliveira (ed.), Marquis R.J. (ed.). The cerrados of Brazil : ecology and natural history of neotropical savanna. New York : Columbia University Press, p. 33-50.

- Ledru, M-P., Salatino, M.L.F., Ceccatini, G., Salaino, A., Pinheiro, F., Pintaud, J-C., 2007. Regional assessment of the impact of climatic change on the distribution of a tropical conifer in the lowlands of South America. *Diversity and Distribution*, **13**, 761 – 771.
- Lehmann CER, Anderson TM, Sankaran M, et al. 2014. Savanna Vegetation-Fire-Climate relationships differ among continents. *Sciences*, **343**, 548-552.
- Lehmann CER, Parr CL. 2016. Tropical grassy biomes: linking ecology, human use and conservation. *Philosophical Transactions B*, **371**: 20160329.
- Lemos HL, Pinto JRR, Mews HA, Lenza, E. 2013. Structure and floristic relationship between Cerrado sensu stricto sites on two types of substrate in northern Cerrado, Brazil. *Biota Neotropical*, **13**, 121-132.
- Leys B, Brewer SC, McConaghy S, Mueller J, McLauchlam KK. 2015. Fire history reconstruction in grassland ecosystems: amount of charcoal reflects local area burned. *Environmental Research Letters*, **10**, 114009.
- Leys B, Commerford JL, McLauchlan KK. 2017. Reconstructing grassland fire history using sedimentary charcoal: Considerin count, size and shape. *PLoS ONE*, **12(4)**, e0176445.
- Li Y, Xu X, Zhao P. 2016. Post-fire dispersal characteristics of charcoal particles in the Daxing'an Mountains of north-east China and their implications for reconstructing past fire activities. *International Journal of Wildland Fire*, **26**(1), 46. doi:10.1071/wf16115
- Lima JFW, da Silva EM, Oliveira-Filho EC, Martins ES, Reatto A, Bufon VB. 2011. The relevance of the Cerrado's water resources to the Brazilian development. *IWRA world water Congress*, Permambuco – Brazil, 11 pag.
- Lima NE, Lima-Ribeiro MS, Tinoco CF, Terribile LC, Collevatti RG. 2014. Phylogeography and ecological niche modelling, coupled with the fossil pollen record, unravel the demographic history of Neotropical swamp palm throught the Quaternary. *Journal of Biogeography*, **41**, 637-686.
- Lima Sabino SM, Cassino RF, Gomes MOS, Sant'Anna EME, Augustin CHRR, de Oliveira DA. 2021. Late Holocene in Central Brazil: vegetation changes and humidity variability in tropical wetland. *Journal of Quaternary Science*, **36**, 1028 – 1039.
- Lira-Martins D, Nascimento DL, Abrahão A, Costa PB, D'Angioli AM, Valézio E, Rowland L, Oliveira RS. 2022. Soil properties and geomorphic processes influence vegetation composition, structure, and function in the Cerrado Domain. *Plant and Soil*, **476**, 549-588.
- Loizeau P-A, Barriera G, Manen J-F, Broennimann O. 2005. Towards an understanding of the distribution of *Ilex* L. (Aquifoliaceae) on a World-wide scale. *Biol. Skr.*, **55**, 501 – 520.
- Lombardo JA. 1996. Five new species of *Cissus* (Vitaceae) from Northern Brazil. *Missouri Botanical Garden Press*, **6**(2), 195-200.
- Longhi-Wagner HM, Welker CAD, Waechter JL. 2012. Floristic affinities in montane grasslands in eastern Brazil. *Systematics and Biodiversity*, **10** (4): 537 - 550.
- Lorente FL and Meyer KEB. 2010. Palinomorfos da vereda da Fazenda Urbano, município de Buritizeiro, Minas Gerais, Brasil. *Heringia*, **65**, 133–169
- Lorente FL, Junior AAB, de Oliveira PE, Pessenda LCR. 2017. Palynological Atlas: 14C Laboratory – CENA/USP. *Piracicaba: FEALQ* – São Paulo, Brazil, 333p.

- Lorente FL, Meyer KEB, Horn AH. 2010. Análise palinológica da vereda da Fazenda Urbano, município de Buritizeiro, Minas Gerais, Brasil. *Geonomos*, **18**(2), 57-72.
- Lorenzi H. 2002. Arvores Brasileiras. In: Instituto Plantarum, nova Odessa, Brazil. 352 pag.
- Marchant JC, Almeida L, Belhing H, et al. 2002. Distribution and ecology of parent taxa of pollen lodged within the Latin American Pollen Database. *Review of Palaeobotany and Palynology*, **121**, 1 – 75.
- Marengo JA, Liebmann B, Grimm AM, Misra V, Silva Dias PL, Cavalcanti, et al. 2012. Recent developments on the South American monsoon system. *International Journal of Climatology*, **32**, 1-21.
- Marengo JA, Soares WR, Saulo C, Nicolini M. 2004. Climatology of the Low-Level Jet East of the Andes as Derived from the NCEP–NCAR Reanalyses: Characteristics and Temporal Variability. *Journal of Climatology*, **17**, 2261-2280.
- Marshall CP, Marshall AO, Aitken JB, Lai B, Vogt S, Breuer P, Steemans P, Lay PA. Imaging of Vanadium in Microfossils: A new potential biosignature. *Astrobiology*, **17**. Doi: 10.1089/ast.2017.1709
- Martin L, Flexor JM, Suguio, K. 1995. Vibrotestemunhador leve. Construção, utilização e potencialidades. *Rev. IG. São Paulo*, **16**, 59-66.
- Martinelli G, Moraes MA. 2013. Livro vermelho da flora do Brasil. Rio de Janeiro: Andrea Jakobsson Estudio, Instituto de Pesquisas Jardim Botânico do Rio do Janeiro, 1000 pag.
- Martinelli LA, Nardoto GB, Soltangheisi A, Reis CRG, Abdalla-Filho AL, Gomes TF, Lins SRM, Mardegan SF, Mariano E, Miatto RC, Moraes R, Moreira MZ, Olveira RS, Ometto JPHB, Santos FLS, Sena-Souza J, Silva DML, Silva JCSS, Vieira SA. 2021. Determining ecosystem functioning, in Brazilian biomes through foliar carbon and nitrogen concentrations and stable isotope ratios. *Biogeochemistry*, **154**, 405 – 423.
- Martinelli LA, Piccolo MC, Townsend AR, Vitousek PM, McDowell W, Robertson GP, Santos OC, Treseder K. 1999. Nitrogen stable isotopic composition of leaves and soil: Tropical versus temperate forest. *Biogeochemistry*, **46**, 45-65.
- Martins FQ, Batalha MA. 2006. Pollination systems and floral traits in cerrado woody species of the upper Taquari region (central Brazil). *Braz. J. Biol.*, **66**(2A), 543–552.
- Martins TO, Siquiera KN, Silv-Neto CM, Fonseca CS, Venturoli F, Calil FN. 2018. Vegetational and edaphic attributes in forest formations in the Cerrado biome. *Floresta*, **50**, 961-970.
- Maslin MA, Ettwein VJ, Wilson KE, Guilderson TP, Burns SJ, Leng MJ. Dynamic boundary-monsoon intensity hypothesis: evidence from the deglacial Amazon river discharge record. *Quaternary Science Review*, **30**, 3823-3833.
- Matias LQ, Guedes FM, do Nascimento HP, Sfair JC. 2021. Breaking the misconception of a dry and lifeless semiarid region: The diversity and distribution of aquatic flora in wetlands of the brazilian northeast. *Acta Botanica Brasilica*, **35**, 46–61.

- McCulloch RD, Mathiasen P, Premoli AC. 2022. Palaeoecological evidence of pollen morphological changes: A climate change adaptation strategy?. *Palaeogeography, Palaeoclimatology, Palaeoecology*, **601**, 111157.
- Medeiros MB, Walter BMT, da Silva GP, Gomes BM, Lima ILP, Silva SR, Moser P, Oliveira WL, Cavalcanti TB. 2012. Vascular flora of the Tocantins river middle basin, Brazil. *Check list*, **8**(5), 852-885.
- Medeiros MB, Walter BMT. 2012. Composição e estrutura de comunidades arbóreas de Cerrado stricto sensu no norte do Tocantins e sul do Maranhão. *Revista Arvore*, **36** (4), 673-683.
- Mistry J, Berardi A, Andrade V, Krahô T, Krahô P, Leonardos O. 2005. Indigenous fire management in the *Cerrado* of Brazil: the case of the Krahô of Tocantins. *Human Ecology*, **33** (3), 365-386.
- Mistry J. 1998. Fire in Cerrado (savannas) of Brazil: an ecological review. *Progress in Physical Geography*, **22** (4), 425-448.
- Moreira SN, Pott A, Pott VJ, Damasceno-Junior GA. 2011. Structure of pond vegetation in the Brazilian Cerrado. *Rodriguesia*, **62**(4), 721-729.
- Moreno de Sousa, J.C. (2016) Lithic technology of an Itaparica industry archeological site: the Gruta das Araras rockshelter, Midwest Brazil. *Journal of Lithis Studies*, **3**, 1-20.
Doi:10.2218/jls.v3il.1298
- Muller J, Kylander M, Wüst RAJ et al., 2008. Possible evidence for wet Heinrich phases in tropical NE Australia: the Lynch's Crater deposit. *Quat. Sci. Rev.*, **27**, 468–475.
- Murphy BP, Bowman DMJS. 2012. What controls the distribution of tropical forest and savannas?. *Ecology letters*, **15**, 748-758.
- Nascimento, D.T.F. and Novais, G.T., 2020. Clima do Cerrado: dinâmica atmosférica e característica, variabilidades e tipologias climáticas. *Elisée*, **9**(2), e922021
- Neves DM, Dexter KG, Baker TR, et al. 2020. Evolutionary diversity in tropical tree communities peaks at intermediate precipitation. *Nature: Scientific reports*, **10**, 1188.
- Neves DM, Dexter KG, Baker TR, et al. 2020. Evolutionary diversity in tropical tree communities peaks at intermediate precipitation. *Scientific reports*, **10**, 1188.
- Nogueira C. 2015. Plano de Pesquisa para a Estação Ecológica Serra Geral do Tocantins. ICMBio (Instituto Chico Mendes de Conservação da Biodiversidade).
- Novello VF, Cruz FW, Karmann I, Burns SJ, Stríkis NM, Vuille M. et al. 2012. Multidecadal climate variability in Brazil's Nordeste during the last 3000 years based on speleothem isotope records, *Geophys. Res. Lett.*, **39**, L23706.
- Novello VF, Vuille M, Cruz FW, Stríkis NM, de Paula MS, Edwards RL, et al. 2016. Centennial-scale solar forcing of the South American Monsoon System recorded in stalagmites. *Nature*, **6**, 24762.
- Numby PJ, Chollett I, Bozec Y-M, Wolff NH. 2014. Ecological resilience, robustness and vulnerability: how do these concepts benefit ecosystem management?. *Current Opinion in Environmental Sustainability*, **7**, 22-27.

- Oliveira, P.E., Barreto, A.M.F., Suguio, K., 1999. Late Pleistocene/Holocene climatic and vegetational history of the Brazilian caatinga: the fossil dunes of the middle São Francisco River. *Palaeogeography, Palaeoclimatology, Palaeoecology*, **152**, 319 – 337.
- Oliveira, U., Soares-Filho, B., Souza Costa, W.L., Gomes, L., Bustamante, M., Miranda, H., 2021. Modeling fuel loads dynamics and fire spread probability in the Brazilian Cerrado. *Forest Ecology and Management*, **482**, 118889.
- Oliveira-Filho AT, Fontes MA. 2000. Patterns of Floristic differentiation among Atlantic forest in Southeastern Brazil and the influence of climate. *Biotropica*, **32**(4b), 793-810.
- Oliveira-Filho AT, Ratter JA. 1995. A study of the origin of Central Brazilian forests by the analysis of plant species distribution patterns. *Edinburg Journal of Botany*, **52**(2), 141-194.
- Oliveira-Filho AT, Ratter JA. 2002. Vegetation physiognomies and wood flora of the Cerrado biome. In: Oliveira, P.S. and Marquis, R.J., Eds., *The Cerrados of Brazil: Ecology and Natural History of a Neotropical Savanna* (91-120). Columbia University, New York.
- Osborne CP, Sack L. 2012. Evolution of C4 plants: a new hypothesis for an interaction of CO₂ and water relations mediated by plant hydraulics. *Philosophical transactions of the Royal Society*, **367**, 583-600.
- Ouarmim S, Paradis L, Asselin H, Bergeron Y, Ali AA, Hély C. 2016. Burning potential of fire refuges in the boreal mixedwood forest. *Forests*, **7** (246). doi.org/10.3390/f7100246.
- Parizzi MG, Salgado-Labouriau ML, Kholer HC. 1998. Genesis and environmental history of Lagoa Santa, Southeastern Brazil. *The Holocene*, **8**, 311-321.
- Parr CL, Lehmann, CER, Bond, WJ, Hoffmann W, Andersen AN. 2014. Tropical grassy biomes: misunderstood, neglected, and under threat. *Trends in Ecology & Evolution*, **29** (4): 205-213.
- Pedro JB, Bostock HL, Bitz CM, He F, Vandergoes MJ, Steig EJ, Chase BM, Krause CE, Rasmussen SO, Markle BR, Cortese G. 2015. The spatial extent and dynamics of the Antarctic Cold Reversal. *Nature Geoscience*, **9**, 51 -56.
- Pennington RT, Hughes CE. 2014. The remarkable congruence of New and Old World savanna origins. *New Phytologist*, **204**: 4-6.
- Pennington RT, Lehmann CER, Rowland LM. 2014. Tropical savannas and dry forest. *Current Biology*, **28**, R541-545.
- Pereira AJ, Oliveira SL, Pereira JM, Turkman MAA. 2014. Modelling fire frequency in a Cerrado Savanna Protected area. *PLoSone*, **6**, e102380.
- Pessenda LC, Aravena R, Melfi AJ, et al. 1996. The use of carbon isotopes (¹³C, ¹⁴C) in soil to evaluate vegetation changes during the Holocene in central Brazil. *Radiocarbon*, **38**(2), 191–201.
- Petit J-R, Jouzel J, Raynaud D, Barkov NI, et al. 1999. Climate and atmospheric history of the past 420,000 years from the Vostok Ice Core, Antarctica. *Nature*, **399**, 429-436.
- Pigati JS, Springer KB. 2022. Hydroclimate response of spring ecosystems to a two-stages Younger Dryas event in the western North America. *Scientific Reports*, **12**, 7323.
- Pinaya JLD, Cruz FW, Ceccatini GCT, Corrêa PLP, et al. 2019. Brazilian montane rainforest expansion induced by Heinrich Stadial 1 event. *Scientific reports*, **9**, 17912. DOI: 10.1038/s41598-019-53036-1

- Pivello VR, Vieira I, Christianini AV, Ribeiro DB, Menezes LdaS, Berlinck CN, et al. 2021. Understanding Brazil's catastrophic fires: Causes, consequences and policy needed to prevent future tragedies. *Perspectives in Ecology and conservation*, **19**, 233 – 255.
- Prado LF, Wainer I, Chiesi CM. 2013b. Mid-Holocene PMIP3/CMIP5 model results: Intercomparison for the South American Monsoon System. *The Holocene*, **23**(12): 1915 – 1920.
- Prado LF, Wainer I, Chiesi CM, Ledru M-P, Turcq B. 2013a. A mid-Holocene climate reconstruction for eastern South America, *Clim. Past*, **9**, 2117–2133.
- Prous A, Fogaça E. 1999. Archaeology of the Pleistocene-Holocene boundary in Brazil. *Quaternary International*, **53**, 21-41.
- Ramos-Neto MB, Pivello VR. 2000. Lightning fires in a Brazilian savanna national park: rethinking management strategies. *Environ. Manag.*, **26** (6), 675-684.
- Ratnam J, Bond WJ, Fensham RJ, Hoffmann WA, Archibald S, Lehmann CE, Anderson MT, Higgins SI, Sankaran M. 2011. When is a ‘forest’ a savanna, and why does it matter?. *Global Ecology and Biogeography*, **20** (5), 653-660.
- Ratter JA, Bridgewater S, Ribeiro JF, Fonseca-Filho J, Rodrigues da Silva M, Milliken W, Pott A, Oliveira-Filho AT, Durigan G, Pennington RT. 2011. Analysis of the floristic composition of the Brazilian Cerrado vegetation IV: revision of the comparison of the woody vegetation of 367 areas and presentation of a revised data-base of 367 areas. Available in <http://www.cerrado.rbge.org.uk>.
- Ratter, J.A., Bridgewater, S., Ribeiro, J.F., 2003. Analysis of the floristic composition of the brazilian Cerrado vegetation III: comparison of the Woody vegetation of 376 areas. *Edinburgh Journal of Botany*, **60**, 57 – 109.
- Reboita MS, Gan MAM, da Rocha RP, Ambrizzi T. 2010. Regimes de precipitação na América do Sul: Um Revisão bibliográfica. *Revista Brasileira de Meteorologia*, **25**, 185-204.
- Reimann, C., Filzmoser, P., Garrett, R.G., et al., 2008. Statistical Data Analysis Explained: Applied Environmental Statistics with R. John Wiley & Sons Ltd: Chichester.
- Ribeiro JF, Walter BMT. 2008. As principais fitofisionomias do bioma Cerrado. In Sano, S.M., Almeida, S.P., Ribeiro, J.F. (Eds.), *Cerrado: Ecologia e Flora* (pp. 153 – 212). Brasilia, DF: Embrapa Cerrados.
- Reis SM, Oliveira EA, Elias F, Gomes L, Monardi PS, Marimon BS, Marimon Jr BH, Neves EC, Oliveira B, Lenza E. 2017. Resistance to fire and the resilience of the woody vegetation of the “Cerradão” in the “Cerrado” – Amazon transition zone. *Braz. J. Bot.*, **40**, 193-201.
- Riris P, Arroyo-Kalin M. 2019. Widespread population decline in South America correlates with mid-Holocene climate change. *Nature*, **9**, 6850.
- Riris P, de Souza JG. 2021. Formal test for resistance-resilience in Archeological time series. *Frontiers in Ecology and Evolution*, **9**, 740629.
- Robrahn González EM. 1996. Os grupos ceramistas pré-Coloniais do centro-oeste Brasileiro. *Rev. do Museo de Arqueología e Etnología*, Sao Paulo, **6**, 83-121.
- Rodrigues, C.A., Zirondi, H.L., Fidelis, A., 2021. Fire frequency affects fire behavior in open savannas of the Cerrado. *Forest Ecology and Management*, **482**, 118850.
- Rother DC, Rodrigues RR, Pizo MA. 2009. Effects of bamboo stand in seed rain and seed limitation in a rainforest. *Forest Ecology and Management*, **257**, 885-892.
- Salgado-Labouriau ML, Barberi M, Ferraz-Vicentini KR, Parizzi MG. 1998. A dry climatic event during the late Quaternary of tropical Brazil. *Review of Palaeobotany and Palynology*, **99**(2), 115-129. doi: 10.1016/S0034-6667(97)00045-6.

- Salgado-Labouriau ML, Cassetti V, Ferraz-Vicentini KR, Martin L, Soubiès F, Suguió K, Turcq B. 1997. Late Quaternary vegetational and climatic changes in cerrado and palm swamp from Central Brazil. *Palaeogeography, Palaeoclimatology, Palaeoecology*, **128**, 215-226.
- Salgado-Labouriau ML. 1973. Contribuição à Palinologia dos Cerrados. *Academia Brasileira de Ciências*, Rio de Janeiro, 291 pp.
- Salvador HF, Mazzottini-dos-Santos HS, Díaz DS, Azevedo AM, Lopes PSN, Nunes YR, Ribeiro LM. 2022. The dynamics of *Mauritia flexuosa* (Arecaceae) recalcitrant seed banks reveal control of their persistence in marsh environments. *Forest Ecology and Management*, **511**, 120155.
- Sampaio ACF, Bianchini JE, Santos PM, Ariati V, Santos LM. 2018. Fitossociologia do Cerrado *sensu stricto* na bacia do Rio Paranaíba no nordeste brasileiro. *Advances in forestry Sciences*, **5**(2), 299 – 307.
- Sano EE, Rodrigues AA, Martins ES, Bettoli GM, Bustamante MM, Bezerra AS, Couto Jr. AF, Vasconcelos V, Schüler J, Bolfe EL. 2019. Cerrado ecoregions: A spatial framework to assess and prioritize Brazilian savanna environmental diversity for conservation. *Journal of Environmental Management*, **232**, 818-828. doi: 10.1016/j.jenvman.2018.11.108
- Sano SM, de Almeida SP, Ribeiro JP. 2008. Cerrado, ecologia e flora vol. II. Embrapa informação tecnológica Brasília, DF, 877 pag.
- Santos FFM, Munhoz CBR. 2012. Diversidade de espécies herbaceo-arbustivas e zonação florística em uma vereda no Distrito Federal. *Heringiana*, **6**(2), 21-27.
- Schmidt IB, Eloy L. 2020. Fire regime in the Brazilian Savanna: Recent changes, policy and management. *Flora*, **268**, 151613.
- Schmidt IB, Fidelis A, Miranda H, Ticktin. 2017. How do the wetlands burn? Fire behavior and intensity in wet grasslands in the Brazilian savanna. *Braz. J. Bot.*, **40**, 167-175.
- Shimizu, M.H., Sampaio ,G., Venancio, I.M., Maksic, J., 2020. Seasonal changes of the South American monsoon system during the mid-Holocene in the CMIP5 simulations. *Climate Dynamics*, **54**, 2697 – 2712.
- Sifeddine, A., Wirrmann, D., Albuquerque, A.L. et al., 2004. Bulk composition of sedimentary organic matter used in palaeoenvironmental reconstructions: Examples from the tropical belt of South America and Africa. *Palaeogeography, Palaeoclimatology, Palaeoecology*, **214**, 41–53.
- Silva FAM, Assad ED, Evangelista BA. 2008. Caracterização climática do Bioma Cerrado. In: Sano SM, Almeida SP, Ribeiro JF, editors. Cerrado: ecologia e flora. Brasília: Embrapa Cerrados/Embrapa Informação Tecnológica, p. 61–88.
- Silva WM, Lolis SF, Viana RH. 2016. Composition and structure of the gallery forest and the Taquaruçu Grande sub-basin, Municipality of Palmas, Tocantins state. *Maringá*, **38**, 17-24.
- Silva-Moraes H, Cordeiro I, Figueiredo N. 2019. Flora and floristic affinities of the cerrados of Maranhão state, Brazil. *Edinburgh Journal of Botany*, **76**, 1-21.
doi:10.1017/S0960428618000215
- Simon, M.F., Grether, R., de Queiroz, L.P., Skema, C., Pennington, R.T., Hughes, C.E. 2009. Recent assembly of the Cerrado, a neotropical plant diversity hotspot, by in situ evolution of adaptations to fire. *Proc. Natl. Acad. Sci.*, **106**, 20359–20364.
- Sjöström, J.K., Martínez Cortizas, A., Hansson, S.V. et al., 2020. Paleodust deposition and peat accumulation rates – Bog size matters. *Chem. Geol.* **554**, 119795.
- Soares EL, Landi LADC, Gasparino EC. 2020. Additions to the knowledge of the pollen morphology of some Fabaceae from Cerrado forest patches of Brazil. *Palynology*. Doi: 10.1080/01916122.2020.1804007

- Souza CM, Shimbo JZ, Rosa MR, et al. 2020. Reconstructign three decades of land use and land cover changes in Brazilian Biomes with landsat Archive and Earth engine. *Remote sensing*, **20**, 2735.
- speciesLink's*. 2013-2023. Brazil: CRIA;[accessed 2023 March 30]. <https://specieslink.net/>
- Strassburg BBN, Brooks T, Feltran-Barberi R, Iribarrem A, Crouzeilles R, Loyola R, Latawiec AE, Oliveira-Filho FJB, Scaramuzza CA de M, Scarano FR, Soares-Filho B, Balmford A. 2017. Moment of truth for the Cerrado Hotspot. *Nature Ecology & Evolution*, **99**, 1-3.
- Stríkis NM, Chiessi CM, Cruz FW, Vuille M, Cheng H, Souza Barreto EA, Mollenhauer G, Kasten S, Karmann I, Edwards RL, Bernal JP, Reis H. 2015. Timing and structure of Mega-SACZ events during the Heinrich Stadial 1. *Geophysical Research Letters*, **42**. Doi: 10.1002/2015GL064048.
- Stríkis NM, Cruz FW, Barreto EAS, Naughton F, Vuille M, Cheng H, Voelker AHL, Zhang H, Karmann I, Edwards L, Auler AS, Santos RV, Sales HR. 2018. South American monsoon response to iceberg discharge in the North Atlantic. *PNAS*, **115** (15), 3788-3793.
- Stríkis NM, Cruz FW, Cheng H, Karmann I, Edwards RL, Vuille M, Wang X, de Paula MS, Novello F, Auler AS. 2011. Abrupt variations in South American monsoon rainfall during the Holocene based on a speleothem record from central-eastern Brazil. *Geology*, **39**, 1075–1078. doi: 10.1130/G32098.1
- Struyf E, Conley D. 2009. Silica an essential nutrient in wetland biogeochemistry. *Frontiers in Ecology and the Environment*, **7**(2), 88-94.
- Stuiver M, Reimer PJ. 1993. CALIB rev. 7. *Radiocarbon*, **35**, 215-230.
- Sulca J, Vuille M, Silva Y, Takahashi K. 2016. Teleconnections between the Peruvian Central Andes and Northeast Brazil during Extreme Rainfall Events in Austral Summer. *Journal of Hydrometeorology*, **17**, 499-515.
- Thomas ER, Wolff EW, Mulvaney R, Steffensen JP, Sigfus JJ, Arrowsmith C, White JWC, Vaughn B, Popp T. 2007. The 8.2 ka evento from Greenland ice cores. *Quaternary Sciences Reviews*, **26**, 70-81.
- Tinner W, Hofstetter S, Zeugin F, Conedera M, Wohlgemuth T, Zimmermann L, Zweifel R. 2006. Long-distance of macroscopic charcoal by an intensive crown fire in the Swiss Alps – implications for fire history reconstruction. *The Holocene*, **16**, 287 – 292.
- Tweddle JC, Edwards KJ. 2010. Pollen preservation zones as an interpretative tool in Holocene palynology. *Review of Paleobotany and Palynology*, **161** (1-2), 59-76.
- Umbanhowar CE, McGrath M. 1998. Experimental production and analysis of microscopic charcoal from wood, leaves and grasses. *The Holocene*, **8**, 341 6 346.
- Utida G, Cruz FW, Etourneau J, Bouloubassi I, Schefuß E, Vuille M, et al. 2019. Tropical South Atlantic influence on Northeastern Brazil precipitation and ITCZ displacement during the past 2300 years. *Nature*, **9**, 1698.
- Utida G, Cruz FW, Santos RV, Sawakuchi AO, Wang H, Pessenda LCR, Novello VF, Vuille M, Strauss AM, Borella AC, Strikis NM, Guedes CCF, de Andrade FRD, Zhang H, Cheng H, Edwards RL. 2020. Climate changes in Northeastern Brazil from deglacial to Meghalayn periods and related environmental impacts. *Quaternary Sciences Reviews*, **250**, 106655.
- Vachula RS, Rehn E. 2023. Modeled dispersal patterns for wood and grass charcoal are different: Implications for paleofire reconstruction. *The Holocene*, **33**(2), 159 – 166.

van den Berg E, Oliveira-Filho AT. 2000. Composição florística e estrutura fitossociológica de uma floresta ripária em Itutinga, MG, e comparação com outras áreas. *Revista Brasileira Botânica*, **23**(3), 231–253.

Velazco SJE, Villalobos F, Galvão F, De Marco Júnior PA. 2019. Dark scenario for Cerrado plant species: Effects of future climate, land use and protected areas ineffectiveness. *Divers Distrib*, **25**, 660– 673.

Vieira JA. 2020. Revisão Taxonômica de Pentaphylacaceae Engl. para o Brasil. Universidade Estadual Paulista "Julio de Mesquita Filho", 242 pag.

Vieira LTA, Azevedo TN, Castro AAJF, Martins FR. 2022. Reviewing the Cerrado's limits, flora distribution patterns, and conservation status for policy decisions. *Land Use Policy*, **115**, 106038. Vieira LTA, Castro AAJF, Coutinho JMCP, de Sousa SR, de Farias RRS, Castro NMCF, Martins FR. 2019. A biogeographic and evolutionary analysis of the flora of the North-eastern cerrado, Brazil. *Plant Ecology & Diversity*, **12**(5), 475-488. doi: 10.1080/17550874.2019.1649311.

Villela FNJ, Nogueira C, 2011. Geologia e geomorfologia da estação Serra Geral do Tocantins. *Biota Neotropica*, **11**, 217 – 229. Doi: 10.1590/S1676-06032011000100023

Wainer I, Prado L, Khodri M, Otto-Bliesner B. 2014. Reconstruction of the South Atlantic subtropical dipole index for the past 12,000 years from surface temperature proxy. *Scientific Reports*, **4**, 5291.

Wainer I, Prado LF, Khodri M, Otto-Bliesner B. 2021. The South Atlantic sub-tropical dipole mode since the last deglaciation and changes in rainfall. *Climate Dynamics*, **56**, 109-122.

Walker, M., Gibbard, P., Head, M.J., et al., 2019. Formal Subdivision of the Holocene Series/Epoch: A Summary. *Journal of the Geological Society of India*, **93**, 135–141. Doi: 10.1007/s12594-019- 1141-9

Wang X, Edwards RL, Auler AS, Cheng H, Ito E. 2007. Millenial-scale interhemispheric asymmetry of low-latitude precipitation: Speleothem evidence and possible high-latitude forcing. pp 279-294. In: Ocean Circulation: mechanism and impacts – Past and future changes of Meridional Overtourning vol. 3. Edited by: Schmittner A, Chiang JCH & Hemming SR, Washington D.C.

Wang, X., Edwards, R.L., Auler, A.S., et al., 2017. Hydroclimate changes across the Amazon lowlands over the past 45,000 years. *Nature*, **541**, 204–207. <https://doi.org/10.1038/nature20787>

Ward BM, Wong CI, Novello VF, McGee D, Santos RV, Silva LCR, Cruz FW, Wang X, Edwards RL, Cheng H. 2019. Reconstruction of Holocene coupling between the South America Monsoon System and local moisture variability from speleothem $\delta^{18}\text{O}$ and $^{87}\text{Sr}/^{86}\text{Sr}$ records. *Quaternary Sciences review*, **210**, 51-63.

Wersal RM. 2010. The conceptual ecology and management of parrotfeather [Myriophyllum aquaticum (Vell. Verdc.)]. Mississippi State University, degree of Doctor of Philosophy. 199 pag.

Wong ML, Wang X, Lutrubesse EM, He S, Bayer M. 2021. Variations in the South Atlantic Convergence Zone over the mid-to-late Holocene inferred from speleothem $\delta^{18}\text{O}$ in central Brazil. *Quaternary Sciences reviews*, **270**, 107178.

- Wortham BR, Wong CI, Silva LCR, McGee D, Montañez IP, Rasbury ET, Cooper KM, Sharp WD, Glessner JHG, Santos RV. 2019. Assessing response of local moisture conditions in central Brazil to variability in regional monsoon intensity using speleothem $^{87}\text{Sr}/^{86}\text{Sr}$ values. *Earth and Planetary Science Letters*, **463**, 310-322.
- Xu Q, Zhang S, Gaillard M-J, Li M, Cao X, T F, Li F. 2016. Studies of modern pollen assemblages for pollen dispersal- deposition- preservation process understanding and for pollen-based reconstructions of past vegetation, climate, and human impact: A review based on case studies in China. *Quaternary Science Reviews*, **149**, 151–166.
- Zhang S, Xu Q, Nielsen AB, Chen H, Li Y, Li M, Hun L, Li J. 2012. Pollen assemblages and their environmental implications in the Qaidam Basin, NW China. *Boreas*, **41**(4), 513-736.
- Zhao Y, Wu F, Fang X, Yang Y. 2015. Topsoil C/N ratios in the Qilian mountains: implications for the use of subaqueous sediment C/N ratios in paleo-environmental reconstructions to indicate organic sources. *Palaeogeography, Palaeoclimatology, Palaeoecology*, **426**, 1-9.
- Zolitschka B, Lee A-S, Bermúdez DP, Giescke T. 2021. Environmental variability at the margin of the South American Monsoon System recorded by a high-resolution sediment record from Lagoa Dourada (South Brazil). *Quaternary Sciences Review*, **272**, 107204.
- Zupo T, Dabies LF, Pausas JG, Fidelis A. 2020. Post-fire regeneration strategies in a frequently burned Cerrado community. *Journal of Vegetation Sciene*, **32**, e12968.